SANDIA REPORT

SAND91–0893/4 • UC–721
Unlimited Release
Printed April 1992

Preliminary Comparison with 40 CFR Part 191, Subpart B for the Waste Isolation Pilot Plant, December 1991

Volume 4: Uncertainty and Sensitivity Analysis Results

J. C. Helton, J. W. Garner, R. P. Rechard, D. K. Rudeen, P. N. Swift

Prepared by
Sandia National Laboratories
Albuquerque, New Mexico 87185 and Livermore, California 94550
for the United States Department of Energy
under Contract DE-AC04-76DP00789

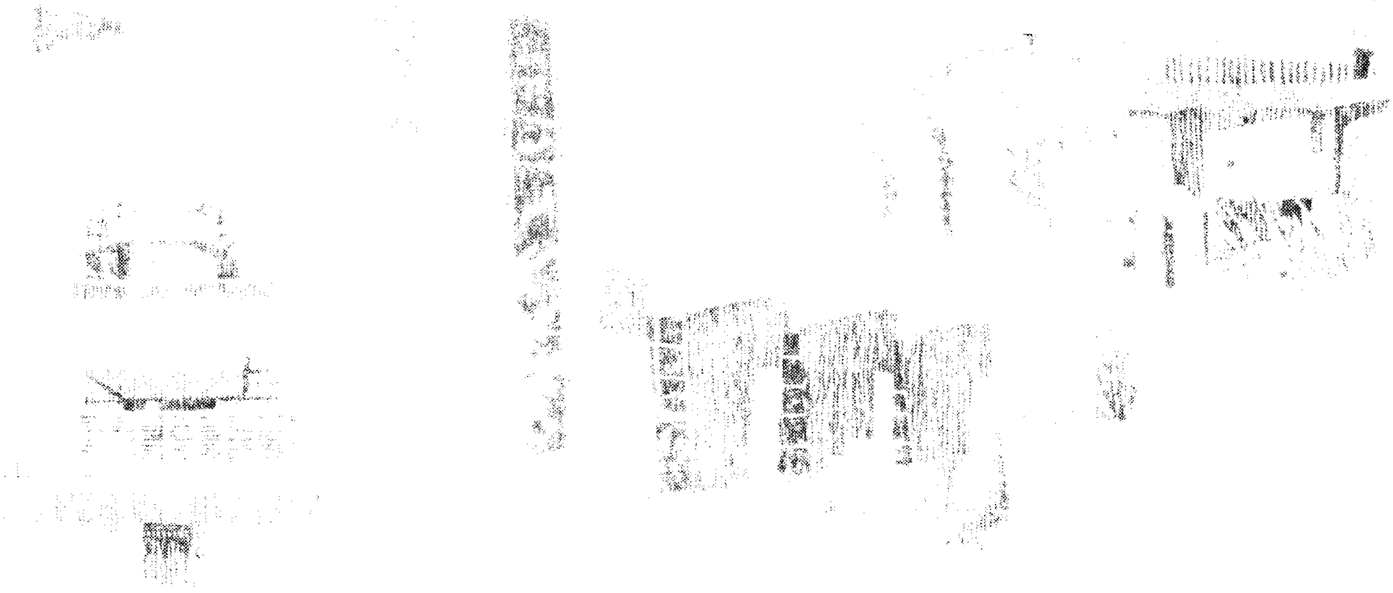

Issued by Sandia National Laboratories, operated for the United States Department of Energy by Sandia Corporation.

Printed in the United States of America. This report has been reproduced directly from the best available copy.

Available to DOE and DOE contractors from
Office of Scientific and Technical Information
PO Box 62
Oak Ridge, TN 37831

Prices available from (615) 576-8401, FTS 626-8401

Available to the public from
National Technical Information Service
US Department of Commerce
5285 Port Royal Rd
Springfield, VA 22161

NTIS price codes
Printed copy: A10
Microfiche copy: A01

SAND91-0893/4
Unlimited Release
Printed April 1992

Distribution
Category UC-721

PRELIMINARY COMPARISON WITH 40 CFR PART 191, SUBPART B FOR THE WASTE ISOLATION PILOT PLANT, DECEMBER 1991

VOLUME 4: UNCERTAINTY AND SENSITIVITY ANALYSIS RESULTS

Jon C. Helton[1]
James W. Garner[2], Rob P. Rechard,
David K. Rudeen[3], Peter N. Swift[4]
WIPP Performance Assessment Division
Sandia National Laboratories
Albuquerque, New Mexico 87185

ABSTRACT

The most appropriate conceptual model for performance assessment at the Waste Isolation Pilot Plant (WIPP) is believed to include gas generation due to corrosion and microbial action in the repository and a dual-porosity (matrix and fracture porosity) representation for solute transport in the Culebra Dolomite Member of the Rustler Formation. Under these assumptions, complementary cumulative distribution functions (CCDFs) summarizing radionuclide releases to the accessible environment due to both cuttings removal and groundwater transport fall substantially below the release limits promulgated by the Environmental Protection Agency (EPA). This is the case even when the current estimates of the uncertainty in analysis inputs are incorporated into the performance assessment. The best-estimate performance-assessment results are dominated by cuttings removal. The releases to the accessible environment due to groundwater transport make very small contributions to the total release. The variability in the distribution of CCDFs that must be considered in comparisons with the EPA release limits is dominated by the variable LAMBDA (rate constant in Poisson model for drilling

[1] Arizona State University, Department of Mathematics, Tempe, AZ 85287
[2] Applied Physics, Inc., Albuquerque, NM 87109
[3] New Mexico Engineering Research Institute, Albuquerque, NM 87131
[4] Tech Reps, Inc, Albuquerque, NM 87110

intrusions). The variability in releases to the accessible environment due to individual drilling intrusions is dominated by DBDIAM (drill bit diameter). Most of the imprecisely known variables considered in the 1991 WIPP performance assessment relate to radionuclide releases to the accessible environment due to groundwater transport. For a single borehole (i.e., an E2-type scenario), whether or not a release from the repository to the Culebra even occurs is controlled by the variable SALPERM (Salado permeability), with no releases for small values (i.e., $< 5 \times 10^{-21}$ m^2) of this variable. When SALPERM is small, the repository never fills with brine and so there is no flow up an intruding borehole that can transport radionuclides to the Culebra. Further, releases that do reach the Culebra for larger values of SALPERM are small and usually do not reach the accessible environment. A potentially important scenario for the WIPP involves two or more boreholes through the same waste panel, of which at least one penetrates a pressurized brine pocket and at least one does not (i.e., an E1E2-type scenario). For these scenarios, the uncertainty in release to the Culebra is dominated by the variables BHPERM (borehole permeability), BPPRES (brine pocket pressure), and the solubilities for the individual elements (i.e., Am, Np, Pu, Th, U) in the projected radionuclide inventory for the WIPP. Once a release reaches the Culebra, the matrix distribution coefficients for the individual elements are important, with releases to the Culebra often failing to reach the accessible environment over the 10,000-yr period specified in the EPA regulations. To provide additional perspective, the following variants of the 1991 WIPP performance assessment have also been considered: (1) no gas generation in the repository and a dual-porosity transport model in the Culebra; (2) gas generation in the repository and a single-porosity (fracture porosity) transport model in the Culebra; (3) no gas generation in the repository and a single-porosity transport model in the Culebra; (4) gas generation in the repository and a dual-porosity transport model in the Culebra without chemical retardation; and (5) gas generation in the repository, a dual-porosity transport model in the Culebra, and extremes of climatic variation. All of these variations relate to groundwater transport and thus do not affect releases due to cuttings removal, which were found to dominate the results of the 1991 WIPP performance assessment. However, these variations do have the potential to increase the importance of releases due to groundwater transport relative to releases due to cuttings removal.

ACKNOWLEDGMENTS

The WIPP Performance Assessment Division is comprised of both Sandia and contractor employees working as a team to produce these annual preliminary comparisons with EPA regulations, assessments of overall long-term safety of the repository, and interim technical guidance to the program. The on-site team, affiliations, and contributions to the 1991 performance assessment are listed in alphabetical order:

Performance Assessment Division

Name	Affil.	Primary Author of Doc: Sect.	Primary Author of Major Code	Area of Responsibility
R. Anderson	SNL			Division Manager
B. Baker	TEC	V.2:§6.4		SECO2D, Hydrology, Office Manager
J. Bean	UNM	V.2:§4.2.1		BRAGFLO & BOASTII, 2-Phase Flow
J. Berglund	UNM	V.2:Ch.7 Editor V.2	CUTTINGS	Task Ldr., Undisturbed Repository, Cuttings/Cavings/ Engr. Mech.
W. Beyeler	SAI	V.2:§5.3; 6.1;6.3	PANEL GARFIELD	Geostatistics, Analytical Models, CAMCON Systems Codes
K. Brinster	SAI			Geohydrology, Conceptual Models
R. Blaine	ECO			SECO2D & CAMCON Systems Codes
T. Blaine	EPE			Drilling Technology, Exposure Pathways Data
J. Garner	API	V.2:§5.3	PANEL	Source Term, Sens. Anal.
A. Gilkey	UNM			CAMCON Systems Codes
L. Gomez	SNL			Task Ldr., Safety Assessments
M. Gruebel	TRI	V.1:Ch.1,2, 8,9,10		EPA Regulations
R. Guzowski	SAI	V.1:Ch.4		Geology, Scenario Construction
J. Helton	ASU	V.1:Ch.3,4 V.2:Ch.2,3	CCDFPERM	Task Ldr., Uncert./Sens. Anal., Probability Models
H. Iuzzolino	GC	Editor V.3	CCDFPERM	LHS & CAMCON System Codes
R. Klett	SNL			EPA Regulations
P. Knupp	ECO			STAFF2D & SECOTR, Comp. Fluid Dyn.
C. Leigh	SNL		GENII-S	Exposure Pathways
M. Marietta	SNL	Editor (Set)		Dep. Div. Manager, Tech. Coord.
G. de Marsily	UP	V.2:§6.2		Task Ldr., Geostatistics
R. McCurley	UNM	V.2:§4.2.3		SUTRA & CAMCON System Codes
A. Peterson	SNL	Editor V.3		Task Ldr., Inventory
J. Rath	UNM	V.2:§4.2.3		SUTRA, Engr. Mech.
R. Rechard	SNL	Editor V.2 & V.3		Task Ldr., CAMCON, QA, Ref. Data
P. Roache	ECO	V.2:§6.4	SECO	Task Ldr., Comp. Fluid Dyn.
D. Rudeen	UNM	V.2:§4.2.2; 6.5		STAFF2D, Transport
J. Sandha	SAI	Editor V.3		INGRES, PA Data Base
J. Schreiber	SAI	V.2:§4.2.1; 5.2.5 Editor V.3		BRAGFLO & BOASTII, 2-Phase Flow

P. Swift	TRI	V.1:Ch.5,11		Task Ldr., Geology, Climate Var.
M. Tierney	SNL	Editor V.3		Task Ldr., CDF Constr., Probability Models
K. Trauth	SNL			Task Ldr., Expert Panels
P. Vaughn	API	V.2:§5.1; 5.2;5.2.5; App.A	BRAGFLO	Task Ldr., 2-Phase Flow & Waste Panel Chemistry
J. Wormeck	ECO			Comp. Fluid Dyn. & Thermodyn.

The foundation of the annual WIPP performance assessment is the underlying data set and understanding of the important processes in the engineered and natural barrier systems. The SNL Nuclear Waste Technology Department is the primary source of these data and understanding. Assistance with the waste inventory comes from WEC and its contractors. We gratefully acknowledge the support of our departmental and project colleagues. Some individuals have worked closely with the performance assessment team, and we wish to acknowledge their contributions individually:

J. Ball	ReS	Computer System Manager
H. Batchelder	WEC	CH & RH Inventories
R. Beauheim	SNL	Natural Barrier System, Hydrologic Parameters
B. Butcher	SNL	Engineered Barrier System, Unmodified Waste-Form Parameters, Disposal Room Systems Parameters
L. Brush	SNL	Engineered Barrier System, Source Term (Solubility) and Gas Generation Parameters
L. Clements	ReS	Computer System Support
T. Corbet	SNL	Natural Barrier System, Geologic & Hydrologic Parameters, Conceptual Models
P. Davies	SNL	Natural Barrier System, Hydrologic & Transport Parameters, & 2-Phase Flow Mechanistic Modeling
P. Drez	IT	CH & RH Inventories
E. Gorham	SNL	Natural Barrier System, Fluid Flow & Transport Parameters
S. Howarth	SNL	Natural Barrier System, Hydrologic Parameters
R. Kehrman	WEC	CH & RH Waste Characterization
R. Lincoln	SNL	Project Integration
F. Mendenhall	SNL	Engineered Barrier System, Unmodified Waste Form Parameters, Waste Panel Closure (Expansion)
D. Munson	SNL	Reference Stratigraphy, Constitutive Models, Physical & Mechanical Parameters
E. Nowak	SNL	Shaft/Panel Seal Design, Seal Material Properties, Reliability
J. Orona	ReS	Computer System Support
J. Tillerson	SNL	Repository Isolation Systems Parameters
S. Webb	SNL	2-Phase Flow Sensitivity Analysis & Benchmarking

API = Applied Physics Incorporated
ASU = Arizona State University
ECO = Ecodynamics Research Associates
EPE = Epoch Engineering
GC = Geo-Centers Incorporated
IT = International Technology
ReS = ReSpec
SAI = Scientific Applications International Corporation
SNL = Sandia National Laboratories
TEC = Technadyne Engineering Consultants
TRI = Tech Reps, Inc.
UNM = Univ. of New Mexico/New Mexico Engineering Research Institute
UP = University of Paris
WEC = Westinghouse Electric Corporation

Peer Review

Internal/Sandia

T. Corbet	Vol. I, II, III
D. Gallegos	Vol. I, II, III
M. LaVenue	Vol. I, II, III
S. Hora	Vol. I, II, III
M. Marietta	Vol. IV
M. Tierney	Vol. IV

Management/Sandia

W. Weart
T. Hunter

PA Peer Review Panel

R. Heath, Chairman	University of Washington
R. Budnitz	Future Resources Associates, Inc.
T. Cotton	JK Research Associates, Inc.
J. Mann	University of Illinois
T. Pigford	University of California, Berkeley
F. Schwartz	Ohio State University

Department of Energy

R. Becker
J. Rhoderick
P. Higgins

Expert Panels

Futures

M. Baram	Boston University
W. Bell	Yale University
G. Benford	University of California, Irvine
D. Chapman	The World Bank, Cornell University
B. Cohen	University of Pittsburgh
V. Ferkiss	Georgetown University
T. Glickman	Resources for the Future
T. Gordon	Futures Group
C. Kirkwood	Arizona State University
H. Otway	Joint Research Center (Ispra), Los Alamos National Laboratory
M. Pasqualetti	Arizona State University
D. Reicher	Natural Resources Defense Council
N. Rosenberg	Resources for the Future
M. Singer	The Potomac Organization
T. Taylor	Consultant
M. Vinovski	University of Michigan

Source Term

C. Bruton	Lawrence Livermore National Laboratory
I-Ming Chou	U.S. Geological Survey
D. Hobart	Los Alamos National Laboratory
F. Millero	University of Miami

Retardation

R. Dosch	Sandia National Laboratories
C. Novak	Sandia National Laboratories
M. Siegel	Sandia National Laboratories

Geostatistics Expert Group

G. de Marsily, Chairman	University of Paris
R. Bras	Massachusetts Institute of Technology
J. Carrera	Universidad Politecnica de Cataluña
G. Dagan	Tel Aviv University
A. Galli	Ecole des Mines de Paris
A. Gutjahr	New Mexico Institute of Mining and Technology
D. McLaughlin	Massachusetts Institute of Technology
S. Neuman	University of Arizona
Y. Rubin	University of California, Berkeley

Report Preparation (TRI)

Editors:

Volume 1: M. Gruebel (text); S. Laundre-Woerner (illustrations)
Volume 2: D. Scott (text); D. Marchand (illustrations)
Volume 3: J. Chapman (text); D. Pulliam (illustrations)
Volume 4: D. Bissell (text); D. Marchand (illustrations)

D. Rivard, D. Miera, T. Allen, and the Word Processing Department
R. Rohac, R. Andree, and the Illustration and Computer Graphics Departments
S. Tullar and the Production Department

J. Stikar (compilation of PA Peer Review Panel comments)

CONTENTS

FIGURES

Figure		Page

Figure		Page

Figure		Page

TABLES

1. INTRODUCTION

This volume is the fourth in a sequence of reports that document the December 1991 preliminary comparison with 40 CFR 191, Subpart B (the Standard; U.S. EPA, 1985) for the Waste Isolation Pilot Plant (WIPP). The three previous volumes describe the background of the project, the performance-assessment methodology, and the 1991 results (Volume 1); the probability and consequence models used in the calculations (Volume 2); and the reference data base (Volume 3). This volume contains the results of uncertainty and sensitivity analyses conducted using the methodology, modeling system, and data described in the earlier volumes. These analyses provide quantitative and qualitative insights on the relationships between uncertainty in the models and data used in the WIPP performance assessment and the resultant uncertainty in the results of the performance assessment.

Performance assessment for the WIPP is an annual iterative process, with each year's preliminary comparison building on the previous year's until a final defensible comparison with the Standard can be prepared. Results of this preliminary comparison cannot be used to evaluate compliance with the Standard because portions of the modeling system are still under development, data is insufficient in some areas, and the level of confidence in the estimated performance remains uncertain. The current status of the compliance-assessment system is summarized in Chapter 11 of Volume 1. A final evaluation of compliance also cannot be made at this time because the Standard was vacated by a Federal Court of Appeals in 1987, and has not been repromulgated by the Environmental Protection Agency (EPA). By agreement with the State of New Mexico, the Department of Energy (DOE) is evaluating compliance with the Standard as first promulgated until a revised Standard is available (U.S. DOE and State of New Mexico, 1981, as modified).

Uncertainty and sensitivity analysis is an important part of the WIPP performance assessment and contributes to the overall analysis in the following areas: (1) assessment of the uncertainty in performance-assessment results that must be used in comparison with regulatory standards, (2) identification of modeling areas where reductions in uncertainty can significantly improve the confidence that can be placed in performance-assessment results, and (3) verification that the models used within the performance-assessment process are operating properly.

This report is organized as follows. Chapter 2 provides an overview of the structure of the WIPP performance assessment. First, the Kaplan and Garrick ordered-triple representation for risk is introduced as the conceptual model for the overall structure of the WIPP performance assessment. Then, the definition of scenarios, the determination of scenario probabilities, and the calculation of scenario consequences in the 1991 WIPP performance assessment are described in the context of this representation. The ordered-triple representation for risk facilitates the separation of stochastic and subjective uncertainty and leads naturally to complementary cumulative distribution functions (CCDFs) that are used in comparisons with the EPA Standard for releases to the accessible environment.

Chapter 3 discusses the 45 imprecisely known variables considered in the 1991 WIPP performance assessment and also summarizes the approach to uncertainty and sensitivity analysis being used. Specifically, a Monte Carlo approach to uncertainty/sensitivity involving the following steps is used in the 1991 WIPP performance assessment: (1) develop distributions characterizing the subjective uncertainty in the variables under consideration; (2) generate sample from variables according to their assigned distributions; (3) propagate sample through performance assessment; (4) summarize uncertainty analysis results with means and variances, distribution functions and box plots; and (5) determine sensitivity of performance-assessment results to the sampled variables with scatterplots, regression analysis, partial correlation analysis and possibly other techniques. The distributions assigned to the 45 variables presented in Chapter 2 characterize subjective uncertainty (i.e., a degree of belief as to the value of a fixed but imprecisely known quantity). In contrast, stochastic uncertainty is characterized by the probabilities assigned to the individual scenarios considered in the performance assessment.

At present, the most appropriate physical model for performance assessment at the WIPP is believed to include gas generation due to both corrosion and microbial action in the repository and a dual-porosity representation for radionuclide transport in the Culebra Dolomite Member of the Rustler Formation. This conceptual view was used in the modeling that produced the best-estimate performance-assessment results presented in Chapter 6 of Vol. 1. Chapter 4 of the present volume presents uncertainty and sensitivity analysis results for these modeling assumptions, including results for cuttings removal, groundwater transport, cuttings removal and groundwater transport combined, and the CCDFs that are used in comparisons with the EPA release limits.

In addition to the best-estimate conceptual model involving gas generation in the repository and a dual-porosity transport model in the Culebra, the 1991 WIPP performance assessment also considered the following alternative conceptual models: (1) no gas generation in the repository and a dual-porosity transport model in the Culebra, (2) gas generation in the repository and a single-porosity transport model in the Culebra, (3) no gas generation in the repository and a single-porosity transport model in the Culebra, (4) gas generation in the repository and dual-porosity transport model without chemical retardation in the Culebra, and (5) climate change with gas generation in the repository and with single- and dual-porosity transport models in the Culebra. Uncertainty and sensitivity analyses for these alternative conceptual models are presented in Chapter 5, including results for groundwater transport, cuttings removal and groundwater transport combined, and the CCDFs that are used in comparison with the EPA release limits.

Chapter 6 contains a concluding discussion that summarizes the uncertainty and sensitivity analysis results and compares the results obtained with the alternative conceptual models.

2. STRUCTURE OF WIPP PERFORMANCE ASSESSMENT

2.1 Conceptual Model

As proposed by Kaplan and Garrick (1981), the outcome of a performance assessment can be represented by a set R of ordered triples of the form

$$R = \{(S_i, pS_i, \mathbf{cS}_i), i=1, \ldots, nS\}, \tag{2.1-1}$$

where

S_i = a set of similar occurrences,

pS_i = probability that an occurrence in the set S_i will take place,

$\mathbf{cS}_i$ = a vector of consequences associated with S_i,

nS = number of sets selected for consideration,

and the sets S_i have no occurrences in common (i.e., the S_i are disjoint sets). This representation formally decomposes the outcome of a performance assessment into what can happen (the S_i), how likely things are to happen (the pS_i), and the consequences for each set of occurrences (the $\mathbf{cS}_i$). The S_i are typically referred to as "scenarios" in radioactive waste disposal. Similarly, the pS_i are scenario probabilities, and the vector $\mathbf{cS}_i$ contains environmental releases for individual isotopes, the normalized EPA release summed over all isotopes, and possibly other information associated with scenario S_i. The set R in Eq. 2.1-1 is used as the conceptual model for the WIPP performance assessment.

Although the representation in Eq. 2.1-1 provides a natural conceptual way to view risk, the set R by itself can be difficult to examine. For this reason, the risk results in R are often summarized with complementary cumulative distribution functions (CCDFs). These functions provide a display of the information contained in the probabilities pS_i and the consequences $\mathbf{cS}_i$. With the assumption that a particular consequence result cS in the vector $\mathbf{cS}$ has been ordered so that $cS_i \le cS_{i+1}$ for $i=1, \ldots, nS$, the associated CCDF is shown in Figure 2.1-1. A consequence result of particular interest in performance assessments for radioactive waste disposal is the EPA normalized release to the accessible environment (U.S. EPA, 1985). As indicated in Figure 2.1-1, the EPA places a bound on the CCDF for normalized release to the accessible environment.

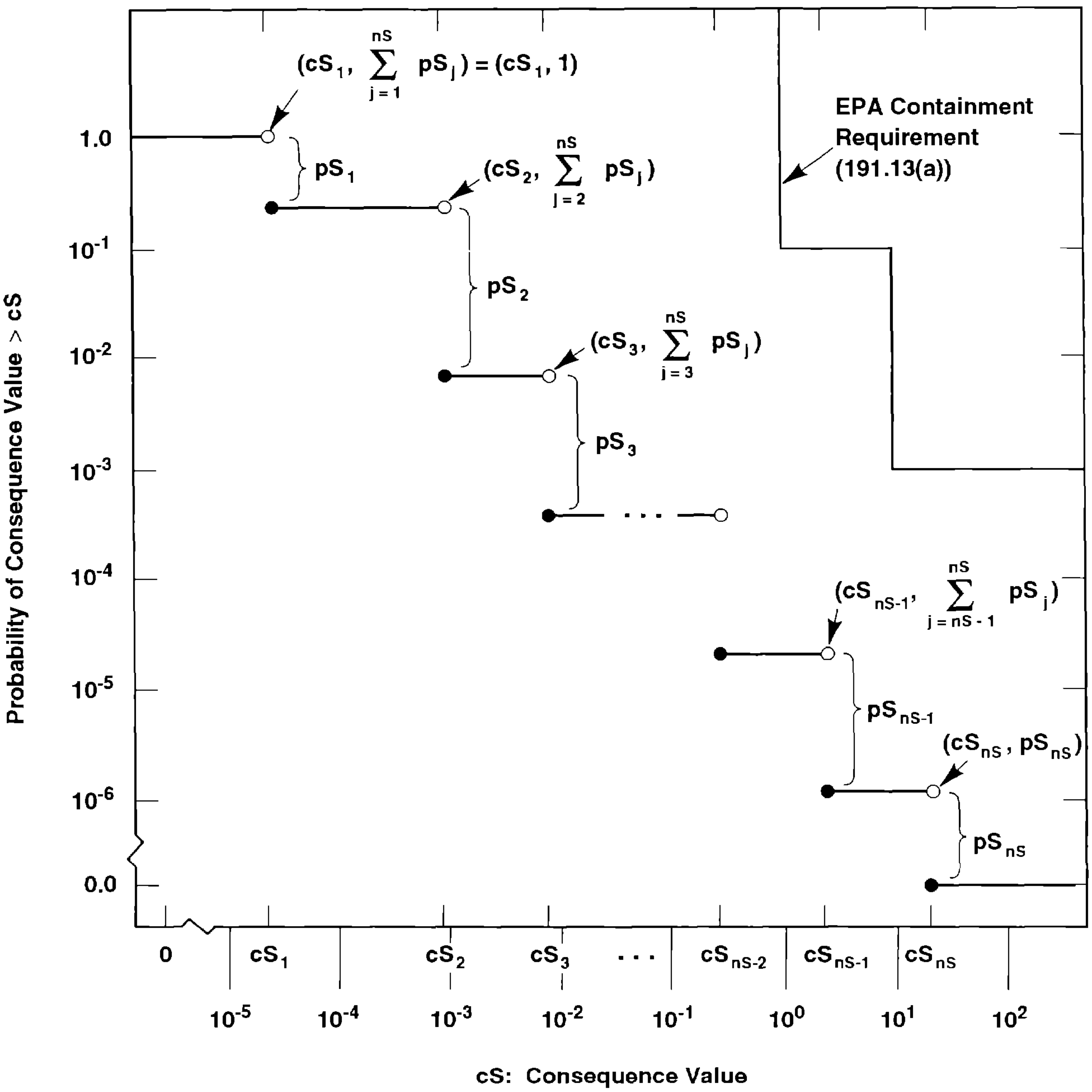

TRI-6342-730-6

Figure 2.1-1. Estimated Complementary Cumulative Distribution Function (CCDF) for Consequence Result cS (Helton et al., 1991). The open and solid circles at the discontinuities indicate the points included on (solid circles) and excluded from (open circles) the CCDF.

In practice, the outcome of a performance assessment depends on many imprecisely known variables. These imprecisely known variables can be represented by a vector

$$\mathbf{x} = [x_1, x_2, \ldots, x_{nV}], \qquad (2.1\text{-}2)$$

where each x_j is an imprecisely known input required in the performance assessment and nV is the total number of such inputs. As a result, the set R is actually a function of $\mathbf{x}$:

$$R(\mathbf{x}) = \{[S_i(\mathbf{x}), pS_i(\mathbf{x}), \mathbf{cS}_i(\mathbf{x})], i=1, \ldots, nS(\mathbf{x})\}. \qquad (2.1\text{-}3)$$

As $\mathbf{x}$ changes, so will $R(\mathbf{x})$ and all summary measures that can be derived from $R(\mathbf{x})$. Thus, rather than a single CCDF for each consequence value contained in $\mathbf{cS}$, there will be a distribution of CCDFs that results from the possible values that $\mathbf{x}$ can take on.

The uncertainty in $\mathbf{x}$ can be characterized by a sequence of probability distributions

$$D_1, D_2, \ldots, D_{nV}, \qquad (2.1\text{-}4)$$

where D_j is the distribution for the variable x_j contained in $\mathbf{x}$. The definition of these distributions may also be accompanied by the specification of correlations and various restrictions that further define the relations between the x_j. These distributions and other restrictions probabilistically characterize where the appropriate input to use in a performance assessment might fall given that the analysis has been structured so that only one value can be used for each variable.

Once the distributions in Eq. 2.1-4 have been developed, Monte Carlo techniques can be used to determine the uncertainty in $R(\mathbf{x})$ that results from the uncertainty in $\mathbf{x}$. First, a sample

$$\mathbf{x}_k = [x_{k1}, x_{k2}, \ldots, x_{k,nV}], k=1, \ldots, nK, \qquad (2.1\text{-}5)$$

is generated according to the specified distributions and restrictions, where nK is the size of the sample. The performance assessment is then performed for each sample element $\mathbf{x}_k$, which yields a sequence of risk results of the form

$$R(\mathbf{x}_k) = \{[S_i(\mathbf{x}_k), pS_i(\mathbf{x}_k), \mathbf{cS}_i(\mathbf{x}_k)], i=1, \ldots, nS(\mathbf{x}_k)\} \qquad (2.1\text{-}6)$$

for k=1, ..., nK. Each set $R(\mathbf{x}_k)$ is the result of one complete performance assessment performed with a set of inputs (i.e., $\mathbf{x}_k$) that the review process producing the distributions in Eq. 2.1-4 concluded was possible. Further, associated with each risk result $R(\mathbf{x}_k)$ in Eq. 2.1-6 is a probability or weight that can be used in making probabilistic statements about the distribution of $R(\mathbf{x})$. When random or Latin hypercube sampling is used, this weight is the reciprocal of the sample size (i.e., 1/nK).

In most performance assessments, CCDFs are the results of greatest interest. For a particular consequence result, a CCDF will be produced for each set $R(\mathbf{x}_k)$ shown in Eq. 2.1-6. This yields a distribution of CCDFs of the form shown in Figure 2.1-2.

An important distinction exists between the uncertainty that gives rise to a single CCDF in Figure 2.1-2 and the uncertainty that gives rise to the distribution of CCDFs in this figure. A single CCDF arises from the fact that a number of different occurrences have a real possibility of taking place. This type of uncertainty is referred to as stochastic variation or uncertainty in this report. A distribution of CCDFs arises from the fact that fixed, but unknown, quantities are needed in the estimation of a CCDF. The development of distributions that characterize what the values for these fixed quantities might be leads to a distribution of CCDFs. In essence, a performance assessment can be viewed as a very complex function that estimates a CCDF. Since there is uncertainty in the values of some of the variables operated on by this function, there will also be uncertainty in the dependent variable produced by this function, where this dependent variable is a CCDF.

Both Kaplan and Garrick (1981) and a recent report by the International Atomic Energy Agency (IAEA, 1989) distinguish between these two types of uncertainty. Specifically, Kaplan and Garrick distinguish between probabilities derived from frequencies and probabilities that characterize degrees of belief. Probabilities derived from frequencies correspond to the probabilities pS_i in Eq. 2.1-1, while probabilities that characterize degrees of belief (i.e., subjective probabilities) correspond to the distributions indicated in Eq. 2.1-4. The IAEA report distinguished between what it calls Type A uncertainty and Type B uncertainty. The IAEA report defines Type A uncertainty to be stochastic variation; as such, this uncertainty corresponds to the frequency-based probability of Kaplan and Garrick and the pS_i of Eq. 2.1-1. Type B uncertainty is defined to be uncertainty that is due to lack of knowledge about fixed quantities; thus, this uncertainty corresponds to the subjective probability of Kaplan and Garrick and the distributions indicated in Equation 2.1-4. This distinction has also been made by other authors, including Vesely and Rasmusen (1984), Paté-Cornell (1986) and Parry (1988).

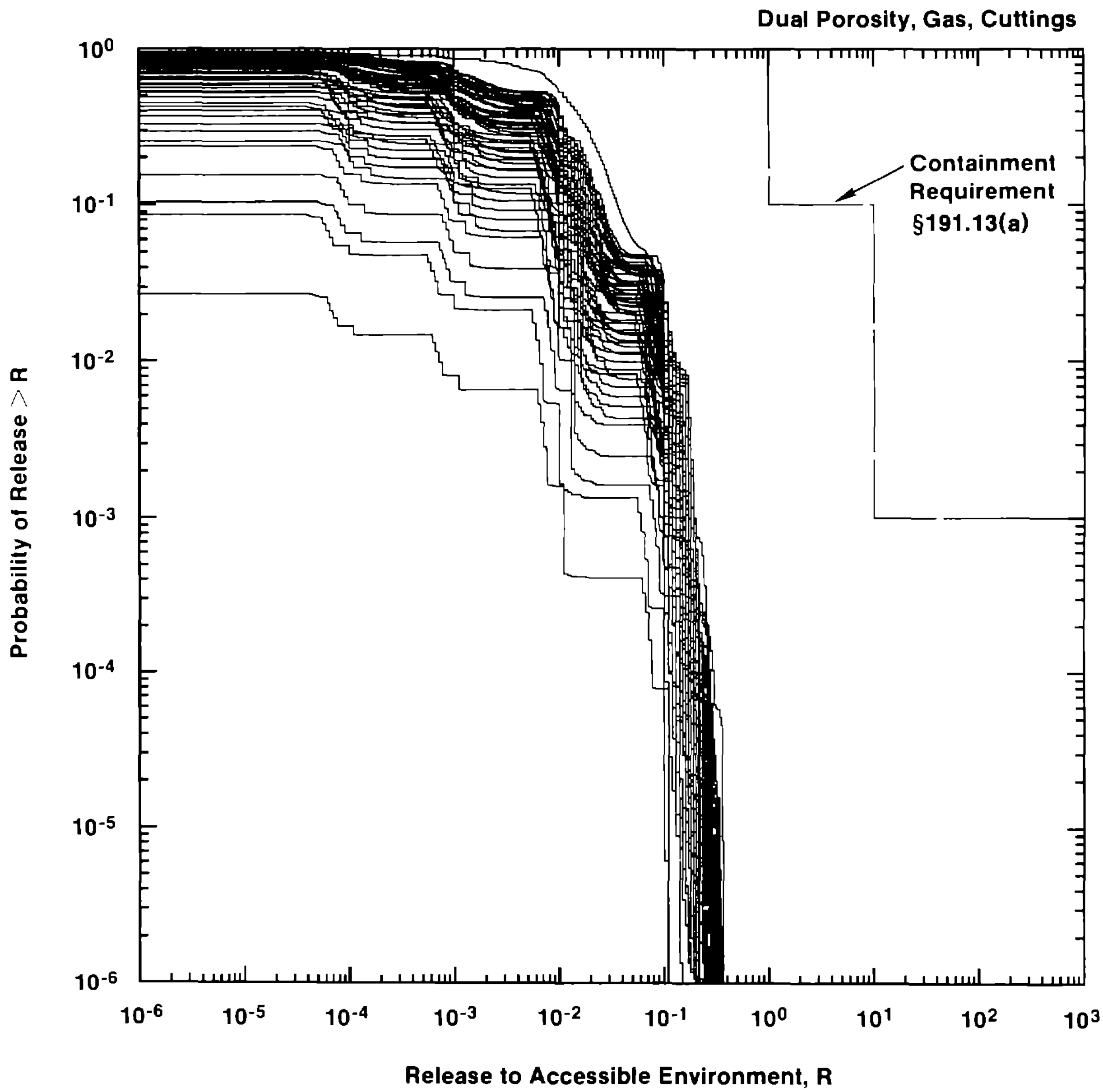

TRI-6342-1293-1

3 Figure 2.1-2. Distribution of Complementary Cumulative Distribution Functions for Normalized Release
4 to the Accessible Environment Including Both Cuttings Removal and Groundwater
5 Transport with Gas Generation in the Repository and a Dual-Porosity Transport Model in
6 the Culebra Dolomite.

As already indicated, the ordered triple representation shown in Eq. 2.1-1 is used as the conceptual model for the WIPP performance assessment. In consistency with this representation, the scenarios S_i, scenario probabilities pS_i and scenario consequences $\mathbf{cS}_i$ used in the 1991 preliminary WIPP performance assessment are discussed in Sections 2.2, 2.3 and 2.4, respectively. Further, the WIPP performance assessment endeavors to maintain a distinction between stochastic uncertainty and subjective uncertainty. The effect of stochastic uncertainty is represented by the probabilities pS_i discussed in Section 2.4. The characterization of the subjective uncertainty in the inputs to the 1991 WIPP performance assessment is discussed in Section 3. The primary focus of this report is the impact of subjective uncertainties on the outcomes of the 1991 WIPP performance assessment. These impacts will be investigated in Chapters 4 and 5.

2.2 Definition of Scenarios

Scenarios constitute the first element S_i of the ordered triples contained in the set R shown in Eq. 2.1-1 and are obtained by subdividing the set

$$S = \{x\text{: x a single 10,000-yr history beginning at decommissioning of the WIPP}\}. \quad (2.2\text{-}1)$$

Each 10,000-yr history is complete in the sense that it includes a full specification, including time of occurrence, for everything of importance to performance assessment that happens in this time period. In the terminology of Cranwell et al. (1990), each history would contain a characterization for a specific sequence of "naturally occurring and/or human-induced conditions that represent realistic future states of the repository, geologic systems, and ground-water flow systems that could affect the release and transport of radionuclides from the repository to humans."

The WIPP performance assessment uses a two stage procedure for scenario development (Vol. 1, Ch. 4). The purpose of the first stage is to develop a comprehensive set of scenarios that includes all occurrences that might reasonably take place at the WIPP. The result of this stage is a set of scenarios, called summary scenarios, that summarize what might happen at the WIPP. These summary scenarios provide a basis for discussing the future behavior of the WIPP and a starting point for the second stage of the procedure, which is the definition of scenarios at a level of detail that is appropriate for use with the computational models employed in the WIPP performance assessment. The scenarios obtained in this second stage of scenario development are referred to as computational scenarios. The development of summary scenarios is directed at understanding what might happen at the WIPP and answering completeness questions. The development of computational scenarios is directed at organizing the actual calculations that must be performed to obtain the consequences $\mathbf{cS}_i$ appearing in Eq. 2.1-1, and as a result, must provide a structure that both permits the $\mathbf{cS}_i$ to be calculated at a reasonable cost and holds the amount of aggregation error that enters the analysis to a reasonable level. Here, aggregation error refers to the inevitable loss of resolution that occurs when an infinite number of occurrences (i.e., the elements of S) must be divided into a finite number of sets for analysis (i.e., the subsets S_i of S). The following discussion describes the computational scenarios used in the 1991 WIPP performance assessment.

The development of summary scenarios for the 1991 WIPP performance assessment led to a set S of the form shown in Eq. 2.2-1 in which all credible disruptions were due to drilling intrusions (Vol. 1, Ch. 4). As a result, computational scenarios were defined to provide a systematic coverage of drilling intrusions. Specifically, computational scenarios were defined on the basis of (1) number of drilling intrusions, (2) time of the drilling intrusions, (3) whether or not a single waste panel is penetrated by two or more boreholes, of which at least one penetrates a pressurized brine pocket and at least one does not, and (4) the activity level of the waste penetrated by the boreholes.

The construction of computational scenarios started with the division of the 10,000-yr time period appearing in the EPA regulations into a sequence

$$[t_{i-1}, t_i],\ i = 1, 2, \ldots, nT, \qquad (2.2\text{-}2)$$

of disjoint time intervals. When the activity levels of the waste are not considered, these time intervals lead to computational scenarios of the form

$$S(\mathbf{n}) = \{x: x \text{ an element of } S \text{ for which exactly } n(i) \text{ intrusions occur in time interval } [t_{i-1}, t_i] \text{ for } i=1, 2, \ldots, nT\} \qquad (2.2\text{-}3)$$

and

$$S^{+-}(t_{i-1},t_i) = \{x: x \text{ an element of } S \text{ for which two or more boreholes penetrate the same waste panel during the time interval } [t_{i-1}, t_i]\text{, with at least one of these boreholes penetrating a pressurized brine pocket and at least one not penetrating a pressurized brine pocket}\}, \qquad (2.2\text{-}4)$$

where

$$\mathbf{n} = [n(1), n(2), \ldots, n(nT)]. \qquad (2.2\text{-}5)$$

For the 1991 WIPP performance assessment, nT = 5, and each time interval $[t_{i-1}, t_i]$ had a length of 2000 yrs.

When the activity levels of the waste are considered, the preceding time intervals lead to computational scenarios of the form

$S(\mathbf{l},\mathbf{n})$ = {x: x an element of $S(\mathbf{n})$ for which the j^{th} borehole encounters waste of activity level $\ell(j)$ for j=1, 2, ..., nBH, where nBH is the total number of boreholes associated with a time history in $S(\mathbf{n})$} (2.2-6)

and

$S^{+-}(\mathbf{l};t_{i-1},t_i)$ = {x: x an element of $S^{+-}(t_{i-1},t_i)$ for which the j^{th} borehole encounters waste of activity level $\ell(j)$ for j=1, 2, ..., nBH, where nBH is the total number of boreholes associated with a time history in $S^{+-}(t_{i-1},t_i)$}, (2.2-7)

where

$$\mathbf{l} = [\ell(1), \ell(2), \ldots, \ell(nBH)] \text{ and } nBH = \sum_{i=1}^{nT} n(i). \qquad (2.2\text{-}8)$$

The computational scenarios $S(\mathbf{l},\mathbf{n})$ and $S^{+-}(\mathbf{l};t_{i-1},t_i)$ were used as the basis for the CCDFs for normalized release to the accessible environment presented in the 1991 WIPP performance assessment (e.g., as shown in Figure 2.1-2).

The definitions of $S^{+-}(t_{i-1},t_i)$ and $S^{+-}(\mathbf{l};t_{i-1},t_i)$ appearing in Eqs. 2.2-4 and 2.2-7 do not use the vector **n** designating the time intervals in which drilling intrusions occur that appears in the definitions of $S(\mathbf{n})$ and $S(\mathbf{l},\mathbf{n})$. However, vectors of this form can be incorporated into the definitions of $S^{+-}(t_{i-1},t_i)$ and $S^{+-}(\mathbf{l};t_{i-1},t_i)$. Specifically, let

$S_i^{+-}(\mathbf{n})$ = {x: x an element of $S(\mathbf{n})$ for which 2 or more boreholes penetrate the same waste panel during the time interval $[t_{i-1},t_i]$ (i.e., $n(i) \geq 2$), with at least one of these boreholes penetrating a pressurized brine pocket and at least one not penetrating a pressurized brine pocket}. (2.2-9)

Then,

$$S^{+-}(t_{i-1},t_i) = \bigcup_{\mathbf{n}\in A(i)} S_i^{+-}(\mathbf{n}), \qquad (2.2\text{-}10)$$

where $\mathbf{n}\in A(i)$ only if $\mathbf{n}$ is a vector of the form defined in Eq. 2.2-5 with $n(i)\geq 2$. The computational scenarios $S_i^{+-}(\mathbf{l},\mathbf{n})$ and $S^{+-}(\mathbf{l};t_{i-1},t_i)$ can be defined analogously for the vector $\mathbf{l}$ indicated in Eq. 2.2-8. In Section 2.3, conservative relations are presented (i.e., Eqs. 2.3-3 and 2.3-4) that bound the probabilities for $S^{+-}(t_{i-1},t_i)$ and $S^{+-}(\mathbf{l};t_{i-1},t_i)$ and are used in the construction of CCDFs of the form appearing in Figure 2.1-2. In Section 2.4, $S^{+-}(t_{i-1},t_i)$ and $S^{+-}(\mathbf{l};t_{i-1},t_i)$, $i = 1, \ldots, nT = 5$, are assigned the groundwater releases (i.e., Eqs. 2.4-13 and 2.4-14) associated with

$$S_1^{+-}(2,0,0,0,0),\ S_2^{+-}(0,2,0,0,0),\ S_3^{+-}(0,0,2,0,0),$$

$$S_4^{+-}(0,0,0,2,0),\ S_5^{+-}(0,0,0,0,2), \qquad (2.2\text{-}11)$$

respectively; these releases are used in the construction of CCDFs of the form appearing in Figure 2.1-2. The subscripts in the preceding notation for $S_1^{+-}(2,0,0,0,0)$ through $S_5^{+-}(0,0,0,0,2)$ are redundant and will be omitted in the remainder of this report.

Additional information on the construction of computational scenarios for the 1991 WIPP performance assessment is available elsewhere (Vol. 2, Ch. 3).

2.3 Determination of Scenario Probabilities

As discussed in Chapters 2 and 3 of Volume 2, probabilities for computational scenarios were determined under the assumption that the occurrence of boreholes through the repository follows a Poisson process with a rate constant λ. The probabilities $pS(\mathbf{n})$ and $pS(\mathbf{l},\mathbf{n})$ for the computational scenarios $S(\mathbf{n})$ and $S(\mathbf{l},\mathbf{n})$ are given by

$$pS(\mathbf{n}) = \left\{\prod_{i=1}^{nT}\left[\frac{\lambda^{n(i)}\left(t_i - t_{i-1}\right)^{n(i)}}{n(i)!}\right]\right\}\exp\left[-\lambda\left(t_{nT} - t_0\right)\right] \qquad (2.3\text{-}1)$$

and

$$pS(\mathbf{l},\mathbf{n}) = \left[\prod_{j=1}^{nBH} pL_{\ell(j)}\right] pS(\mathbf{n}), \qquad (2.3\text{-}2)$$

where **n** and **l** are defined in Eqs. 2.2-5 and 2.2-8, respectively, and pL_ℓ is the probability that a randomly placed borehole through a waste panel will encounter waste of activity level ℓ. Table 2.3-1 provides an example of probabilities $pS(\mathbf{n})$ calculated as shown in Eq. 2.3-1 with $\lambda = 3.28 \times 10^{-4}$ yr^{-1}, which corresponds to the maximum drilling rate suggested for use by the EPA.

The probabilities $pS^{+-}(t_{i-1},t_i)$ and $pS^{+-}(\mathbf{l};t_{i-1},t_i)$ for the computational scenarios $S^{+-}(t_{i-1},t_i)$ and $S^{+-}(\mathbf{l};t_{i-1},t_i)$ are given by

$$pS^{+-}(t_{i-1},t_i) \doteq \sum_{\ell=1}^{nP} \left\{1 - \exp[-\alpha(\ell)(t_i - t_{i-1})]\right\} \left\{1 - \exp[-\beta(\ell)(t_i - t_{i-1})]\right\} \tag{2.3-3}$$

and

$$pS^{+-}(\mathbf{l};t_{i-1},t_i) \doteq \left[\prod_{j=1}^{nBH} pL_{\ell(j)}\right] pS^{+-}(t_{i-1},t_i), \tag{2.3-4}$$

where

$$\alpha(\ell) = [aBP(\ell)]\lambda/aTOT$$

$$\beta(\ell) = [aTOT(\ell) - aBP(\ell)]\lambda/aTOT$$

$aBP(\ell)$ = area (m^2) of pressurized brine pocket under waste panel ℓ,

$aTOT(\ell)$ = total area (m^2) of waste panel ℓ,

$aTOT$ = total area (m^2) of waste panels,

and

nP = number of waste panels.

For the 1991 WIPP performance assessment, $aTOT(\ell)$ and $aBP(\ell)$ were assumed to be the same for all waste panels due to an absence of information on $aBP(\ell)$ for individual panels.

The relations appearing in Eqs. 2.3-1 through 2.3-4 are derived in Volume 2, Chapter 2 of this report under the assumption that drilling intrusions follow a Poisson process (i.e., are random in time and space). The derivations are quite general and include both the stationary (i.e., constant λ) and nonstationary (i.e., time-dependent λ) cases.

TABLE 2.3-1. PROBABILITIES FOR COMPUTATIONAL SCENARIOS INVOLVING MULTIPLE INTRUSIONS OVER 10,000 YRS FOR $\lambda = 3.28 \times 10^{-4}$ YR^{-1}, A 100-YR PERIOD OF ADMINISTRATIVE CONTROL DURING WHICH NO DRILLING INTRUSIONS CAN OCCUR AND 2,000-YR TIME INTERVALS

0 Intrusions
(prob = 3.888E-2)
(cum prob = 3.888E-2)
(# scenarios = 1)

Scenario	Prob
S(0,0,0,0,0)	3.888E-02

1 Intrusion
(prob = 1.263E-1)
(cum prob = 1.651E-1)
(# scenarios = 5)

Scenario	Prob
S(1,0,0,0,0)	2.423E-2
S(0,1,0,0,0)	2.551E-2
S(0,0,1,0,0)	2.551E-2
S(0,0,0,1,0)	2.551E-2
S(0,0,0,0,1)	2.551E-2
	1.263E-1

2 Intrusions
(prob = 2.050E-1)
(cum prob = 3.701E-1)
(# scenarios = 15)

Scenario	Prob
S(2,0,0,0,0)	7.551E-3
S(1,1,0,0,0)	1.590E-2
S(1,0,1,0,0)	1.590E-2
S(1,0,0,1,0)	1.590E-2
S(1,0,0,0,1)	1.590E-2
S(0,2,0,0,0)	8.366E-3
S(0,1,1,0,0)	1.673E-2
S(0,1,0,1,0)	1.673E-2
S(0,1,0,0,1)	1.673E-2
S(0,0,2,0,0)	8.366E-3
S(0,0,1,1,0)	1.673E-2
S(0,0,1,0,1)	1.673E-2
S(0,0,0,2,0)	8.366E-3
S(0,0,0,1,1)	1.673E-2
S(0,0,0,0,2)	8.366E-3
	2.050E-1

3 Intrusions
(prob = 2.219E-1)
(cum prob = 5.920E-1)
(# scenarios = 35)

Scenario	Prob
S(3,0,0,0,0)	1.569E-3
S(2,1,0,0,0)	4.953E-3
S(2,0,1,0,0)	4.953E-3
S(2,0,0,1,0)	4.953E-3
S(2,0,0,0,1)	4.953E-3
S(1,2,0,0,0)	5.214E-3
S(1,1,1,0,0)	1.043E-2
S(1,1,0,1,0)	1.043E-2
S(1,1,0,0,1)	1.043E-2
S(1,0,2,0,0)	5.214E-3
S(1,0,1,1,0)	1.043E-2
S(1,0,1,0,1)	1.043E-2
S(1,0,0,2,0)	5.214E-3
S(1,0,0,1,1)	1.043E-2
S(1,0,0,0,2)	5.214E-3
S(0,3,0,0,0)	1.829E-3
S(0,2,1,0,0)	5.488E-3
S(0,2,0,1,0)	5.488E-3
S(0,2,0,0,1)	5.488E-3
S(0,1,2,0,0)	5.488E-3
S(0,1,1,1,0)	1.098E-2
S(0,1,1,0,1)	1.098E-2
S(0,1,0,2,0)	5.488E-3
S(0,1,0,1,1)	1.098E-2
S(0,1,0,0,2)	5.488E-3
S(0,0,3,0,0)	1.829E-3
S(0,0,2,1,0)	5.488E-3
S(0,0,2,0,1)	5.488E-3
S(0,0,1,2,0)	5.488E-3
S(0,0,1,1,1)	1.098E-2
S(0,0,1,0,2)	5.488E-3
S(0,0,0,3,0)	1.829E-3
S(0,0,0,2,1)	5.488E-3
S(0,0,0,1,2)	5.488E-3
S(0,0,0,0,3)	1.829E-3
	2.219E-1

4 Intrusions
(prob = 1.801E-1)
(cum prob = 7.722E-1)
(# scenarios = 70)

Scenario	Prob
S(4,0,0,0,0)	2.444E-4
S(3,1,0,0,0)	1.029E-3
.	.
.	.
.	.
S(1,1,1,1,0)	6.841E-3
.	.
.	.
.	.
S(0,0,0,1,3)	1.200E-3
S(0,0,0,0,4)	3.000E-4
	1.801E-1

5 Intrusions
(prob = 1.170E-1)
(cum prob = 8.891E-1)
(# scenarios = 126)

6 Intrusions
(prob = 6.331E-2)
(cum prob = 9.525E-1)
(# scenarios = 210)

7 Intrusions
(prob = 2.937E-2)
(cum prob = 9.818E-1)
(# scenarios = 330)

TABLE 2.3-1. PROBABILITIES FOR COMPUTATIONAL SCENARIOS INVOLVING MULTIPLE INTRUSIONS OVER 10,000 YRS FOR λ = 3.28 x 10^{-4} YR^{-1}, A 100-YR PERIOD OF ADMINISTRATIVE CONTROL DURING WHICH NO DRILLING INTRUSIONS CAN OCCUR AND 2,000-YR TIME INTERVALS (concluded)

8 Intrusions (prob = 1.192E-2) (cum prob = 9.937E-1) (# scenarios = 495)	11 Intrusions (prob = 4.123E-4) (cum prob = 9.999E-1) (# scenarios = 1365)	14 Intrusions (prob = 6.464E-6) (cum prob = 1.000E+0) (# scenarios = 3060)
9 Intrusions (prob = 4.301E-3) (cum prob = 9.980E-1) (# scenarios = 715)	12 Intrusions (prob = 1.116E-4) (cum prob = 1.000E+0) (# scenarios = 1820)	15 Intrusions (prob = 1.399E-6) (cum prob = 1.000E+0) (# scenarios = 3876)
10 Intrusions (prob = 1.397E-3) (cum prob = 9.994E-1) (# scenarios = 1001)	13 Intrusions (prob = 2.787E-5) (cum prob = 1.000E+0) (# scenarios = 2380)	

2.4 Calculation of Scenario Consequences

As indicated in Figure 2.4-1, the following five computer models were used to estimate scenario consequences in the 1991 WIPP performance assessment: CUTTINGS, BRAGFLO, PANEL, SECO2D and STAFF2D. Brief descriptions of these models are given in Table 2.4-1. Further, more detailed descriptions of these models and their use in the 1991 WIPP performance assessment are given in Vol. 2 of this report.

As can be seen from Table 2.3-1, there are too many computational scenarios (e.g., $S(\mathbf{n})$ and $S(\mathbf{l},\mathbf{n})$) to perform a detailed calculation for each scenario with the models discussed in Table 2.4-1. For example, 3003 senarios of the form $S(\mathbf{n})$ (i.e., all scenarios involving less than or equal to 10 intrusions) are required to reach a cumulative probability of 0.9994. Construction of a CCDF for comparison against the EPA release limits requires the estimation of cumulative probability through at least the 0.999 level. Thus, depending on the value for the rate constant λ in the Poisson model for drilling intrusions, this may require the inclusion of computational scenarios involving as many as 10 to 12 drilling intrusions, which results in a total of several thousand computational scenarios. Further, this number does not include the effects of different activity levels in the waste. To obtain results for such a large number of computational scenarios, it is necessary

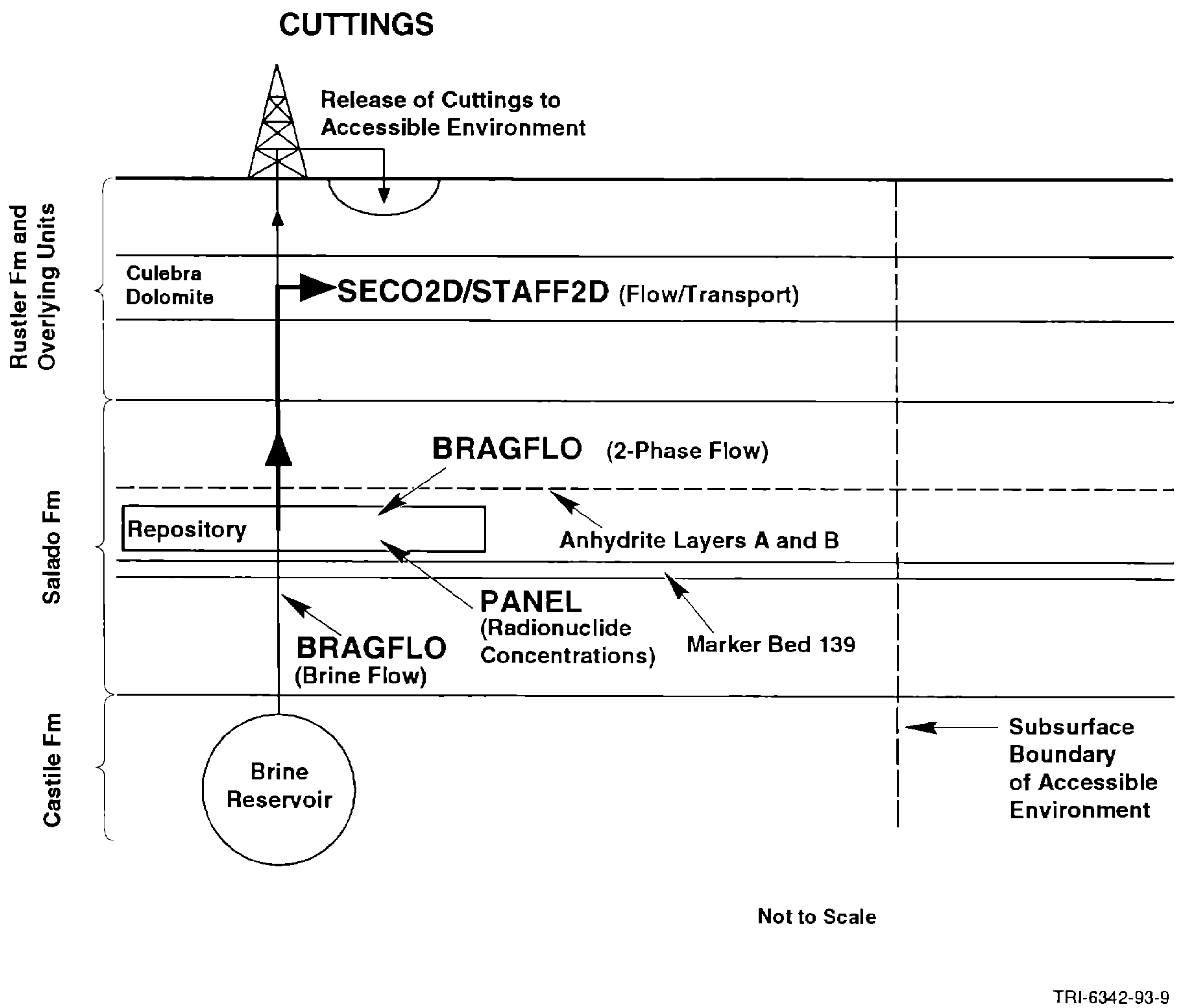

3 Figure 2.4-1. Models Used in 1991 WIPP Performance Assessment. The names for computer models
4 (i.e., computer codes) are shown in capital letters.

TABLE 2.4-1. SUMMARY OF COMPUTER MODELS USED IN THE 1991 WIPP PERFORMANCE ASSESSMENT

Model	Description
BRAGFLO	Describes the multiphase flow of gas and brine through a porous, heterogenous reservoir. BRAGFLO solves simultaneously the coupled partial differential equations that describe the mass conservation of gas and brine along with appropriate constraint equations, initial conditions, and boundary conditions (Volume 2, Chapter 5 of this report).
CUTTINGS	Calculates the quantity of radioactive material brought to the surface as cuttings and cavings generated by an exploratory drilling operation that penetrates a waste panel (Volume 2, Chapter 7 of this report).
PANEL	Calculates rate of discharge and cumulative discharge of radionuclides from a repository panel through an intrusion borehole. Discharge is a function of fluid flow rate, elemental solubility, and remaining inventory (Volume 2, Chapter 5 of this report).
SECO2D	Calculates single-phase Darcy flow for groundwater-flow problems in two dimensions. The formulation is based on a single partial differential equation for hydraulic head using fully implicit time differencing (Volume 2, Chapter 6 of this report).
STAFF2D	Simulates fluid flow and transport of radionuclides in fractured porous media. STAFF2D is a two-dimensional finite element code (Huyakorn et al., 1989; Volume 2, Chapter 6 of this report).

to plan and implement the overall calculations very carefully. The manner in which this can be done is not unique. The following describes the approach used in the 1991 WIPP performance assessment.

As indicated in Eq. 2.2-2, the 10,000-yr time interval that must be considered in the construction of CCDFs for comparison with the EPA release limits is divided into disjoint subintervals $[t_{i-1}, t_i]$, i = 1, 2, ..., nT, in the definition of computational scenarios. The following results can be calculated for each time interval:

rC_i = EPA normalized release to the surface environment for cuttings removal due to a single borehole in time interval i with the assumption that the waste is homogeneous (i.e., waste of different activity levels is not present), (2.4-1)

rC_{ij} = EPA normalized release to the surface environment for cuttings removal due to a single borehole in time interval i that penetrates waste of activity level j, (2.4-2)

$rGW1_i$ = EPA normalized release to the accessible environment due to groundwater transport initiated by a single borehole in time interval i (i.e., an E2-type scenario), (2.4-3) and

$rGW2_i$ = EPA normalized release to the accessible environment due to groundwater transport initiated by two boreholes in the same waste panel in time interval i, of which one penetrates a pressurized brine pocket and one does not (i.e., an E1E2-type scenario), (2.4-4)

with the assumption that the intrusions occur at the midpoints of the time intervals (i.e., at 1000, 3000, 5000, 7000 and 9000 yrs). For the calculation of $rGW1_i$ and $rGW2_i$ in the 1991 WIPP performance assessment, the accessible environment is assumed to begin 5 km from the waste panels (e.g., see Figures 1.5-4, 2.1-1 and 2.1-2 in Vol. 3).

In general, rC_i, rC_{ij} $rGW1_i$ and $rGW2_i$ will be vectors containing a large variety of information; however, for notational simplicity, a vector representation will not be used. For the 1991 WIPP performance assessment, the cuttings release to the accessible environment (i.e., rC_i and rC_{ij}) is determined by the CUTTINGS program, and the groundwater release to the accessible environment (i.e., $rGW1_i$ and $rGW2_i$) is determined through a sequence of linked calculations involving the BRAGFLO, PANEL, SECO2D and STAFF2D programs.

The cuttings releases

$$rC_1,\ rC_2,\ rC_3,\ rC_4,\ rC_5 \tag{2.4-5}$$

correspond to the cuttings releases associated with the computational scenarios

$$S(1,0,0,0,0),\ S(0,1,0,0,0),\ S(0,0,1,0,0),\ S(0,0,0,1,0),\ S(0,0,0,0,1) \tag{2.4-6}$$

under the assumption that all waste is of the same average activity level. Similarly, the groundwater releases

$$rGW1_1,\ rGW1_2,\ rGW1_3,\ rGW1_4,\ rGW1_5 \tag{2.4-7}$$

correspond to the groundwater releases associated with the preceding five scenarios, while

$$rGW2_1,\ rGW2_2,\ rGW2_3,\ rGW2_4,\ rGW2_5 \tag{2.4-8}$$

correspond to the groundwater releases associated with the computational scenarios

$$S^{+-}(2,0,0,0,0),\ S^{+-}(0,2,0,0,0),\ S^{+-}(0,0,2,0,0),\ S^{+-}(0,0,0,2,0),\ S^{+-}(0,0,0,0,2). \qquad (2.4\text{-}9)$$

In like manner, rC_{1j} corresponds to the cuttings release associated with the computational scenario $S(j;\ 1,0,0,0,0)$; rC_{2j} corresponds to the cuttings release associated with $S(j;\ 0,1,0,0,0)$, and so on.

The releases rC_i, rC_{ij}, $rGW1_i$ and $rGW2_i$ are used to construct the releases associated with the many individual computational scenarios that are used in the construction of a CCDF for comparison with the EPA release limits. The following assumptions are made:

(1) With the exception of E1E2-type scenarios, no synergistic effects result from multiple boreholes, and thus, the total release for a scenario involving multiple intrusions can be obtained by adding the releases associated with the individual intrusions.

(2) An E1E2-type scenario can only take place when the necessary boreholes occur within the same time interval $[t_{i-1}, t_i]$.

(3) An E1E2-type scenario involving more than two boreholes will have the same release as an E1E2-type scenario involving exactly two boreholes.

The preceding assumptions are used to construct the releases for individual computational scenarios.

The normalized releases rC_i, rC_{ij} and $rGW1_i$ can be used to construct the EPA normalized releases for the scenarios $S(\mathbf{n})$ and $S(\mathbf{l},\mathbf{n})$. For $S(\mathbf{n})$, the normalized release to the accessible environment, $cS(\mathbf{n})$, can be approximated by

$$cS(\mathbf{n}) = \sum_{j=1}^{nBH} (rC_{m(j)} + rGW1_{m(j)}), \qquad (2.4\text{-}10)$$

where m(j) designates the time interval in which the j^{th} borehole occurs. The vector

$$\mathbf{m} = [m(1),\ m(2),\ \ldots,\ m(nBH)] \qquad (2.4\text{-}11)$$

is uniquely determined once the vector $\mathbf{n}$ appearing in the definition of $S(\mathbf{n})$ is specified. The definition of $S(\mathbf{n})$ in Eq. 2.2-3 contains no information on the activity levels encountered by the individual boreholes, and so $cS(\mathbf{n})$ was constructed with the assumption that all waste is of the same average activity. However, the definition of $S(\mathbf{l},\mathbf{n})$ in Eq. 2.2-6 does contain information on activity levels, and the associated normalized release to the accessible environment, $cS(\mathbf{l},\mathbf{n})$, can be approximated by

$$cS(\mathbf{l},\mathbf{n}) = \sum_{j=1}^{nBH} \left[rC_{m(j),\ell(j)} + rGW1_{m(j)} \right], \qquad (2.4\text{-}12)$$

which does incorporate the activity levels encountered by the individual boreholes.

For $S^{+-}(t_{i-1},t_i)$, the normalized release to the accessible environment, $cS^{+-}(t_{i-1},t_i)$, can be approximated by

$$cS^{+-}(t_{i-1},t_i) = 2\ rC_i + rGW2_i, \qquad (2.4\text{-}13)$$

where it is assumed that all waste is of the same average activity for cuttings removal. Similarly, the normalized release $cS^{+-}(\mathbf{l};t_{i-1},t_i)$ for $S^{+-}(\mathbf{l};t_{i-1},t_i)$ can be approximated by

$$cS^{+-}(\mathbf{l};t_{i-1},t_i) = \sum_{j=1}^{2} rC_{i,\ell(j)} + rGW2_i, \qquad (2.4\text{-}14)$$

which incorporates the activity level of the waste. The approximations for $cS^{+-}(t_{i-1},t_i)$ and $cS^{+-}(\mathbf{l};t_{i-1},t_i)$ in Eqs. 2.4-13 and 2.4-14 are based on exactly two intrusions in the time interval $[t_{i-1},t_i]$. More complicated expressions could be developed to define releases for multiple E1E2-type intrusions. However, due to the low probability of such patterns of intrusion (e.g., compare the probabilities for 2 and ≥2 boreholes in Tables 2-4 and 2-6 of Vol. 2), the use of such expressions would have little impact on the CCDFs used for comparison with the EPA release limits.

The construction process shown in Eqs. 2.4-10 and 2.4-13 to obtain the normalized releases $cS(\mathbf{n})$ and $cS^{+-}(t_{i-1},t_i)$ for scenarios $S(\mathbf{n})$ and $S^{+-}(t_{i-1},t_i)$ is illustrated in Table 3-4 of Vol. 3. Further, the construction process shown in Eqs. 2.4-12 and 2.4-14 to obtain normalized releases $cS(\mathbf{l},\mathbf{n})$ and $cS^{+-}(\mathbf{l};t_{i-1},t_i)$ for scenarios $S(\mathbf{l},\mathbf{n})$ and $S^{+-}(\mathbf{l};t_{i-1},t_i)$ is illustrated in Table 3-5 of Vol. 3.

Before continuing, this is a natural place to introduce some additional information on the consequence calculations. Specifically, Table 2.4-2 lists the initial inventory of waste used in the 1991 calculations, Table 2.4-3 lists the decay chains used for transport calculations in the Culebra Dolomite, and Table 2.4-4 lists the activity levels considered in the estimation of cuttings releases. Further, Figure 2.4-2 presents time-dependent inventories expressed in EPA units (i.e., the normalizations used in comparisons with the EPA release limits) used for a single waste panel in the 1991 WIPP performance assessment; the total WIPP inventory is ten times the quantities indicated in this figure. This information will facilitate the interpretation of later uncertainty and sensitivity analysis results.

The cuttings releases used in the 1991 WIPP performance assessment were calculated with the program CUTTINGS for waste of average activity level. Then, the releases for activity levels 1 through 5 shown in Table 2.4-4 were obtained by multiplying the average activity level releases by scale factors of the form

$$SF_{i\ell} = AL_{i\ell}/AL_i, \qquad (2.4\text{-}15)$$

where

$AL_{i\ell}$ = projected radioactivity (Ci/m^2) contained in waste of activity level ℓ at time i, where 1 ~ 1000 yrs, 2 ~ 3000 yrs, 3 ~ 5000 yrs, 4 ~ 7000 yrs and 5 ~ 9000 yrs,

and

AL_i = projected radioactivity (Ci/m^2) contained in waste of average activity at time i.

For example, the scale factor

$$SF_{24} = 184.01/7.9658 = 23.100 \qquad (2.4\text{-}16)$$

is used to convert from a release of average activity at 3000 yrs to a release of activity level 4 at 3000 yrs.

TABLE 2.4-2. POTENTIALLY IMPORTANT RADIONUCLIDES ASSOCIATED WITH INITIAL CONTACT-HANDLED WASTE INVENTORY USED IN CALCULATIONS FOR CUTTINGS REMOVAL AND RELEASE TO CULEBRA DOLOMITE (adapted from Table 3.3-5 of Vol. 3)

Radionuclide	$t_{1/2}$(yr)	Curies	Grams
Pu-238	8.77×10^1	9.26×10^6	5.41×10^5
Pu-239	2.41×10^4	8.45×10^5	1.36×10^7
Pu-240	6.53×10^3	1.07×10^5	4.69×10^5
Pu-242	3.76×10^5	2.16×10^0	5.50×10^2
U-233	1.59×10^5	1.037×10^2	1.07×10^4
U-234	2.44×10^5	0	0
U-236	2.34×10^7	0	0
Am-241	4.32×10^2	1.64×10^6	4.79×10^5
Np-237	2.14×10^6	2.14	3.04×10^3
Th-229	7.43×10^3	0	0
Th-230	7.70×10^4	0	0
Ra-226	1.60×10^3	0	0

TABLE 2.4-3. SIMPLIFIED RADIONUCLIDE DECAY CHAINS USED FOR TRANSPORT CALCULATIONS IN THE CULEBRA DOLOMITE (from Ch. 6 of Vol. 2)

(1) Pu-240

(2) Am-241 → Np-237 → U-233

(3) U-234 → Th-230

(4) Pu-239

TABLE 2.4-4. PROJECTED ACTIVITY LEVELS (Ci/m²) IN THE WIPP DUE TO WASTE THAT IS CURRENTLY STORED AND MAY BE SHIPPED TO THE WIPP (based on Table 3.4-11 of Vol. 3)

Activity Level	Type[a]	Probability[b]	Time (years) 0	1000	3000	5000	7000	9000
1	CH	0.40023	3.4833	0.2718	0.1840	0.1688	0.1575	0.1473
2	CH	0.2998	34.8326	2.7177	1.8401	1.6875	1.5748	1.4729
3	CH	0.2242	348.326	27.117	18.401	16.875	15.748	14.729
4	CH	0.0149	3483.26	271.77	184.01	168.75	157.48	147.29
5	RH	0.0588	117.6717	0.1546	0.1212	0.1139	0.1082	0.1030
	Average for CH Waste:		150.7905	11.7648	7.9658	7.3053	6.8174	6.3764

[a] CH designates contact-handled waste; RH designates remote-handled waste

[b] Probability that a randomly placed borehole through the waste panels will intersect waste of activity level ℓ, $\ell = 1,2,3,4,5$.

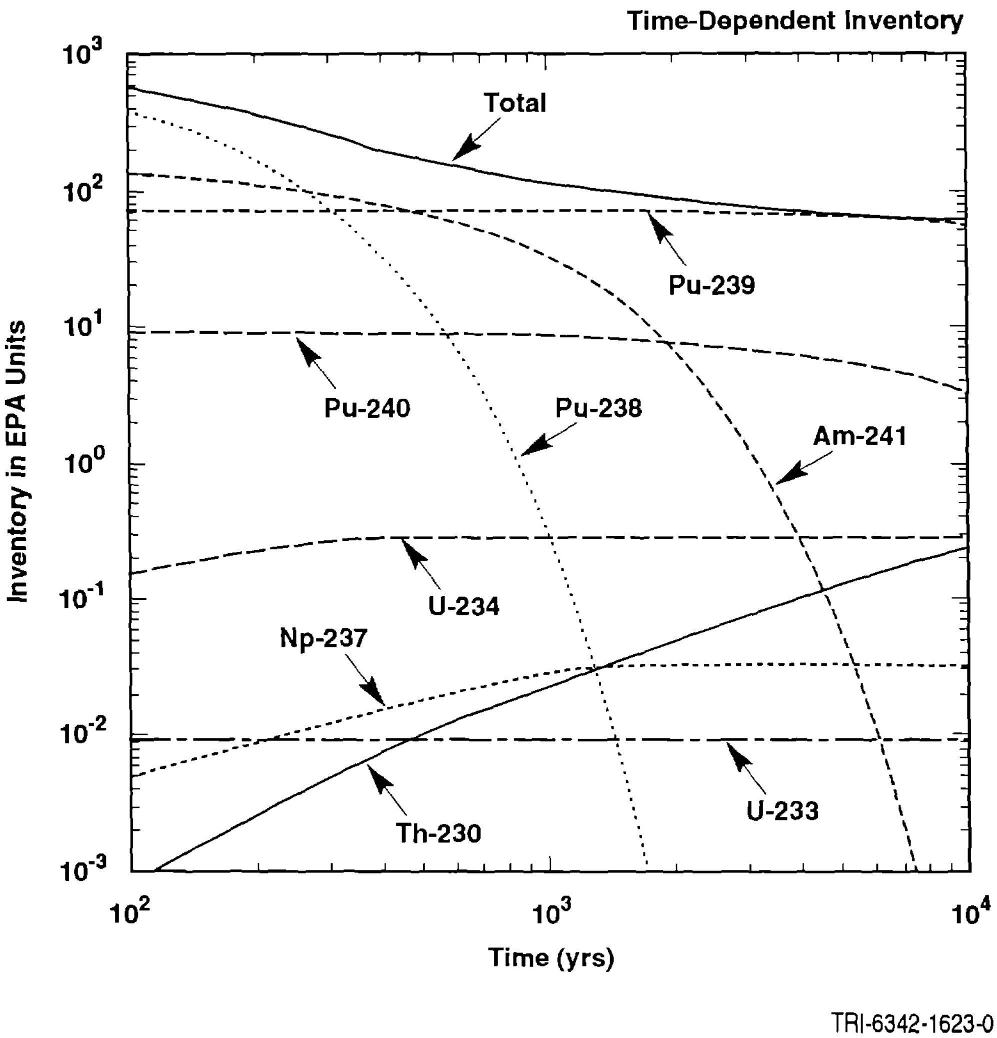

3 Figure 2.4-2. Time-Dependent Inventory Expressed in EPA Units (i.e., the normalized units used in showing compliance with 40 CFR 191) for a Single Waste Panel. The total WIPP inventory used in the 1991 performance assessment is 10 times the values shown in this figure.

3. UNCERTAIN VARIABLES

The 1991 WIPP performance assessment selected 45 imprecisely known variables for consideration. These variables are listed in Table 3-1 and correspond to the elements x_j, j=1, 2, ..., nV = 45, of the vector **x** shown in Eq. 2.1-2. The distributions indicated in Table 3-1 correspond to the distributions appearing in Eq. 2.1-4 and characterize subjective, or type B, uncertainty.

TABLE 3-1. VARIABLES SAMPLED IN 1991 WIPP PERFORMANCE ASSESSMENT (adapted from Tables 6.0-1, 6.0-2 and 6.0-3 of Vol. 3 of this report)

Variable	Definition
BHPERM	Borehole permeability (k) (m^2). Used in BRAGFLO. Range: 1×10^{-14} to 1×10^{-11}. Median: 3.16×10^{-12}. Distribution: Lognormal. Additional information: Freeze and Cherry, 1979, Table 2-2 (clean sand); Section 4.2.1, Vol. 3. Variable 16 in Latin hypercube sample (LHS).
BPPRES	Initial pressure (p) of pressurized brine pocket in Castile Formation (Pa). Used in BRAGFLO. Range: 1.1×10^7 to 2.1×10^7. Median: 1.26×10^7. Distribution: Piecewise linear. Additional information: Popielak et al., 1983, p. H-52; Lappin et al., 1989, Table 3-19; Section 4.3.1, Vol. 3. Variable 14 in LHS.
BPSTOR	Bulk storativity (S_b) of pressurized brine pocket in Castile Formation (m^3). Used in BRAGFLO. Range: 2×10^{-2} to 2. Median: 2×10^{-1}. Distribution: Lognormal. Additional information: Section 4.3.1, Vol. 3. Variable 15 in LHS.
BPAREAFR	Fraction of waste panel area underlain by a pressurized brine pocket (dimensionless). Used in CCDFPERM in calculation of probability of E1E2-type scenarios. Range: 2.5×10^{-1} to 5.52×10^{-1}. Median: 4×10^{-1}. Distribution: Approximately uniform. Additional information: Section 5.1, Vol. 3. Variable 44 in LHS.
BRSAT	Initial fluid (brine) saturation of waste (dimensionless). Used in BRAGFLO. Range: 0 to 2.76×10^{-1}. Median: 1.38×10^{-1}. Distribution: Uniform. Additional information: Section 3.4.9, Vol. 3. Variable 1 in LHS is uniformly distributed on interval [0,1] and used to select value for BRSAT by preprocessor to BRAGFLO.

TABLE 3-1. VARIABLES SAMPLED IN 1991 WIPP PERFORMANCE ASSESSMENT (adapted from Tables 6.0-1, 6.0-2 and 6.0-3 of Vol. 3 of this report) (continued)

Variable	Definition
CULCLIM	Recharge amplitude factor (A_m) for Culebra (dimensionless). Used in SECO2D. Range: 1 to 1.16. Median: 1.08. Distribution: Uniform. Used in definition of time-dependent heads in Culebra, with the maximum head increasing from the estimated present-day head in the Culebra (i.e., 880 m) for CULCLIM = 1 to a head corresponding to land-surface level (i.e., 1030 m) for CULCLIM = 1.16. Additional information: Section 4.4.3, Vol. 3. Variable 28 in LHS is uniformly distributed on [0,1] and used to select value for CULCLIM by preprocessor to SECO2D. Note: Range of 0 to 0.16 for CULCLIM stated in Section 4.4.3 and Table 6.0-3 of Vol. 3 is incorrect.
CULDISP	Longitudinal dispersivity (α_L) in Culebra (m). Used in STAFF2D. Range : 5×10^1 to 3×10^2. Median: 1×10^2. Distribution: Piecewise uniform. Additional information: Table E-6, Lappin et al., 1989; Section 2.6.2, Vol. 3. Variable 29 in LHS.
CULFRPOR	Fracture porosity (θ_f) in Culebra (dimensionless). Used in STAFF2D and SECO2D. Range: 1×10^{-4} to 1×10^{-2}. Median: 1×10^{-3}. Distribution: Lognormal. Additional information: Tables 1-2 and E-6, Lappin et al. 1989; Section 2.6.4, Vol. 3. Variable 9 in LHS.
CULFRSP	Fracture spacing (2B) in Culebra (m). Used in STAFF2D. Range: 6×10^{-2} to 8. Median: 4×10^{-1} Distribution: Piecewise uniform. Additional information: Memo from Beauheim et al., June 10, 1991, contained in Appendix A, Vol. 3; Section 2.6.4, Vol. 3. Variable 36 in LHS.
CULPOR	Matrix porosity (θ_m) in Culebra (dimensionless). Used in STAFF2D. Range: 9.6×10^{-2} to 2.08×10^{-1}. Median: 1.39×10^{-1}. Distribution: Piecewise uniform. Additional information: Table 4.4, Kelley and Saulnier, 1990; Table E-8, Lappin et al., 1989; Section 2.6.4, Vol. 3. Variable 37 in LHS.
CULTRFLD	Transmissivity field for Culebra. Sixty transmissivity fields consistent with available field data were constructed and ranked with respect to travel time to the accessible environment. CULTRFLD in a pointer variable used to select from these 60 fields, with travel time increasing monotonically with CULTRFLD. Used in STAFF2D and SECO2D. Range: 0 to 1. Distribution: Uniform. Additional information: Sections 6.1 to 6.3, Vol. 2; Section 2.6.9, Vol. 3. Variable 27 in LHS.
DBDIAM	Drill bit diameter (m). Used in CUTTINGS. Range = 2.67×10^{-1} to 4.44×10^{-1}. Median: 3.55×10^{-1}. Distribution: Uniform. Additional information: Section 4.2.2, Vol. 3. Variable 17 in LHS.

TABLE 3-1. VARIABLES SAMPLED IN 1991 WIPP PERFORMANCE ASSESSMENT (adapted from Tables 6.0-1, 6.0-2 and 6.0-3 of Vol. 3 of this report) (continued)

Variable	Definition
EHPH	Index variable used to select the relative areas of the stability regimes for different oxidation states of Np, Pu and U. Used in PANEL in the determination of solubilities. Range: 0 to 1. Median: 0.5. Distribution: Uniform. Additional information: Section 3.3.6, Vol. 3. Variable 18 in LHS.
FKDAM	Fracture distribution coefficient (k_d) for Am in Culebra (m^3/ kg). Used in STAFF2D. Range: 0 to 1×10^3. Median: 9.26×10^1. Distribution: Piecewise uniform. Additional information: Section 2.6.10, Vol. 3. Variable 15 in LHS.
FKDNP	Fracture distribution coefficient (k_d) for Np in Culebra (m^3/kg). Used in STAFF2D. Range: 0 to 1×10^3. Median: 1. Distribution: Piecewise uniform. Additional information: Section 2.6.10, Vol. 3. Variable 16 in LHS.
FKDPU	Fracture distribution coefficient (k_d) for Pu in Culebra (m^3/kg). Used in STAFF2D. Range: 0 to 1×10^3. Median: 2.02×10^2. Distribution: Piecewise uniform. Additional information: Section 2.6.10, Vol. 3. Variable 17 in LHS.
FKDTH	Fracture distribution coefficient (k_d) for Th in Culebra (m^3/kg). Used in STAFF2D. Range: 0 to 1×10^1. Median: 1×10^{-1}. Distribution: Piecewise uniform. Additional information: Section 2.6.10, Vol. 3. Variable 18 in LHS.
FKDU	Fracture distribution coefficient (k_d) for U in Culebra (m^3/kg). Used in STAFF2D. Range: 0 to 1. Median: 7.5×10^{-3}. Distribution: Piecewise uniform. Additional information: Section 2.6.10, Vol. 3. Variable 19 in LHS.
GRCORH	Gas generation rate for corrosion of steel under humid conditions (mol/m^2 surface area steel•s). Used in BRAGFLO. Range: 0 to 5×10^{-1}. Median: 1×10^{-1}. Distribution: Piecewise uniform. Additional information: Memo from Brush, July 8, 1991, contained in Appendix A, Vol.3; Section 3.3.8, Vol. 3. Variable 3 in LHS.
GRCORI	Gas generation rate for corrosion of steel under inundated conditions (mol/m^2 surface area steel•s). Used in BRAGFLO. Range: 0 to 1.3×10^{-8}. Median: 6.3×10^{-9}. Distribution: Piecewise uniform. Additional information: Same as GRCORH. Variable 4 in LHS.
GRMICH	Gas generation rate due to microbial degradation of cellulosics under humid conditions (mol/kg cellulosics•s). Used in BRAGFLO. Range: 0 to 2×10^{-1}. Median: 1×10^{-1}. Distribution: Piecewise uniform. Aditional information: Same as GRCORH. Variable 5 in LHS.

TABLE 3-1. VARIABLES SAMPLED IN 1991 WIPP PERFORMANCE ASSESSMENT (adapted from Tables 6.0-1, 6.0-2 and 6.0-3 of Vol. 3 of this report) (continued)

Variable	Definition
GRMICI	Gas generation rate due to microbial degradation of cellulosics under inundated conditions (mol/kg cellulosics•s). Used in BRAGFLO. Range: 0 to 1.6×10^{-8}. Median: 3.2×10^{-9}. Distribution: Piecewise uniform. Additional information: Same as GRCORH. Variable 6 in LHS.
LAMBDA	Rate constant (λ) in Poisson model for drilling intrusions (s^{-1}). Used in CCDFPERM. Range: 0 to 1.04×10^{-11}. Median: 5.2×10^{-12}. Maximum value corresponds to 30 boreholes per km^2 per 10,000 yr as suggested in 40 CFR 191. Distribution: Uniform. Additional information: Chapters 2 and 3, Vol. 2; Section 5.2, Vol. 3. Variable 43 in LHS.
MBPERM	Permeability (k) in Marker Bed 139 under undisturbed conditions (m^2). Used in BRAGFLO. Range: 6.8×10^{-20} to 9.5×10^{-19}. Median: 7.8×10^{-20}. Distribution: Piecewise uniform with a 0.8 rank correlation with SALPERM. Additional information: Memo from Beauheim, June 14, 1991, contained in Appendix A, Vol. 3; Section 2.4.5, Vol. 3. Variable 12 in LHS.
MBPOR	Porosity (ϕ) in Marker Bed 139 under undisturbed conditions (dimensionless). Used in BRAGFLO. Range: 1×10^{-3} to 3×10^{-2}. Median: 1×10^{-2}. Distribution: Piecewise uniform. Additional information: Section 2.4.7, Vol. 3. Variable 13 in LHS.
MBTHPRES	Threshold displacement pressure (p_t) in Marker Bed 139 (Pa). Used in BRAGFLO. Range: 3×10^3 to 3×10^7. Median: 3×10^5. Distribution: Lognormal. Additional information: Davies, 1991; memo from Davies, June 2, 1991, contained in Appendix A, Vol. 3; Section 2.4.1, Vol. 3. Variable 45 in LHS.
MKDAM	Matrix distribution coefficient (k_d) for AM in Culebra (m^3/kg). Used in STAFF2D. Range: 0 to 1×10^2. Median: 1.86×10^{-1}. Distribution: Piecewise uniform. Additional information: Section 2.6.10, Vol. 3. Variable 38 in LHS.
MKDNP	Matrix distribution coefficient (k_d) for Np in Culebra (m^3/kg). Used in STAFF2D. Range: 0 to 1×10^2. Median: 4.8×10^{-2}. Distribution: Piecewise uniform. Additional information: Section 2.6.10, Vol. 3. Variable 39 in LHS.
MKDPU	Matrix distribution coefficient (k_d) for Pu in Culebra (m^3/kg). Used in STAFF2D. Range: 0 to 1×10^2. Median: 2.61×10^{-1}. Distribution: Piecewise uniform. Additional information: Section 2.6.10, Vol. 3. Variable 40 in LHS.
MKDTH	Matrix distribution coefficient (k_d) for Th in Culebra (m^3/kg). Used in STAFF2D. Range: 0 to 1. Median: 1×10^{-2}. Distribution: Piecewise uniform. Additional information: Section 2.6.10, Vol. 3. Variable 41 in LHS.

TABLE 3-1. VARIABLES SAMPLED IN 1991 WIPP PERFORMANCE ASSESSMENT (adapted from Tables 6.0-1, 6.0-2 and 6.0-3 of Vol. 3 of this report) (continued)

Variable	Definition
MKDU	Matrix distribution coefficient (k_d) for U in Culebra (m^3/kg). Used in STAFF2D. Range: 0 to 1. Median: 2.58×10^{-2}. Distribution: Piecewise uniform. Additional information: Section 2.6.10, Vol. 3. Variable 42 in LHS.
SALPERM	Permeability (k) in Salado (m^2). Used in BRAGFLO. Range: 8.6×10^{-22} to 5.4×10^{-20}. Median: 5.7×10^{-21}. Distribution: Piecewise uniform. Additional information: Memo from Beauheim, June 14, 1991, contained In Appendix A, Vol. 3; Section 2.3.5, Vol. 3. Variable 10 in LHS.
SALPRES	Pressure (p) in Salado (halite and anhydrite components) under undisturbed conditions (Pa). Used in BRAGFLO. Range: 9.3×10^6 to 1.39×10^7. Median: 1.28×10^7. Distribution: Piecewise uniform. Additional information: Memos from Beauheim, June 14, 1991, and Howarth, June 12, 1991, contained in Appendix A, Vol. 3; Section 2.4.6, Vol. 3. Variable 11 in LHS.
SOLAM	Solubility of Am^{+3} in brine (mol/ℓ). Used in PANEL. Range: 5×10^{-14} to 1.4. Median: 1×10^{-9}. Distribution: Piecewise uniform. Additional information: Trauth et al., 1991; Section 3.3.5, Vol. 3. Variable 19 in LHS.
SOLNP4	Solubility of Np^{+4} in brine (mol/ℓ). Used in PANEL. Range: 3×10^{-16} to 2×10^{-5}. Median: 6×10^{-9}. Distribution: Piecewise uniform with 0.99 rank correlation with SOLNP5. For each sample element, value for SOLNP4 is used if EHPH $< 0.474/(0.474 + 0.503) = 0.485$; otherwise, value for SOLNP4 is used; see Figure 3.3-9, Vol. 3. Additional information: Same as SOLAM. Variable 20 in LHS. Due to the 0.99 rank correlation between SOLNP4 and SOLNP5, the variables SOLNP4 and SOLNP5 are essentially indistinguishable in a rank regression; because of this high correlation, rank regressions presented later in this report use the symbol SOLNP for Np solubility.
SOLNP5	Solubility of Np^{+5} in brine (mol/ℓ). Used in PANEL. Range: 3×10^{-11} to 1.2×10^{-2}. Median: 6×10^{-7}. Distribution: Piecewise uniform with 0.99 rank correlation with SOLNP4. Additional information: Same as SOLAM. Variable 21 in LHS.
SOLPU4	Solubility of Pu^{+4} in brine (mol/ℓ). Used in PANEL. Range: 2×10^{-16} to 4×10^{-6}. Median: 6×10^{-10}. Distribution: Piecewise uniform with 0.99 rank correlation with SOLPU5. For each sample element, value for SOLPU4 is used if EHPH $< 0.539/(0.539 + 0.152) = 0.780$; otherwise, value for SOLPU5 is used; see Figure 3.3-9, Vol. 3. Additional information: Same as SOLAM. Variable 22 in LHS. Due to the 0.99 rank correlation between SOLPU4 and SOLPU5, the variables SOLPU4 and SOLPU5 are essentially indistinguishable in a rank regression; because of this high correlation, rank regressions presented later in this report use the symbol SOLPU for Pu solubility.

TABLE 3-1. VARIABLES SAMPLED IN 1991 WIPP PERFORMANCE ASSESSMENT (adapted from Tables 6.0-1, 6.0-2 and 6.0-3 of Vol. 3 of this report) (concluded)

Variable	Definition
SOLPU5	Solubility of Pu^{+5} in brine (mol/ℓ). Used in PANEL. Range: 2.5×10^{-17} to 5.5×10^{-4}. Median: 6×10^{-10}. Distribution: Piecewise uniform with 0.99 rank correlation with SOLPU4. Additional information: Same as SOLAM. Variable 23 in LHS.
SOLTH	Solubility of Th in brine (mol/ℓ). Used in PANEL. Range: 5.5×10^{-16} to 2.2×10^{-6}. Median: 1×10^{-10}. Distribution: Piecewise uniform. Additional information: Same as SOLAM. Variable 24 in LHS.
SOLU4	Solubility of U^{+4} in brine (mol/ℓ). Used in PANEL. Range: 1×10^{-15} to 5×10^{-2}. Median: 1×10^{-4}. Distribution: Piecewise uniform with 0.99 rank correlation with SOLU6. For each sample element, value for SOLU4 is used if EHPH $< 0.299/(0.299 + .701) = 0.299$; otherwise, value for SOLU6 is used; see Figure 3.3-9, Vol. 3. Additional information: Same as SOLAM. Variable 25 in LHS. Due to the 0.99 rank correlation between SOLU4 and SOLU6, the variables SOLU4 and SOLU6 are essentially indistinguishable in a rank regression; because of this high correlation, rank regressions presented later in this report use the symbol SOLU for U solubility.
SOLU6	Solubility of U^{+6} in brine (mol/ℓ). Used in PANEL. Range: 1×10^{-7} to 1. Median: 2×10^{-3}. Distribution: Piecewise uniform with 0.99 rank correlation with SOLU4. Additional information: Same as SOLAM. Variable 26 in LHS.
STOICCOR	Stoichiometric coefficient for corrosion of steel (mol H_2/mol Fe). Used in BRAGFLO. Range: 0 to 1. Median: 5×10^{-1}. Distribution: Uniform. Additional information: Brush and Anderson in Lappin et al., 1989, p. A-6; Section 3.3.8, Vol. 3. Variable 2 in LHS.
STOICMIC	Stoichiometric coefficient for microbial degradation of cellulosics (mol gas/mol CH_2O). Used in BRAGFLO. Range: 0 to 1.67. Median: 8.35×10^{-1}. Distribution: Uniform. Additional information: Brush and Anderson in Lappin et al., 1989, p. A-10; Section 3.3.9, Vol. 3. Variable 9 in LHS.
VMETAL	Fraction of total waste volume that is occupied by IDB (Integrated Data Base) metals and glass waste category (dimensionless). Used in BRAGFLO. Range: 2.76×10^{-1} to 4.76×10^{-1}. Median: 3.76×10^{-1}. Distribution: Normal. Additional information: Section 3.4.1, Vol. 3. Variable 7 in LHS.
VWOOD	Fraction of total waste volume that is occupied by IDB combustible waste category (dimensionless). Used in BRAGFLO. Range: 2.84×10^{-1} to 4.84×10^{-1}. Median: 3.84×10^{-1}. Distribution: Normal. Additional Information: Section 3.4.1, Vol. 3. Variable 8 in LHS.

As discussed in conjunction with Eq. 2.1-5, a Latin hypercube sample (McKay et al., 1979; Iman and Shortencarier, 1984) of size nK = 60 was generated from the variables listed in Table 3-1. The restricted pairing technique developed by Iman and Conover (1982) was used to induce the correlations between variables indicated in Table 3-1 and also to assure that the correlations between other variables were close to zero.

Once the sample indicated in Eq. 2.1-5 was generated from the variables in Table 3-1, the individual sample elements $\mathbf{x}_k$, k=1, ..., 60, were used in the generation of the risk results shown in Eq. 2.1-6. An overview of this process is provided in Sections 2.2, 2.3 and 2.4. In addition to many intermediate results, the final outcome of this process is a distribution of CCDFs of the form shown in Figure 2.1-2.

The analyses leading to the risk results shown in Eq. 2.1-6 were actually repeated a number of times with different modeling assumptions. The specific cases considered are listed in Table 3-2. The first case listed in Table 3-2, gas generation in the repository and a dual-porosity transport model in the Culebra Dolomite, is believed to be the most creditable and is presented as the best-estimate analysis in the 1991 WIPP preliminary performance assessment. The other cases listed in Table 3-2 can be viewed as *ceteris paribus* sensitivity studies that explore various perturbations on this best-estimate analysis.

In addition to the variation between the cases shown in Table 3-2, the sampling-based approach to the treatment of subjective uncertainty also produces uncertainty and sensitivity results for the individual cases. In the following two chapters, box plots and distributions of CCDFs will be used to display the effect of subjective uncertainty on the cases listed in Table 3-2, and the impact of individual variables will be investigated with sensitivity analysis techniques based on scatterplots, regression analysis and partial correlation analysis. Scatterplots will also be used to compare results obtained with the different analysis cases listed in Table 3-2.

Additional information on the uncertainty and sensitivity analysis techniques in use is available elsewhere (Ch. 3, Vol. 1: Helton et al., 1991).

TABLE 3-2. DIFFERENT ANALYSIS CASES SELECTED FOR CONSIDERATION IN THE 1991 WIPP PERFORMANCE ASSESSMENT

Case	Description
1	Gas generation in repository and a dual-porosity (matrix and fracture porosity) transport model in Culebra Dolomite with drilling intrusions occurring at 1000, 3000, 5000, 7000, and 9000 yrs. Considered best-estimate analysis in 1991 WIPP performance assessment. Discussion in Chapter 4.
2	No gas generation in repository and a dual-porosity (matrix and fracture porosity) transport model in Culebra with drilling intrusions occurring at 1000 yrs. The 1991 preliminary comparison is the first one to include a two-phase (brine and gas), Darcy-flow model in the compliance assessment system. Previous deterministic two-phase calculations (Bertram-Howery et al., 1990, Chapter 6) implied that including waste-generated gas would not negatively affect compliance status with the containment requirements when compared to previous comparisons that assumed fully brine-saturated repository conditions. To understand the impact of including new processes associated with waste-generated gas, Case 1 with waste-generated gas is compared with Case 2 without waste-generated gas. Discussion in Section 5.1.
3	Gas generation in repository and a single-porosity (fracture porosity) transport model in Culebra with drilling intrusions occurring at 1000, 3000, 5000, 7000, and 9000 yrs. For fully brine-saturated repository conditions, the 1990 preliminary comparison (Bertram-Howery et al., 1990; Helton et al., 1991) analyzed the importance of a dual-porosity assumption (Reeves et al., 1987) for modeling radionuclide transport. A study to assess the defensibility of this assumption has started. To establish the continuing importance of this work with the new modeling system that includes waste-generated gas, Case 1 with a dual-porosity (matrix and fracture porosity) model for transport is compared with Case 3 with a single-porosity (fracture porosity) model for transport. Discussion in Section 5.2.
4	No gas generation in repository and a single-porosity (fracture porosity) transport model in Culebra with drilling intrusions occurring at 1000 yrs. Included for completeness and to provide an analysis for single-porosity transport that was not complicated by the effects of gas generation. Discussion in Section 5.3.
5	Gas generation in repository and a dual-porosity (matrix and fracture porosity) transport model without chemical retardation in Culebra with drilling intrusions occurring at 1000 yrs. Under agreement with the State of New Mexico (U.S. DOE and State of New Mexico, 1981, as modified, Vol. 1, Appendix B, p. B-14, Comment 14), a case using zero distribution coefficients will continue to be included in these preliminary comparisons until site-specific information becomes available. Case 5 with zero distribution coefficients in a dual-porosity transport model (physical retardation is included) is compared to Case 1 with nonzero distribution coefficients to assess the importance of obtaining a defensible data set for chemical retardation. Discussion in Section 5.4.

TABLE 3-2. DIFFERENT ANALYSIS CASES SELECTED FOR CONSIDERATION IN THE 1991 WIPP PERFORMANCE ASSESSMENT (concluded)

Case	Description
6	Effect of climate change with gas generation in repository and with single- and dual-porosity transport models in the Culebra and intrusions occurring at 1000 yrs. To date, the preliminary comparisons have not addressed the problem of conceptual model uncertainty except for the dual-porosity and waste-generated gas cases. Future comparisons will need to consider alternative conceptual models throughout the modeling system. Case 6 is a first attempt to assess the importance of a simple model (not intended to be a bounding case) for including climate variability through a recharge and infiltration modeling assumption for use with the 2-D confined aquifer conceptual model of the Culebra. Discussion in Section 5.5.

General: The preliminary comparisons are interim analyses to assess the status of compliance and provide annual guidance to the project through uncertainty/sensitivity analyses. The cases included here are intended to help identify and understand important processes in the modeling system for the 1991 guidance.

4. UNCERTAINTY AND SENSITIVITY ANALYSIS RESULTS FOR 1991 PRELIMINARY COMPARISON

At present, the most appropriate conceptual model for performance assessment at the WIPP is believed to include gas generation due to both corrosion and microbial action in the repository and a dual-porosity (matrix and fracture porosity) representation for transport in the Culebra Dolomite Member of the Rustler Formation (i.e., Case 1 in Table 3-2). This conceptual view was used in the modeling that produced the best-estimate performance-assessment results for the WIPP presented in Chapter 6 of Vol. 1. This chapter presents uncertainty and sensitivity analysis results associated with these current best-estimate calculations.

4.1 Uncertainty in CCDFs

The distribution of CCDFs for normalized release to the accessible environment, including both cuttings and cavings removal (hereafter called cuttings removal) and groundwater transport, that results from the imprecisely known variables presented in Chapter 3 is given in Figure 2.1-1. This figure was constructed with a Latin hypercube sample of size 60 generated from the 45 variables in Table 3-1. The construction of each CCDF appearing in Figure 2.1-1 was based on the scenarios, scenario probabilities and scenario consequences described in Sections 2.2, 2.3 and 2.4, respectively. As is the case for all results involving groundwater transport presented in Chapter 4, gas generation is assumed to take place in the repository and a dual-porosity model is used to represent radionuclide transport in the Culebra. The results contained in Figure 2.1-1 are presented in Chapter 6, Vol. 1, of this report as the current best estimate of the CCDFs for comparison with the EPA release limits. As examination of Figure 2.1-1 shows, consideration of gas generation in the repository and a dual-porosity transport model in the Culebra results in all CCDFs being below the EPA release limits.

Although Figure 2.1-1 presents all 60 CCDFs that result for the sample indicated in Eq. 2.1-5, it is rather cluttered and hard to read. A less crowded summary can be obtained by plotting the mean value and selected percentile values for the individual releases appearing on the abscissa. The mean and percentile values are obtained from the exceedance probabilities associated with the individual release values and the weights, or "probabilities" (i.e., 1/60), associated with the individual sample elements. The result of this calculation is shown in Figure 4.1-1 for the mean plus the 10th, 50th (i.e., median) and 90th percentile values. The calculated mean and percentile values are for specific releases on the abscissa of Figure 2.1-1; the curves in Figure 4.1-1 result from connecting these individual

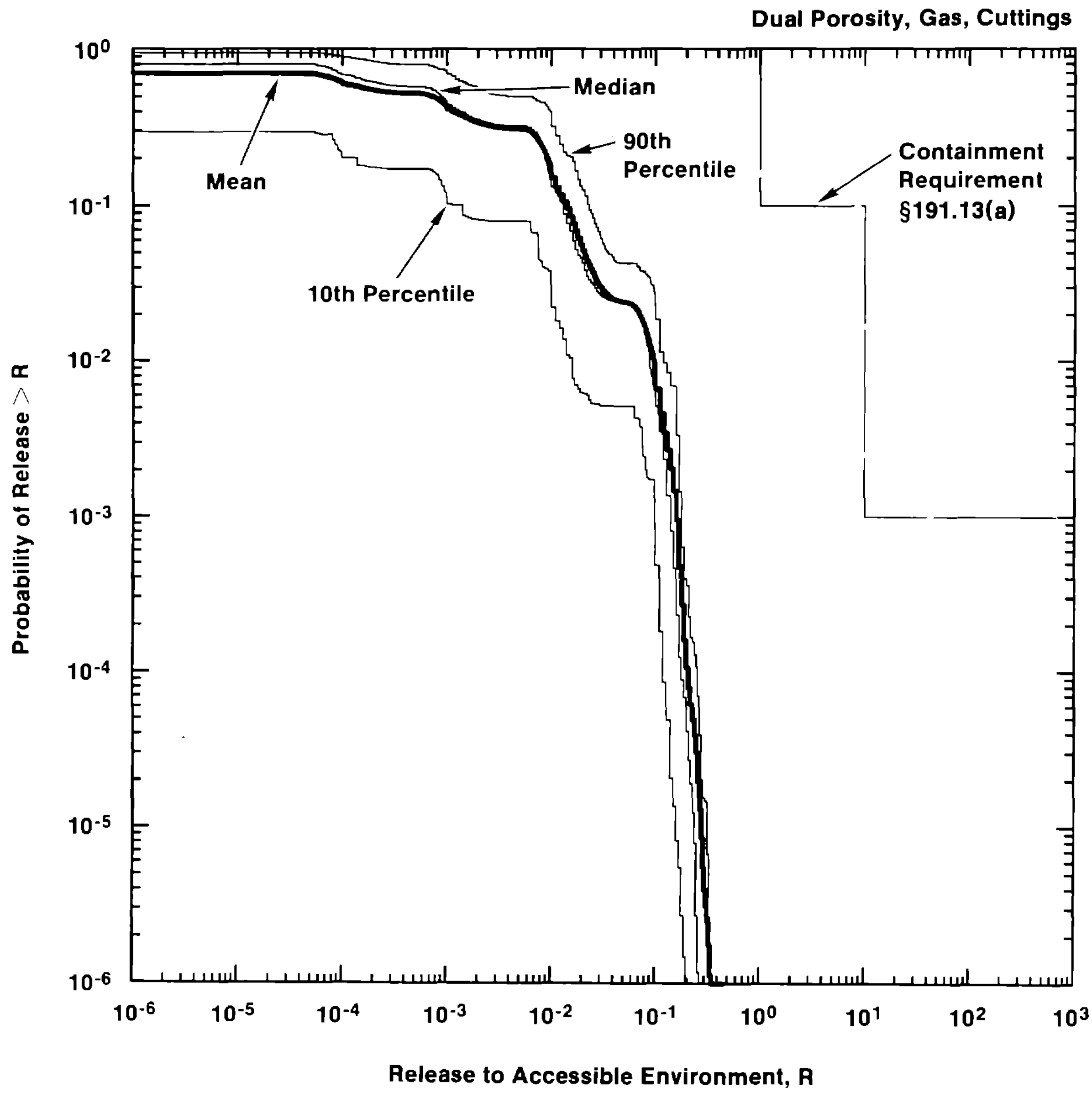

Figure 4.1-1. Mean and Percentile Curves for Distribution of Complementary Cumulative Distribution Functions Shown in Figure 2.1-1 for Normalized Releases to the Accessible Environment Including Both Cuttings Removal and Groundwater Transport with Gas Generation in the Repository and a Dual-Porosity Transport Model in the Culebra Dolomite.

values. The mean and percentile curves appearing in Figure 4.1-1 result from the subjective uncertainty in the variables in Table 3-1, as does the distribution of CCDFs in Figure 2.1-1. In contrast, the individual CCDFs in Figure 2.1-1 provide a representation for stochastic uncertainty.

As indicated in Eqs. 2.4-10 through 2.4-14, the total release to the accessible environment for a given scenario is the sum of a release due to cuttings removal and a release due to groundwater transport. For comparison, Figure 4.1-2 shows the CCDFs that result when only releases due to cuttings removal are considered (upper two frames) and only releases due to groundwater transport are considered (lower two frames). As examination of Figure 4.1-2 shows, releases to the accessible environment are dominated by cuttings removal. The only exception to this occurs for the upper-right CCDF in Figure 2.1-2, which is dominated by the groundwater release. Otherwise, the CCDFs in Figure 2.1-2 are essentially identical to the cuttings-release-only CCDFs in Figure 4.1-2.

As shown in Figure 4.1-2, only 4 groundwater-release-only CCDFs involve normalized releases to the accessible environment that are greater than 10^{-6} at an exceedance probability of 10^{-6}. Further, only 16 CCDFs involve releases that are greater than 10^{-12} at an exceedance probability of 10^{-6}. Thus, the uncertainty characterization and associated modeling for the variables in Table 3-1 lead to limited releases to the accessible environment due to groundwater transport.

The releases associated with the individual release modes (i.e., cuttings removal and groundwater transport) are now considered. Specifically, uncertainty and sensitivity analysis results for cuttings removal are presented in Sections 4.2 and 4.3, followed by similar results for groundwater transport in Sections 4.4 and 4.5. Then, sensitivity analysis results for the CCDFs in Figure 2.1-1 are presented in Section 4.6.

4.2 Uncertainty in Cuttings Removal

The variation in the total normalized release to the accessible environment due to cuttings removal resulting from boreholes intersecting waste of average activity level is shown in Figure 4.2-1 for intrusions occurring at 1000, 3000, 5000, 7000 and 9000 yrs. Specifically, box plots in Figure 4.2-1 show the normalized releases due to cuttings removal (i.e., the rC_i defined in Eq. 2.4-1) for scenarios $S(1,0,0,0,0)$, $S(0,1,0,0,0)$, $S(0,0,1,0,0)$, $S(0,0,0,1,0)$ and $S(0,0,0,0,1)$ as defined in Eq. (2.2-3). Each box plot summarizes the distribution of results obtained with the previously discussed Latin hypercube sample of size 60 from the variables in Table 3-1; thus, each box plot is based on 60 observations.

Cuttings Releases Only

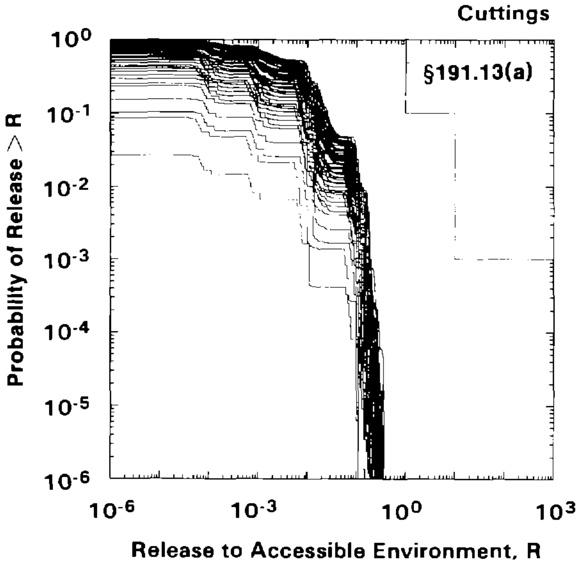

TRI-6342-1383-1

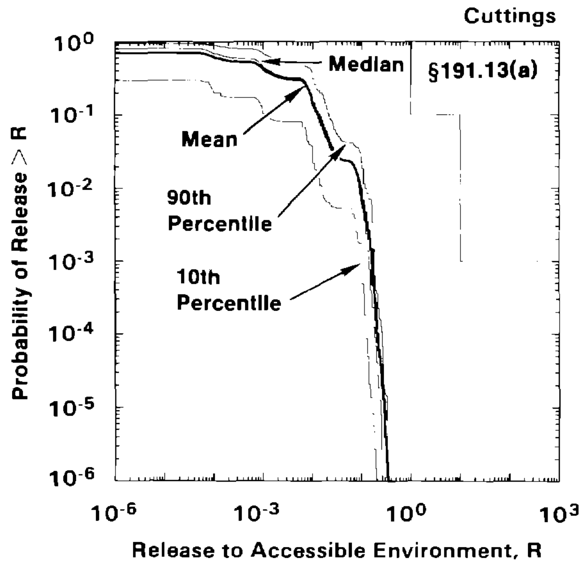

TRI-6342-1561-0

Groundwater Transport Releases Only

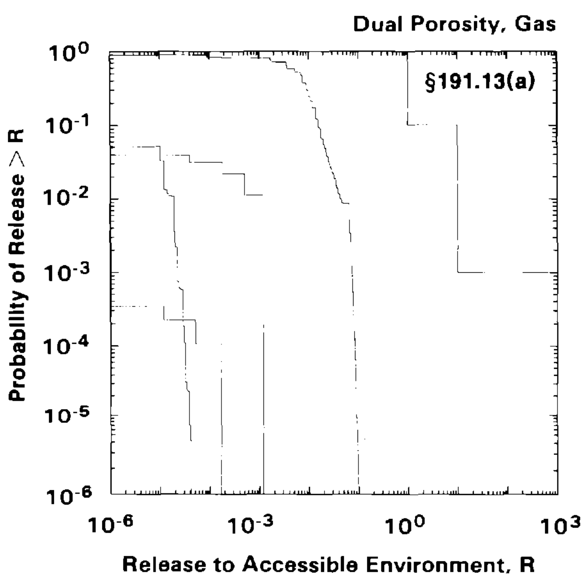

TRI-6342-1562-0

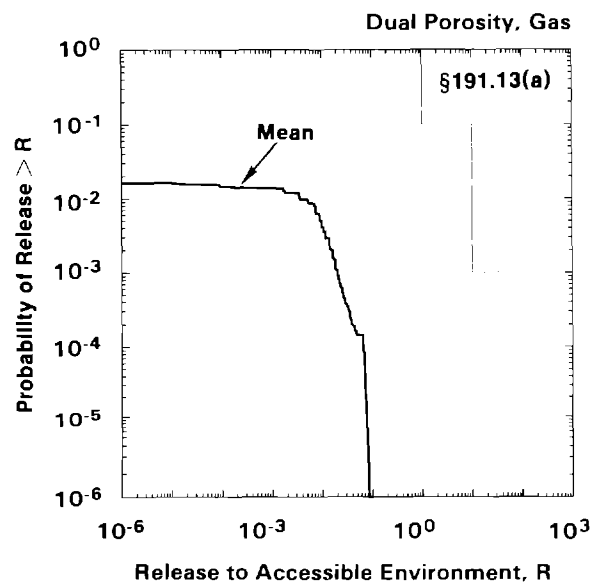

TRI-6342-1563-0

Figure 4.1-2. Comparison of Complementary Cumulative Distribution Functions for Normalized Releases to the Accessible Environment for Cuttings Removal Only (upper two frames) and Groundwater Transport with Gas Generation in the Repository and a Dual-Porosity Transport Model in the Culebra Dolomite (lower two frames).

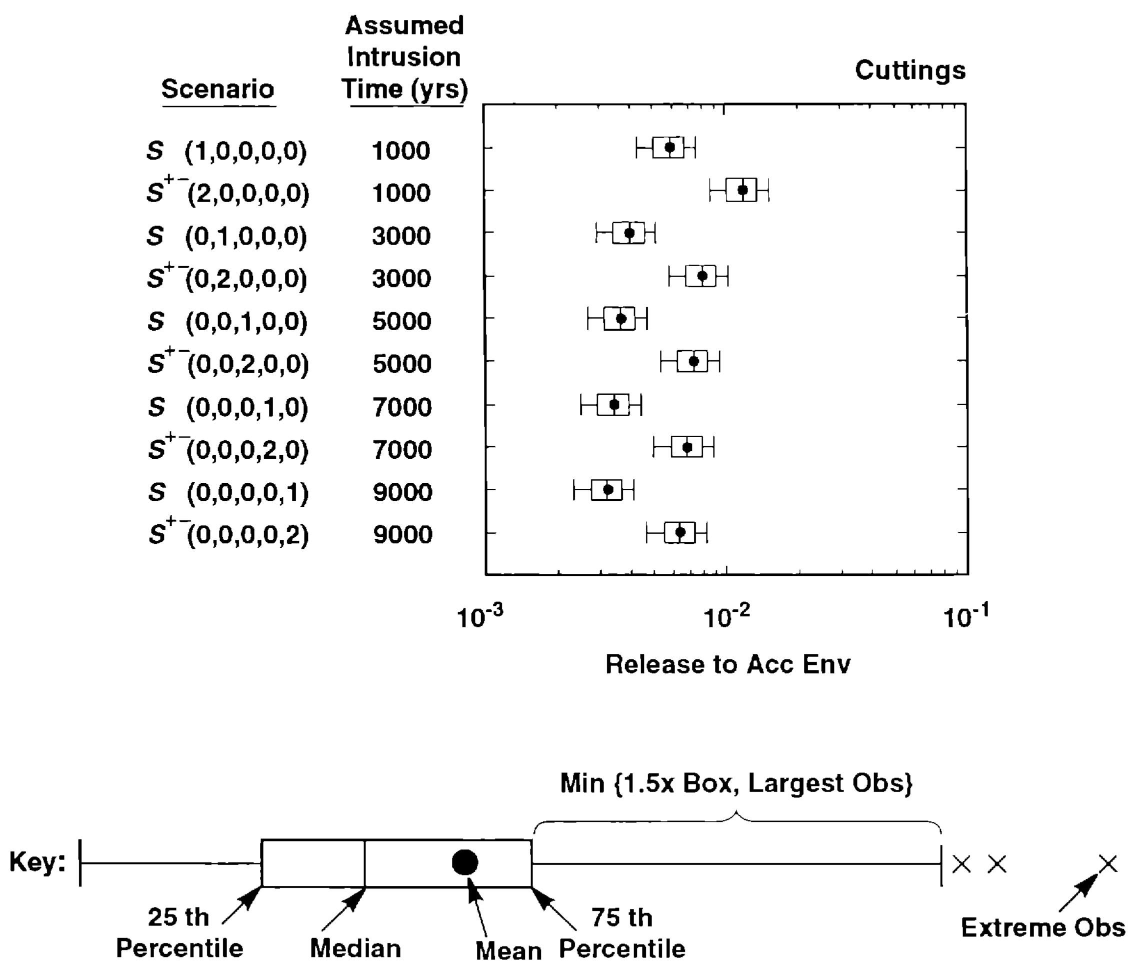

TRI-6342-1529-0

Figure 4.2-1. Total Normalized Release to the Accessible Environment Due to Cuttings Removal from Waste of Average Activity Level.

As a reminder, the endpoints of the boxes in Figure 4.2-1 are formed by the lower and upper quartiles of the data, that is $x_{.25}$ and $x_{.75}$. The vertical line within the box represents the median, $x_{.50}$. The sample mean is identified by the large dot. The bar on the right of the box extends to the minimum of $x_{.75} + 1.5(x_{.75} - x_{.25})$ and the maximum observation. In a similar manner, the bar on the left of the box extends to the maximum of $x_{.25} - 1.5(x_{.75} - x_{.25})$ and the minimum observation. Observations falling outside of these bars are shown with x's. In symmetric distributions, these values would be considered outliers. Extreme values of this type do not appear in Figure 4.2-1 but will be present in most box plots presented in this report. The structure of box plots is illustrated in the key appearing at the bottom of Figure 4.2-1.

All results involving cuttings removal in the 1991 WIPP performance assessment are derived from the total normalized releases for scenarios $S(1,0,0,0,0)$ through $S(0,0,0,0,1)$ summarized in Figure 4.2-1. For comparison and consistency with later figures, Figure 4.2-1 also shows the normalized releases due to cuttings removal (i.e., $2\ rC_i$) for scenarios $S^{+-}(2,0,0,0,0)$ through $S^{+-}(0,0,0,0,2)$ as defined in Eq. 2.2-9, with the subscript i appearing in the definition of $S_i^{+-}(\mathbf{n})$ in Eq. 2.2-9 omitted due to redundancy. As discussed in conjunction with Eq. 2.4-15, a scale factor is used to convert from releases of waste of average activity level to releases of waste of the five activity levels shown in Table 2.4-4. These scaled releases are then used in the construction of releases due to cuttings removal of waste of different activity levels for scenarios $S(\mathbf{l},\mathbf{n})$ and $S^{+-}(\mathbf{l}; t_{i-1}, t_i)$ as shown in Eqs. 2.4-12 and 2.4-14, respectively.

As examination of Figure 4.2-1 shows, all of the normalized releases associated with a single borehole and average activity level waste are between 0.001 and 0.01. The largest scale factor defined by Eq. 2.4-15 to convert from an average activity level release to a release of a specified activity level is approximately 23.1, which results for time steps $i=1,2,3,4,5$ and waste of activity level $\ell=4$ (e.g., SF_{24} as shown in Eq. 2.4-16). Thus, a single borehole at the first time step used in the analysis (i.e., 1000 yrs) will not result in a normalized release that exceeds 1, although it is possible that a single borehole into waste of activity level 4 at an earlier time might result in a normalized release greater than 1.

The contribution of individual isotopes to the total normalized release to the accessible environment due to cuttings removal resulting from a single borehole intersecting waste of average activity level is shown in Figure 4.2-2. Only three isotopes contribute to the total release at 1000 yrs:

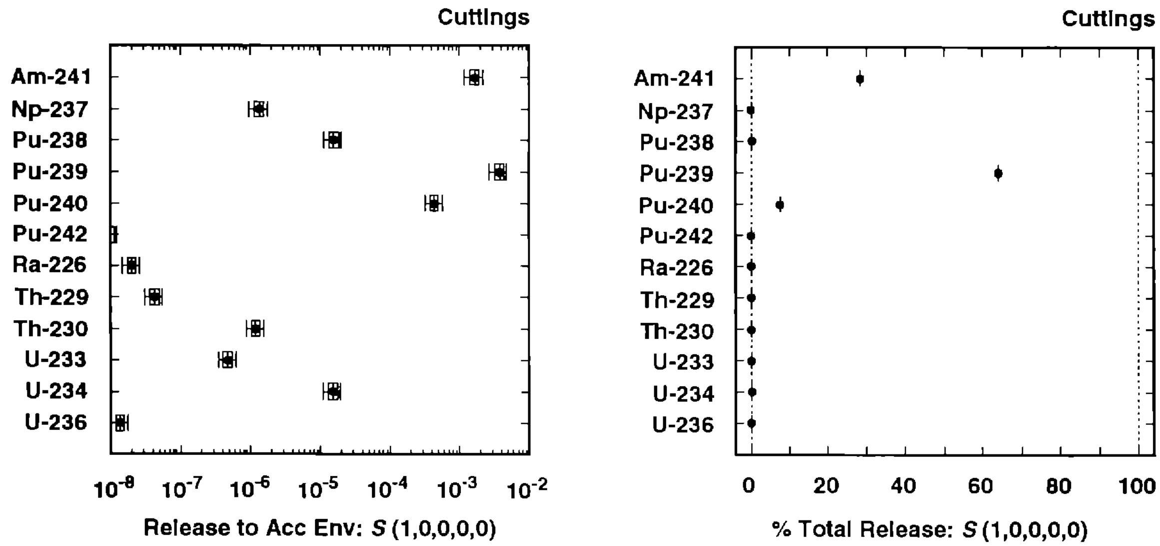

TRI-6342-1525-0 TRI-6342-1526-0

Figure 4.2-2. Normalized Releases to the Accessible Environment for Individual Isotopes and Percent Contribution to the Total Normalized Release for Cuttings Removal Resulting from a Single Borehole Intersecting Waste of Average Activity Level at 1000 Yrs. The results shown in this figure correspond to the releases associated with scenario *S*(1,0,0,0,0).

Am-241, Pu-239 and Pu-240. No other isotopes make an appreciable contribution to the total release. At later times, the total release is dominated by Pu-239 due to the decay of Am-241, with a small contribution from Pu-240.

4.3 Sensitivity Analysis for Cuttings Removal

Drill bit diameter (DBDIAM) is the only variable in Table 3-1 that affects cuttings removal. This variable is used as an input to the CUTTINGS program, where it is used in the calculation of an eroded or "effective" diameter for the borehole as it passes through the repository. The eroded diameter is the actual determinant of the amount of waste that is removed to the surface.

The relationships between drill bit diameter (DBDIAM), eroded diameter and normalized release to the accessible environment due to cuttings removal are shown in the scatterplots appearing in Figure 4.3-1. Scatterplots present the points (x_k, y_k), $k = 1,2,\ldots, nK$, where x_k and y_k are results associated

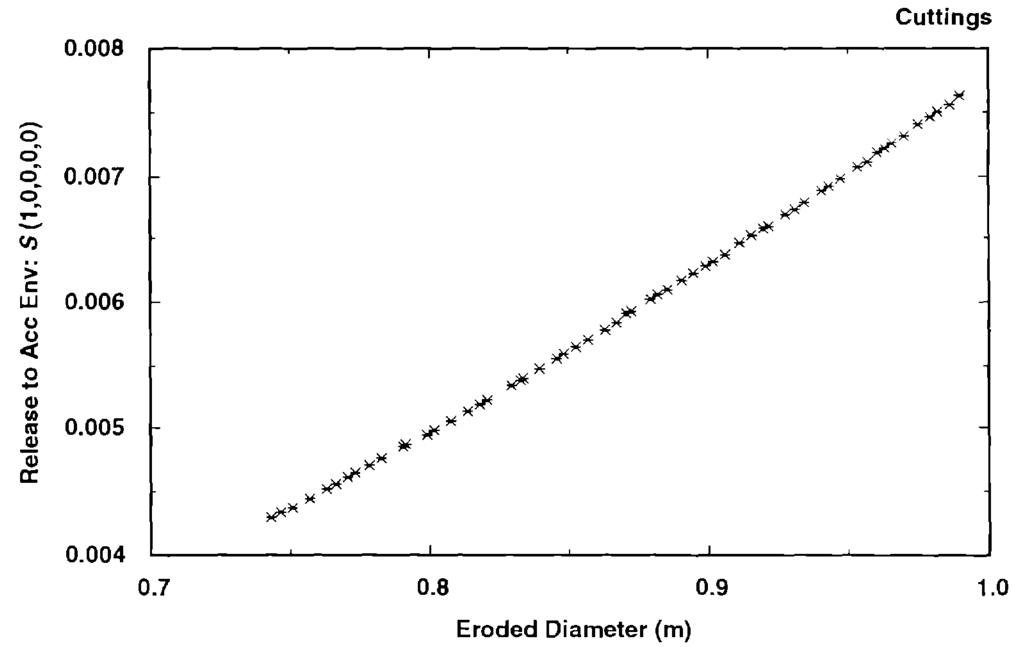

TRI-6342-1630-0

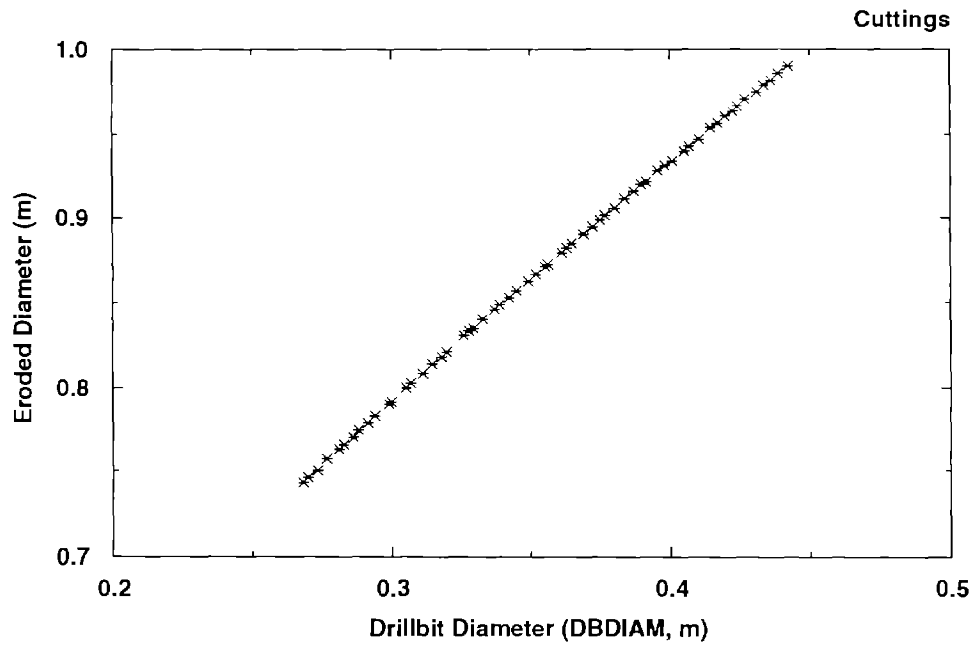

TRI-6342-1631-0

Figure 4.3-1. Scatterplots Displaying Relationships between Drill Bit Diameter (DBDIAM, a sampled variable), Eroded Diameter of Borehole (a calculated variable), and Associated Normalized Cuttings Release to the Accessible Environment (a calculated variable) for Waste of Average Activity Level with Intrusion Occurring at 1000 Yrs (i.e., the release for scenario $S(1,0,0,0,0)$).

with sample element $\mathbf{x}_k$ shown in Eq. 2.1-5 and nK is the sample size. Often, x_k is the value for a particular sampled variable contained in $\mathbf{x}_k$, and y_k is the value for a particular calculated variable contained in one of the vectors $\mathbf{cS}_i(\mathbf{x}_k)$ shown in Eq. 2.1-6. A scatterplot of this type appears in the lower frame of Figure 4.3-1, where x_k corresponds to the value for DBDIAM (drill bit diameter) in $\mathbf{x}_k$ and y_k corresponds to the eroded diameter of the resultant borehole calculated for $\mathbf{x}_k$. In other cases, both x_k and y_k are values calculated for $\mathbf{x}_k$. A scatterplot of this type appears in the upper frame of Figure 4.3-1, where x_k corresponds to the eroded diameter of the resultant borehole calculated for $\mathbf{x}_k$ and y_k corresponds to the normalized release to the accessible environment due to cuttings removal calculated for $\mathbf{x}_k$. Scatterplots facilitate the examination of the results obtained for individual sample elements.

As examination of Figure 4.3-1 shows, release to the accessible environment varies in an almost linear manner with drill bit and eroded borehole diameter. The relationship between normalized release and eroded borehole diameter shown in Figure 4.3-1 is actually quadratic. However, due to the relatively small range for eroded diameter (i.e., approximately 0.75 m to 1.0 m), the relationship is also very close to being linear.

Drill bit diameter provides an excellent example of the choice that must be made in deciding whether a particular variable involves stochastic (i.e., type A) uncertainty or subjective (i.e., type B) uncertainty. Clearly, drill bits of different diameters are used now and also will be used in the future. Thus, the occurrence of boreholes initiated by drill bits of different diameters is a stochastic uncertainty. If this stochastic uncertainty was felt to be important, then drill bit diameter would have to be one of the characteristics used to define the scenarios S_i appearing in Eq. 2.1-1. Further, a probability distribution D_A would have to be developed that described the likelihood that boreholes initiated by drill bits of different sizes would occur. This distribution would be one of the determinants of the probabilities pS_i appearing in Eq. 2.1-1. In contrast, it is also possible to decide that drill bit diameter is not sufficiently important to merit incorporation into the definition of the scenarios S_i, which is equivalent to deciding that the performance assessment can be reasonably carried out with only one value for drill bit diameter. However, given the decision that use of a single appropriately selected drill bit diameter will not compromise the results of the analysis, it may not be clear what this single value should be. In this case, a subjective distribution D_B can be used to characterize where this appropriate value is located. The distributions D_A and D_B are being used to characterize different aspects of the same physical process, and thus will not be the same. For the 1991 WIPP performance assessment, the distribution assigned to drill bit diameter characterizes subjective uncertainty.

4.4 Uncertainty in Groundwater Releases

As discussed in conjunction with Eqs. 2.4-3 and 2.4-4, two types of groundwater releases to the accessible environment are considered in the 1991 WIPP performance assessment: a release initiated by a single borehole (i.e., E2-type scenarios) and a release initiated by two or more boreholes in the same waste panel and time interval, of which at least one penetrates a pressurized brine pocket and at least one does not penetrate a pressurized brine pocket (i.e., E1E2-type scenarios). As already indicated by the groundwater-release-only CCDFs shown in Figure 4.1-2, the releases due to groundwater transport are very small. Additional perspective is provided by Figure 4.4-1, which shows the normalized releases to the accessible environment for scenarios of the E2- and E1E2-type, respectively. Of the 60 sample elements considered in this analysis, only 7 resulted in nonzero releases for an E2-type scenario with intrusion occurring at 1000 yrs (i.e., for $S(1,0,0,0,0)$) and only 15 resulted in nonzero releases for an E1E2-type scenario with intrusion occurring at 1000 yrs (i.e., for $S^{+-}(2,0,0,0,0)$). Further, even the few nonzero releases are small.

The normalized releases shown in Figure 4.4-1 correspond to the releases $rGW1_i$ and $rGW2_i$ shown in Eqs. 2.4-3 and 2.4-4. As shown in Eqs. 2.4-12 and 2.4-14, these releases are used to construct the groundwater releases to the accessible environment for scenarios of the form $S(\mathbf{l},\mathbf{n})$ and $S^{+-}(\mathbf{l};t_{i-1},t_i)$. The best-estimate comparisons with the EPA release limits in the 1991 WIPP performance assessment used the groundwater transport results summarized in Figure 4.4-1.

For additional perspective, Figure 4.4-2 summarizes the normalized releases to the accessible environment and the percent contributions to the total release for individual isotopes for intrusions occurring at 1000 yrs. The percent contributions can only be calculated for the nonzero releases. Specifically, the distributions summarized in Figure 4.4-2 and other similar figures for percent contribution to total release are conditional in the sense that they are based only on the sample elements that have a nonzero total release. As examination of Figure 4.4-2 shows, total release to the accessible environment, when it occurs, is usually dominated by U-234, although there are sample elements in which the release is completely dominated by Np-237, Pu-239 or Th-230. However, the total normalized release is very small in all cases (i.e., always less than 10^{-1} and usually less than 10^{-3}). The releases due to intrusions occurring at later times (i.e., 3000, 5000, 7000, and 9000 yrs) are even smaller than those shown in Figure 4.4-2 due to increased time for decay and decreased time for transport.

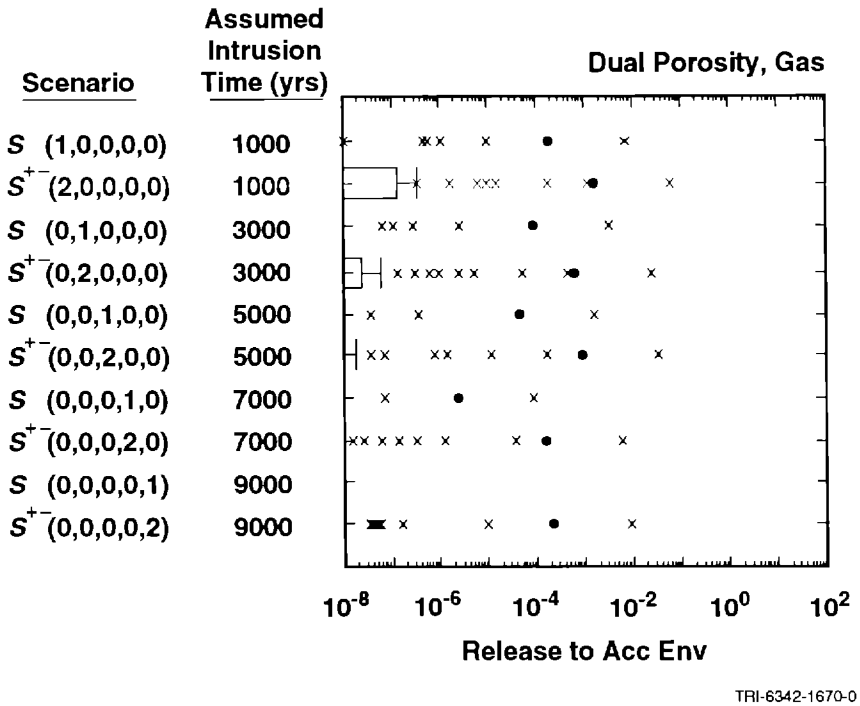

Figure 4.4-1. Total Normalized Release to the Accessible Environment Due to Groundwater Transport with Gas Generation in the Repository and a Dual-Porosity Transport Model in the Culebra Dolomite.

As described in Eqs. 2.4-10 through 2.4-14, the total release to the accessible environment for a scenario is the sum of a cuttings-removal component and a groundwater-transport component. The uncertainty in these individual components is summarized in Figures 4.2-1 and 4.4-1. Total release to the accessible environment, including cuttings removal and groundwater transport, is summarized in Figure 4.4-3. As comparison with Figure 4.2-1 shows, inclusion of releases due to groundwater transport has little effect on the total releases for the individual scenarios.

The large number of zero releases associated with the results shown in Figure 4.4-1 is reassuring with respect to the possible suitability of the WIPP as a disposal facility for transuranic waste. However, these zero releases tend to obscure what is going on in the analysis. Additional insight can be obtained by examining the releases from the repository to the Culebra. The total normalized release to the Culebra as predicted by the PANEL program is shown in Figure 4.4-4. The individual releases summarized in this figure constitute the initial input to the STAFF2D program for radionuclide transport in the Culebra. For the 60 sample elements, 38 result in zero releases to the Culebra due to an E2-type scenario with intrusion occurring at 1000 yrs (i.e., for scenario $S(1,0,0,0,0)$), while only 2 sample elements result in a zero release to the Culebra due to an E1E2-type scenario with intrusion occurring at 1000 yrs (i.e., for scenario $S^{+-}(2,0,0,0,0)$).

Scenario: $S(1,0,0,0,0)$, Assumed Intrusion Time: 1000 yrs

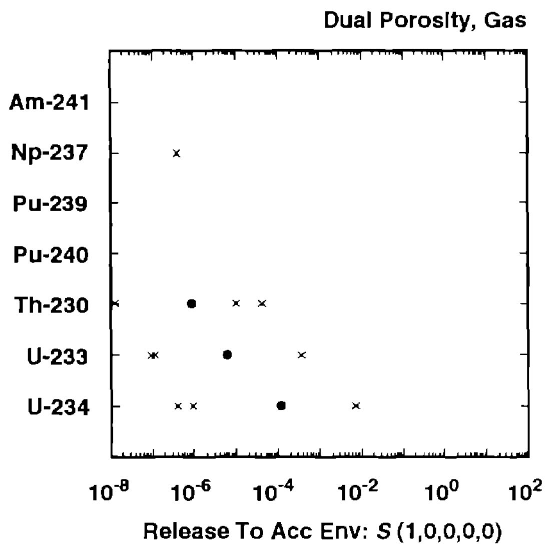

TRI-6342-1532-0

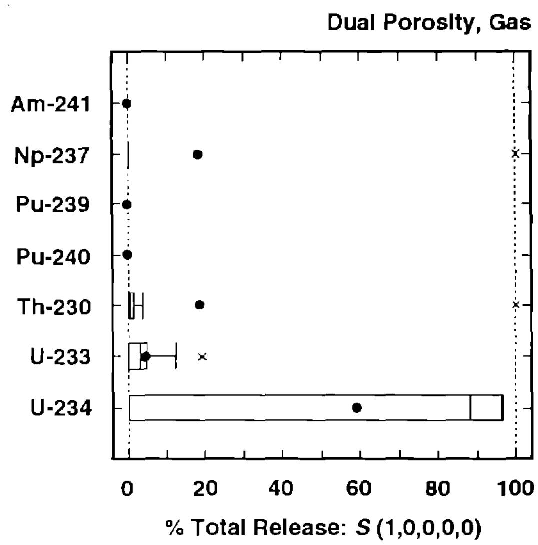

TRI-6342-1533-0

Scenario: $S^{+-}(2,0,0,0,0)$, Assumed Intrusion Time: 1000 yrs

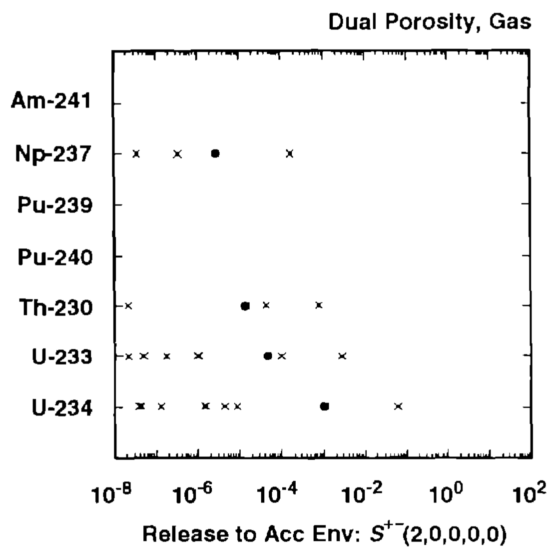

TRI-6342-1530-0

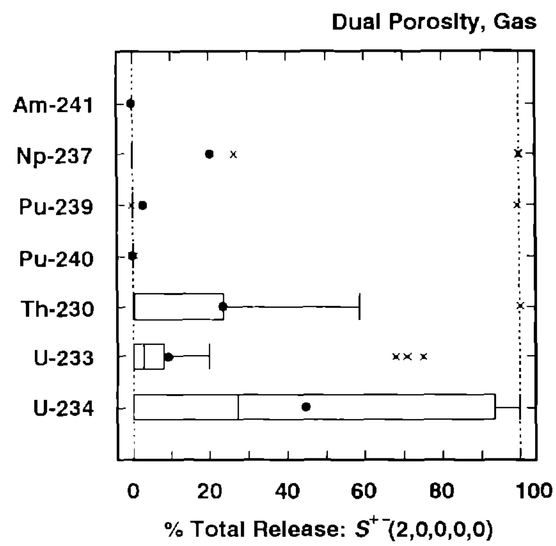

TRI-6342-1531-0

Figure 4.4-2. Normalized Releases for Individual Isotopes to the Accessible Environment Due to Groundwater Transport with Intrusion Occurring at 1000 Yrs, Gas Generation in the Repository and a Dual-Porosity Transport Model in the Culebra Dolomite.

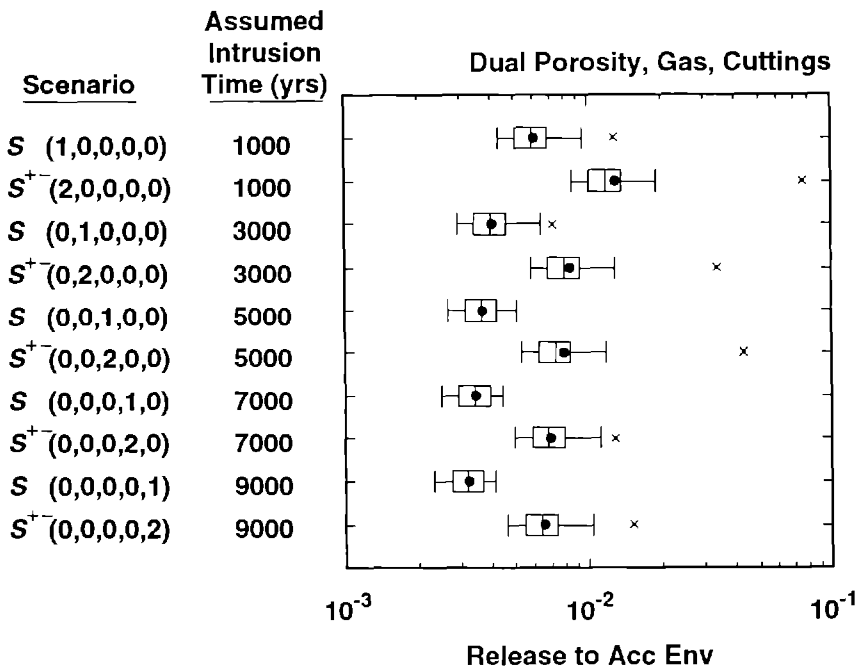

TRI-6342-1534-0

Figure 4.4-3. Total Normalized Release to the Accessible Environment Due to Cuttings Removal and Groundwater Transport with Gas Generation in the Repository and a Dual-Porosity Transport Model in the Culebra Dolomite.

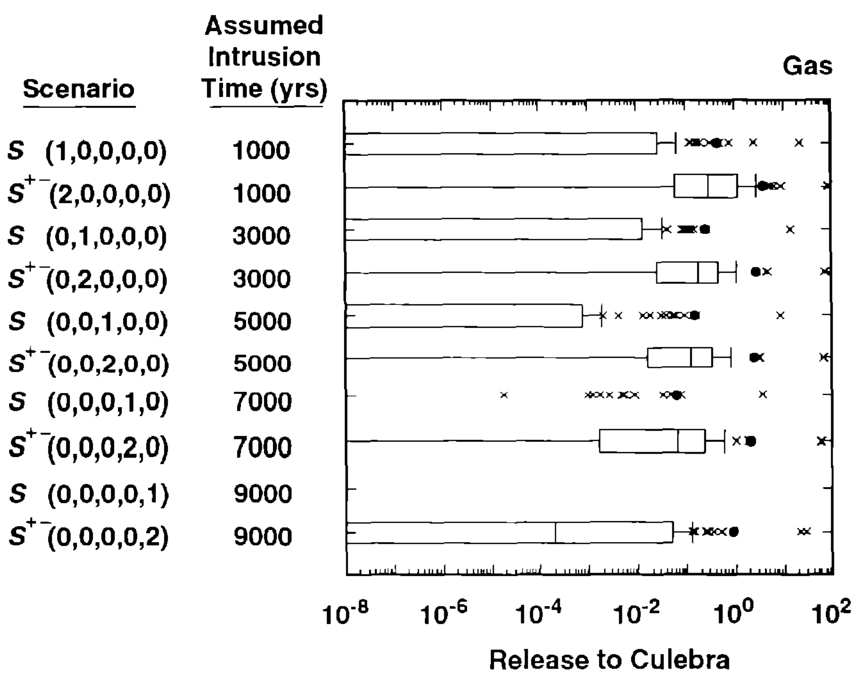

TRI-6342-1535-0

Figure 4.4-4. Total Normalized Release to the Culebra Dolomite as Predicted by the PANEL Program with Gas Generation in the Repository.

Three insights emerge from the information summarized in Figures 4.4-1 and 4.4-4. First, the Culebra appears to provide an effective barrier in reducing groundwater transport releases to the accessible environment. For example, scenario $S(1,0,0,0,0)$ has 22 nonzero releases to the Culebra but only 7 nonzero releases to the accessible environment, and scenario $S^{+-}(2,0,0,0,0)$ has 58 nonzero releases to the Culebra but only 15 nonzero releases to the accessible environment. The extent of this reduction is illustrated for scenario $S^{+-}(2,0,0,0,0)$ by the scatterplot appearing in Figure 4.4-5. Second, even the release to the Culebra for E2-type scenarios is often zero. At present, the probability of E2-type scenarios at the WIPP is estimated to be considerably larger than the probability for E1E2-type scenarios. (e.g., see Chapters 2 and 3 of Vol. 2). Third, the releases to the Culebra may be several orders of magnitude larger for E1E2-type scenarios than for E2-type scenarios. This pattern is illustrated for scenarios $S^{+-}(2,0,0,0,0)$ and $S(1,0,0,0,0)$ by the scatterplot appearing in Figure 4.4-6.

For additional perspective, Figure 4.4-7 summarizes the normalized release to the Culebra for individual isotopes for intrusions occurring at 1000 yrs. As examination of this figure shows, total release into the Culebra tends to be dominated by U-234, although Pu-239 is an important contributor for some sample elements. Further, Am-241 is also an important contributor at 1000 yrs but is unimportant at later times to radioactive decay.

The releases summarized in Figure 4.4-7 are carried into the Culebra by the upward flow of brine from the repository through an intruding borehole. The total brine release to the Culebra is summarized in Figure 4.4-8. The variables that cause the variation in brine flow to the Culebra shown in Figure 4.4-8 are determined in a sensitivity analysis presented in the next section.

4.5 Sensitivity Analysis for Groundwater Releases

Stepwise regression analysis can be used to examine the relationships between the sampled variables listed in Table 3-1 and groundwater releases to the accessible environment. Such analyses can be carried out with the original variables or with these variables transformed in some manner (e.g., logarithms, ranks, ...). The present analysis tried regressions with both the original variables and with their rank-transformed values (Iman and Conover, 1979). The regressions with rank-transformed variables (i.e., rank regressions) generally outperformed the regressions with the original variables.

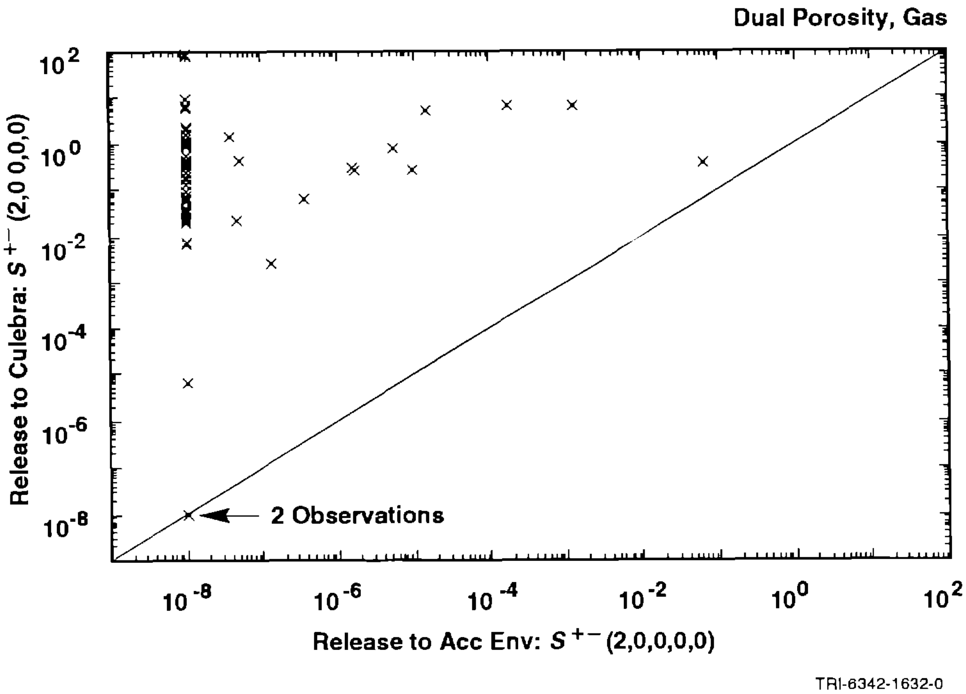

Figure 4.4-5. Scatterplot of Total Normalized Release to the Culebra Dolomite and Total Normalized Release to the Accessible Environment for Scenario S^{+-}(2,0,0,0,0) with Gas Generation in the Repository, a Dual-Porosity Transport Model in the Culebra Dolomite and Intrusion Occurring at 1000 Yrs. For plotting purposes, values less than 10^{-8} are set to 10^{-8}.

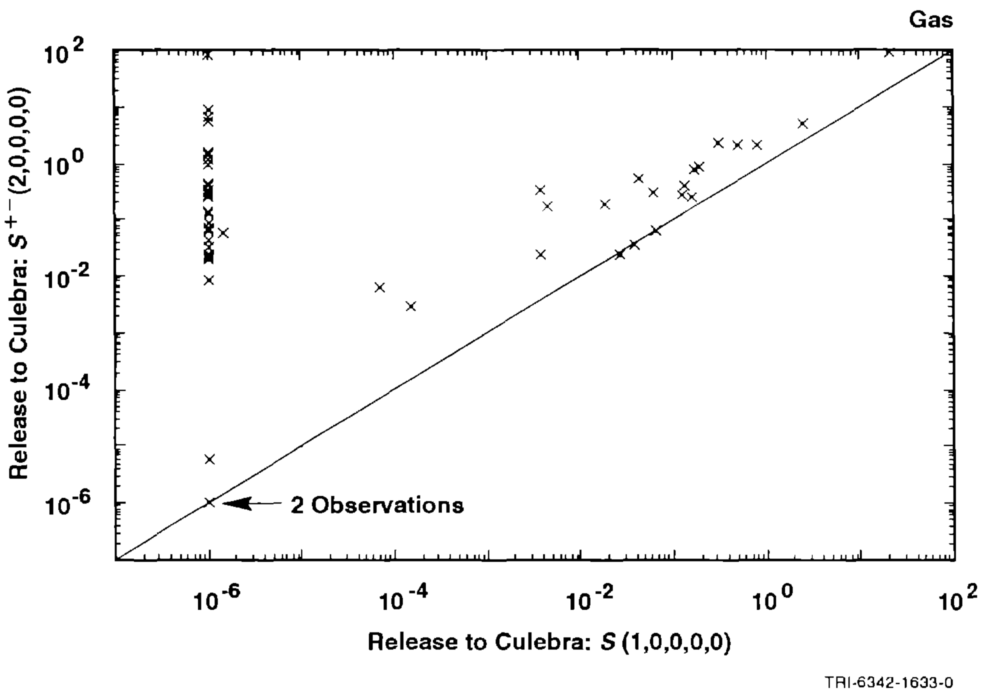

Figure 4.4-6. Scatterplot of Total Normalized Release to the Culebra Dolomite with Gas Generation in the Repository and Intrusion Occurring at 1000 Yrs for Scenarios S(1,0,0,0,0) and S^{+-}(2,0,0,0,0). For plotting purposes, values less than 10^{-6} are set to 10^{-6}.

Scenario: $S(1,0,0,0,0)$, Assumed Intrusion Time: 1000 yrs

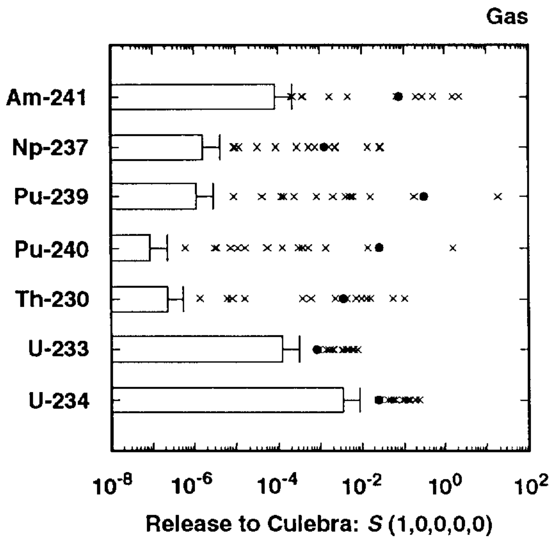

TRI-6342-1536-0

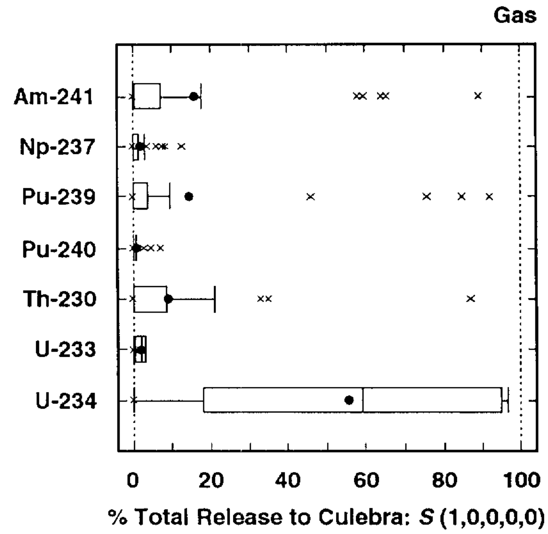

TRI-6342-1537-0

Scenario: $S^{+-}(2,0,0,0,0)$, Assumed Intrusion Time: 1000 yrs

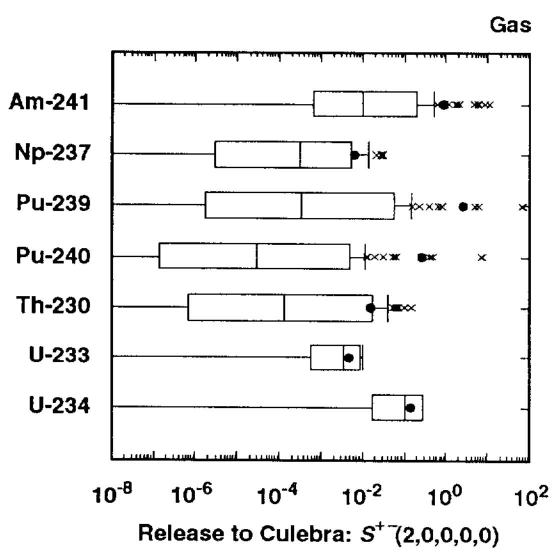

TRI-6342-1538-0

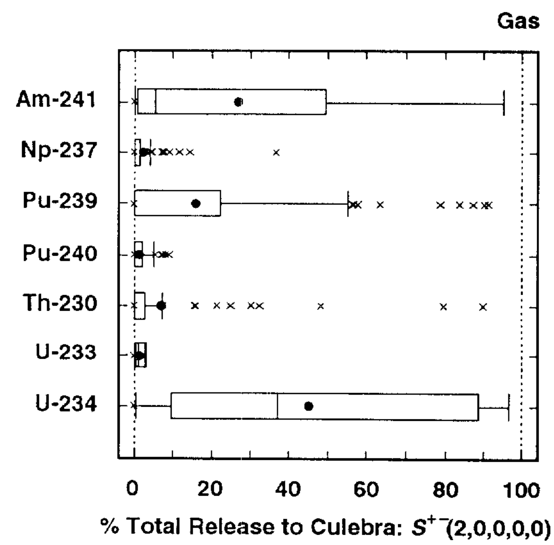

TRI-6342-1539-0

Figure 4.4-7. Normalized Releases for Individual Isotopes to the Culebra Dolomite with Intrusion Occurring at 1000 Yrs and Gas Generation in the Repository.

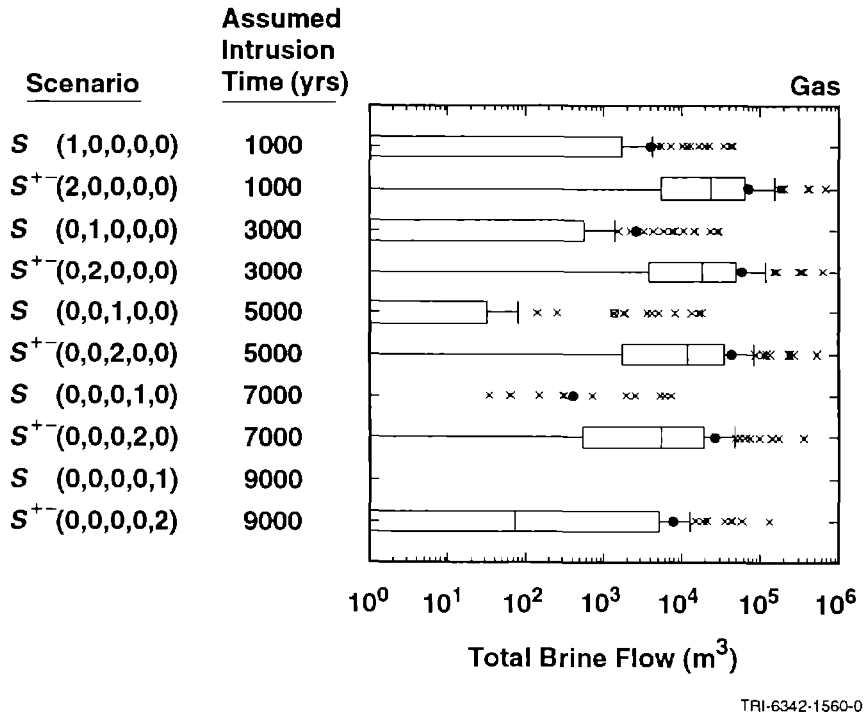

Figure 4.4-8. Total Brine Flow (m^3) from the Repository to the Culebra Dolomite with Gas Generation in the Repository.

Rank regressions for scenario $S(1,0,0,0,0)$ are presented in Table 4.5-1 for release from the repository to the Culebra Dolomite and for groundwater transport one-quarter, one-half and the full distance to the accessible environment. As indicated in Figures 1.5-4, 2.1-1 and 2.1-2 of Vol. 3, the accessible environment is assumed to begin 5 km from the waste panels. The actual dependent variables in the regression analyses are the integrated releases from time of intrusion (i.e., 1000 yrs for scenario $S(1,0,0,0,0)$) to 10,000 yrs. Thus, the dependent variables in the regression analyses summarized in the columns labeled "Release to Culebra", "Quarter Distance", "Half Distance" and "Full Distance" in Table 4.5-1 and other similar tables are integrated radionuclide releases from time of intrusion to 10,000 yrs into the Culebra, through a surface 1.25 km from the repository, through a surface 2.5 km from the repository and through a surface 5 km from the repository, respectively. Further, the column labeled "Variable" lists the variables in the order that they entered the stepwise regression analysis, and the column labeled "R^2" lists the cumulative R^2 value for all variables included in the regression model through the step under consideration. The "+" or "-" appearing in parentheses after the R^2 value designates the sign of the regression coefficient for the variable entering the regression model at the step under consideration. Regression diagnostics (i.e., α-values and the

TABLE 4.5-1. STEPWISE REGRESSION ANALYSES WITH RANK-TRANSFORMED DATA FOR SCENARIO $S(1,0,0,0,0)$ WITH GAS GENERATION IN THE REPOSITORY, A DUAL-POROSITY TRANSPORT MODEL IN THE CULEBRA DOLOMITE AND INTRUSION OCCURRING 1000 YRS AFTER REPOSITORY CLOSURE

	Release to Culebra		Quarter Distance		Half Distance		Full Distance	
Step	Variable	R^2	Variable	R^2	Variable	R^2	Variable	R^2
Dependent Variable: Integrated Discharge Am-241								
1	SALPERM	0.59(+)	--	--	SALPERM	0.14 (+)	--	--
2					FKDAM	0.24 (+)		
3					MKDAM	0.32 (-)		
4					CULFRPOR	0.39 (+)		
Dependent Variable: Integrated Discharge Np-237								
1	SALPERM	0.53(+)	MBPERM	0.20 (+)	SALPERM	0.19 (+)	MBPERM	0.11 (+)
2					MKDNP	0.30 (-)		
Dependent Variable: Integrated Discharge Pu-239								
1	SALPERM	0.56(+)	CULCLIM	0.09 (+)	MBPERM	0.18 (+)	--	--
2					FKDPU	0.27 (+)		
3					VWOOD	0.34 (-)		
Dependent Variable: Integrated Discharge Pu-240								
1	SALPERM	0.56(+)	CULCLIM	0.09 (+)	MBPERM	0.18 (+)	--	--
2					FKDPU	0.27 (+)		
3					VWOOD	0.34 (-)		
Dependent Variable: Integrated Discharge Th-230								
1	SALPERM	0.55(+)	SALPERM	0.48 (+)	SALPERM	0.23 (+)	MKDU	0.20 (-)
2			CULFRPOR	0.57 (+)	MKDU	0.39 (-)	SALPERM	0.34 (+)
3			MKDU	0.65 (-)	CULFRPOR	0.45 (+)	CULCLIM	0.52 (+)
Dependent Variable: Integrated Discharge U-233								
1	SALPERM	0.59(+)	SALPERM	0.32 (+)	SALPERM	0.18 (+)	MKDU	0.17 (-)
2			MKDU	0.46 (-)	MKDU	0.33 (-)	SALPERM	0.32 (+)
3			CULFRPOR	0.56 (+)				
4			CULCLIM	0.61 (+)				

TABLE 4.5-1. STEPWISE REGRESSION ANALYSES WITH RANK-TRANSFORMED DATA FOR SCENARIO *S*(1,0,0,0,0) WITH GAS GENERATION IN THE REPOSITORY, A DUAL-POROSITY TRANSPORT MODEL IN THE CULEBRA DOLOMITE AND INTRUSION OCCURRING 1000 YRS AFTER REPOSITORY CLOSURE (concluded)

	Release to Culebra		Quarter Distance		Half Distance		Full Distance	
Step	Variable	R^2	Variable	R^2	Variable	R^2	Variable	R^2
Dependent Variable: Integrated Discharge U-234								
1	SALPERM	0.59(+)	SALPERM	0.38 (+)	SALPERM	0.23 (+)	MKDU	0.26 (-)
2			MKDU	0.54 (-)	MKDU	0.43 (-)	SALPERM	0.36 (+)
3			CULFRPOR	0.61 (+)	CULFRPOR	0.51 (+)	CULTRFLD	0.42 (+)
4					CULCLIM	0.57 (+)		
Dependent Variable: EPA Sum for Total Integrated Discharge								
1	SALPERM	0.58(+)	SALPERM	0.51 (+)	SALPERM	0.42 (+)	SALPERM	0.20 (+)
2			CULFRPOR	0.59 (+)	MKDU	0.51 (-)	MKDU	0.32 (-)
3			MKDU	0.64 (-)	CULFRPOR	0.59 (+)	CULCLIM	0.41 (+)
4			CULCLIM	0.69 (+)				
5			MKDAM	0.73 (-)				

PRESS criterion) were used to provide guidance on the variables selected for inclusion in the final regression models. However, the final selection of variables had a significant subjective component, with spurious variables being excluded from the final regression models. The stepwise regression analyses presented in this report were performed with the STEPWISE program (Iman et al., 1980). An overview of the regression-based sensitivity analysis techniques used in the generation of Table 4.5-1 and other similar tables in this report is provided in Section 3.5.2 of Vol. 1, and a more detailed description of these techniques is given in Helton et al. (1991).

As examination of the R^2 values associated with the individual regression analyses in Table 4.5-1 shows, none of the regressions are particularly successful in accounting for the observed variation in either the releases for the individual isotopes or the total EPA normalized release. Specifically, the largest R^2 value in Table 4.5-1 is 0.73 and most R^2 values are considerably smaller. This lack of resolution in the regression models is not surprising given the large number of zero releases associated with the scenario *S*(1,0,0,0,0).

When thresholds and other complex relationships are present, the examination of scatterplots is often revealing. The scatterplots presented in Figure 4.5-1 for the normalized release of Pu-239 to the Culebra provide an excellent example of the type of information that can sometimes be extracted from scatterplots. As a reminder, the stepwise regression analysis presented in Table 4.5-1 for the release of Pu-239 to the Culebra for scenario $S(1,0,0,0,0)$ selected only the variable SALPERM (Salado permeability) with an R^2 value of 0.56, which indicates that the release is dominated by SALPERM but also that much of the variability in the release is not accounted for. The upper two scatterplots in Figure 4.5-1 provide significantly more insight into what controls the release of Pu-239 to the Culebra.

As shown by the scatterplot appearing in the upper left of Figure 4.5-1, the variable SALPERM acts as a switch for scenario $S(1,0,0,0,0)$ with zero (i.e., $< 10^{-8}$) releases of Pu-239 resulting for SALPERM $< 5 \times 10^{-21}$ m^2, and nonzero releases resulting for SALPERM $> 5 \times 10^{-21}$ m^2. However, given that there is a nonzero release, there is little relationship between SALPERM and the size of the release. As shown by the scatterplot appearing in the upper right of Figure 4.5-1, the size of the nonzero releases is dominated by SOLPU (solubility for Pu).* Thus, SALPERM determines whether or not there is a Pu-239 release to the Culebra, and given that there is a release, SOLPU determines how big the release is. The variable SALPERM acts as a switch for scenario $S(1,0,0,0,0)$ because it determines how long will be required for a waste panel to fill with brine. If the pore space in a waste panel does not fill with brine due to a low value for SALPERM, then there can be no fluid flow to the Culebra and hence no radionuclide release.

For comparison, the lower two frames in Figure 4.5-1 show scatterplots of Pu-239 release to the Culebra versus SALPERM (Salado permeability) and SOLPU (solubility for Pu) for scenario $S^{+-}(2,0,0,0,0)$. As examination of these scatterplots shows, SALPERM has no effect on the Pu-239 release to the

---

* The elements Np, Pu and U were assigned two solubilities (i.e., SOLNP4, SOLNP5, SOLPU4, SOLPU5, SOLU4, SOLU6), with only one solubility being used in each sample element as determined by the variable EHPH (index variable used to select the relative areas of the stability regimes for different oxidation states of Np, Pu and U). All scatterplots involving solubilities presented in this report display the actual solubilities used in the calculation of the releases shown in the plot. Further, the solubilities SOLNP4 and SOLNP5 were sampled with a rank correlation of 0.99, as were the solubilities SOLPU4 and SOLPU5 and also the solubilities SOLU4 and SOLU6. As a result, the variables in the pairs (SOLNP4, SOLNP5), (SOLPU4, SOLPU5) and (SOLU4, SOLU6) are essentially indistinguishable in a regression analysis with rank-transformed data. Therefore, the regression analyses presented in this report use the symbols SOLNP, SOLPU and SOLU to designate the solubility limits for Np, Pu and U.

Scenario: $S(1,0,0,0,0)$, Assumed Intrusion Time: 1000 yrs

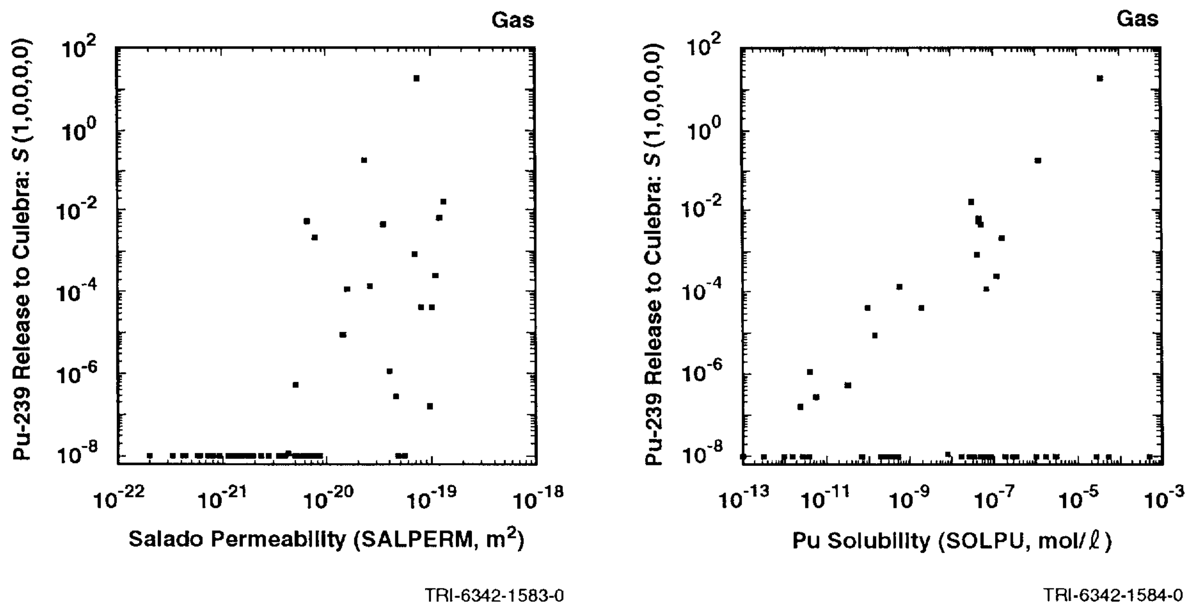

Scenario: $S^{+-}(2,0,0,0,0)$, Assumed Intrusion Time: 1000 yrs

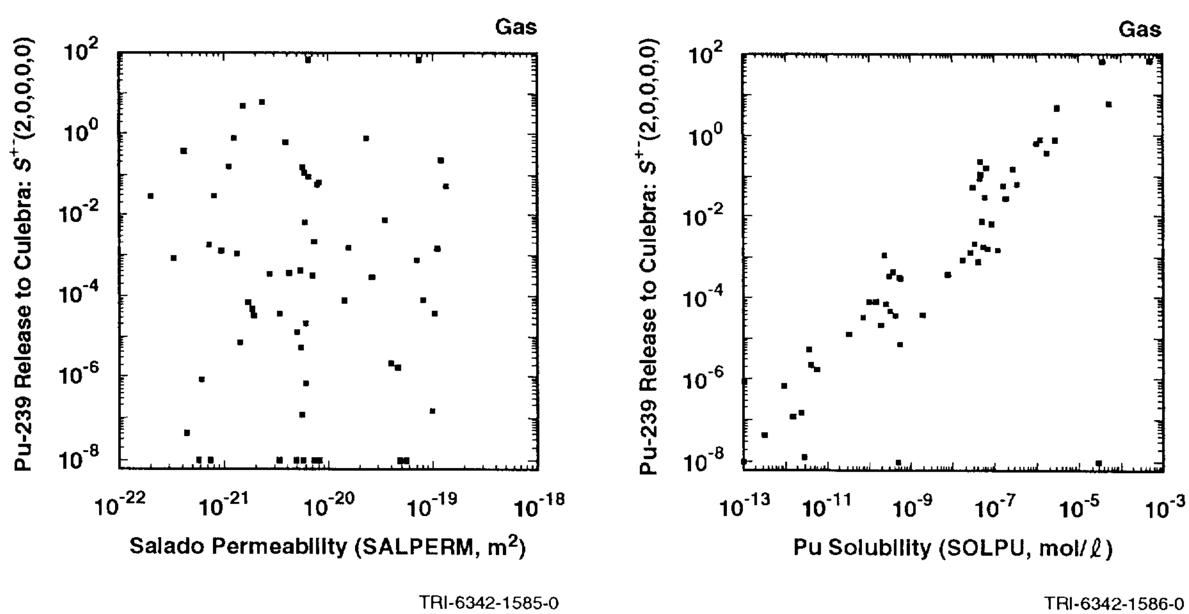

Figure 4.5-1. Scatterplots for Normalized Release of Pu-239 to the Culebra Dolomite with Gas Generation in the Repository and Intrusion Occurring at 1000 Yrs for Variables SALPERM (Salado permeability) and SOLPU (solubility for Pu) and Scenarios $S(1,0,0,0,0)$ and $S^{+-}(2,0,0,0,0)$.

Culebra for scenario $S^{+-}(2,0,0,0,0)$, with the release being dominated by SOLPU. Large brine flows take place through a waste panel for scenario $S^{+-}(2,0,0,0,0,)$ due to the penetration of a pressurized brine pocket, with the result that additional brine inflow that might be influenced by SALPERM is of reduced importance.

Due to its role in determining whether or not the waste panels resaturate, SALPERM (Salado permeability) acts as a switch for all isotopes for scenario $S(1,0,0,0,0)$. Further, the release patterns shown by Pu-239 in Figure 4.5-1 for scenarios $S(1,0,0,0,0)$ and $S^{+-}(2,0,0,0,0)$ are also displayed by Pu-240 and Th-230. A related, but somewhat different, pattern is shown by U-234. As before, SALPERM acts as a switch for scenario $S(1,0,0,0,0)$ but the impact of solubility is reduced due to inventory limits. Scatterplots for BHPERM (borehole permeability) and SOLU (solubility for U) are shown in Figure 4.5-2. The scatterplots for the release of U-234 to the Culebra for scenario $S(1,0,0,0,0)$ show small positive effects for BHPERM and SOLU. However, these effects are not very strong. As a reminder, the numerous zero releases are resulting from the effect of SALPERM as a switch.

Examination of the scatterplots in Figure 4.5-2 for scenario $S^{+-}(2,0,0,0,0)$ gives a clearer view of what is happening. As indicated by the straight lines of points in the two lower scatterplots, many sample elements are resulting in equal releases for scenario $S^{+-}(2,0,0,0,0)$. As shown in Figure 2.4-2, these equal releases correspond to the inventory of U-234 in a single panel. Thus, the release of U-234 for scenario $S^{+-}(2,0,0,0,0)$ is often inventory limited. As the two lower scatterplots in Figure 4.5-2 show, the release of U-234 to the Culebra for scenario $S^{+-}(2,0,0,0,0)$ tends to increase as BHPERM (borehole permeability) and SOLU (solubility for U) increase. However, the larger values assigned to either of these variables result in a complete removal of the U-234 inventory. The indicated effect for BHPERM results because large values for BHPERM lead to large brine flows through the repository and hence a complete removal of U-234 even for the smaller values of SOLU. Similarly, large values of SOLU result in a complete removal of U-234 unless the brine flows are very small (i.e., there are a few sample elements in which a large value for SOLU does not lead to a complete removal of U-234).

The scatterplots shown in Figure 4.5-2 for scenario $S(1,0,0,0,0)$ do not display patterns that are as well-defined as in the scatterplots for scenario $S^{+-}(2,0,0,0,0)$. However, with the insights gained from the scatterplots for scenario $S^{+-}(2,0,0,0,0)$, it is possible to get a better feeling for what is happening for scenario $S(1,0,0,0,0)$. As shown in Figure 4.4-8, the brine

Scenario: $S(1,0,0,0,0)$, Assumed Intrusion Time: 1000 yrs

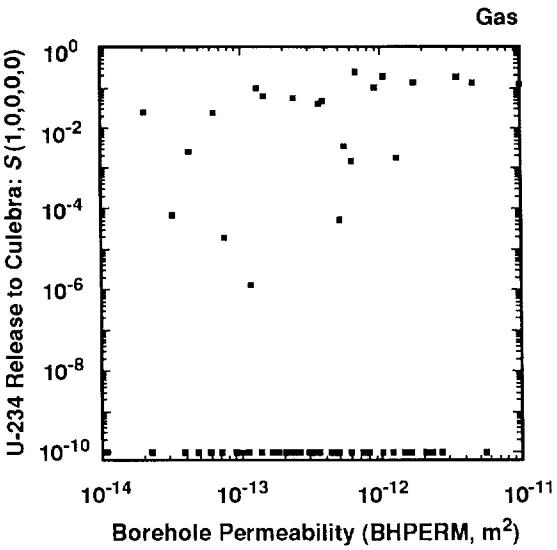

TRI-6342-1619-0

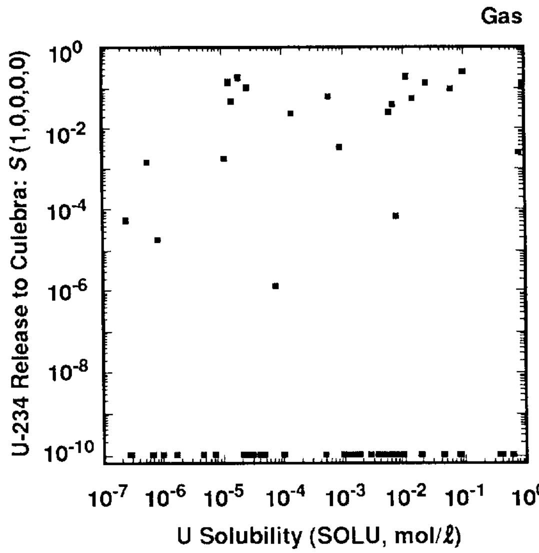

TRI-6342-1620-0

Scenario: $S^{+-}(2,0,0,0,0)$, Assumed Intrusion Time: 1000 yrs

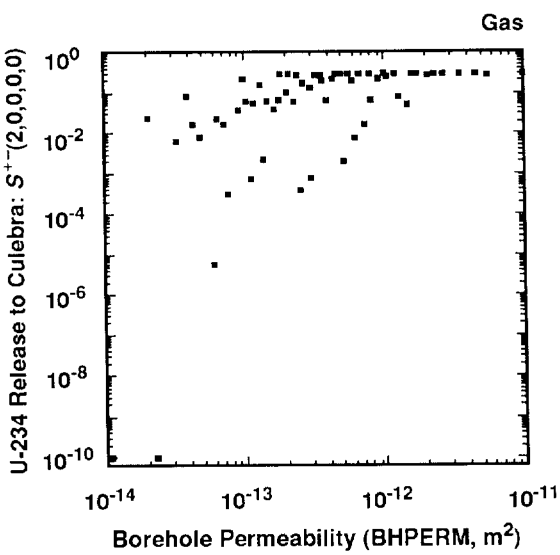

TRI-6342-1621-0

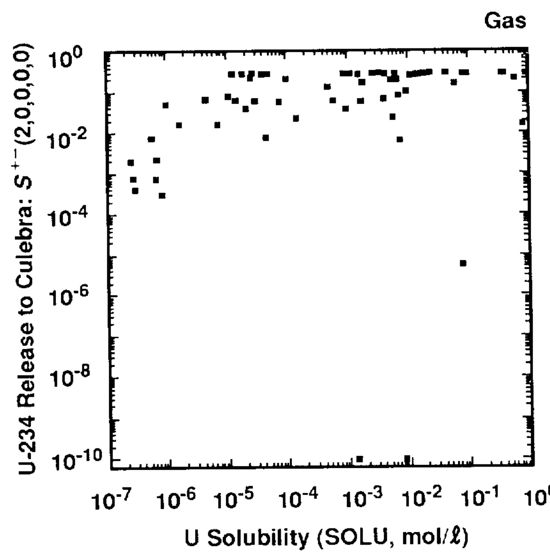

TRI-6342-1622-0

Figure 4.5-2. Scatterplots for Normalized Release of U-234 to the Culebra Dolomite with Gas Generation in the Repository and Intrusion Occurring at 1000 Yrs for Variables BHPERM (borehole permeability) and SOLU (solubility for U) and Scenarios $S(1,0,0,0,0)$ and $S^{+-}(2,0,0,0,0)$.

flows out of the repository are much smaller for scenario $S(1,0,0,0,0)$ than for scenario $S^{+-}(2,0,0,0,0)$. Increasing BHPERM increases this flow and hence tends to increase the release; similarly, increasing SOLU increases the amount of U-234 that can be dissolved and hence tends to increase the size of the release. However, the small size of these flows and their variability due to the effects of other variables such as SALPERM (Salado permeability) and SALPRES (Salado pressure)* produces a more diffuse pattern. Further, the larger values of BHPERM and SOLU for scenario $S(1,0,0,0,0)$ come very close to producing inventory-limited results, although the inventory limits are not quite reached and so the scatterplots for scenario $S(1,0,0,0,0)$ in Figure 4.5-2 do not have the flattened tops displayed by the scatterplots for scenario $S^{+-}(2,0,0,0,0)$.

Scatterplots for the release of Am-241 to the Culebra for BHPERM (borehole permeability) and SOLAM (solubility for Am) are given in Figure 4.5-3 for scenarios $S(1,0,0,0,0)$ and $S^{+-}(2,0,0,0,0)$. The release behavior for Am-241 is similar to that of U-234, although it is complicated by the relatively short half-life (i.e., 432 yrs) of Am-241. For scenario $S(1,0,0,0,0)$, the release to the Culebra tends to increase as BHPERM and SOLAM increase, and many zero releases occur due to the previously discussed role of SALPERM (Salado permeability). However, except for the role of SALPERM as a switch, the relations between the sampled variables and release to the Culebra tend to be rather diffuse for scenario $S(1,0,0,0,0)$.

A somewhat clearer pattern of relationships is shown in Figure 4.5-3 for scenario $S^{+-}(2,0,0,0,0)$. A well-defined relationship between release to the Culebra and BHPERM (borehole permeability) is shown, with the release tending to increase as BHPERM increases. As discussed with respect to U-234, increasing BHPERM increases brine flow through the waste panel and hence release to the Culebra. This effect is particularly important for Am-241 because release to the Culebra is competing with radioactive decay; if Am-241 is not transported to the Culebra relatively early in the 10,000-yr time period that must be considered in the EPA regulations, very little release can occur. The scatterplot for SOLAM (solubility for Am) shows the Am-241 releases to the Culebra increasing as SOLAM increases, with a tendency for the release to level off for larger values of SOLAM (i.e., $> 10^{-7}$ mol/ℓ). As shown in Figure 2.4-2, the inventory of Am-241 in a single waste panel at 1000 yrs is approximately 30 EPA units, which declines rapidly with increasing time due to radioactive decay. The flattening shown in the relationship between release to the Culebra and SOLAM for Am-241, which is bounded above by approximately 10 EPA units, is probably due to inventory

---

* See Tables 4.5-3 and 5.1-1.

Scenario: $S(1,0,0,0,0)$, Assumed Intrusion Time: 1000 yrs

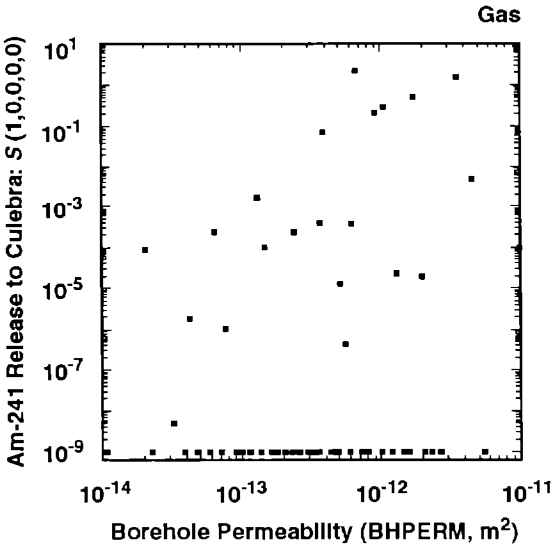

TRI-6342-1684-0

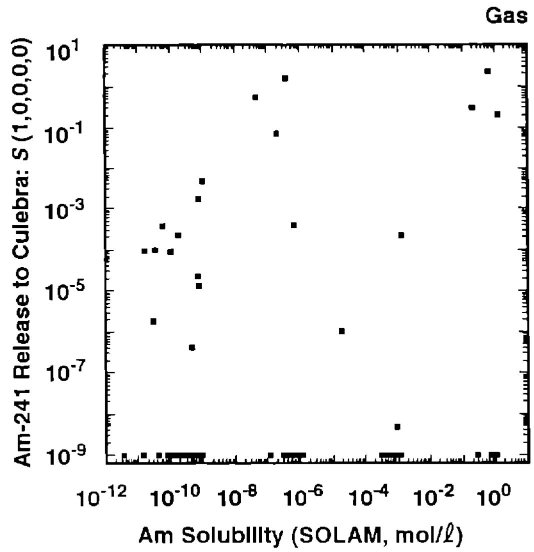

TRI-6342-1685-0

Scenario: $S^{+-}(2,0,0,0,0)$, Assumed Intrusion Time: 1000 yrs

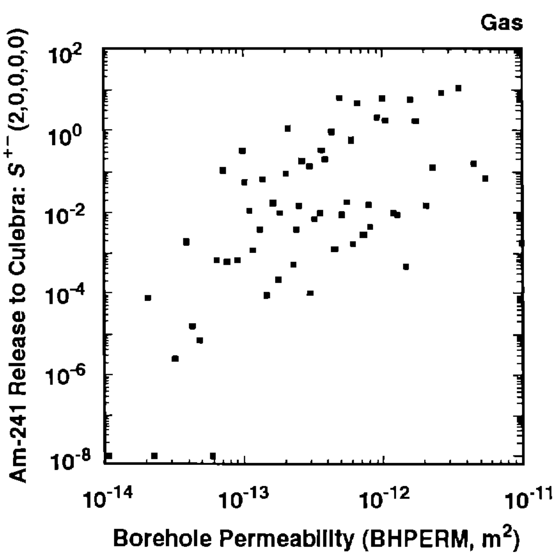

TRI-6342-1686-0

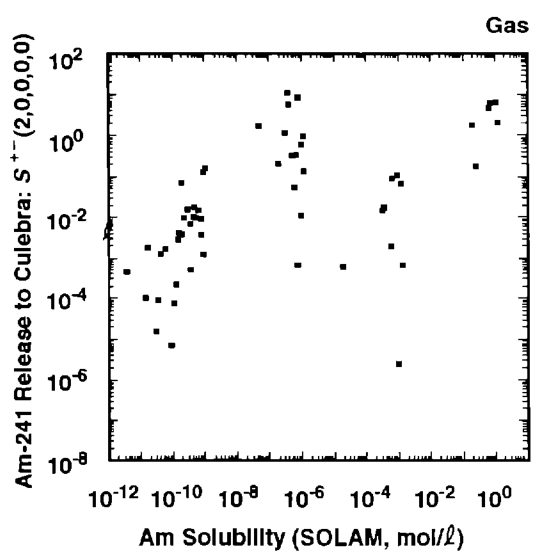

TRI-6342-1687-0

Figure 4.5-3. Scatterplots for Normalized Release of Am-241 to the Culebra Dolomite with Gas Generation In the Repository and Intrusion Occurring at 1000 Yrs for Variables BHPERM (borehole permeability) and SOLAM (solubility for Am) and Scenarios $S(1,0,0,0,0)$ and $S^{+-}(2,0,0,0,0)$.

limitations. The pattern for Am-241 is not as clean as the corresponding pattern shown in Figure 4.5-2 for U-234 due to the strong time dependence of the Am-241 inventory (i.e., compare the time-dependent inventories of Am-241 and U-234 shown in Figure 2.4-2).*

Thus far, the discussion of the sensitivity analysis results in Table 4.5-1 for scenario $S(1,0,0,0,0)$ has focused on the release of individual isotopes to the Culebra. Corresponding releases for scenario $S^{+-}(2,0,0,0,0)$ have also been discussed. Total releases (i.e., summed over all isotopes) to the Culebra and also to the accessible environment for scenario $S(1,0,0,0,0)$ are now considered. As shown by the R^2 values for the regressions for "EPA Sum for Total Integrated Discharge" in Table 4.5-1, the regression models are performing poorly in determining the relationships between the sampled variables and total release, which is not surprising given the complex relationships involving individual isotopes that are shown in Figures 4.5-1 through 4.5-3. Specifically, the final R^2 values for the four regressions are 0.58, 0.73, 0.59 and 0.41. Additional insight on what is causing the variation in total release for scenario $S(1,0,0,0,0)$ can be obtained from the scatterplots in Figure 4.5-4.

The top pair of scatterplots in Figure 4.5-4 is for the total normalized release from the repository to the Culebra. As previously observed for the individual isotopes (e.g., see Figure 4.5-1), SALPERM (Salado permeability) acts as a switch, with a value of approximately 5×10^{-21} m^2 determining whether or not a release to the Culebra will occur. Further, given that a release occurs, its value tends to increase as SALPERM increases. Similarly, releases also tend to increase as BHPERM (borehole permeability) increases, although zero releases are interspersed throughout the range of BHPERM due to the effects of SALPERM. The lower pair of scatterplots in Figure 4.5-4 is for the total normalized release to the accessible environment. As examination of these scatterplots shows, only seven sample elements result in nonzero releases to the accessible environment. Further, these releases tend to increase as BHPERM and SALPERM increase. The large number of zero releases indicated by the scatterplots in Figure 4.5-4 are obscuring (i.e., censoring) the effects of individual variables and, as a result, are leading to regression models with low R^2 values.

---

* The results presented in Figure 4.5-3 are for gas generation in the repository, which does have an effect on the time required to fill the pore space in a waste panel with brine. This effect is more important for isotopes such as Am-241 that have short half-lives than for isotopes with longer half-lives. The effects discussed in this paragraph can be seen more clearly in Figure 5.1-7, which presents the same results but without the assumption of gas generation in the repository.

Scatterplots for Normalized Release to Culebra Dolomite

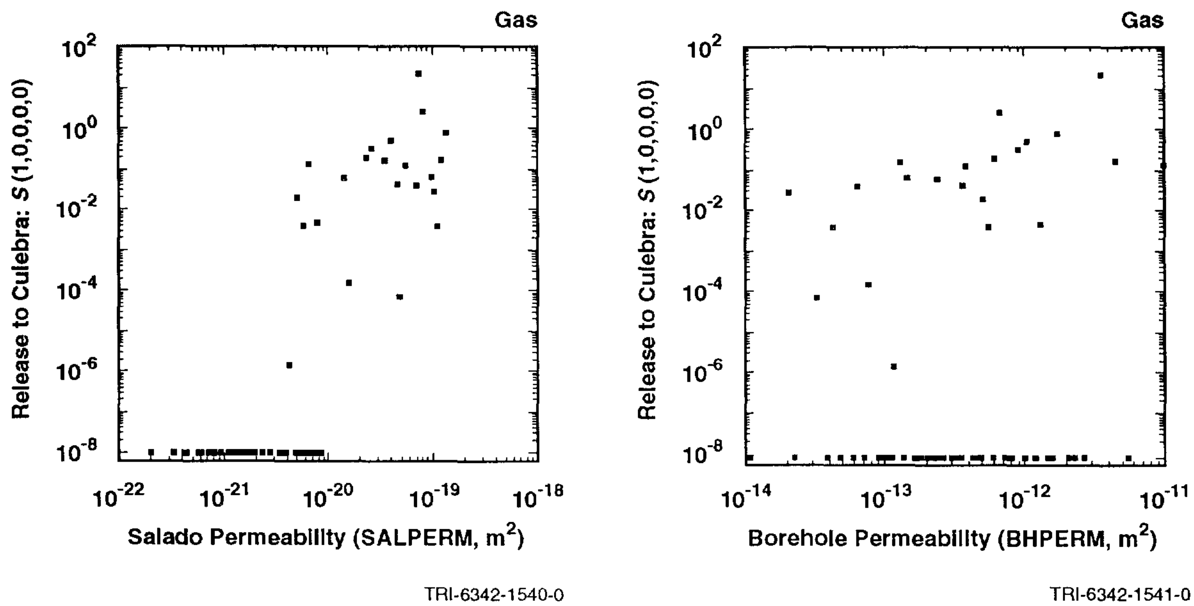

Scatterplots for Normalized Release to Accessible Environment

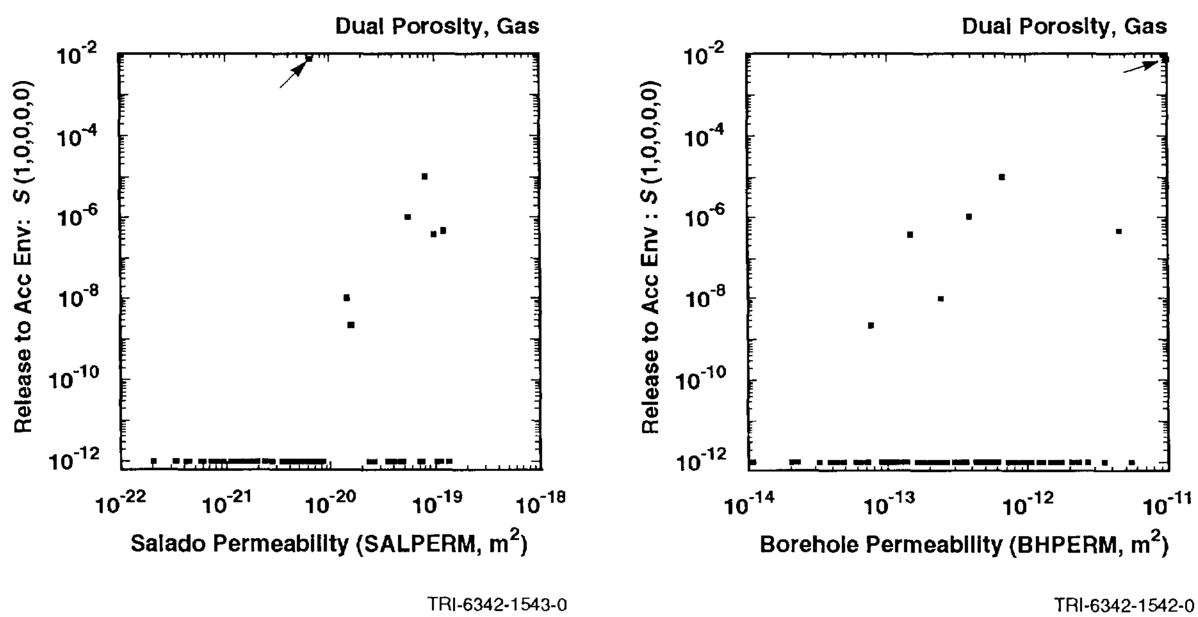

Figure 4.5-4. Scatterplots for Total Normalized Release Associated with Scenario $S(1,0,0,0,0)$ for Groundwater Transport with Gas Generation in the Repository, a Dual-Porosity Transport Model in the Culebra Dolomite and Intrusion Occurring at 1000 Yrs.

Table 4.5-1 also contains analyses for the integrated releases of individual isotopes at one-quarter, one-half and the full distance to the accessible environment. The regressions are very poor, with most analyses leading to final regression models with R^2 values less than 0.5. The reason for this is simple: most of the releases are zero. As already discussed, SALPERM (Salado permeability) causes approximately half the releases to the Culebra to be zero. Further, retardation prevents all isotopes from reaching the accessible environment for most sample elements. The limited releases due to transport within the Culebra as illustrated are Figures 4.4-1, 4.4-2 and 4.5-4.

Rank regressions for scenario $S^{+-}(2,0,0,0,0)$ are presented in Table 4.5-2. The individual regression analyses in Table 4.5-2 generally have higher R^2 values than the corresponding analyses in Table 4.5-1 for scenario $S(1,0,0,0,0)$, which is not surprising given the larger number of nonzero releases for scenario $S^{+-}(2,0,0,0,0)$. As previously discussed in conjunction with Figures 4.5-1 through 4.5-3, the most important variables for release to the Culebra are BHPERM (borehole permeability) and the solubilities for the individual elements (i.e., SOLU, SOLNP, SOLAM, SOLTH and SOLPU). As an example, Figure 4.5-5 contains the scatterplot for BHPERM and total normalized release to the Culebra and shows the well-defined trend between increasing values for BHPERM and increasing releases to the Culebra. After BHPERM and the solubilities, the most important variable is BPPRES (brine pocket pressure).

The matrix distributions coefficients (i.e, MKDU, MKDNP, MKDTH and MKDPU) tend to be the most important variables for integrated release at various points along the transport path in the Culebra. The R^2 values tend to decrease as the length of the transport path increases due to both an increasing number of variables that can affect the results and an increasing number of zero releases. The scatterplots in Figure 4.5-6 for integrated radionuclide transport in the Culebra for one-quarter the distance to the accessible environment provide a graphical representation for what is happening. The top two scatterplots are for Am-241 and Pu-239 versus their matrix distribution coefficients MKDAM and MKDPU. Effectively, all the releases for these two isotopes are zero even though transport is for only one-quarter the distance to the accessible environment (i.e., the largest integrated release values for Am-241 and Pu-239 are less than 10^{-19} and 10^{-9}, respectively). The lower two scatterplots for U-234 are more interesting. The U-234 releases tend to decrease as MKDU (matrix distribution coefficient for U) increases until a switch is reached at a value of approximately 10^{-3} m^3/kg for MKDU, after which the integrated release values for U-234 are zero (i.e., $< 10^{-10}$). Further, given that there is a nonzero release for U-234, this release tends to increase as BHPERM (borehole permeability)

TABLE 4.5-2. STEPWISE REGRESSION ANALYSES WITH RANK-TRANSFORMED DATA FOR SCENARIO S^{+-}(2,0,0,0,0) WITH GAS GENERATION IN THE REPOSITORY, A DUAL-POROSITY TRANSPORT MODEL IN THE CULEBRA DOLOMITE AND INTRUSION OCCURRING 1000 YRS AFTER REPOSITORY CLOSURE

	Release to Culebra		Quarter Distance		Half Distance		Full Distance	
Step	Variable	R^2	Variable	R^2	Variable	R^2	Variable	R^2
Dependent Variable: Integrated Discharge Am-241								
1	SOLAM	0.36 (+)	--	--	--	--	--	--
2	BHPERM	0.74 (+)						
3	BPPRES	0.78 (+)						
Dependent Variable: Integrated Discharge Np-237								
1	SOLNP	0.65 (+)	FKDNP	0.18 (-)	MKDNP	0.55 (-)	MKDNP	0.26 (-)
2	BHPERM	0.78 (+)	MKDNP	0.34 (-)	GRCORI	0.36 (-)		
3	BPPRES	0.82 (+)	BHPERM	0.41 (+)				
4	EHPH	0.85 (+)						
5	GRCORI	0.88 (-)						
Dependent Variable: Integrated Discharge Pu-239								
1	SOLPU	0.74 (+)	MKDPU	0.16 (-)	MKDPU	0.16 (-)	--	--
2	BHPERM	0.85 (+)	FKDPU	0.28 (-)				
3			CULPOR	0.35 (-)				
Dependent Variable: Integrated Discharge Pu-240								
1	SOLPU	0.74 (+)	CULPOR	0.15 (-)	MKDPU	0.17 (-)	--	--
2	BHPERM	0.85 (+)	MKDPU	0.25 (-)				
3			FKDPU	0.35 (-)				
Dependent Variable: Integrated Discharge Th-230								
1	SOLTH	0.69 (+)	MKDU	0.30 (-)	MKDU	0.32 (-)	MKDU	0.35 (-)
2	BHPERM	0.82 (+)	MKDTH	0.45 (-)	MKDTH	0.43 (-)	CULFRSP	0.46 (+)
3			CULFRSP	0.53 (+)	CULFRSP	0.52 (+)	CULCLIM	0.55 (+)
4			DBDIAM	0.58 (+)	CULCLIM	0.58 (+)	MKDTH	0.61 (-)
5			FKDPU	0.63 (-)	FKDPU	0.63 (-)		
6			CULCLIM	0.68 (+)				
7			BHPERM	0.72 (+)				

TABLE 4.5-2. STEPWISE REGRESSION ANALYSES WITH RANK-TRANSFORMED DATA FOR SCENARIO $S^{+-}(2,0,0,0,0)$ WITH GAS GENERATION IN THE REPOSITORY, A DUAL-POROSITY TRANSPORT MODEL IN THE CULEBRA DOLOMITE AND INTRUSION OCCURRING 1000 YRS AFTER REPOSITORY CLOSURE (concluded)

	Release to Culebra		Quarter Distance		Half Distance		Full Distance	
Step	Variable	R^2	Variable	R^2	Variable	R^2	Variable	R^2
Dependent Variable: Integrated Discharge U-233								
1	BHPERM	0.43 (+)	MKDU	0.46 (-)	MKDU	0.48 (-)	MKDU	0.41 (-)
2	SOLU	0.58 (+)	GRCORI	0.53 (-)	SOLNP	0.55 (+)	SOLNP	0.49 (+)
3	BPPRES	0.70 (+)	SOLNP	0.60 (+)	FKDNP	0.60 (-)	FKDNP	0.54 (-)
4	SOLNP	0.74 (-)	BHPERM	0.66 (+)				
5			CULFRSP	0.71 (+)				
6			MKDNP	0.75 (-)				
7			FKDNP	0.77 (-)				
Dependent Variable: Integrated Discharge U-234								
1	BHPERM	0.47 (+)	MKDU	0.62 (-)	MKDU	0.61 (-)	MKDU	0.61 (-)
2	SOLU	0.60 (+)	CULFRSP	0.67 (+)	SOLNP	0.68 (+)	SOLNP	0.68 (+)
3	BPPRES	0.72 (+)	BHPERM	0.71 (+)	CULCLIM	0.71 (+)		
4			CULCLIM	0.74 (+)				
5			EHPH	0.77 (-)				
Dependent Variable: EPA Sum for Total Integrated Discharge								
1	BHPERM	0.46 (+)	MKDU	0.26 (-)	MKDU	0.25 (-)	MKDU	0.24 (-)
2	SOLAM	0.57 (+)	CULFRSP	0.40 (+)	CULFRSP	0.43 (+)	CULFRSP	0.44 (+)
3	BPPRES	0.66 (+)	GRCORI	0.46 (-)	GRCORI	0.49 (-)	GRCORI	0.51 (-)
4	SOLPU	0.69 (+)	BHPERM	0.52 (+)	BHPERM	0.55 (+)	SOLNP	0.58 (+)
5	BPSTOR	0.73 (+)	SOLNP	0.58 (+)	FKDPU	0.60 (-)		
6	SOLU	0.76 (+)	FKDPU	0.63 (-)	MKDNP	0.64 (-)		
7			MKDNP	0.68 (-)	SOLNP	0.68 (+)		
8			FKDNP	0.71 (-)				

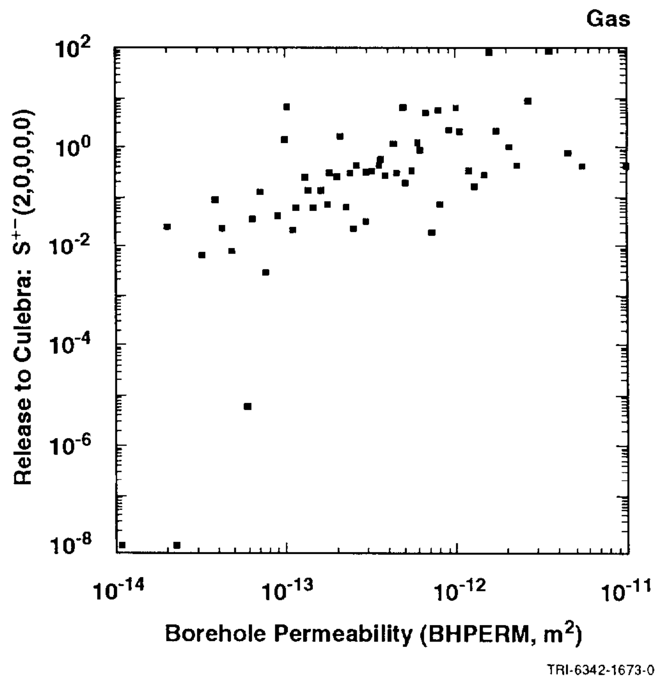

Figure 4.5-5. Scatterplot for Borehole Permeability (BHPERM) versus Total Normalized Release to the Culebra Dolomite for Scenario S^{+-}(2,0,0,0,0) with Gas Generation in the Repository and Intrusion Occurring at 1000 Yrs.

increases. The variable BHPERM is important because it influences both how much U-234 is released to the Culebra and when this release occurs. Specifically, large values for BHPERM result in earlier releases to the Culebra, which allows more time for groundwater transport.

Additional perspective on the variables affecting total release to the accessible environment for scenario S^{+-}(2,0,0,0,0) is provided by the scatterplots appearing in Figure 4.5-7. Of the four variables shown in this figure, only MKDU (matrix distribution coefficient for U) and CULFRSP (Culebra fracture spacing) are selected in the corresponding regression analysis shown in Table 4.5-2 (i.e., the analysis for "EPA Sum for Total Integrated Discharge" at "Full Distance"). As examination of the scatterplots for these variables shows, zero releases tend to be associated with large values of MKDU and the larger releases tend to be associated with the larger values of CULFRSP, which is consistent with the negative regression coefficient determined for MKDU and the positive regression coefficient determined for CULFRSP. The scatterplots for BHPERM (borehole permeability) and CULFRPOR (Culebra fracture porosity) show that both these variables have a positive effect on total release to the accessible environment (i.e., there is a tendency for the release to increase as each of these variables increases). However, neither of these variables is selected

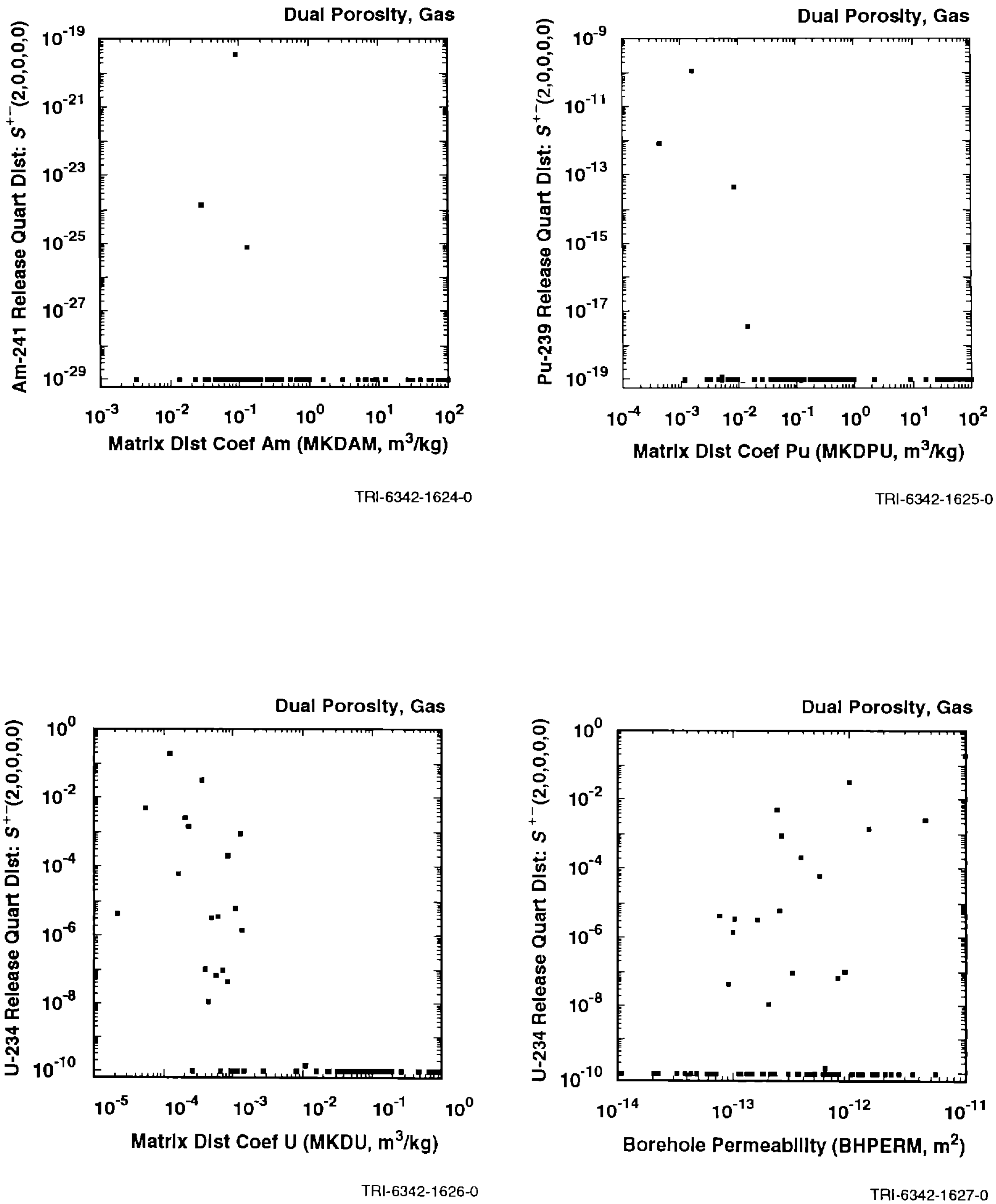

Figure 4.5-6. Scatterplots for Normalized Releases of Individual Isotopes at One-Quarter the Distance to the Accessible Environment for Scenario $S^{+-}(2,0,0,0,0)$ for Groundwater Transport with Gas Generation in the Repository, a Dual-Porosity Transport Model in the Culebra Dolomite and Intrusion Occurring at 1000 Yrs.

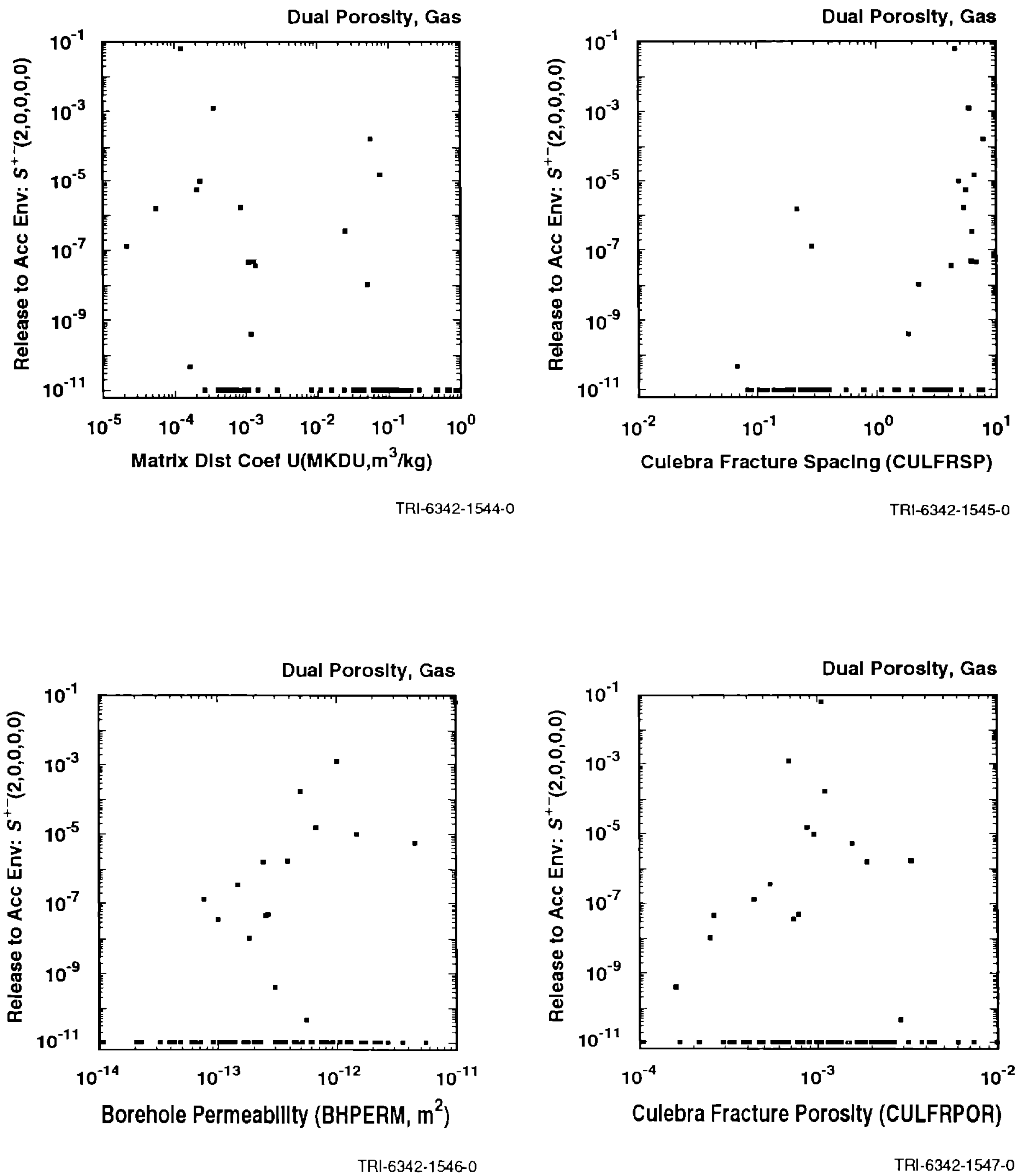

Figure 4.5-7. Scatterplots for Total Normalized Release to the Accessible Environment for Scenario $S^{+-}(2,0,0,0,0)$ for Groundwater Transport with Gas Generation in the Repository, a Dual-Porosity Transport Model in the Culebra Dolomite and Intrusion Occurring at 1000 Yrs.

in the corresponding regression analysis presented in Table 4.5-2 due to the large number of zero releases randomly interspersed over their ranges as a result of the effects of other variables. Thus, total release to the accessible environment for scenario $S^{+-}(2,0,0,0,0)$ provides another example of the fact that, when complex patterns of behavior are present, it is not possible to blindly rely on regression analyses to reveal what is going on. An earlier example of this type of complex behavior was provided by the effect of SALPERM (Salado permeability) on the release to the Culebra for scenario $S(1,0,0,0,0)$.

The sensitivity analysis results in Tables 4.5-1 and 4.5-2 are for groundwater releases to the accessible environment resulting from intrusions occurring at 1000 yrs (i.e., for scenarios $S(1,0,0,0,0)$ and $S^{+-}(2,0,0,0,0)$). Due to the increasing number of zero releases, additional sensitivity analyses for releases to the accessible environment due to intrusions occurring at later times are not particularly revealing. However, due to the larger number of nonzero releases, it is interesting to consider the releases from the repository to the Culebra at additional times.

The total normalized releases to the Culebra due to intrusions occurring at different times are summarized in Figure 4.4-4. Further, the brine flows that carry these releases from the repository to the Culebra are summarized in Figure 4.4-8. Stepwise regression analyses for the brine flows and radionuclide releases summarized in these figures are given in Table 4.5-3. For the E2-type scenarios (i.e., $S(1,0,0,0,0)$, ..., $S(0,0,0,0,1)$), both the brine flows and the normalized releases are dominated by SALPERM (Salado permeability), BHPERM (borehole permeability) and MBPERM (marker bed permeability). For the E1E2-type scenarios (i.e., $S^{+-}(2,0,0,0,0)$ through $S^{+-}(0,0,0,0,2)$), the brine flows are dominated by BHPERM, BPPRES (brine pocket pressure) and DBDIAM (drill bit diameter), and the normalized releases are dominated by BHPERM, BPPRES and solubilities for individual elements (e.g., SOLAM, SOLPU, SOLU). For releases into the Culebra overall, SALPERM is the most important variable for E2-type scenarios, and BHPERM is the most important variable for E1E2-type scenarios.

The elements Np, Pu and U were assigned two solubilities (i.e., SOLNP4, SOLNP5, SOLPU4, SOLPU5, SOLU4 and SOLU6), with only one solubility being used in each sample element as determined by the variable EHPH (index variable used to select the relative areas of the stability regimes for different oxidation states of Np, Pu and U) (Trauth et al., 1991). Specifically, EHPH has a value between 0 and 1 for each sample element. As indicated in Table 3-1 and discussed in more detail in Section 3.5-5 of Vol. 3, solubilities (i.e., SOLNP, SOLPU and SOLU) are then assigned in the following manner for calculations with the PANEL program for each sample element:

TABLE 4.5-3. STEPWISE REGRESSION ANALYSES WITH RANK-TRANSFORMED DATA FOR TOTAL BRINE RELEASE AND TOTAL NORMALIZED RELEASE TO THE CULEBRA DOLOMITE WITH GAS GENERATION IN THE REPOSITORY

	Total Brine		Total Release		Total Brine		Total Release	
Step	Variable	R^2	Variable	R^2	Variable	R^2	Variable	R^2
Time of Intrusion: 1000 yrs								
	Scenario: $S(1,0,0,0,0)$				Scenario: $S^{+-}(2,0,0,0,0)$			
1	SALPERM	0.58(+)	SALPERM	0.58(+)	BHPERM	0.81(+)	BHPERM	0.46(+)
2					BPPRES	0.94(+)	SOLAM	0.57(+)
3					DBDIAM	0.96(+)	BPPRES	0.66(+)
4							SOLPU	0.69(+)
5							BPSTOR	0.73(+)
6							SOLU	0.76(+)
Time of Intrusion: 3000 yrs								
	Scenario: $S(0,1,0,0,0)$				Scenario: $S^{+-}(0,2,0,0,0)$			
1	SALPERM	0.59(+)	SALPERM	0.59(+)	BHPERM	0.81(+)	BHPERM	0.49(+)
2			MBPERM	0.63(+)	BPPRES	0.94(+)	BPPRES	0.62(+)
3					DBDIAM	0.96(+)	SOLPU	0.69(+)
Time of Intrusion: 5000 yrs								
	Scenario: $S(0,0,1,0,0)$				Scenario: $S^{+-}(0,0,2,0,0)$			
1	SALPERM	0.54(+)	SALPERM	0.54(+)	BHPERM	0.82(+)	BHPERM	0.51(+)
2	BHPERM	0.58(+)	BHPERM	0.58(+)	BPPRES	0.94(+)	BPPRES	0.64(+)
3					DBDIAM	0.96(+)	SOLPU	0.70(+)
4							SOLU	0.73(+)
Time of Intrusion: 7000 yrs								
	Scenario: $S(0,0,0,1,0)$				Scenario: $S^{+-}(0,0,0,2,0)$			
1	MBPERM	0.39(+)	MBPERM	0.40(+)	BHPERM	0.83(+)	BHPERM	0.60(+)
2	BHPERM	0.49(+)	BHPERM	0.50(+)	BPPRES	0.92(+)	BPPRES	0.71(+)
3					DBDIAM	0.95(+)	SOLPU	0.75(+)
4							SOLU	0.77(+)
Time of Intrusion: 9000 yrs								
	Scenario: $S(0,0,0,0,1)$				Scenario: $S^{+-}(0,0,0,0,2)$			
1	--	--	--	--	BHPERM	0.78(+)	BHPERM	0.72(+)
2					BPPRES	0.83(+)	BPPRES	0.78(+)
3					DBDIAM	0.85(+)	SOLU	0.80(+)

$$SOLNP = \begin{cases} SOLNP4 \text{ if } EHPH < 0.485 \\ SOLNP5 \text{ if } EHPH \geq 0.485, \end{cases}$$

$$SOLPU = \begin{cases} SOLPU4 \text{ if } EHPH < 0.539 \\ SOLPU5 \text{ if } EHPH \geq 0.539 \end{cases}$$

and

$$SOLU = \begin{cases} SOLU4 \text{ if } EHPH < 0.299 \\ SOLU6 \text{ if } EHPH \geq 0.299. \end{cases}$$

Three scatterplots and one box plot showing the effects of these assignments on release to the Culebra for scenario $S^{+-}(2,0,0,0,0)$ are given in Figure 4.5-8.

The scatterplots are for EHPH (index variable used to select the relative areas of the stability regimes for different oxidation states of Np, Pu and U) versus normalized release of Np, Pu and U to the Culebra. The vertical lines in the scatterplots indicate where the transition from the use of the solubility for one oxidation state to the solubility for the other oxidation state takes place. Although EHPH provides no ordering on the solubilities actually used for a given oxidation state, there should be a general shift in the locations of the points associated with the two oxidation states for a given element if the solubility for one oxidation state tends to produce larger releases than the solubility for the other oxidation state. The three scatterplots give little indication of such a shift. Use of SOLNP5 produces somewhat larger releases for Np than use of SOLNP4, although the effect is not very striking given the large overall variation in release size. Basically, the ranges associated with the individual solubilities are so large and overlap to such an extent that the effects of the different oxidation states are lost. The box plot in Figure 4.5-8 provides a more compact representation of the information contained in the scatterplots and clearly shows the great extent to which the releases predicted with the solubilities for different oxidation states overlap. As indicated in the figure, the number of observations used in the construction of each box plot depends on how many times the corresponding solubility was used in the original sample of size 60 (e.g., 29 observations were used in the construction of the box plot for Np^{+4}).

The distribution of CCDFs for normalized release to the accessible environment due to groundwater transport is shown in the lower left frame of Figure 4.1-2. This is not a particularly interesting distribution as only 4 CCDFs out of a total of 60 are nonzero within the probability and consequence ranges under consideration. For comparison, Figure 4.5-9 shows the

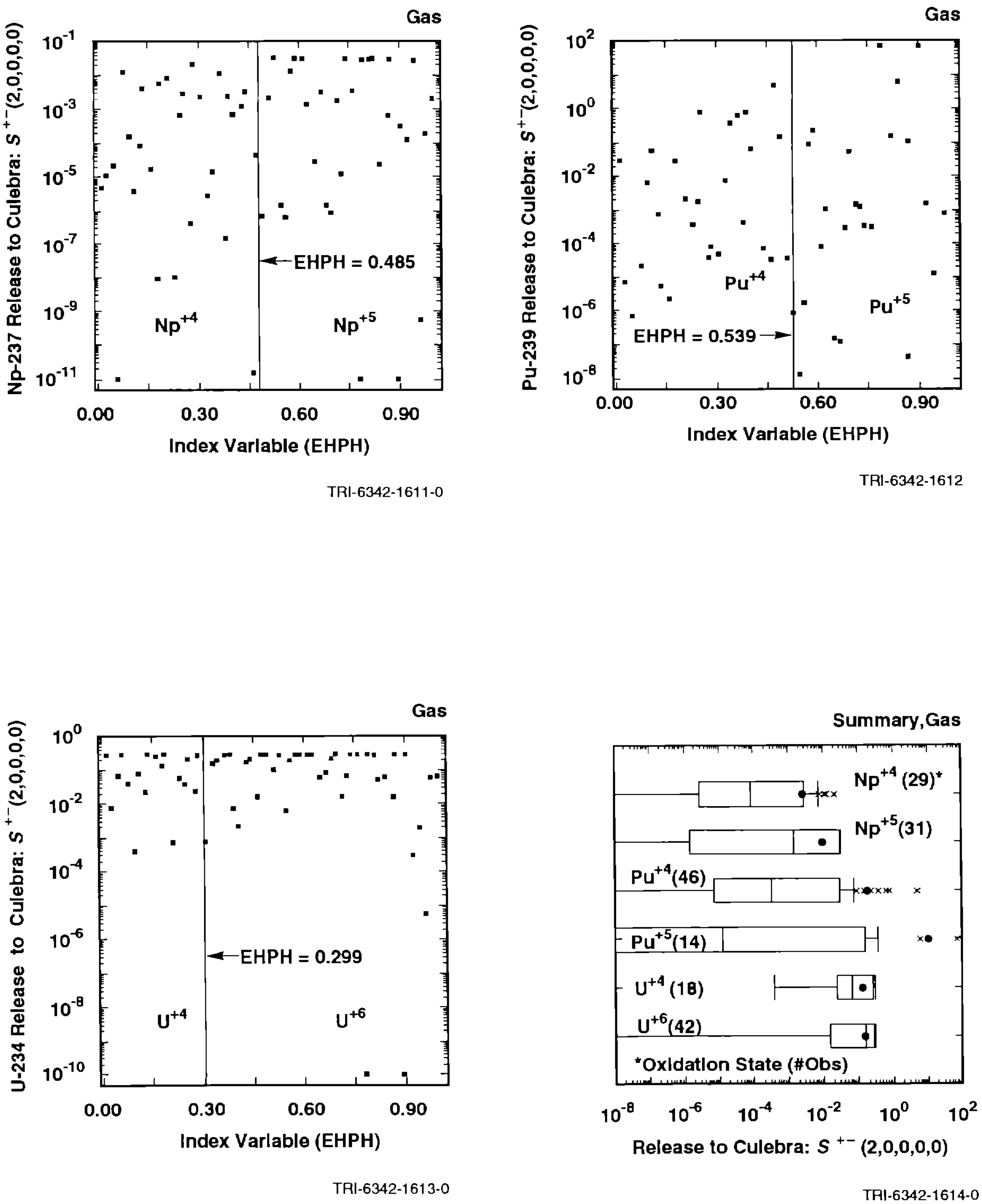

Figure 4.5-8. Effect of Solubilities Determined on the Basis of Oxidation State on the Normalized Releases of Np, Pu and U to the Culebra Dolomite for Scenario S^{+-}(2,0,0,0,0) with Gas Generation in the Repository and Intrusion Occurring at 1000 Yrs.

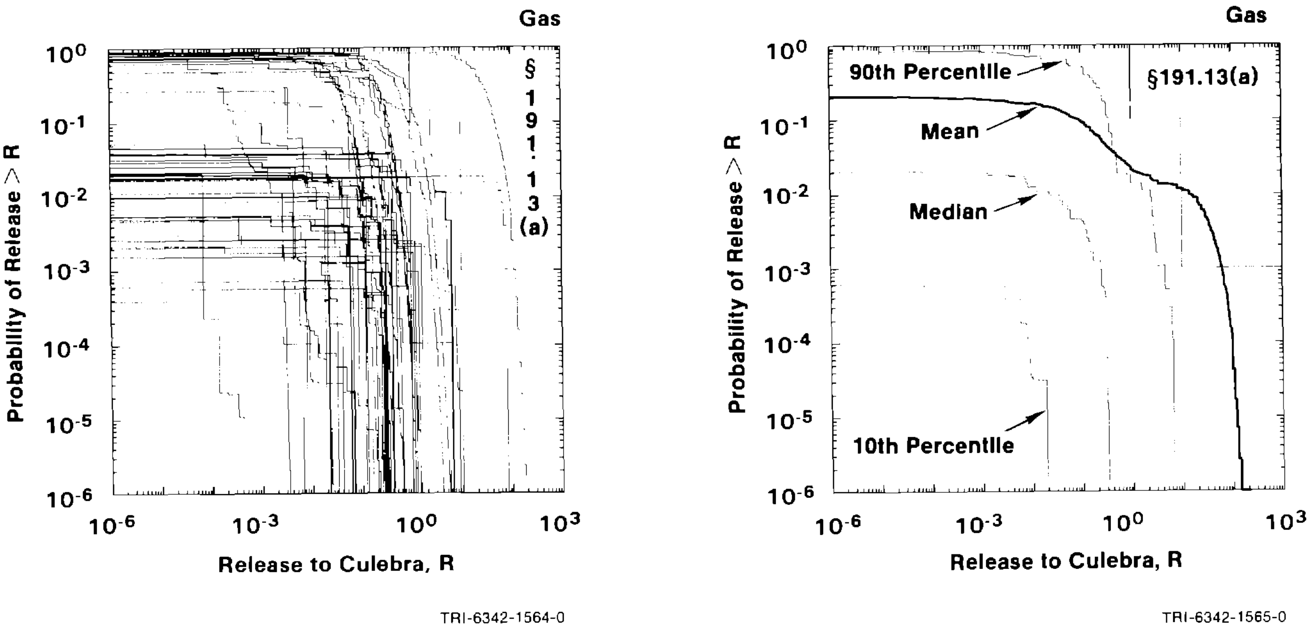

Figure 4.5-9. Distribution of Complementary Cumulative Distribution Functions for Normalized Release to the Culebra Dolomite with Gas Generation in the Repository. The CCDFs in this figure are for release to the Culebra, not release to the accessible environment; the corresponding CCDFs for release to the accessible environment are given in the lower two frames of Figure 4.1-2.

corresponding distribution of CCDFs for normalized release to the Culebra. The CCDFs appearing in Figure 4.5-9 are constructed in the same manner as the CCDFs for release to the accessible environment due to groundwater transport shown in Figure 4.1-2 (see Vol. 2, Chapters 2 and 3) except that releases to the Culebra rather than releases to the accessible environment are used as the consequences associated with the individual scenarios. In contrast to the 4 nonzero CCDFs in Figure 4.1-2 for normalized release to the accessible environment due to groundwater transport, Figure 4.5-9 contains 58 nonzero CCDFs for normalized release to the Culebra. However, only 4 of the CCDFs in Figure 4.5-9 for release to the Culebra cross the EPA release limits. Thus, transport in the Culebra with a dual-porosity model is causing a substantial reduction in radionuclide release to the accessible environment from what is already a small release from the repository.

Distributions of CCDFs of the form shown in Figure 4.5-9 can also be considered in sensitivity studies by performing regression-based analyses for the exceedance probabilities associated with individual release values on the abscissa. Specifically, each value on the abscissa has 60 exceedance probabilities associated with it, where 60 is the sample size being used in the present analysis. Regression coefficients or partial correlation coefficients can be calculated which relate the variability in the exceedance probabilities associated with a particular release value to the sampled variables listed in Table 3-1. The coefficients calculated in this manner can then be plotted above the corresponding releases. The result of such an analysis for the CCDFs shown in Figure 4.5-9 is presented in Figure 4.5-10. The upper frame contains partial rank correlation coefficients, and the lower frame contains standardized rank regression coefficients. The results obtained for individual values on the abscissa are connected to form the curves displayed in the figure. To control the number of curves, a variable was required to have a partial rank correlation coefficient with an absolute value of at least 0.4 for some release value to be included in the figure. The results appearing in Figure 4.5-10 were calculated with the PCCSRC program (Iman et al., 1985).

As examination of Figure 4.5-10 shows, SALPERM (Salado permeability) and LAMBDA (rate constant in Poisson model for drilling intrusions) are the two most important variables with respect to the exceedance probabilities for small release values, with the values for these probabilities tending to increase as SALPERM and LAMBDA increase. The variables BHPERM (borehole permeability) and SOLPU (solubility of Pu) are less important than SALPERM and LAMBDA for the exceedance probabilities for small release values but become more important for the exceedance probabilities for larger release values, with the values for these probabilities again tending to increase as BHPERM and SOLPU increase.

4.6 Sensitivity Analysis for CCDFs

The most general result of the 1991 WIPP performance assessment is the distribution of CCDFs shown in Figure 2.1-2, which include the releases due to both cuttings removal and groundwater transport to the accessible environment. As discussed in conjunction with Figures 4.5-9 and 4.5-10, a sensitivity analysis can be performed for the CCDFs in Figure 2.1-2 by analyzing the variability associated with the exceedance probabilities for individual normalized releases. The result of this analysis is shown in Figure 4.6-1.

As examination of Figure 4.6-1 shows, the variability of the CCDFs in Figure 2.1-2 is dominated by LAMBDA (rate constant in Poisson model for drilling intrusions) and DBDIAM (drill bit diameter). Of the two variables, LAMBDA is the more important and almost completely dominates the variability in the CCDFs. In particular, the partial rank correlation coefficients and standardized rank regression coefficients shown for LAMBDA in Figure 4.6-1 are very close to one. For perspective, plots of R^2 values for regression

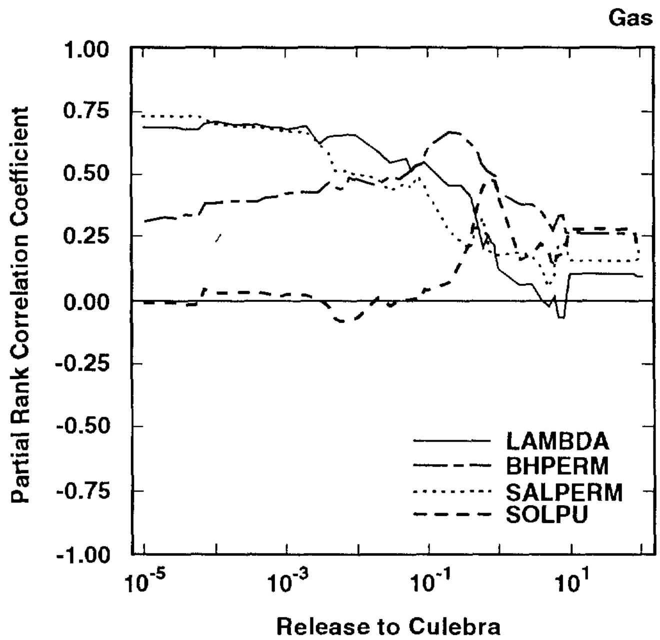

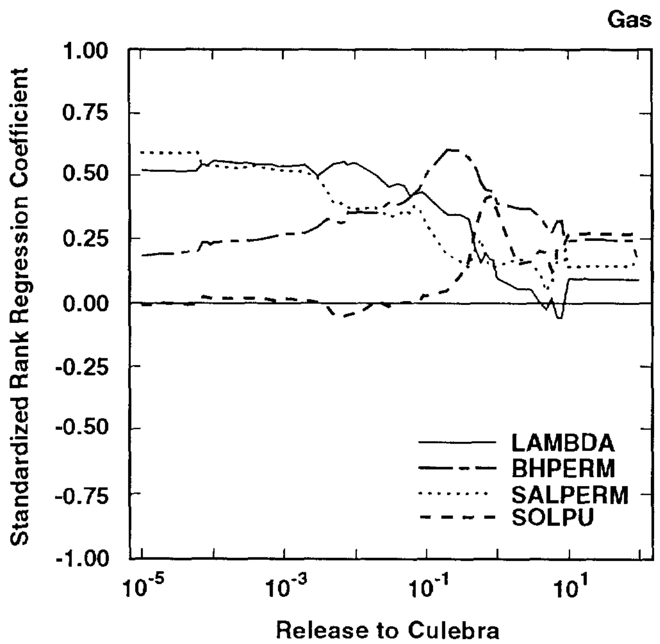

TRI-6342-1681-0

Figure 4.5-10. Partial Rank Correlation Coefficients and Standardized Rank Regression Coefficients for Exceedance Probabilities Associated with the Individual Complementary Cumulative Distribution Functions in Figure 4.5-9 for Normalized Release to the Culebra Dolomite with Gas Generation in the Repository.

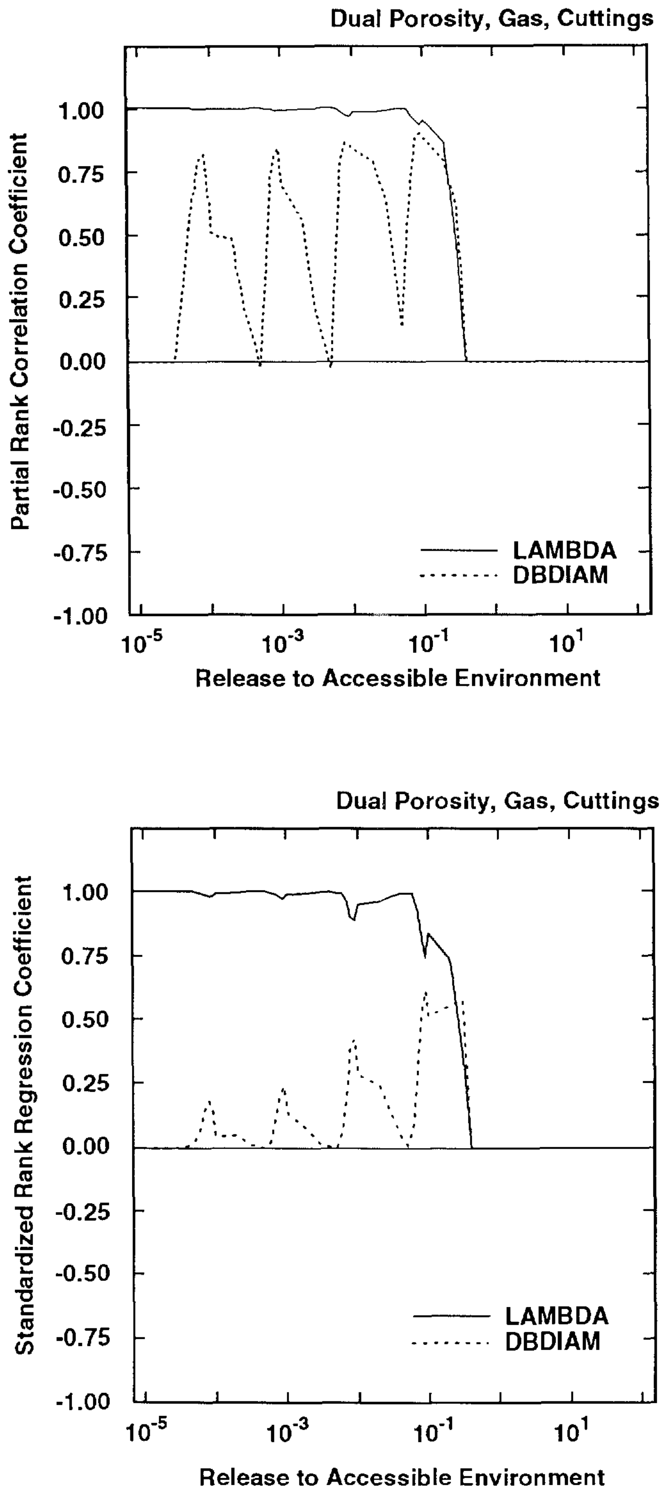

TRI-6342-1682-0

Figure 4.6-1. Partial Rank Correlation Coefficients and Standardized Rank Regression Coefficients for Exceedance Probabilities Associated with Individual Complementary Cumulative Distribution Functions in Figure 2.1-2 for Normalized Release to the Accessible Environment Including Both Cuttings Removal and Groundwater Transport with Gas Generation in the Repository and a Dual-Porosity Transport Model in the Culebra Dolomite.

models using just LAMBDA (upper frame) and both LAMBDA and DBDIAM (lower frame) are shown in Figure 4.6-2. Except for a few downward spikes, the R^2 values for regression models using only LAMBDA are close to one. Further, the downward spikes are substantially reduced and the R^2 values move close to one for regression models using both LAMBDA and DBDIAM.

The spikes involving DBDIAM (drill bit diameter) in Figure 4.6-1 are quite striking and merit additional discussion. These spikes are the result of the discretization of the waste into 5 activity levels as shown in Table 2.4-4 for the calculation of cuttings removal. The effect of this discretization can be seen in the structure of the CCDFs in Figure 2.1-2. As illustrated in Figure 4.6-3, the individual CCDFs in Figure 2.1-2 have 4 plateaus and 4 associated regions of rapid decrease. The first plateau corresponds to no intrusion. The region of rapid decrease between the first and second plateau corresponds to cuttings releases dominated by waste of activity level 1. The second plateau corresponds to a range of releases between releases dominated by activity level 1 and releases dominated by activity level 2. The region of rapid decrease between the second and third plateau corresponds to releases dominated by waste of activity level 2. This pattern continues for the other plateaus. The cuttings release for activity level 5 falls midway between the releases for activity levels 2 and 3 (see Vol. 2, Table 3-3) but does not have a large impact on the structure of the CCDF because the conditional probability of encountering waste of activity level 5 (i.e., 0.0588 as shown in Table 2.4-4) is less than the conditional probability of encountering waste of activity level 3 (i.e., 0.2242). The regions of rapid decrease between plateaus tend to be more stretched out when DBDIAM (drill bit diameter) is large. In particular, DBDIAM affects the location at which the transition from rapid decrease to a plateau occurs but does not affect the height of the plateau, which is determined entirely by LAMBDA (rate constant in Poisson model for drilling intrusions). With respect to Figure 4.6-1, the maximums for DBDIAM are occurring within the regions of rapid descent while the minimums are occurring within the plateaus, which are determined by LAMBDA. The use of more activity levels would eliminate the plateaus and regions of rapid decrease in the CCDFs in Figure 2.1-2 and thus would also eliminate the spikes associated with DBDIAM in Figure 4.6-1. However, although this added resolution would produce smoother CCDFs, it would not cause a significant change in the distribution of CCDFs shown in Figure 2.1-2.

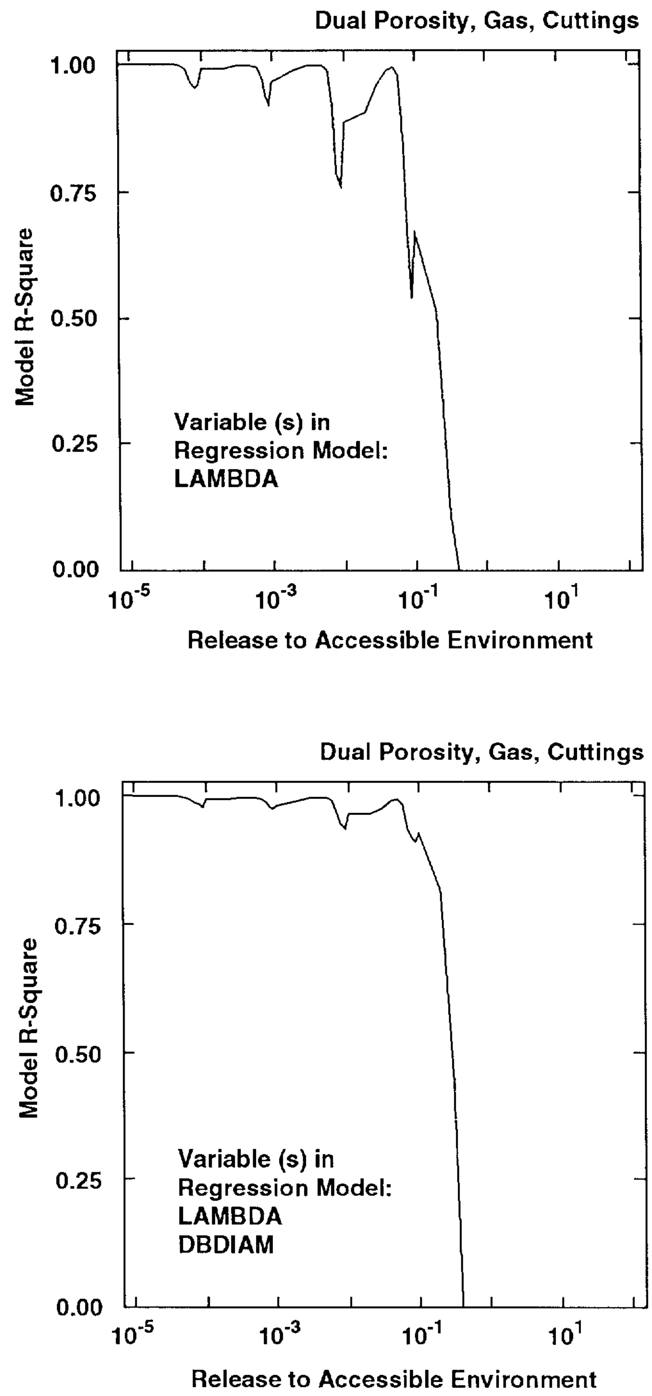

TRI-6342-1683-0

Figure 4.6-2. Coefficient of Determination (R^2 value) in Rank Regression Models for Exceedance Probabilities Associated with Individual Complementary Cumulative Distribution Functions in Figure 2.1-2 for Normalized Release to the Accessible Environment Including Both Cuttings Removal and Groundwater Transport with Gas Generation in the Repository and a Dual-Porosity Transport Model in the Culebra Dolomite.

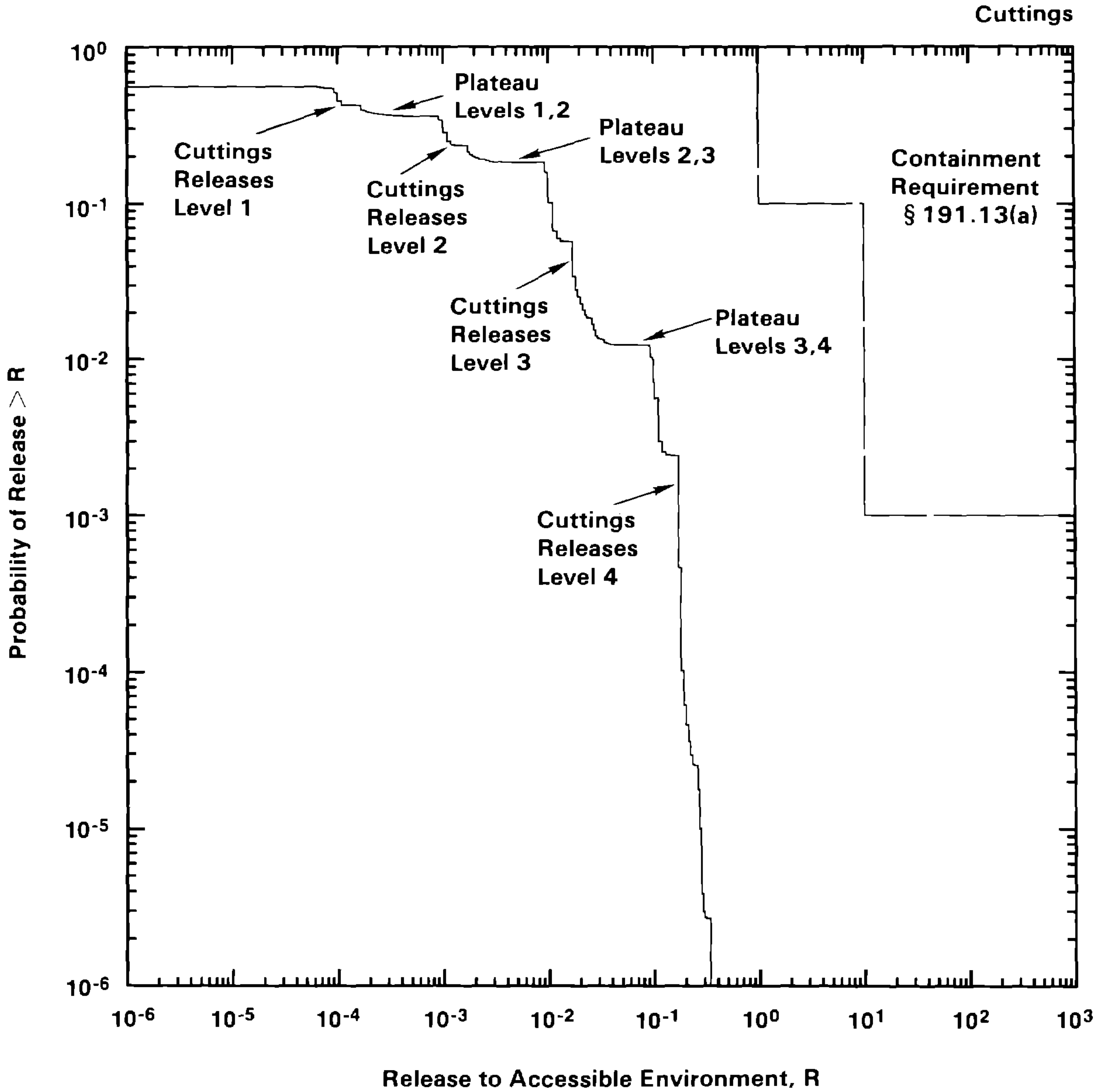

TRI-6342-1566-0

Figure 4.6-3. Structure of Individual Complementary Cumulative Distribution Function in Figure 2.1-2. This figure displays the cuttings release CCDF for sample element 46; the cuttings releases used in the construction of this CCDF are given in Table 3-3 of Vol. 2 of this report.

5. EFFECT OF ALTERNATIVE CONCEPTUAL MODELS

As described in Table 3-2, several alternative conceptual models were considered as part of the 1991 WIPP performance assessment. A summary of the results obtained with these alternative models is presented in this chapter.

5.1 Effect of Waste Generated Gas

The analyses presented in Chapter 4 were performed with the assumption that the production of waste-generated gas would take place due to corrosion and microbial action. The variables GRCORH, GRCORI, GRMICH, GRMICI, STOICCOR, STOICMIC, VMETAL and VWOOD in Table 3-1 relate to the generation of such gas. The presence and impact of waste-generated gas is a topic of considerable interest and uncertainty (Brush, 1990) in the WIPP performance assessment, with 1991 being the first year in which gas generation was incorporated into the annual performance assessment.

To help provide perspective on the impact of gas generation, the analyses presented in Chapter 4 were repeated for scenarios $S(1,0,0,0,0)$ and $S^{+-}(2,0,0,0,0)$ for the same Latin hypercube sample used in Chapter 4 but with an assumption of no gas generation. Results obtained with and without gas generation are compared in Figure 5.1-1, which contains scatterplots for brine flow into the Culebra and total normalized release into the Culebra with and without gas generation for scenarios $S(1,0,0,0,0)$ and $S^{+-}(2,0,0,0,0)$.

As examination of Figure 5.1-1 shows, the presence or absence of gas generation can have a significant impact on radionuclide release to the Culebra. For scenario $S(1,0,0,0,0)$, many sample elements result in no release to the Culebra when gas generation in the repository is assumed to take place. As shown in Figure 4.5-1, the variable SALPERM (Salado permeability) acts as a switch in the presence of gas generation, with no releases to the Culebra occurring for values of SALPERM less than approximately 5×10^{-21} m^2. The removal of gas generation also removes the effect of SALPERM as a switch, which can be seen in the two upper frames in Figure 5.1-1 in the appearance of points indicating nonzero flows and releases above what were zero values for analyses performed with gas generation. Due to the low values for SALPERM, the additional nonzero brine flows into the Culebra in the absence of gas generation are small (see upper left frame in Figure 5.1-1). However, little relationship exists between the size of these brine flows and the actual releases into the Culebra (see upper

Scenario: $S(1,0,0,0,0)$, Assumed Intrusion Time: 1000 yrs

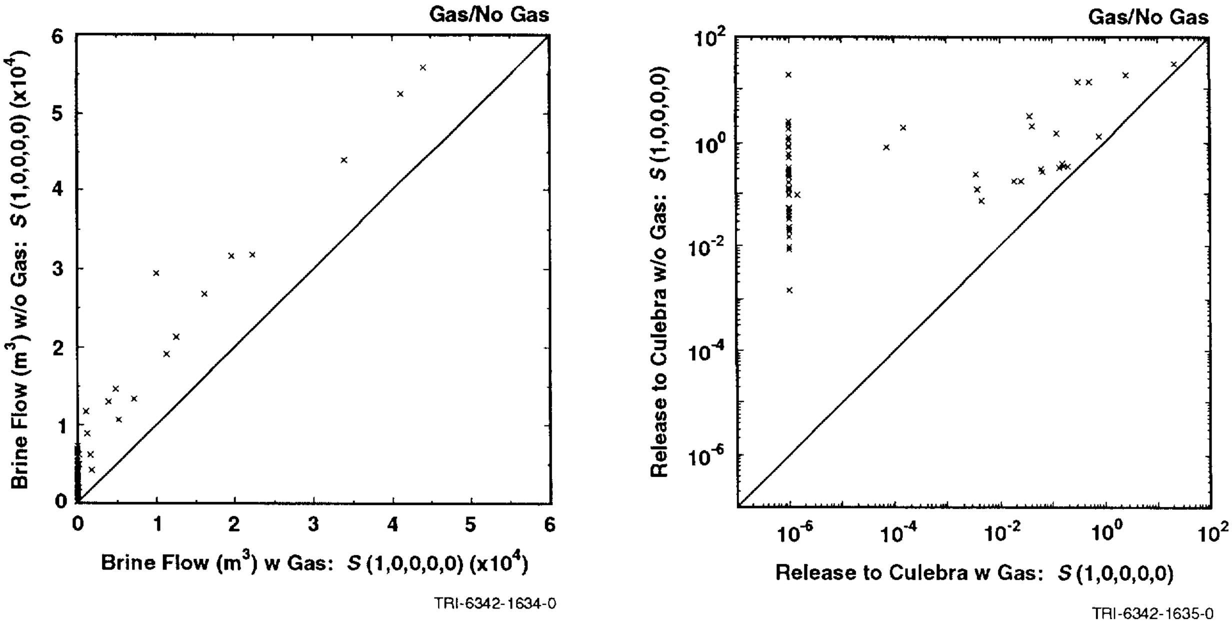

Scenario: $S^{+-}(2,0,0,0,0)$, Assumed Intrusion Time: 1000 yrs

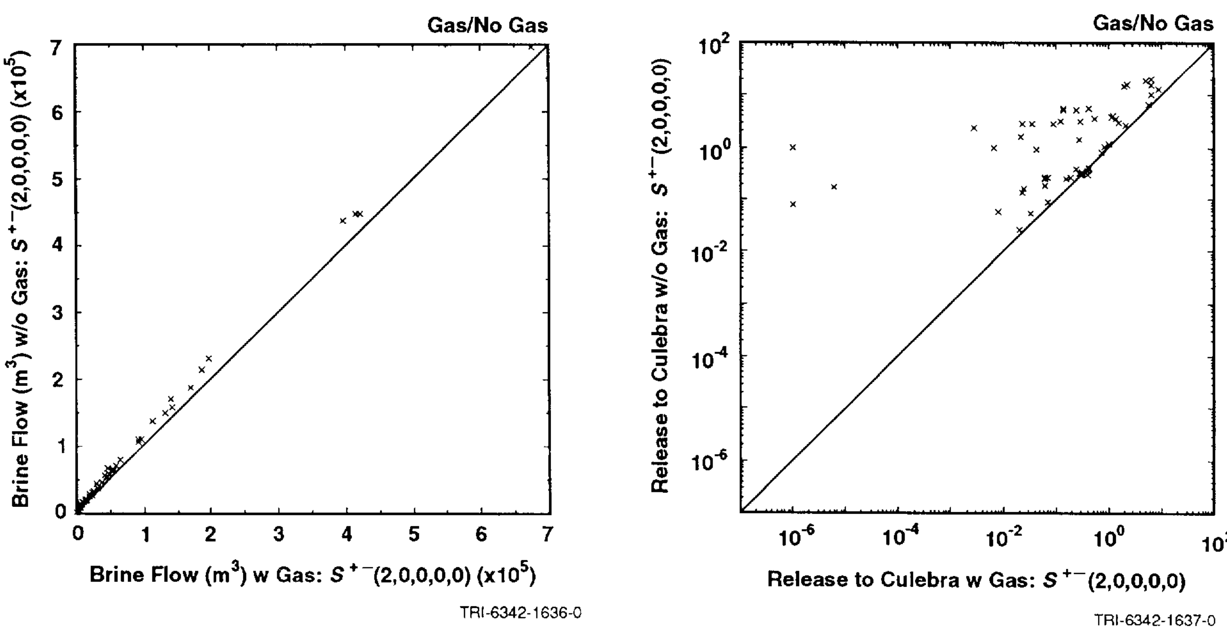

Figure 5.1-1. Scatterplots of Total Brine Flow (m^3) and Total Normalized Release from the Repository to the Culebra Dolomite with and without Gas Generation in the Repository for Scenarios $S(1,0,0,0,0)$ and $S^{+-}(2,0,0,0,0)$ with an Assumed Intrusion Time of 1000 Yrs. For plotting purposes when a logarithmic scale is used, numbers less than 10^{-6} are assigned a value of 10^{-6}.

right frame in Figure 5.1-1). In addition, the nonzero brine flows and radionuclide releases that result for scenario $S(1,0,0,0,0)$ increase in the absence of gas generation, which is indicated by the presence of points above the diagonal lines in the upper two frames of Figure 5.1-1.

For scenario $S^{+-}(2,0,0,0,0)$, the presence or absence of gas generation has little effect on whether or not a release to the Culebra occurs. However, the absence of gas generation does increase the size of the release (see lower right frame in Figure 5.1-1). As most of the brine flow into the Culebra is coming from a pressurized brine pocket in the Castile Formation for the scenario $S^{+-}(2,0,0,0,0)$, gas generation has only a limited effect on this flow (see lower left frame in Figure 5.1-1).

Releases of individual isotopes to the Culebra and to the accessible environment due to groundwater transport are summarized in Figures 5.1-2 and 5.1-3. As examination of these figures shows, transport in the Culebra results in substantial reductions in the releases for the individual isotopes. In particular, Am-241 and Pu-239 are important contributors to the release into the Culebra but make little contribution to the release to the accessible environment.

The radionuclide releases summarized in Figures 5.1-2 and 5.1-3 were calculated with the assumption that no gas generation takes place in the repository. The corresponding results for gas generation in the repository appear in Figures 4.4-7 and 4.4-2, respectively. As already discussed, the releases in Figures 4.4-7 and 4.4-2 tend to be smaller than those in Figures 5.1-2 and 5.1-3 due to the effect that gas generation has on reducing brine inflow to the repository from the Salado Formation.

The CCDFs summarizing groundwater transport releases to the accessible environment for gas generation in the repository and a dual-porosity transport model in the Culebra are given in the lower left frame of Figure 4.1-2. If the no-gas-generation results presented in this section had been calculated for all ten scenarios appearing in Figure 4.4-1, then the equivalent distribution of CCDFs could be obtained for no gas generation, and comparison of the two CCDF distributions would provide an indication of the effect of gas generation on the actual results (i.e., CCDFs) used in comparisons with the EPA release limits. However, to reduce computational costs, the no-gas-generation calculations presented in this section were only performed for scenarios $S(1,0,0,0,0)$ and $S^{+-}(2,0,0,0,0)$. As a result, it is not possible to generate a distribution of CCDFs with the available results for groundwater transport to the accessible environment that is equivalent to the one appearing in Figure 4.1-2.

Scenario: *S*(1,0,0,0,0), Assumed Intrusion Time: 1000 yrs

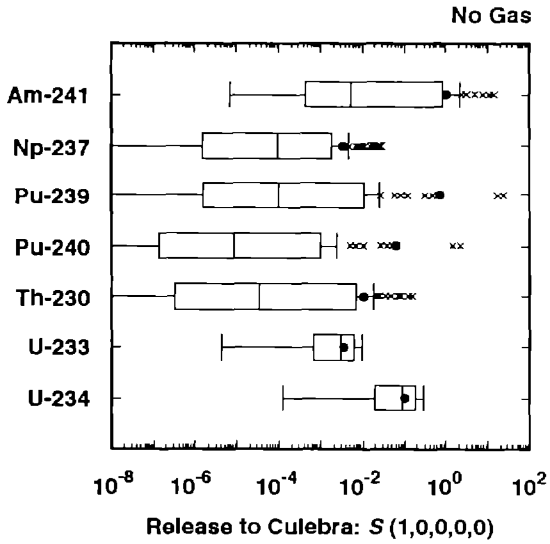

TRI-6342-1548-0

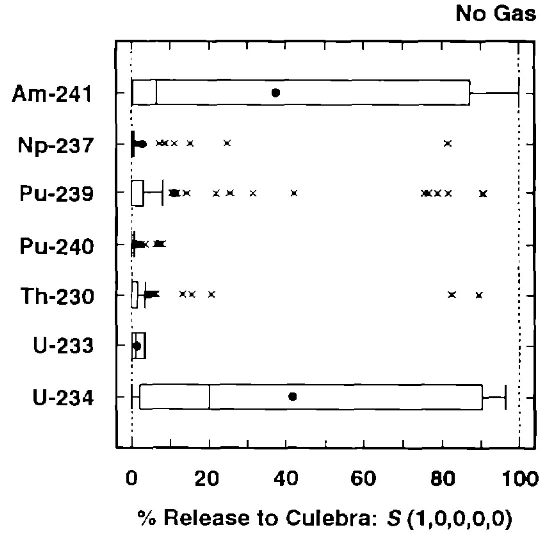

TRI-6342-1549-0

Scenario: S^{+-}(2,0,0,0,0), Assumed Intrusion Time: 1000 yrs

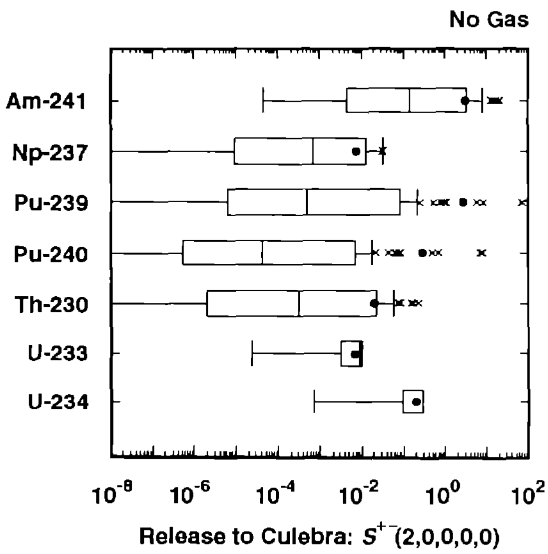

TRI-6342-1550-0

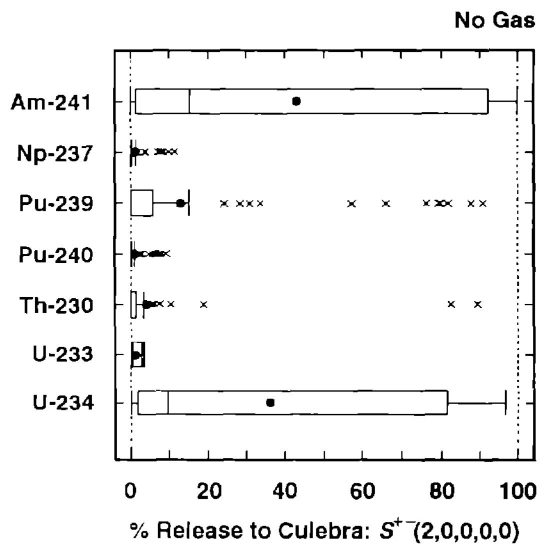

TRI-6342-1551-0

Figure 5.1-2. Normalized Releases for Individual Isotopes into the Culebra Dolomite with Intrusion Occurring at 1000 Yrs and No Gas Generation in the Repository.

Scenario: *S*(1,0,0,0,0), Assumed Intrusion Time: 1000 yrs

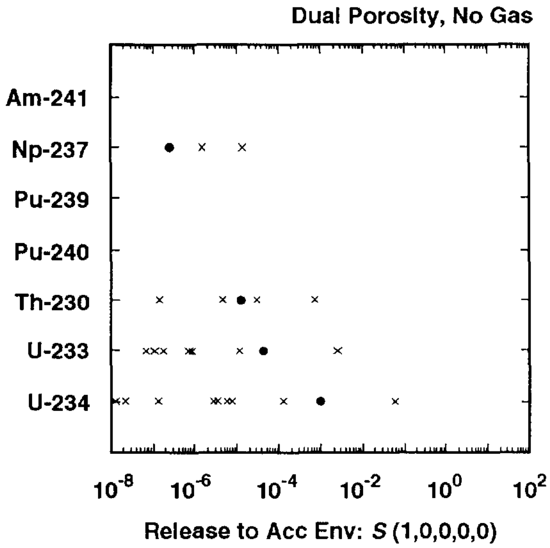

TRI-6342-1552-0

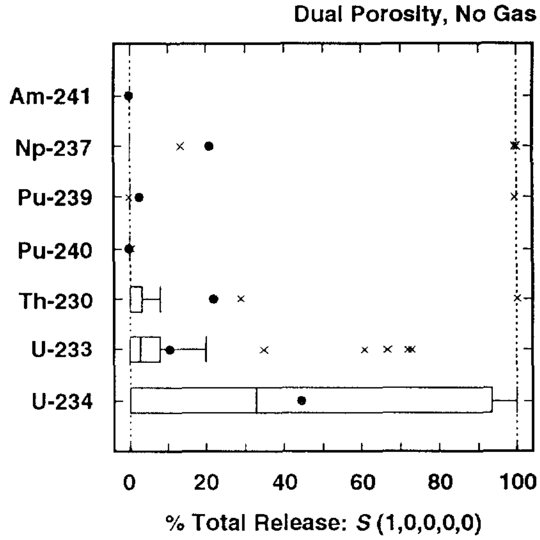

TRI-6342-1553-0

Scenario: S^{+-}(2,0,0,0,0), Assumed Intrusion Time: 1000 yrs

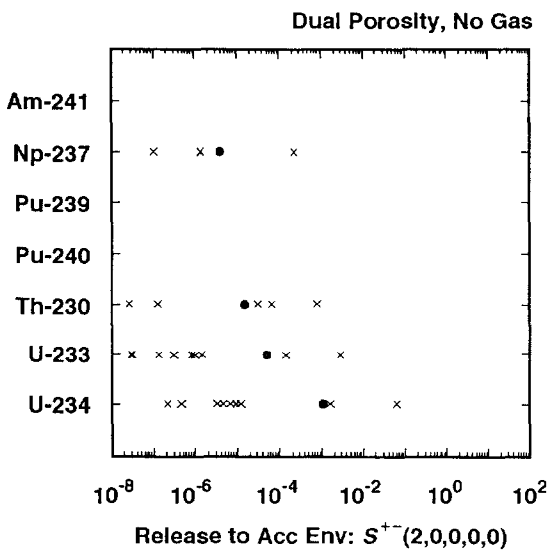

TRI-6342-1554-0

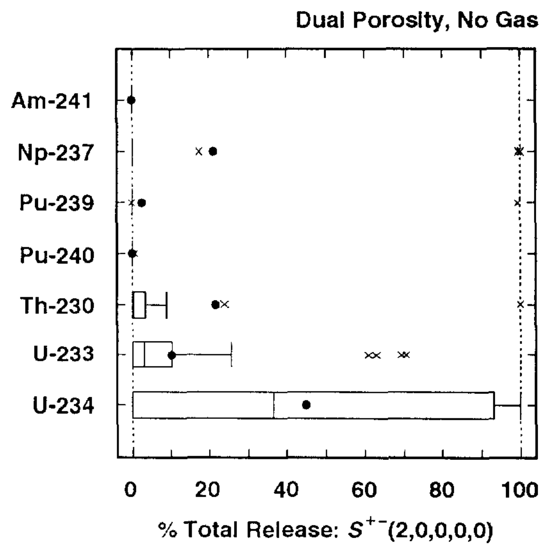

TRI-6342-1555-0

Figure 5.1-3. Normalized Releases for Individual Isotopes to the Accessible Environment Due to Groundwater Transport with Intrusion Occurring at 1000 Yrs, No Gas Generation in the Repository and a Dual-Porosity Transport Model in the Culebra Dolomite.

Another possibility for comparing CCDFs constructed with and without gas generation in the repository is to use only the results for scenarios $S(1,0,0,0,0)$ and $S^{+-}(2,0,0,0,0)$ (i.e., the results for intrusions occurring at 1000 yrs), which is equivalent to assuming that the rate constant λ in the Poisson model for drilling intrusions is equal to zero after 2000 yrs. Such an assumption is actually consistent with recommendations obtained in an external review of potential human disruptions at the WIPP (Hora et al., 1991).

Distributions of CCDFs constructed in this manner for release with and without gas generation in the repository are shown in Figure 5.1-4. As comparison of the results in Figure 5.1-4 shows, both the inclusion and exclusion of gas generation produce distributions of CCDFs that are substantially below the EPA release limits, although the CCDFs obtained without gas generation tend to be somewhat closer to the limits.

As shown in Figure 4.4-1, intrusions occurring after 1000 yrs result in smaller releases than intrusions occurring at 1000 yrs due to increased time for radioactive decay and reduced time for groundwater transport. As a result, consideration of a constant-valued, nonzero λ in the Poison model for drilling intrusions out to 10,000 yrs is unlikely to shift the CCDFs in Figure 5.1-4 up by more than a factor of 5 and an upward shift of 2 is more reasonable. Further, due to the low probability of compounding a large number of independent intrusions in different time intervals, the shift of the CCDFs to the right by more than a factor of 2 or 3 for a constant-valued, nonzero λ out to 10,000 yrs is also unlikely.

Sensitivity analyses for total brine release and total normalized release to the Culebra for scenarios $S(1,0,0,0,0)$ and $S^{+-}(2,0,0,0,0)$ with no gas generation in the repository are presented in Table 5.1-1. For scenario $S(1,0,0,0,0)$, brine release is dominated by SALPERM (Salado permeability), BHPERM (borehole permeability) and SALPRES (Salado pressure), and normalized release is dominated by SOLAM (solubility of Am) and SALPERM. For scenario $S^{+-}(2,0,0,0,0)$, brine release is dominated by BHPERM, BPPRES (brine pocket pressure) and DBDIAM (drill bit diameter), and normalized release is dominated by SOLAM, BHPERM, SOLPU (solubility of Pu) and BPPRES.

The corresponding analyses for brine releases and normalized releases with gas generation are presented in Table 4.5-3 for intrusions occurring at 1000 yrs. For the analyses for scenario $S(1,0,0,0,0)$ with gas generation, the results are dominated by SALPERM (Salado permeability) due to its previously discussed role as a switch. In contrast, additional important variables are identified in the analyses for scenario $S(1,0,0,0,0)$ in Table 5.1-1 because SALPERM does not introduce a discontinuity into the results in the absence

With Gas Generation in the Repository

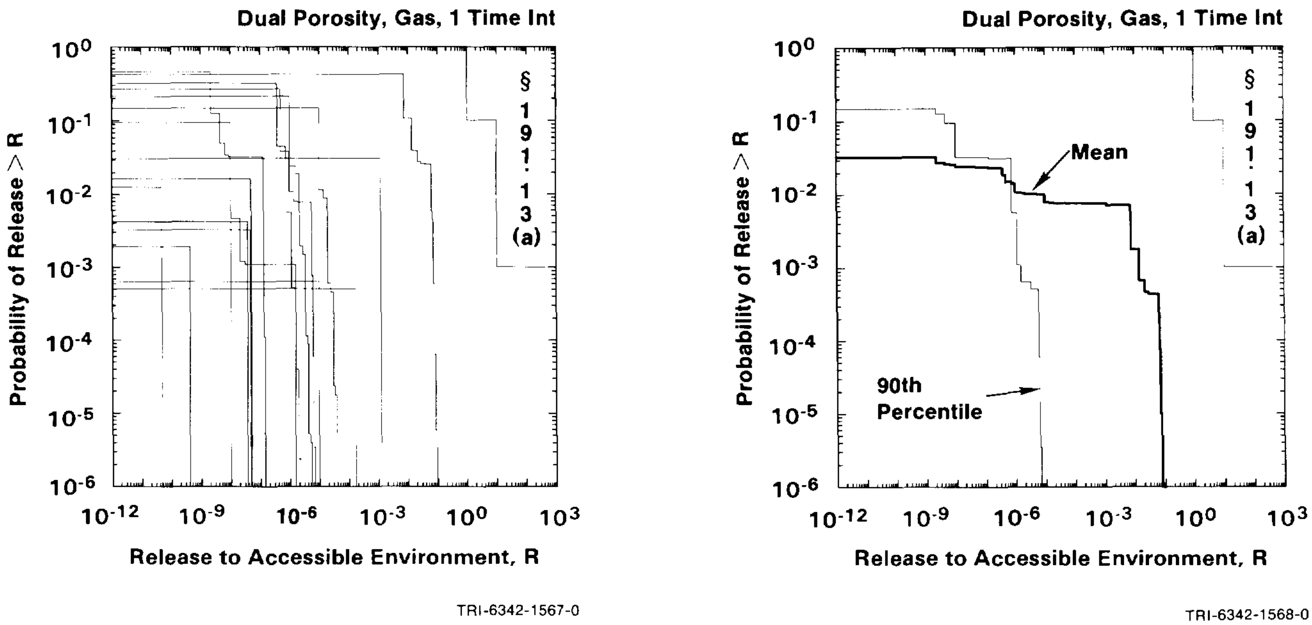

Without Gas Generation in the Repository

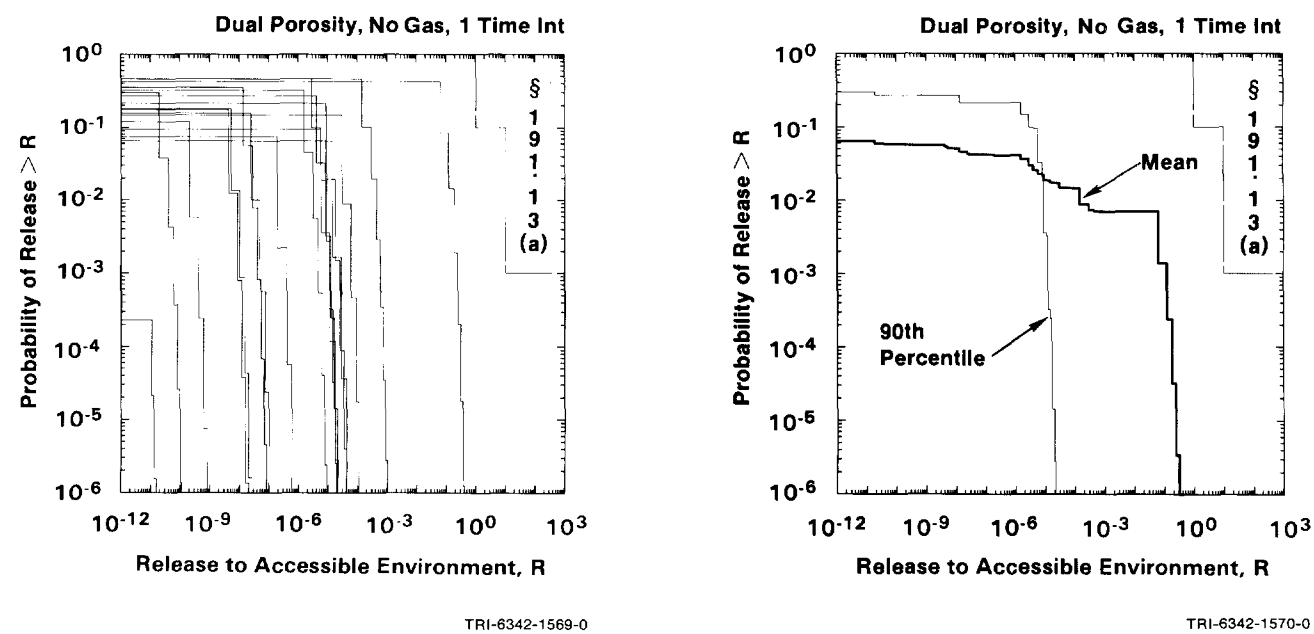

Figure 5.1-4. Comparison of Complementary Cumulative Distribution Functions for Normalized Release to the Accessible Environment with Gas Generation in the Repository (upper two frames) and without Gas Generation in the Repository (lower two frames) for a Dual-Porosity Transport Model in the Culebra Dolomite and the Rate Constant λ in the Poisson Model for Drilling Intrusions Equal to Zero After 2000 Yrs.

TABLE 5.1-1. STEPWISE REGRESSION ANALYSES WITH RANK-TRANSFORMED DATA FOR TOTAL BRINE RELEASE AND TOTAL NORMALIZED RELEASE TO THE CULEBRA DOLOMITE WITH NO GAS GENERATION IN THE REPOSITORY AND INTRUSION OCCURRING 1000 YRS AFTER REPOSITORY CLOSURE

	Scenario: *S*(1,0,0,0,0)				Scenario: S^{+-}(2,0,0,0,0)			
	Total Brine		Total Release		Total Brine		Total Release	
Step	Variable	R^2	Variable	R^2	Variable	R^2	Variable	R^2
1	SALPERM	0.51(+)	SOLAM	0.42(+)	BHPERM	0.82(+)	SOLAM	0.62(+)
2	BHPERM	0.69(+)	SALPERM	0.65(+)	BPPRES	0.95(+)	BHPERM	0.71(+)
3	SALPRES	0.79(+)			DBDIAM	0.97(+)	SOLPU	0.77(+)
4							BPPRES	0.81(+)

of gas generation. The analyses for scenario S^{+-}(2,0,0,0,0) with and without gas generation are similar. However, there is a reversal in the order of importance of BHPERM (borehole permeability) and SOLAM (solubility of Am) for normalized release to the Culebra, with BHPERM being the most important variable in the presence of gas generation and SOLAM being the most important variable in the absence of gas generation. This switch in order of importance probably results because the presence of gas generation delays the release of material to the Culebra and thus allows more time for the decay of Am-241 before it can be released to the Culebra.

Sensitivity analyses of the groundwater transport results for individual isotopes for scenarios *S*(1,0,0,0,0) and S^{+-}(2,0,0,0,0) with no gas generation in the repository are presented in Tables 5.1-2 and 5.1-3 for release to the Culebra and for transport one-quarter, one-half and the full distance to the accessible environment. The results presented in these tables are generally similar to those presented in Tables 4.5-1 and 4.5-2 for results obtained with gas generation in the repository, although the analyses for scenario *S*(1,0,0,0,0) in Table 5.1-2 tend to have larger R^2 values than those in Table 4.5-1 due to the absence of the effect of SALPERM (Salado permeability) as a switch. As shown in Table 5.1-2, the appropriate elemental solubility is the most important variable with respect to the release of each radionuclide to the Culebra, and the appropriate elemental matrix distribution coefficient is the most important variable for the transport of each isotope in the Culebra.

As for the analyses with gas generation in the repository, the examination of scatterplots helps supplement the sensitivity results contained in Tables 5.1-2 and 5.1-3. Scatterplots for the release of Pu-239 to the Culebra without gas generation in the repository are presented in Figure 5.1-5. The top two frames are for scenario *S*(1,0,0,0,0). As the top left frame shows, SALPERM (Salado permeability) does not act as a switch for releases to the Culebra in the absence of gas generation; for comparison, the corresponding

TABLE 5.1-2. STEPWISE REGRESSION ANALYSES WITH RANK-TRANSFORMED DATA FOR SCENARIO *S*(1,0,0,0,0) WITH NO GAS GENERATION IN THE REPOSITORY, A DUAL-POROSITY TRANSPORT MODEL IN THE CULEBRA DOLOMITE AND INTRUSION OCCURRING 1000 YRS AFTER REPOSITORY CLOSURE

	Release to Culebra		Quarter Distance		Half Distance		Full Distance	
Step	Variable	R^2	Variable	R^2	Variable	R^2	Variable	R^2
Dependent Variable: Integrated Discharge Am-241								
1	SOLAM	0.81(+)	CULFRSP	0.11 (+)	FKDAM	0.27 (+)	--	--
2	SALPERM	0.90(+)			MKDAM	0.47 (-)		
3	BHPERM	0.92(+)			CULFRPOR	0.53 (+)		
4	SALPRES	0.93(+)						
Dependent Variable: Integrated Discharge Np-237								
1	SOLNP	0.77(+)	FKDNP	0.22 (-)	MKDNP	0.50 (-)	MKDNP	0.26 (-)
2	EHPH	0.86(+)	MKDNP	0.32 (-)			FKDNP	0.37 (-)
3	SALPERM	0.90(+)						
Dependent Variable: Integrated Discharge Pu-239								
1	SOLPU	0.92(+)	MKDPU	0.17 (-)	MKDPU	0.28 (-)	--	--
2	SALPERM	0.94(+)	FKDPU	0.30 (-)	FKDPU	0.37 (+)		
3	BHPERM	0.95(+)			CULFRPOR	0.46 (+)		
4					CULFRSP	0.52 (+)		
Dependent Variable: Integrated Discharge Pu-240								
1	SOLPU	0.91(+)	MKDPU	0.14 (-)	MKDPU	0.19 (-)	--	--
2	SALPERM	0.94(+)	FKDPU	0.24 (-)	FKDPU	0.29 (+)		
3	BHPERM	0.95(+)	CULPOR	0.34 (-)	CULFRSP	0.36 (+)		
4					CULFRPOR	0.43 (+)		
Dependent Variable: Integrated Discharge Th-230								
1	SOLTH	0.94(+)	MKDU	0.42 (-)	MKDU	0.43 (-)	MKDU	0.38 (-)
2	SALPERM	0.96(+)	MKDTH	0.64 (-)	MKDTH	0.58 (-)	CULFRSP	0.49 (+)
3	BHPERM	0.97(+)	CULFRSP	0.72 (+)	CULFRSP	0.68 (+)	MKDTH	0.57 (-)
4	SALPRES	0.97(+)	CULCLIM	0.77 (+)	CULCLIM	0.73 (+)	CULCLIM	0.63 (+)
5			FKDPU	0.80 (-)	FKDPU	0.76 (-)		

TABLE 5.1-2. STEPWISE REGRESSION ANALYSES WITH RANK-TRANSFORMED DATA FOR SCENARIO $S(1,0,0,0,0)$ WITH NO GAS GENERATION IN THE REPOSITORY, A DUAL-POROSITY TRANSPORT MODEL IN THE CULEBRA DOLOMITE AND INTRUSION OCCURRING 1000 YRS AFTER REPOSITORY CLOSURE (concluded)

	Release to Culebra		Quarter Distance		Half Distance		Full Distance	
Step	Variable	R^2	Variable	R^2	Variable	R^2	Variable	R^2
Dependent Variable: Integrated Discharge U-233								
1	SOLU	0.34(+)	MKDU	0.64 (-)	MKDU	0.59 (-)	MKDU	0.47 (-)
2	SALPERM	0.42(+)	SOLNP	0.73 (+)	SOLNP	0.65 (+)	SOLNP	0.54 (+)
3	SALPRES	0.49(+)	CULFRSP	0.79 (+)	FKDNP	0.71 (-)	FKDNP	0.58 (-)
4			FKDNP	0.82 (-)	CULFRSP	0.74 (+)	CULFRSP	0.63 (+)
Dependent Variable: Integrated Discharge U-234								
1	SOLU	0.29(+)	MKDU	0.81 (-)	MKDU	0.72 (-)	MKDU	0.70 (-)
2	SALPERM	0.37(+)	CULFRSP	0.87 (+)	CULFRSP	0.75 (+)		
3	SALPRES	0.43(+)	CULCLIM	0.89 (+)	CULCLIM	0.78 (+)		
Dependent Variable: EPA Sum for Total Integrated Discharge								
1	SOLAM	0.42(+)	MKDU	0.38 (-)	MKDU	0.36 (-)	MKDU	0.29 (-)
2	SALPERM	0.65(+)	CULFRSP	0.54 (+)	CULFRSP	0.54 (+)	CULFRSP	0.48 (+)
3			SOLNP	0.60 (+)	SOLNP	0.61 (+)	SOLNP	0.55 (+)
4			FKDNP	0.65 (-)			FKDNP	0.59 (-)

TABLE 5.1-3. STEPWISE REGRESSION ANALYSES WITH RANK-TRANSFORMED DATA FOR SCENARIO S^{+-}(2,0,0,0,0) WITH NO GAS GENERATION IN THE REPOSITORY, A DUAL-POROSITY TRANSPORT MODEL IN THE CULEBRA DOLOMITE AND INTRUSION OCCURRING 1000 YRS AFTER REPOSITORY CLOSURE

	Release to Culebra		Quarter Distance		Half Distance		Full Distance	
Step	Variable	R^2	Variable	R^2	Variable	R^2	Variable	R^2
Dependent Variable: Integrated Discharge Am-241								
1	SOLAM	0.84(+)	--	--	FKDAM	0.30 (+)	--	--
2	BHPERM	0.93(+)			MKDAM	0.53 (-)		
3	BPPRES	0.94(+)			CULFRPOR	0.58 (+)		
Dependent Variable: Integrated Discharge Np-237								
1	SOLNP	0.77(+)	FKDNP	0.21 (-)	MKDNP	0.50 (-)	MKDNP	0.24 (-)
2	EHPH	0.84(+)	MKDNP	0.35 (-)			FKDNP	0.34 (-)
3	BHPERM	0.88(+)						
4	BPPRES	0.91(+)						
Dependent Variable: Integrated Discharge Pu-239								
1	SOLPU	0.90(+)	MKDPU	0.28 (-)	MKDPU	0.33 (-)	--	--
2	BHPERM	0.94(+)	FKDPU	0.39 (-)	FKDPU	0.41 (+)		
3	BPPRES	0.95(+)			CULFRSP	0.47 (+)		
4	DBDIAM	0.96(+)						
5	EHPH	0.96(+)						
Dependent Variable: Integrated Discharge Pu-240								
1	SOLPU	0.90(+)	MKDPU	0.17 (-)	MKDPU	0.26 (-)	--	--
2	BHPERM	0.94(+)	FKDPU	0.33 (-)	FKDPU	0.36 (+)		
3	BPPRES	0.95(+)						
4	DBDIAM	0.96(+)						
5	EHPH	0.96(+)						
Dependent Variable: Integrated Discharge Th-230								
1	SOLTH	0.90(+)	MKDU	0.40 (-)	MKDU	0.41 (-)	MKDU	0.38 (-)
2	BHPERM	0.95(+)	MKDTH	0.63 (-)	MKDTH	0.58 (-)	CULFRSP	0.50 (+)
3			CULFRSP	0.72 (+)	CULFRSP	0.67 (+)	MKDTH	0.59 (-)
4			CULCLIM	0.78 (+)	CULCLIM	0.74 (+)	CULCLIM	0.65 (+)
5			CULDISP	0.80 (+)	FKDPU	0.76 (-)		
6			FKDPU	0.82 (-)				

TABLE 5.1-3. STEPWISE REGRESSION ANALYSES WITH RANK-TRANSFORMED DATA FOR SCENARIO S^{+-}(2,0,0,0,0) WITH NO GAS GENERATION IN THE REPOSITORY, A DUAL-POROSITY TRANSPORT MODEL IN THE CULEBRA DOLOMITE AND INTRUSION OCCURRING 1000 YRS AFTER REPOSITORY CLOSURE (concluded)

	Release to Culebra		Quarter Distance		Half Distance		Full Distance	
Step	Variable	R^2	Variable	R^2	Variable	R^2	Variable	R^2
Dependent Variable: Integrated Discharge U-233								
1	SOLU	0.25 (+)	MKDU	0.63 (-)	MKDU	0.59 (-)	MKDU	0.48 (-)
2	BHPERM	0.39 (+)	SOLNP	0.71 (+)	SOLNP	0.65 (+)	SOLNP	0.55 (+)
3	SOLNP	0.50 (-)	CULFRSP	0.78 (+)	FKDNP	0.71 (-)	CULFRSP	0.60 (+)
4	BPPRES	0.58 (+)	FKDNP	0.80 (-)	SOLU	0.75 (-)	SOLU	0.65 (-)
					CULFRSP	0.78 (+)	FKDNP	0.69 (-)
Dependent Variable: Integrated Discharge U-234								
1	SOLU	0.20 (+)	MKDU	0.79 (-)	MKDU	0.71 (-)	MKDU	0.70 (-)
2	BHPERM	0.36 (+)	CULFRSP	0.86 (+)	SOLNP	0.77 (+)	SOLNP	0.75 (+)
3			CULCLIM	0.89 (+)	CULFRSP	0.81 (+)	SOLU	0.78 (-)
4					SOLU	0.86 (-)		
Dependent Variable: EPA Sum for Total Integrated Discharge								
1	SOLAM	0.62 (+)	MKDU	0.37 (-)	MKDU	0.36 (-)	MKDU	0.30 (-)
2	BHPERM	0.71 (+)	CULFRSP	0.53 (+)	CULFRSP	0.56 (+)	CULFRSP	0.49 (+)
3	SOLPU	0.77 (+)	SOLNP	0.60 (+)	SOLNP	0.62 (+)	SOLNP	0.56 (+)
4	BPPRES	0.81 (+)	FKDNP	0.65 (-)			FKDNP	0.60 (-)

Scenario: $S(1,0,0,0,0)$, Assumed Intrusion Time: 1000 yrs

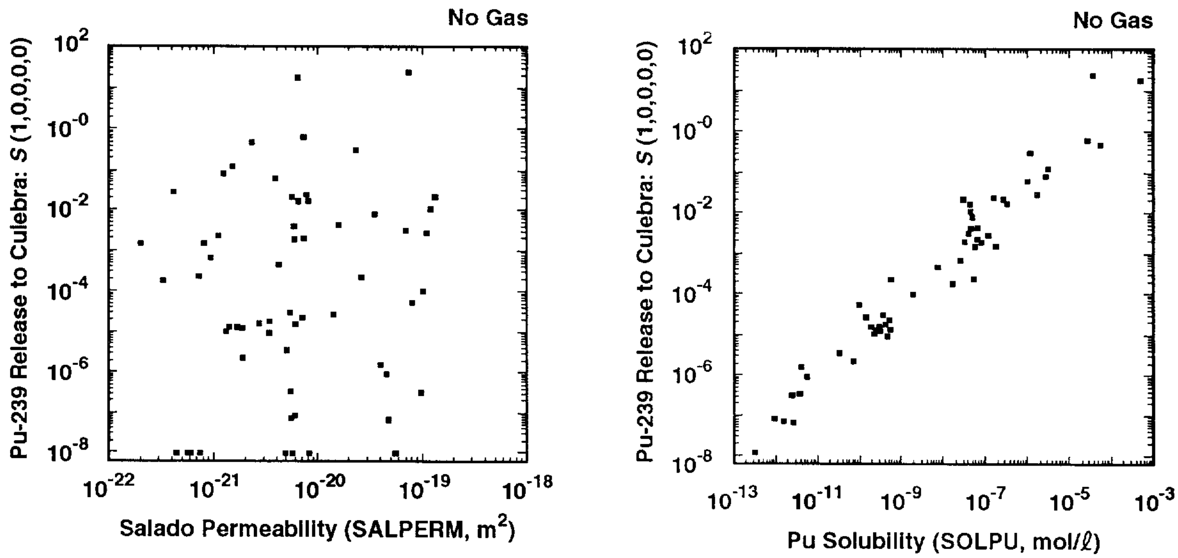

TRI-6342-1607

TRI-6342-1608-0

Scenario: $S^{+-}(2,0,0,0,0)$, Assumed Intrusion Time: 1000 yrs

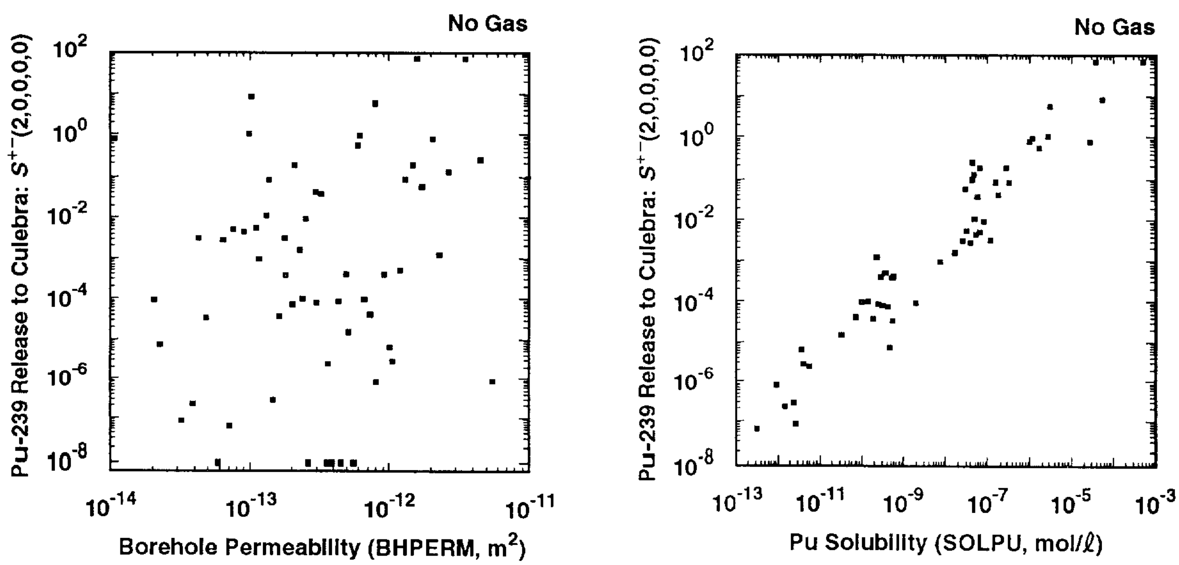

TRI-6342-1609-0

TRI-6342-1610-0

Figure 5.1-5. Scatterplots for Normalized Release of Pu-239 to the Culebra Dolomite without Gas Generation in the Repository for Variables SALPERM (Salado permeability), BHPERM (borehole permeability) and SOLPU (solubility for Pu) and Scenarios $S(1,0,0,0,0)$ and $S^{+-}(2,0,0,0,0)$ with an Assumed Intrusion Time of 1000 Yrs.

scatterplot for gas generation in the repository appears in the upper left frame of Figure 4.5-1 and shows the importance of SALPERM in the presence of gas generation. Rather, as shown in the upper right frame of Figure 5.1-5, the release of Pu-239 to the Culebra for scenario $S(1,0,0,0,0)$ in the absence of gas generation is completely dominated by SOLPU (solubility for Pu). The lower two frames in Figure 4.5-1 are for scenario $S^{+-}(2,0,0,0,0)$. As the right frame shows, the release of Pu-239 to the Culebra for scenario $S^{+-}(2,0,0,0,0)$ is also dominated by SOLPU. The lower left frame is for BHPERM (borehole permeability) and indicates little, if any, visually identifiable relationship between release to the Culebra and BHPERM, although BHPERM is the second variable picked in the regression analysis in Table 5.1-3 for the release of Pu-239 to the Culebra for scenario $S^{+-}(2,0,0,0,0)$. Although BHPERM is an important variable for the release of some isotopes for scenario $S^{+-}(2,0,0,0,0)$ (e.g., see Figure 4.5-2 and 4.5-3 for the gas generation case), its effect is being overwhelmed for Pu-239 by the large range assigned to SOLPU.

Scatterplots for the release of U-234 to the Culebra without gas generation are presented in Figure 5.1-6. The top two frames are for scenario $S(1,0,0,0,0)$. With a little thought, it is easy to understand the pattern shown in the scatterplots contained in these two frames. The upper right frame is for SOLU (solubility for U) and shows the U-234 release to the Culebra initially increasing with SOLU and then flattening off for larger values of SOLU. As shown in Figure 2.4-2, this flattening off corresponds to an inventory-imposed limit (i.e., 0.3 EPA units) on the amount of U-234 available for release to the Culebra. However, there is a great deal of variability in the actual releases associated with the flattened region in the scatterplot for SOLPU due to the effects of SALPERM (Salado permeability), SALPRES (Salado pressure) and BHPERM (borehole permeability). As shown in Table 5.1-1 for scenario $S(1,0,0,0,0)$, increasing each of these variables increases brine flow from the repository to the Culebra and hence tends to increase the U-234 release. However, as shown in the upper left frame in Figure 5.1-1, many of the resultant brine flows are small (i.e., $< 10^4$ m^3), with the result that it is not possible to deplete the U-234 inventory in 10,000 yrs for scenario $S(1,0,0,0,0)$. The scatterplot for SALPERM appears in the upper left frame of Figure 5.1-6. The releases in the scatterplot for SALPERM that are less than 10^{-2} all result from small values for SOLU; when these points are ignored, an increasing relationship between SALPERM and U-234 release to the Culebra can be seen. A similar pattern of relationships involving BHPERM and SOLU can be seen in the two upper scatterplots in Figure 4.5-2 for the release of U-234 for scenario $S(1,0,0,0,0)$ with gas generation in the repository. However, the patterns in Figure 4.5-2 for the gas generation case are much more diffuse due to the many zero releases that result from the interaction of gas generation and SALPERM.

Scenario: $S(1,0,0,0,0)$, Assumed Intrusion Time: 1000 yrs

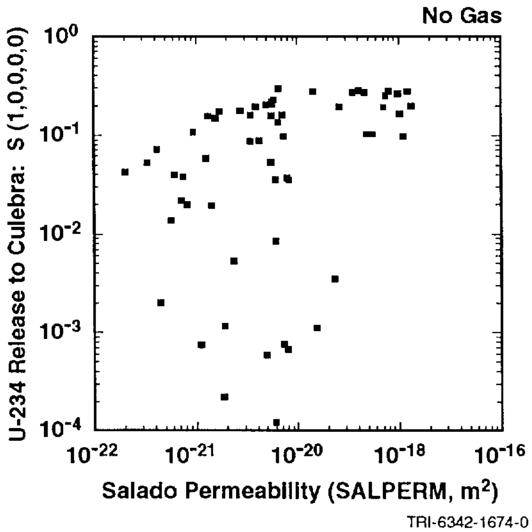

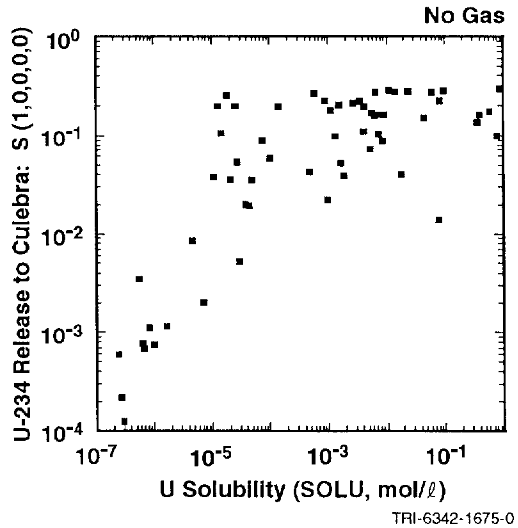

Scenario: $S^{+-}(2,0,0,0,0)$, Assumed Intrusion Time: 1000 yrs

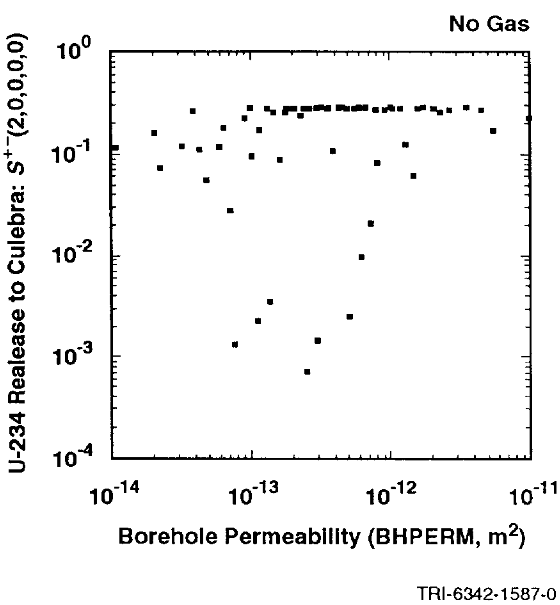

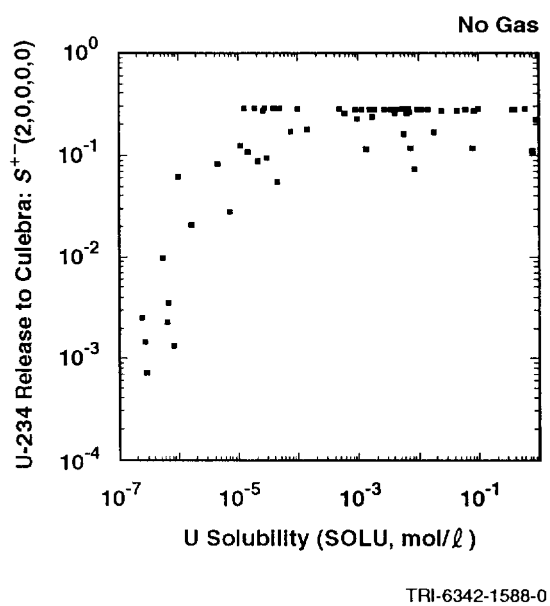

Figure 5.1-6. Scatterplots for Normalized Release of U-234 to the Culebra Dolomite without Gas Generation in the Repository for Variables SALPERM (Salado permeability), BHPERM (borehole permeability) and SOLU (solubility for U) and Scenarios $S(1,0,0,0,0)$ and $S^{+-}(2,0,0,0,0)$ with an Assumed Intrusion Time of 1000 Yrs.

The lower two frames in Figure 5.1-6 are for scenario $S^{+-}(2,0,0,0,0)$. The associated scatterplots show U-234 release to the Culebra increasing with BHPERM (borehole permeability) and SOLU (solubility for U). Further, the effect of an inventory limit on the U-234 release to the Culebra can be clearly seen in the line of equal releases across the top of the two scatterplots. The lower two scatterplots in Figure 5.1-6 for scenario $S^{+-}(2,0,0,0,0)$ show essentially the same pattern as the upper two scatterplots for scenario $S(1,0,0,0,0)$. However, the results for scenario $S^{+-}(2,0,0,0,0)$ are better defined than those for scenario $S(1,0,0,0,0)$ due to the larger brine flows through the panel and into the Culebra. A similar pattern is also shown in Figure 4.5-2 for scenario $S^{+-}(2,0,0,0,0)$ for gas generation in the repository.

Scatterplots for the release of Am-241 to the Culebra without gas generation are presented in Figure 5.1-7. The top two frames are for scenario $S(1,0,0,0,0)$, and the lower two frames are for scenario $S^{+-}(2,0,0,0,0)$. The patterns shown in this figure are similar to those appearing in Figure 5.1-6 for U-234. For both scenarios, the releases initially increase as SOLAM (solubility for Am) increases and then tend to level off for larger values of SOLAM due to inventory limitations. As shown in Figure 2.4-2, the Am-241 inventory in one waste panel at 1000 yrs is approximately 30 EPA units.

Interesting patterns appear in the scatterplots for SALPERM (Salado permeability) and BHPERM (borehole permeability) in Figure 5.1-7 for scenarios $S(1,0,0,0,0)$ and $S^{+-}(2,0,0,0,0)$, respectively. These two scatterplots have two bands that result from the sampling procedure used for SOLAM (solubility for Am). Specifically, the distribution for SOLAM was assumed to be piecewise uniform over several subintervals of a range extending from 5×10^{-14} to 1.4 mol/ℓ, which leads to the clusters of values for SOLAM that can be seen in the two scatterplots involving SOLAM in Figure 5.1-7. The top bands in the scatterplots for SALPERM and BHPERM are associated with the larger values for SOLAM; similarly, the lower bands are associated with the smaller values for SOLAM. If SOLAM had been sampled from a loguniform distribution over the range 5×10^{-14} to 1.4 mol/ℓ, the bands appearing in the scatterplots for SALPERM and BHPERM would be less apparent, although it is possible that they would still be present due to the leveling off of the releases to the Culebra because of inventory limitations. This behavior provides an excellent example of the fact that whether or not a particular variable appears to be important often depends on the ranges assigned to other variables. In this case, SALPERM and BHPERM have well-defined effects when SOLAM is restricted to values below or above the point at which inventory limits are important (i.e., SOLAM $\doteq 10^{-7}$ mol/ℓ). However, the scatterplots for the two variables would show a much more diffuse pattern if SOLAM had been sampled from a loguniform distribution on the interval [5×10^{-14}, 1.4].

Scenario: $S(1,0,0,0,0)$, Assumed Intrusion Time: 1000 yrs

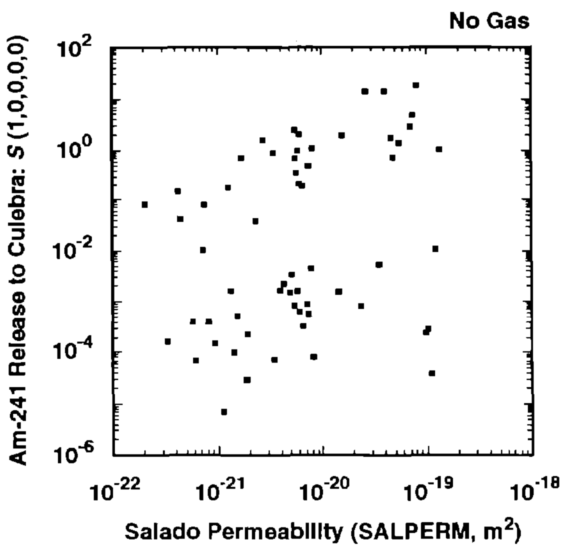

TRI-6342-1589-0

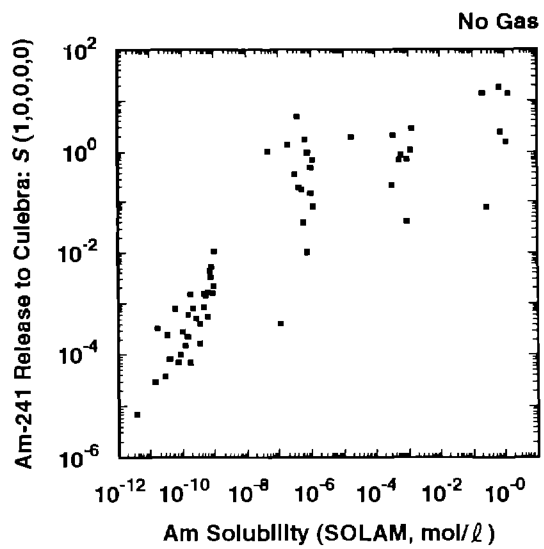

TRI-6342-1590-0

Scenario: $S^{+-}(2,0,0,0,0)$, Assumed Intrusion Time: 1000 yrs

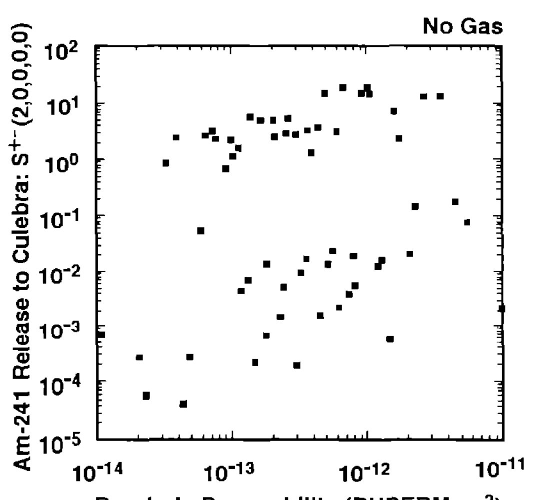

TRI-6342-1676-0

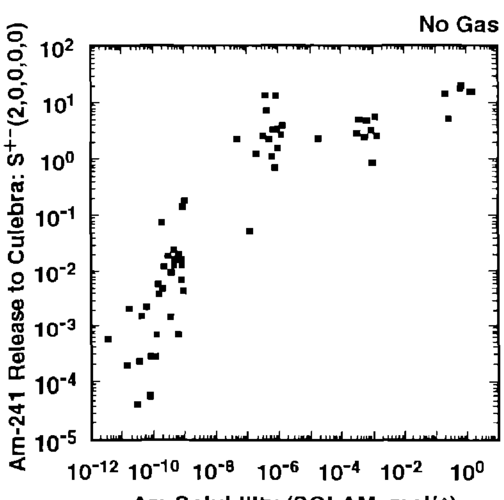

TRI-6342-1677-0

Figure 5.1-7. Scatterplots for Normalized Release of Am-241 to the Culebra Dolomite without Gas Generation in the Repository for Variables SALPERM (Salado permeability), BHPERM (borehole permeability) and SOLAM (solubility for Am) and Scenarios $S(1,0,0,0,0)$ and $S^{+-}(2,0,0,0,0)$ with an Assumed Intrusion Time of 1000 Yrs.

The corresponding scatterplots for Am-241 release to the Culebra with gas generation are shown in Figure 4.5-3. As comparison of the scatterplots in Figures 4.5-3 and 5.1-7 shows, gas generation and no gas generation lead to similar patterns of behavior, although the results shown in Figure 5.1-7 for releases in the absence of gas generation are considerably sharper than those shown in Figure 4.5-3 for releases in the presence of gas generation. In particular, the releases with gas generation shown in Figure 4.5-3 are both smaller and more diffuse than the releases without gas generation shown in Figure 5.1-7 as a result of both less brine inflow to the repository from the Salado Formation and more time for radioactive decay.

The presence or absence of gas generation in the repository only affects release to the Culebra. The groundwater transport analyses for both cases were performed with the same dual porosity transport model in the Culebra and the same sample elements. Thus, the same patterns of behavior shown in Figures 4.5-6 and 4.5-7 for transport in the Culebra with gas generation also hold for transport without gas generation. In particular, as shown by the scatterplot for U-234 in the lower left frame of Figure 4.5-6 for scenario $S^{+-}(2,0,0,0,0)$ and transport one-quarter the distance to the accessible environment, retardation resulting from the matrix distribution coefficients (i.e., MKDAM, MKDNP, MKDPU, MKDTH, MKDU) is very effective in preventing individual isotopes from being transported to the accessible environment. As shown by the upper two frames in Figure 4.5-6, the retardations for Am-241 and Pu-239 effectively cutoff transport in the Culebra with the dual-porosity model.

5.2 Effect of Single-Porosity Transport Model in Culebra Dolomite

Although a dual-porosity transport model is believed to be an appropriate representation for radionuclide transport in the Culebra, the use of a single-porosity transport model has also been proposed (Reeves et al., 1987). To help provide perspective on the impact of a single-porosity rather than a dual-porosity transport model in the Culebra, the analyses presented in Chapter 4 were repeated with a single-porosity transport model.

The CCDFs for groundwater transport to the accessible environment that result from the use of a single-porosity transport model are presented in Figure 5.2-1. The upper left frame displays the CCDFs for the individual sample elements; the corresponding distribution of CCDFs from the analysis with a dual-porosity transport model is shown in the lower left frame of Figure 4.1-2. As comparison of the CCDFs in Figures 5.2-1 and 4.1-2 shows, use of a single-porosity transport model results in considerably larger releases than the use of a dual-porosity transport model.

Groundwater Transport Releases Only

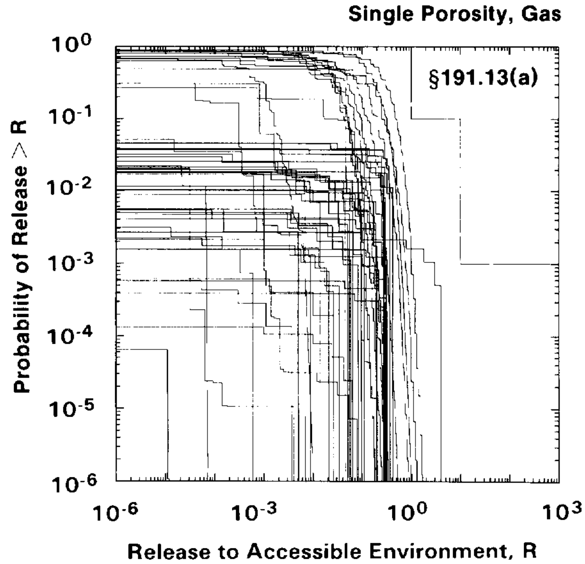

TRI-6342-1582-0

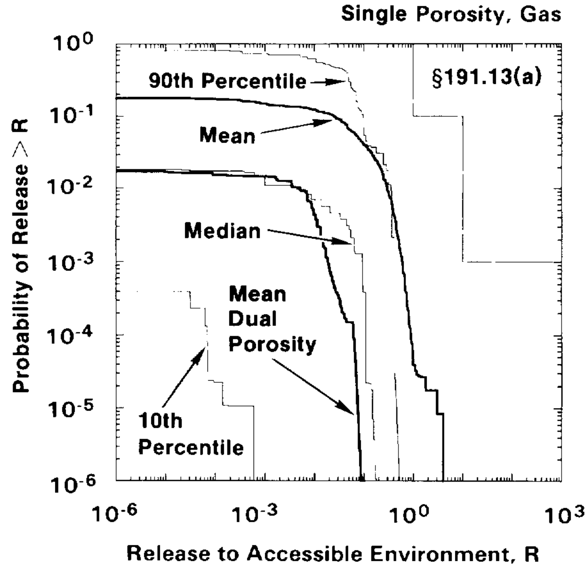

TRI-6342-1581-0

Total Release: Groundwater Transport and Cuttings Releases

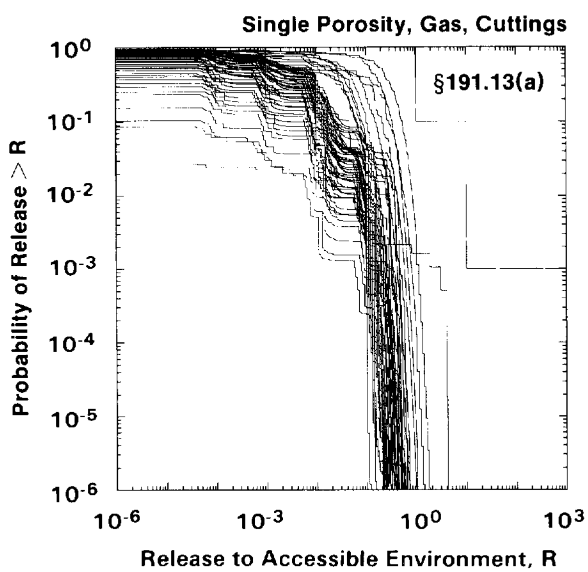

TRI-6342-1615-0

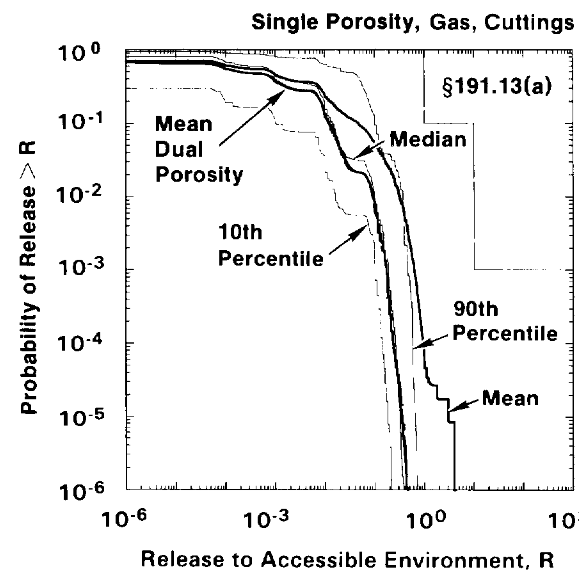

TRI-6342-1616-0

Figure 5.2-1. Complementary Cumulative Distribution Functions for Normalized Release to the Accessible Environment for Gas Generation in the Repository and a Single-Porosity Transport Model in the Culebra Dolomite.

The upper right frame in Figure 5.2-1 shows the mean and selected percentile curves for the distribution of CCDFs shown in the upper left frame. The mean CCDF obtained with the dual-porosity transport model is also shown. As comparison of the two mean curves shows, use of the single-porosity model results in a significant increase in the mean CCDF for radionuclide release to the accessible environment. Due to the large variability in the individual CCDFs, the mean CCDFs tend to be dominated by the few larger CCDFs. As a result, simply comparing mean CCDFs probably underestimates the impact of the single-porosity transport model. However, although the single-porosity transport model results in larger releases to the accessible environment than the dual-porosity transport model, none of the individual CCDFs in Figure 5.2-1 cross the EPA release limits.

The two lower frames in Figure 5.2-1 summarize the CCDFs for total release to the accessible environment. As comparison of the results in the upper and lower frames of Figure 5.2-1 shows, release to the accessible environment is still dominated by cuttings removal when the single-porosity transport model is used, although the CCDFs closest to the EPA release limits are determined primarily by groundwater transport releases (i.e., compare the CCDFs closest to the EPA release limits in the upper left and lower left frames of Figure 5.2-1). For comparison, the CCDFs due to cuttings releases only are shown in the upper left frame of Figure 4.1-2. The lower right frame in Figure 5.2-1 contains the mean CCDFs for total release to the accessible environment, including releases due to groundwater transport and cuttings removal, for single- and dual-porosity transport models in the Culebra. As comparison of these two CCDFs shows, the assumption of a single-porosity transport model does cause an upward shift in the mean CCDF.

An alternate comparison of the effects of single-porosity and dual-porosity transport models in the Culebra for scenarios $S(1,0,0,0,0)$ and $S^{+-}(2,0,0,0,0)$ is shown in Figure 5.2-2. As the scatterplots in this figure show, the single-porosity transport model causes the releases associated with the individual sample elements to be shifted upward. For many sample elements, zero releases with the dual-porosity transport model are nonzero releases with the single-porosity transport model. This effect is most pronounced for scenario $S^{+-}(2,0,0,0,0)$. As shown in Figure 4.5-4, the presence of gas generation in the repository results in no releases to the Culebra for many sample elements for scenario $S(1,0,0,0,0)$, with the result that the transport model in use for the Culebra has no effect on the predicted release to the accessible environment for these sample elements.

The total normalized releases to the accessible environment due to groundwater transport with a single-porosity transport model in the Culebra for individual scenarios are summarized in Figure 5.2-3. The corresponding results for the dual-porosity transport model appear in Figure 4.4-1. As

Scenario: $S(1,0,0,0,0)$, Assumed Intrusion Time: 1000 yrs

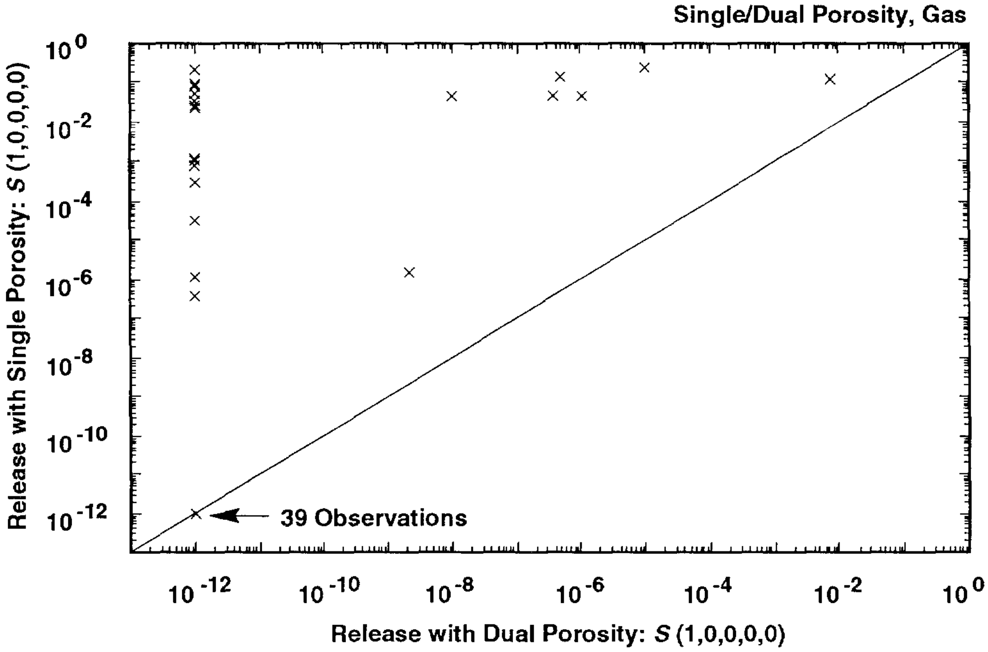

TRI-6342-1638-0

Scenario: $S^{+-}(2,0,0,0,0)$, Assumed Intrusion Time: 1000 yrs

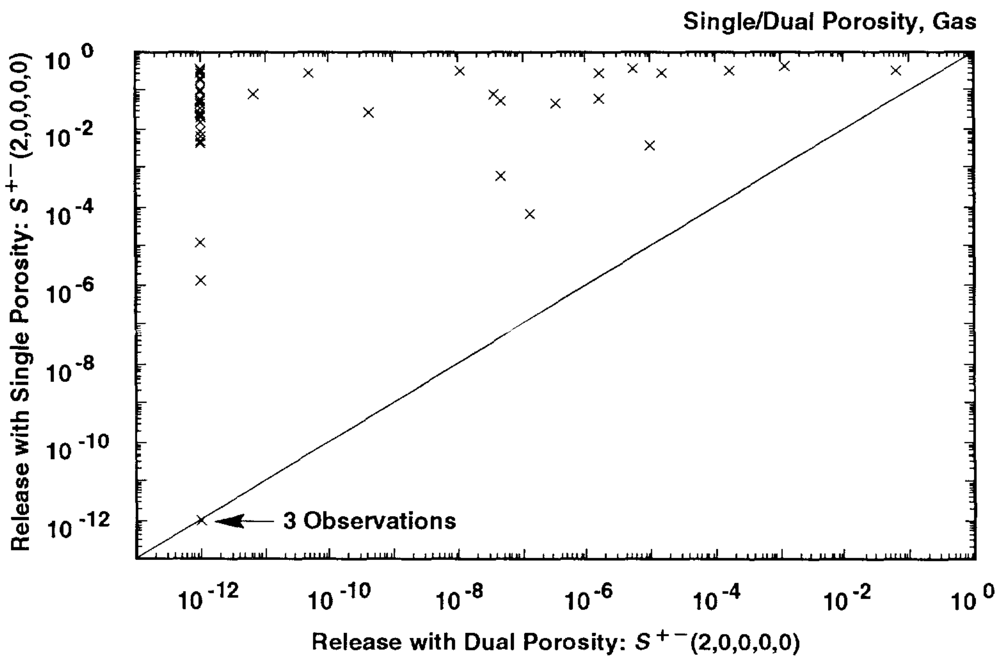

TRI-6342-1639-0

Figure 5.2-2. Scatterplots Comparing Total Normalized Release to the Accessible Environment Due to Groundwater Transport with Gas Generation in the Repository and Intrusion Occurring at 1000 Yrs for Single-Porosity and Dual-Porosity Transport Models in the Culebra Dolomite. For plotting purposes, values less than 10^{-12} are set to 10^{-12}.

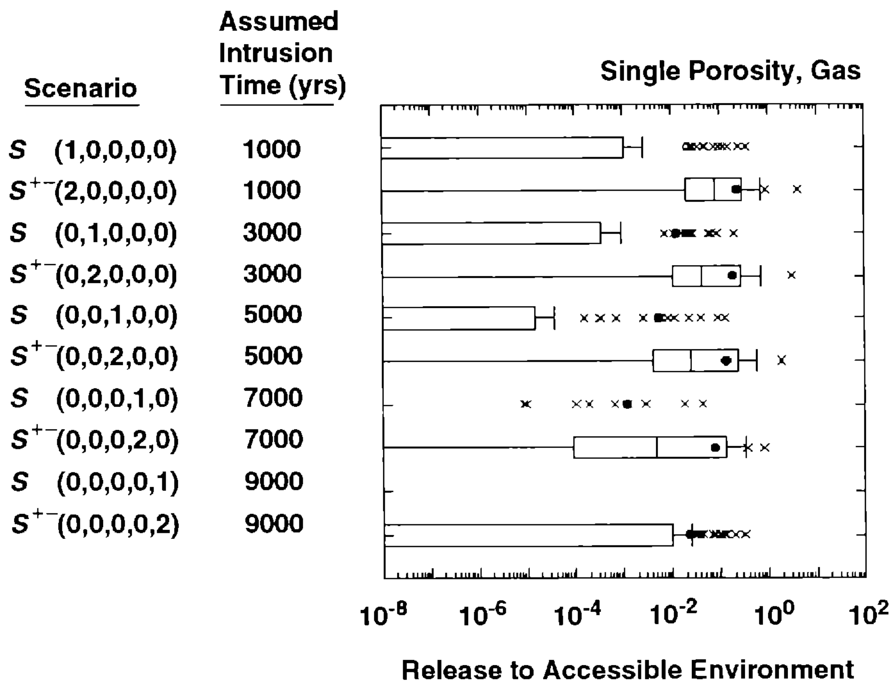

TRI-6342-1688-0

Figure 5.2-3. Total Normalized Release to the Accessible Environment Due to Groundwater Transport with Gas Generation in the Repository and a Single-Porosity Transport Model in the Culebra Dolomite.

already discussed, the releases in Figure 5.2-3 for the single-porosity model are considerably larger than the releases in Figure 4.4-1 for the dual-porosity transport model. The transport model used in the Culebra does not affect cuttings removal. Thus, the cuttings removal results used in the construction of the total releases to the accessible environment are the same regardless of the transport model used in the Culebra. The total releases for individual scenarios due to cuttings removal and groundwater transport with a single-porosity transport model are summarized in Figure 5.2-4. The corresponding results for the dual-porosity transport model are given in Figure 4.4-3. As comparison of Figures 5.2-4 and 4.4-3 shows, total releases to the accessible environment are not completely dominated by cuttings removal when the single-porosity transport model is used, which is the case for the dual-porosity transport model. In particular, the groundwater transport releases for E1E2-type scenarios (i.e., $S^{+-}(2,0,0,0,0)$, ..., $S^{+-}(0,0,0,0,2)$) are often considerably larger than the corresponding releases due to cuttings removal.

Releases of individual isotopes to the Culebra with gas generation in the repository for scenarios $S(1,0,0,0,0)$ and $S^{+-}(2,0,0,0,0)$ are summarized in Figure 4.4-7. The resultant releases to the accessible environment due to groundwater transport with a single-porosity transport model are summarized

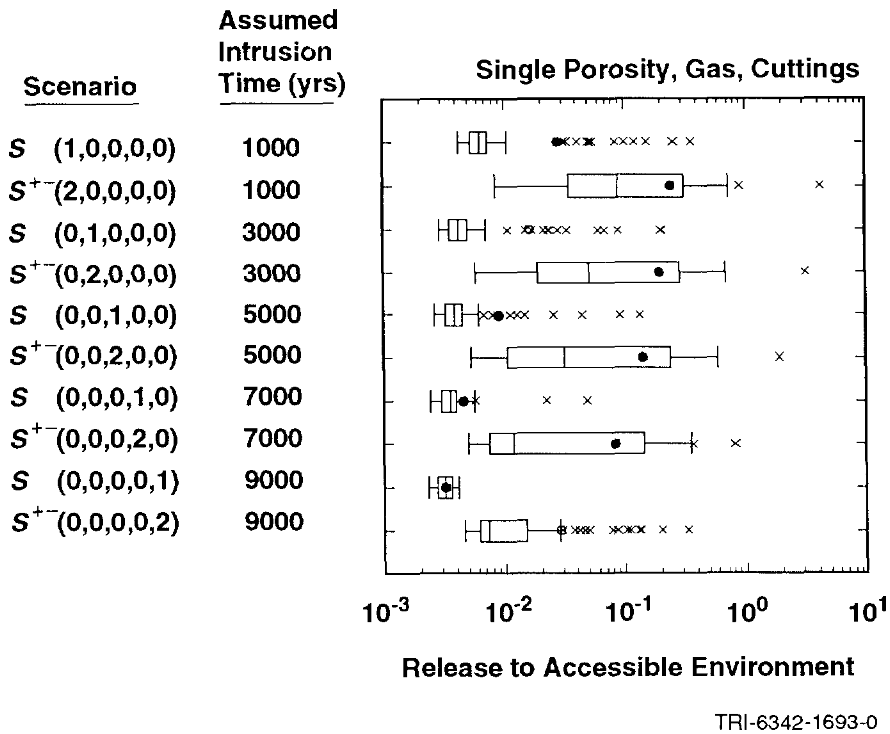

Figure 5.2-4. Total Normalized Release to the Accessible Environment Due to Cuttings Removal and Groundwater Transport with Gas Generation in the Repository and a Single-Porosity Transport Model in the Culebra Dolomite.

in Figure 5.2-5; the corresponding releases for a dual-porosity transport model are summarized in Figure 4.4-2. As already discussed in conjunction with Figures 5.2-1 through 5.2-4, the single-porosity model results in larger total releases to the accessible environment due to groundwater transport than the dual-porosity transport model. As comparison of Figures 4.4-2 and 5.2-5 shows, this pattern also holds for the individual isotopes, with the single-porosity model consistently producing larger releases for the individual isotopes than the dual-porosity transport model.

Sensitivity analyses of the groundwater transport results for individual isotopes for scenarios $S(1,0,0,0,0)$ and $S^{+-}(2,0,0,0,0)$ with gas generation in the repository and a single-porosity transport model in the Culebra are presented in Tables 5.2-1 and 5.2-2 for transport one-quarter, one-half and the full distance to the accessible environment. For convenience, these tables also contain the corresponding sensitivity analysis results for release to the Culebra, although these results have appeared previously in Tables 4.5-1 and 4.5-2.

As discussed in Section 4.5, SALPERM (Salado permeability) acts as switch for scenario $S(1,0,0,0,0)$ that determines whether or not a release from the repository to the Culebra will take place, with the result that the analyses

Scenario: $S(1,0,0,0,0)$, Assumed Intrusion Time: 1000 yrs

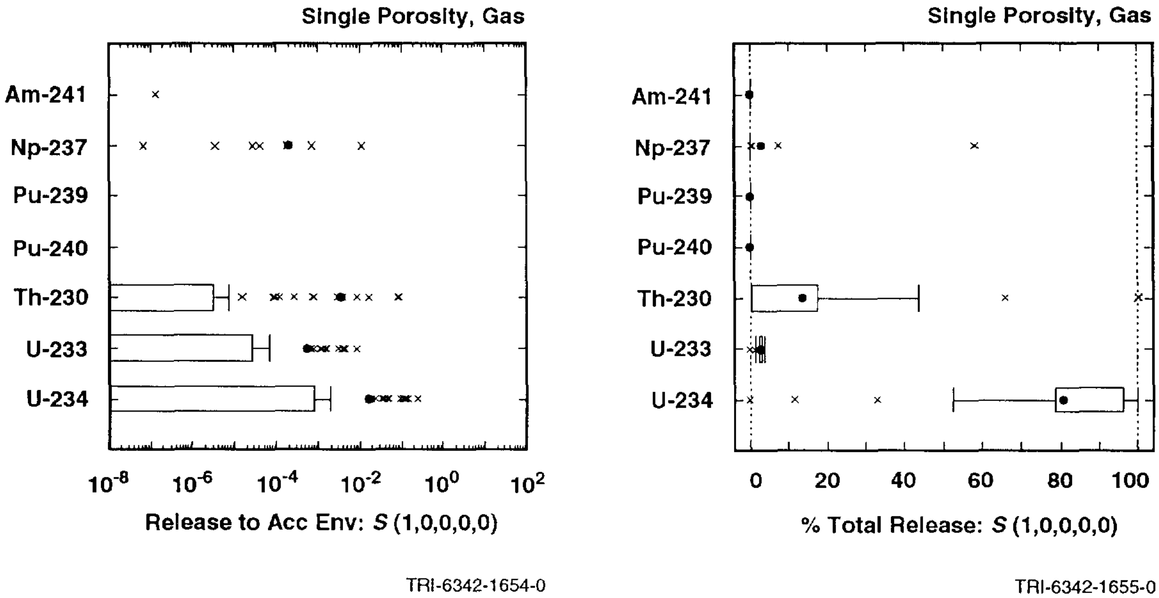

Scenario: $S^{+-}(2,0,0,0,0)$, Assumed Intrusion Time: 1000 yrs

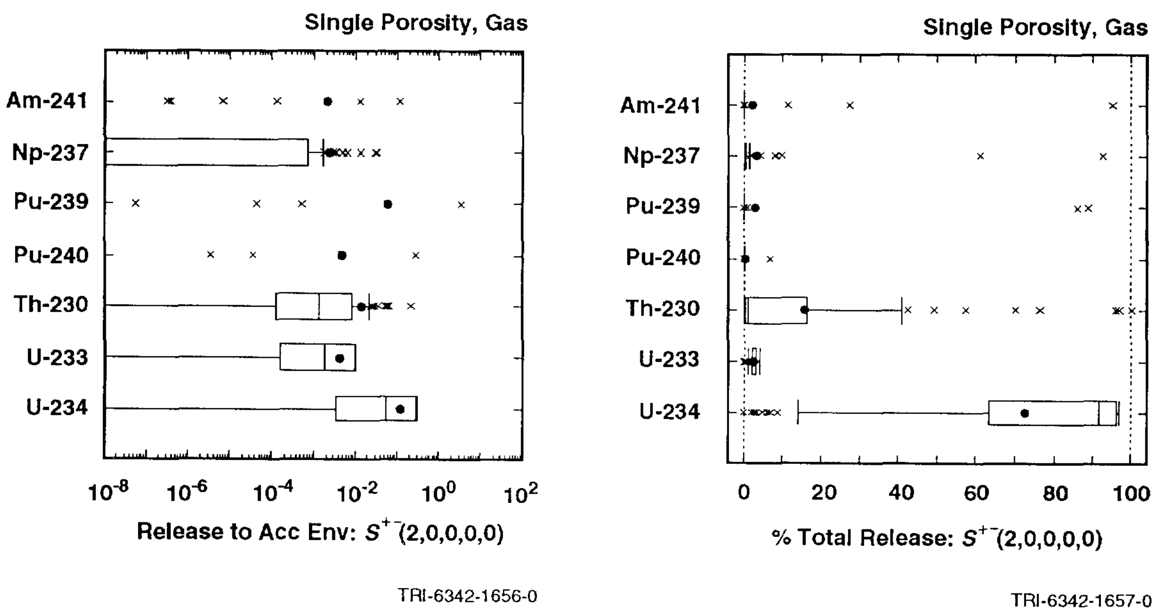

Figure 5.2-5. Normalized Releases for Individual Isotopes to the Accessible Environment Due to Groundwater Transport with Intrusion Occurring at 1000 Yrs, Gas Generation in the Repository and a Single-Porosity Transport Model in the Culebra Dolomite.

TABLE 5.2-1. STEPWISE REGRESSION ANALYSES WITH RANK-TRANSFORMED DATA FOR SCENARIO *S*(1,0,0,0,0) WITH GAS GENERATION IN THE REPOSITORY, A SINGLE-POROSITY TRANSPORT MODEL IN THE CULEBRA DOLOMITE AND INTRUSION OCCURRING 1000 YRS AFTER REPOSITORY CLOSURE

	Release to Culebra*		Quarter Distance		Half Distance		Full Distance	
Step	Variable	R^2	Variable	R^2	Variable	R^2	Variable	R^2
Dependent Variable: Integrated Discharge Am-241								
1	SALPERM	0.59(+)	SALPERM	0.20 (+)	SALPERM	0.55 (+)	SALPERM	0.20 (+)
2			FKDAM	0.35 (-)			FKDAM	0.35 (-)
Dependent Variable: Integrated Discharge Np-237								
1	SALPERM	0.53(+)	MBPERM	0.21 (+)	SALPERM	0.47 (+)	SALPERM	0.24 (+)
2			FKDNP	0.31 (-)				
Dependent Variable: Integrated Discharge Pu-239								
1	SALPERM	0.56(+)	FKDPU	0.16 (-)	SALPERM	0.47 (+)	SALPERM	0.19 (+)
2			SALPERM	0.31 (+)	MBPERM	0.52 (+)	FKDPU	0.27 (-)
Dependent Variable: Integrated Discharge Pu-240								
1	SALPERM	0.56(+)	SALPERM	0.22 (+)	SALPERM	0.53 (+)	SALPERM	0.13 (+)
2			FKDPU	0.38 (-)	MBPERM	0.59 (+)	FKDPU	0.26 (-)
Dependent Variable: Integrated Discharge Th-230								
1	SALPERM	0.55(+)	SALPERM	0.53 (+)	SALPERM	0.53 (+)	SALPERM	0.54 (+)
Dependent Variable: Integrated Discharge U-233								
1	SALPERM	0.59(+)	SALPERM	0.57 (+)	SALPERM	0.56 (+)	SALPERM	0.52 (+)
Dependent Variable: Integrated Discharge U-234								
1	SALPERM	0.59(+)	SALPERM	0.57 (+)	SALPERM	0.56 (+)	SALPERM	0.56 (+)
Dependent Variable: EPA Sum for Total Integrated Discharge								
1	SALPERM	0.58(+)	SALPERM	0.57 (+)	SALPERM	0.57 (+)	SALPERM	0.57 (+)

*Analysis results in this column are the same as those presented in the corresponding column of Table 4.5-1.

TABLE 5.2-2. STEPWISE REGRESSION ANALYSES WITH RANK-TRANSFORMED DATA FOR SCENARIO S^{+-}(2,0,0,0,0) WITH GAS GENERATION IN THE REPOSITORY, A SINGLE-POROSITY TRANSPORT MODEL IN THE CULEBRA DOLOMITE AND INTRUSION OCCURRING 1000 YRS AFTER REPOSITORY CLOSURE

	Release to Culebra*		Quarter Distance		Half Distance		Full Distance	
Step	Variable	R^2	Variable	R^2	Variable	R^2	Variable	R^2
Dependent Variable: Integrated Discharge Am-241								
1	SOLAM	0.36 (+)	FKDAM	0.59 (-)	FKDAM	0.23 (-)	FKDAM	0.38 (-)
2	BHPERM	0.74 (+)	CULFRPOR	0.65 (-)	CULFRPOR	0.44 (-)	CULFRPOR	0.50 (-)
3	BPPRES	0.78 (+)			GRMICH	0.51 (+)		
4					CULFRPOR	0.58 (-)		
Dependent Variable: Integrated Discharge Np-237								
1	SOLNP	0.65 (+)	FKDNP	0.56 (-)	FKDNP	0.49 (-)	FKDNP	0.54 (-)
2	BHPERM	0.78 (+)	SOLNP	0.63 (+)	SOLNP	0.58 (+)	SOLNP	0.64 (+)
3	BPPRES	0.82 (+)	SOLAM	0.68 (+)	SOLAM	0.63 (+)	SOLAM	0.68 (+)
4	EHPH	0.85 (+)	BHPERM	0.72 (+)	BHPERM	0.67 (+)		
5	GRCORI	0.88 (-)						
Dependent Variable: Integrated Discharge Pu-239								
1	SOLPU	0.74 (+)	FKDPU	0.59 (-)	FKDPU	0.24 (-)	FKDPU	0.39 (-)
2	BHPERM	0.85 (+)	CULTRFLD	0.63 (-)				
Variable: Integrated Discharge Pu-240								
1	SOLPU	0.74 (+)	FKDPU	0.63 (-)	FKDPU	0.25 (-)	FKDPU	0.48 (-)
2	BHPERM	0.85 (+)	CULTRFLD	0.67 (-)				
Dependent Variable: Integrated Discharge Th-230								
1	SOLTH	0.69 (+)	FKDTH	0.26 (-)	FKDTH	0.29 (-)	FKDTH	0.33 (-)
2	BHPERM	0.82 (+)	SOLTH	0.37 (+)	BHPERM	0.39 (+)	BHPERM	0.43 (+)
3			BHPERM	0.47 (+)	SOLTH	0.48 (+)	BPPRES	0.52 (+)
4			BPPRES	0.54 (+)	CULFRPOR	0.55 (-)	CULFRPOR	0.58 (-)
5			CULFRPOR	0.61 (-)	BPPRES	0.62 (+)	SOLTH	0.64 (+)
6			DBDIAM	0.67 (+)	DBDIAM	0.68 (+)	DBDIAM	0.69 (+)

*Analysis results in this column are the same as those presented in the corresponding column of Table 4.5-2.

TABLE 5.2-2. STEPWISE REGRESSION ANALYSES WITH RANK-TRANSFORMED DATA FOR SCENARIO S^{+-}(2,0,0,0,0) WITH GAS GENERATION IN THE REPOSITORY, A SINGLE-POROSITY TRANSPORT MODEL IN THE CULEBRA DOLOMITE AND INTRUSION OCCURRING 1000 YRS AFTER REPOSITORY CLOSURE (concluded)

	Release to Culebra*		Quarter Distance		Half Distance		Full Distance	
Step	Variable	R^2	Variable	R^2	Variable	R^2	Variable	R^2
Dependent Variable: Integrated Discharge U-233								
1	BHPERM	0.43 (+)	BHPERM	0.32 (+)	BHPERM	0.32 (+)	BHPERM	0.30 (+)
2	SOLU	0.58 (+)	BPPRES	0.45 (+)	FKDU	0.45 (-)	FKDU	0.46 (-)
3	BPPRES	0.70 (+)	SOLU	0.57 (+)	SOLU	0.55 (+)	SOLU	0.55 (+)
4	SOLNP	0.74 (-)	FKDU	0.68 (-)	BPPRES	0.65 (+)	BPPRES	0.64 (+)
5			CULFRPOR	0.75 (-)	CULFRPOR	0.71 (-)	CULFRPOR	0.71 (-)
6			CULDISP	0.79 (+)	CULDISP	0.75 (+)	CULDISP	0.74 (+)
Dependent Variable: Integrated Discharge U-234								
1	BHPERM	0.47 (+)	BHPERM	0.31 (+)	BHPERM	0.31 (+)	BHPERM	0.30 (+)
2	SOLU	0.60 (+)	BPPRES	0.44 (+)	FKDU	0.43 (-)	FKDU	0.44 (-)
3	BPPRES	0.72 (+)	SOLU	0.55 (+)	BPPRES	0.53 (+)	SOLU	0.53 (+)
4			FKDU	0.64 (-)	SOLU	0.62 (+)	BPPRES	0.62 (+)
5			CULFRPOR	0.71 (-)	CULFRPOR	0.69 (-)	CULFRPOR	0.69 (-)
6			CULDISP	0.75 (+)	CULDISP	0.73 (+)	CULDISP	0.73 (+)
Dependent Variable: EPA Sum for Total Integrated Discharge								
1	BHPERM	0.46 (+)	BHPERM	0.39 (+)	BHPERM	0.38 (+)	BHPERM	0.37 (+)
2	SOLAM	0.57 (+)	BPPRES	0.54 (+)	BPRES	0.51 (+)	BPPRES	0.50 (+)
3	BPPRES	0.66 (+)	FKDU	0.61 (-)	FKDU	0.58 (-)	FKDU	0.58 (-)
4	SOLPU	0.69 (+)	CULFRPOR	0.68 (-)	CULFRPOR	0.66 (-)	CULFRPOR	0.65 (-)
5	BPSTOR	0.73 (+)	SOLU	0.75 (+)	SOLU	0.73 (+)	SOLU	0.72 (+)
6	SOLU	0.76 (+)	FKDNP	0.80 (-)	FKDNP	0.78 (-)	FKDNP	0.77 (-)
7			BPSTOR	0.82 (+)	CULDISP	0.81 (+)	CULDISP	0.80 (+)
8			CULDISP	0.84 (+)	BPSTOR	0.83 (+)		

*Analysis results in this column are the same as those presented in the corresponding column of Table 4.5-2.

presented in Table 5.2-1 are dominated by SALPERM. Due to the greater number of nonzero releases to the Culebra, the analyses in Table 5.2-2 for scenario $S^{+-}(2,0,0,0,0)$ are considerably more interesting than those in Table 5.2-1 for scenario $S(1,0,0,0,0)$. The variables BHPERM (borehole permeability), BPPRES (brine pocket pressure) and CULFRPOR (Culebra fracture porosity) tend to be important for all isotopes for scenario $S^{+-}(2,0,0,0,0)$. Further, the appropriate solubilities and fracture distribution coefficients are important for the individual isotopes.

Scatterplots for the release of Pu-239, U-234 and Am-241 to the Culebra with gas generation in the repository are given in Figures 4.5-1, 4.5-2 and 4.5-3, respectively, and help provide insights into the regression-based sensitivity analyses for release to the Culebra. Scatterplots can also provide insights on the analyses for transport in the Culebra with a single-porosity model. Scatterplots for the normalized release of Pu-239 and Am-241 to the accessible environment for scenario $S^{+-}(2,0,0,0,0)$ are given in Figure 5.2-6. The top two scatterplots in Figure 5.2-6 are for Pu-239 and show that the release decreases with increasing values for FKDPU (fracture distribution coefficient for Pu) and increases with increasing values for SOLPU (solubility for Pu). However, the releases are small, with only 7 sample elements resulting in release values that exceed 10^{-9}. Thus, even for single-porosity transport, the fracture distribution coefficient FKDPU is leading to retardations that prevent Pu-239 from reaching the accessible environment by groundwater transport.

The stepwise regression analysis presented in Table 5.2-2 for the release of Pu-239 to the accessible environment (i.e., the analysis for "Integrated Discharge Pu-239" at "Full Distance") selected only the variable FKDPU (fracture distribution coefficient for plutonium) with an R^2 value of 0.39, which is not a particularly good regression result. Examination of the two scatterplots in Figure 5.2-6 for Pu-239 provides considerably more information. In particular, these plots show not only the effect of FKDPU but also the effect of SOLPU (solubility for Pu), which was not identified in the regression analysis. This is another example of an analysis in which one variable (i.e., FKDPU) acts as a switch and causes all results to be effectively zero (i.e., $< 10^{-9}$) after a some value for the switch variable (i.e., FKDPU $\doteq 10^1$ m^3/kg). This switch produces a more complex pattern of relationships than can be captured by a simple regression model. It is sometimes possible to design regression models that will represent patterns of this type but the effort requires *a priori* knowledge of the relationships involved.

The lower two scatterplots in Figure 5.2-6 are for Am-241 and show that the release decreases with increasing values for FKDAM (fracture distribution

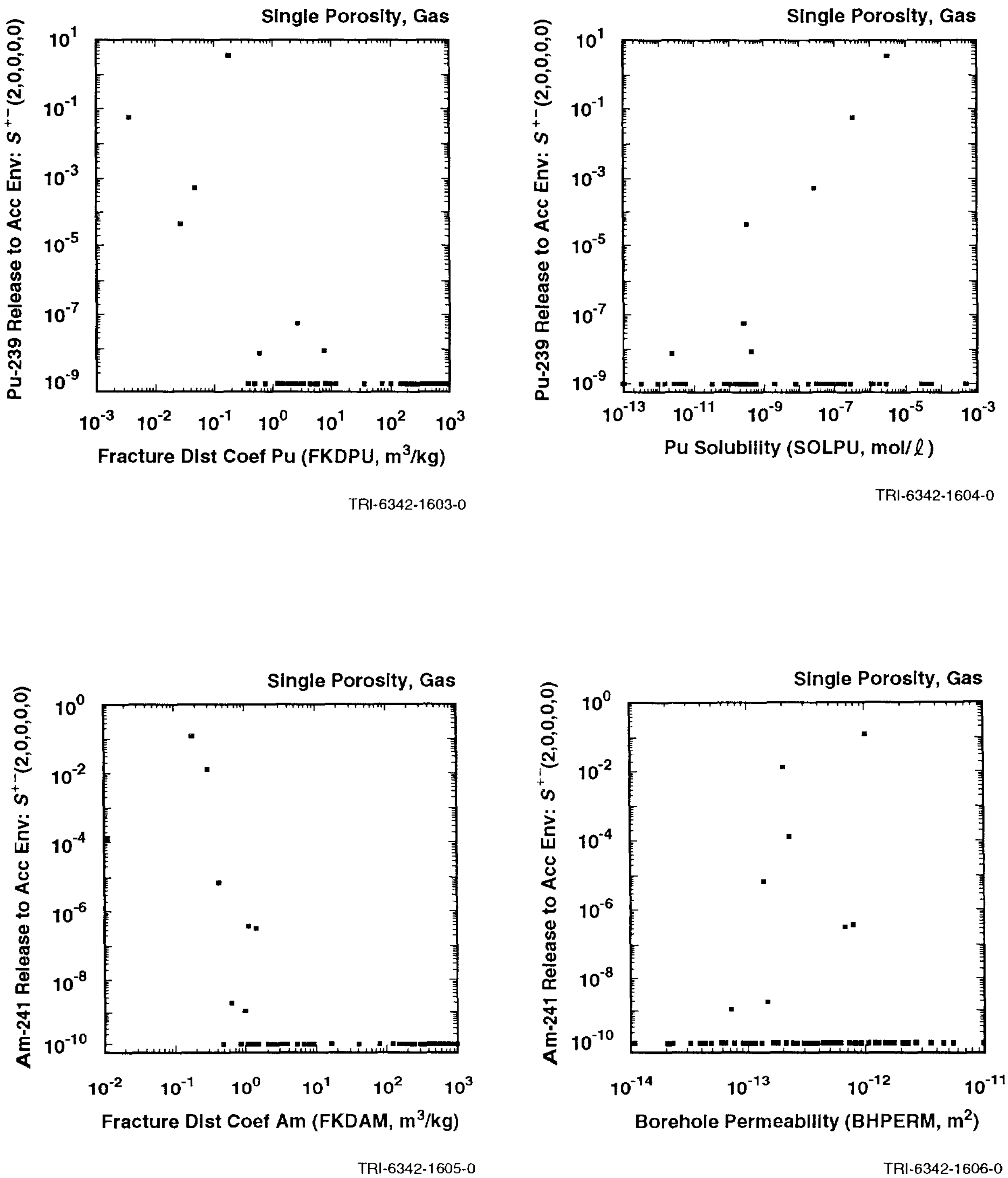

Figure 5.2-6. Scatterplots for Normalized Release of Pu-239 and Am-241 to the Accessible Environment for Scenario $S^{+-}(2,0,0,0,0)$ for Groundwater Transport with Gas Generation in the Repository, a Single-Porosity Transport Model in the Culebra Dolomite and Intrusion Occurring at 1000 Yrs.

coefficient for Am) and increases with increasing values for BHPERM (borehole permeability). The scatterplot for SOLAM (solubility for Am) was not included because the scatterplot for BHPERM showed a stronger relationship. Due to the short half-life of Am-241 (i.e., 432 yr), high values for BHPERM facilitate the release of Am-241 to the Culebra before it is lost due to radioactive decay. As with Pu-239, the two scatterplots in Figure 5.2-6 are more revealing of the factors that control the release of Am-241 to the accessible environment than the corresponding regression analysis in Table 5.2-2.

Scatterplots for the normalized release of U-234 to the accessible environment for scenario $S^{+-}(2,0,0,0,0)$ are given in Figure 5.2-7. The top two scatterplots are for BHPERM (borehole permeability) and SOLU (solubility for U) and show that the release to the accessible environment increases as each of these variables increases. The equal release values appearing at the top of these two scatterplots correspond to the entire inventory of U-234 in a single waste panel (see Figure 2.4-2). Thus, the larger values for BHPERM and SOLU are leading to the release of the entire U-234 inventory to the accessible environment. The lower scatterplot in Figure 5.2-7 is for FKDU (fracture distribution coefficient for U). As examination of this plot shows, the relatively low distribution coefficient values assigned to uranium (i.e., 0 to 1 m^3/kg) result in little retardation, with the result that both BHPERM and SOLU have a more pronounced effect on the U-234 releases to the accessible environment than FKDU. In contrast, the scatterplots in Figure 5.2-6 show more pronounced relationships between FKDPU (fracture distribution coefficient for Pu) and FKDAM (fracture distribution coefficient for Am) and the corresponding releases to the accessible environment for Pu-239 and Am-241 due to the larger values assigned to FKDPU and FKDAM relative to those assigned to FKDU.

Scatterplots similar to those appearing in Figures 5.2-6 and 5.2-7 could also be generated for scenario $S(1,0,0,0,0)$. However, they would be less revealing due to both the smaller releases into the Culebra and the large number of zero releases induced by the role of SALPERM (Salado permeability) in determining whether or not any release into the Culebra will take place.

As indicated by the regressions in Table 5.2-2, there is a negative relationship between CULFRPOR (fracture porosity in Culebra) and integrated discharge in the Culebra. This pattern of decreasing transport with increasing values for CULFRPOR is illustrated by the scatterplot appearing in Figure 5.2-8 for CULFRPOR versus total release to the accessible environment for groundwater transport with a single-porosity model in the Culebra. The negative effect indicated for CULFRPOR in Figure 5.2-8 for single-porosity

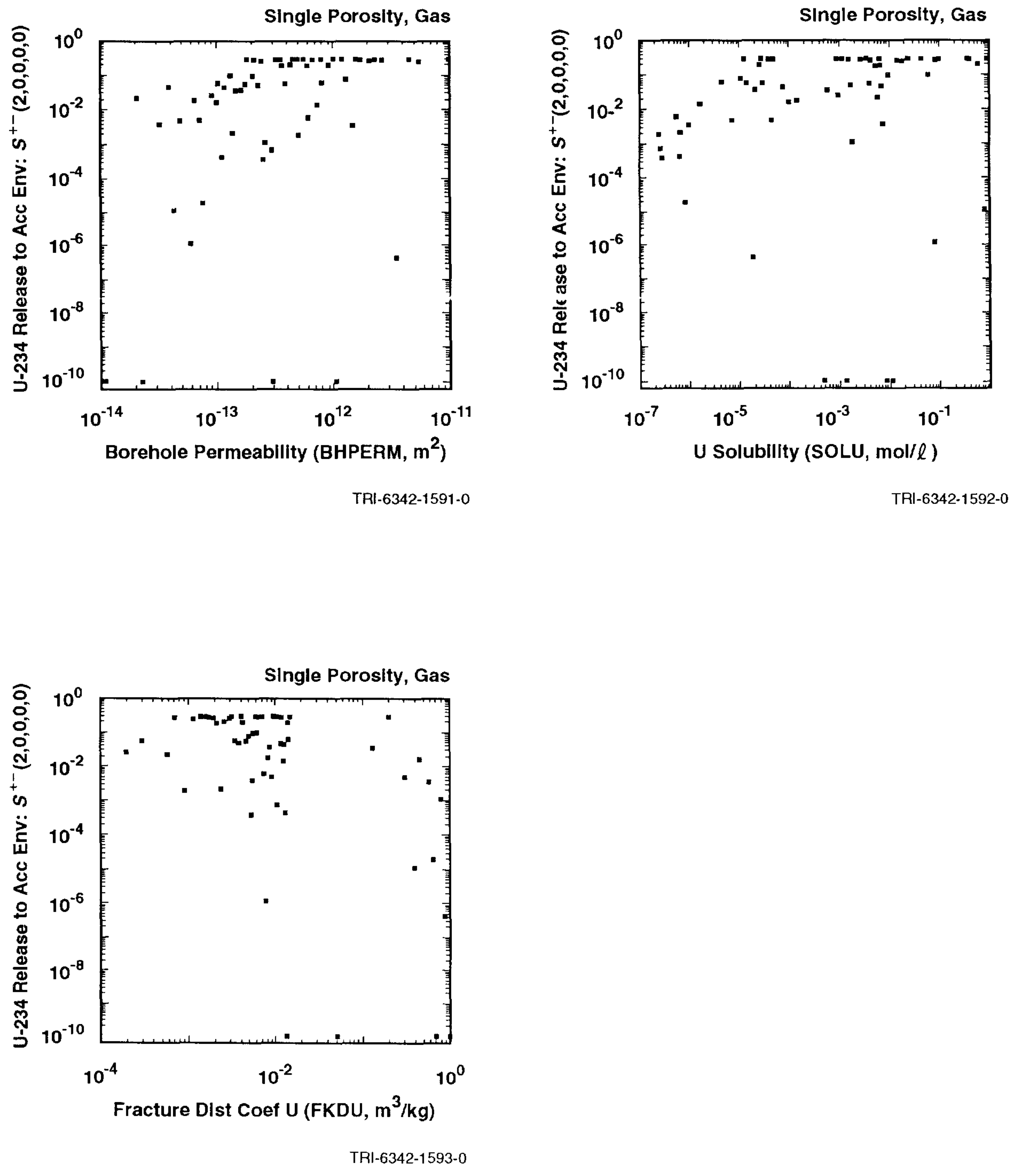

Figure 5.2-7. Scatterplots for Normalized Release of U-234 to the Accessible Environment for Scenario $S^{+-}(2,0,0,0,0)$ for Groundwater Transport with Gas Generation in the Repository, a Single-Porosity Transport Model in the Culebra Dolomite and Intrusion Occurring at 1000 Yrs.

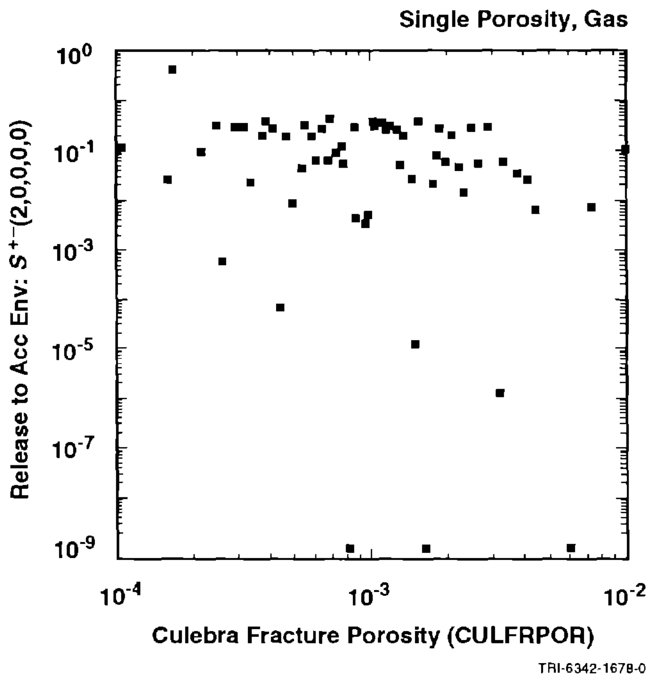

Figure 5.2-8. Scatterplot for Fracture Porosity in Culebra Dolomite (CULFRPOR) versus Total Normalized Release to the Accessible Environment Due to Groundwater Transport for Scenario $S^{+-}(2,0,0,0,0)$ with Gas Generation in the Repository, a Single Porosity Transport Model in the Culebra and Intrusion Occurring at 1000 Yrs.

transport is the reverse of the positive effect indicated for CULFRPOR in Figure 4.5-7 for dual-porosity transport. As shown in these two figures, increasing CULFRPOR decreases release for a single-porosity transport model and causes the reverse effect for a dual-porosity transport model. For the single-porosity transport model, the negative effect of CULFRPOR results because increasing CULFRPOR decreases groundwater velocity, with a resultant decrease in radionuclide transport. The positive effect for the CULFRPOR for the dual-porosity transport model will be explained in Section 5.4 after results for dual-porosity transport without chemical retardation have been presented.

5.3 Effect of No Gas Generation and Single-Porosity Transport Model in Culebra Dolomite

The best estimate analyses presented in Chapter 4 include gas generation in the repository and a dual-porosity transport model in the Culebra. As shown in Sections 5.1 and 5.2, relaxing these assumptions leads to larger releases to the accessible environment due to groundwater transport, although the total release is not significantly affected due to the dominance of the cuttings releases. For perspective, this section presents the results of analyses performed with no gas generation in the repository and a single-porosity transport model for the Culebra.

Scatterplots comparing releases to the accessible environment with and without gas generation in the repository and with a single-porosity transport model in the Culebra are shown in Figure 5.3-1 for scenarios $S(1,0,0,0,0)$ and $S^{+-}(2,0,0,0,0)$. As examination of this figure shows, no gas generation results in larger releases than those obtained with gas generation. This effect is particularly pronounced for scenario $S(1,0,0,0,0)$ due to the large number of zero releases to the Culebra that occur in the presence of gas generation. As discussed in conjunction with Figure 4.5-1, this effect is due to the role of SALPERM (Salado permeability) as a switch in the presence of gas generation.

The releases to the accessible environment for individual isotopes calculated with no gas generation in the repository and a single-porosity transport model in the Culebra for scenarios $S(1,0,0,0,0)$ and $S^{+-}(2,0,0,0,0)$ are summarized in Figure 5.3-2. The corresponding releases for gas generation in the repository and a dual-porosity transport model in the Culebra are shown in Figure 4.4-2. As is the case for the total release, the releases for the individual isotopes are substantially increased with the assumption of no gas generation and a single-porosity transport model for the Culebra. Even so, the releases for the individual isotopes shown in Figure 5.3-2 tend to be small, with only a few sample elements producing individual isotope releases for scenario $S^{+-}(2,0,0,0,0)$ that exceed 1.

Although the single-porosity transport calculations with gas generation in the repository were performed for intrusions occurring in each of the five time intervals under consideration, the single-porosity transport calculations without gas generation were only performed for intrusions occurring at 1000 yrs. Thus, it is not possible to construct a distribution of CCDFs for single-porosity transport without gas generation in the repository that is equivalent to the distribution shown in Figure 5.2-1 for single-porosity transport with gas generation in the repository. However, as discussed in conjunction with Figure 5.1-4, CCDFs can be constructed for single-porosity transport with and without gas generation under the assumption that the rate constant λ in the Poisson model for drilling intrusions is equal to zero after 2000 yrs. The outcome of this construction is shown in Figure 5.3-3, with the results for gas generation appearing in the two upper frames and the results without gas generation appearing in the two lower frames. When considered in the context of the EPA release limits,

Scenario: $S(1,0,0,0,0)$, Assumed Intrusion Time: 1000 yrs

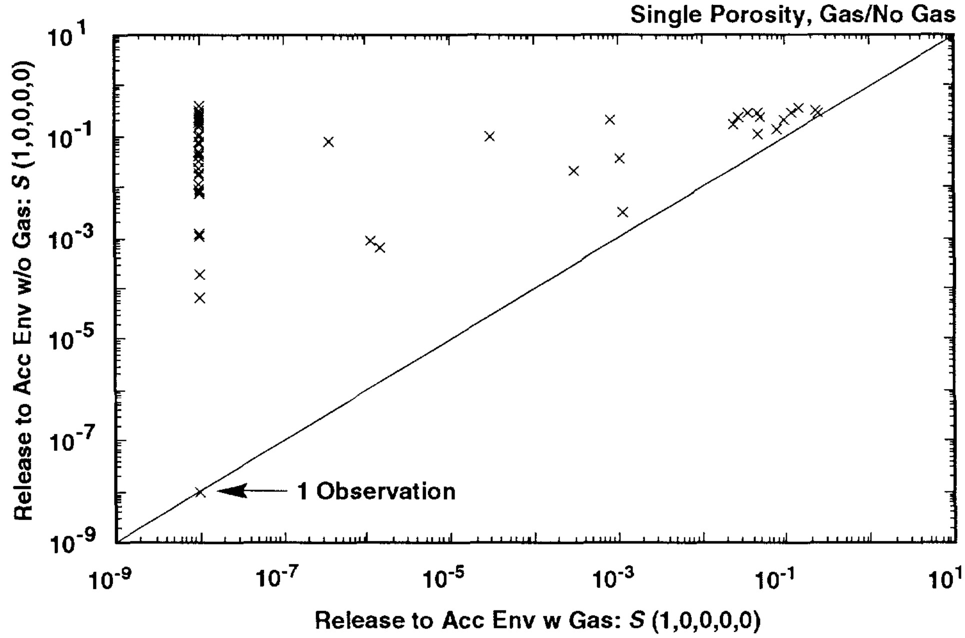

TRI-6342-1640-0

Scenario: $S^{+-}(2,0,0,0,0)$, Assumed Intrusion Time: 1000 yrs

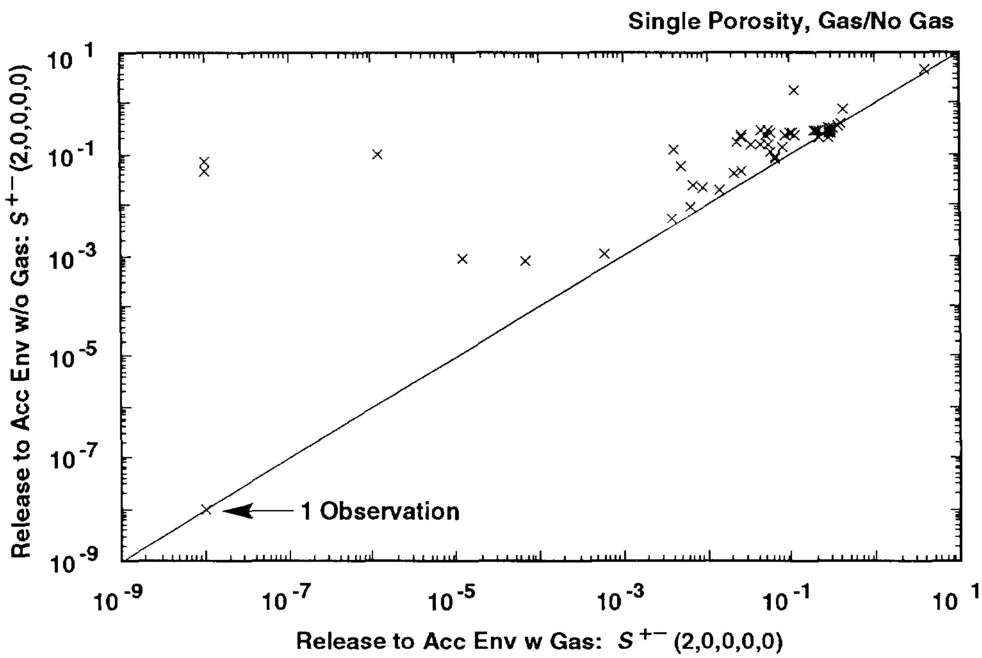

TRI-6342-1641-0

Figure 5.3-1. Scatterplots for Total Normalized Release to the Accessible Environment Due to Groundwater Transport with and without Gas Generation in the Repository for a Single-Porosity Transport Model in the Culebra Dolomite and an Assumed Intrusion Time of 1000 Yrs. For plotting purposes, values less than 10^{-8} are set to 10^{-8}.

Scenario: *S*(1,0,0,0,0), Assumed Intrusion Time: 1000 yrs

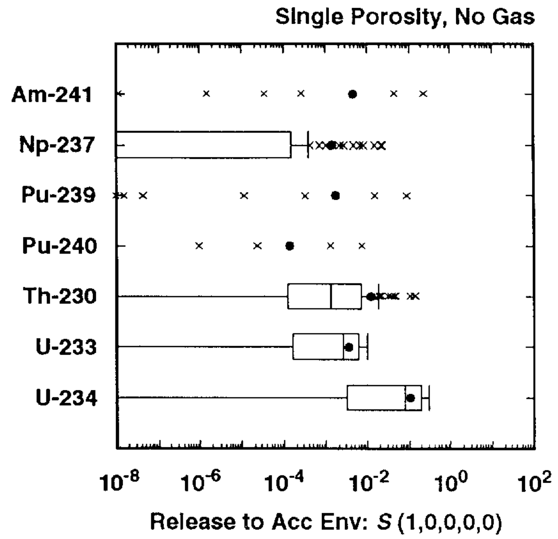

TRI-6342-1650-0

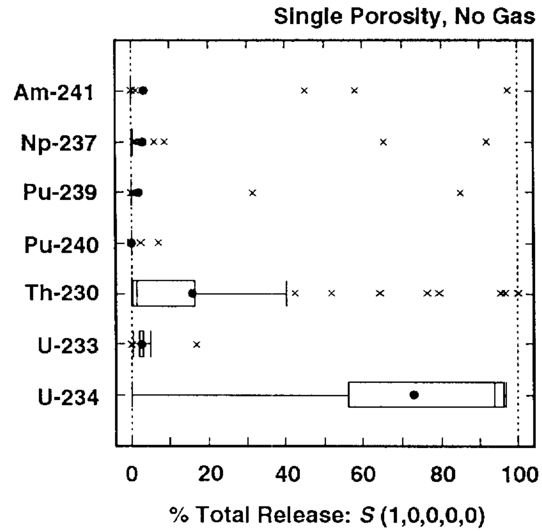

TRI-6342-1651-0

Scenario: S^{+-}(2,0,0,0,0), Assumed Intrusion Time: 1000 yrs

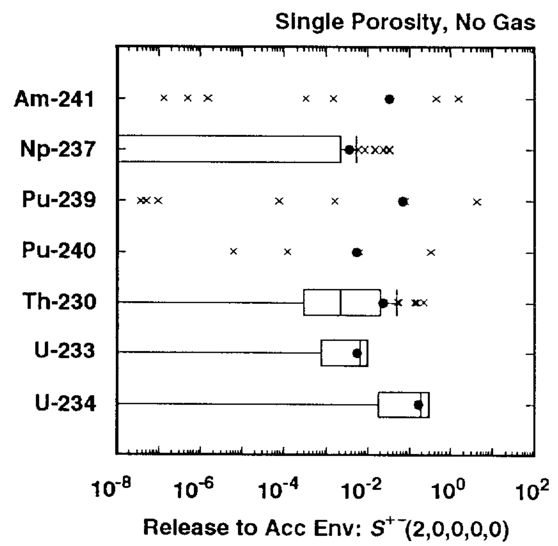

TRI-6342-1652-0

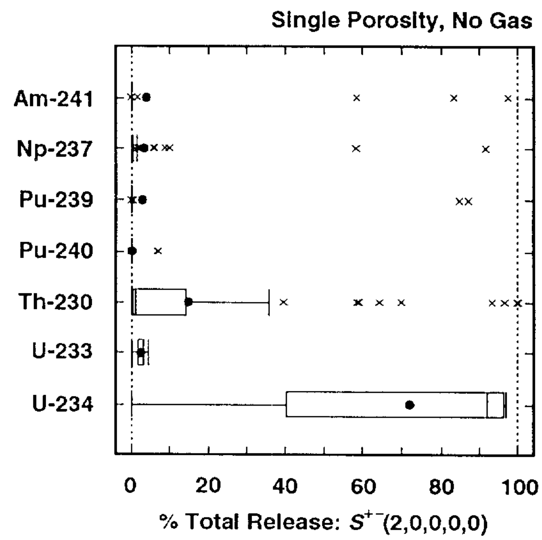

TRI-6342-1653-0

Figure 5.3-2. Normalized Releases for Individual Isotopes to the Accessible Environment Due to Groundwater Transport with Intrusion Occurring at 1000 Yrs, No Gas Generation in the Repository and a Single-Porosity Transport Model in the Culebra Dolomite.

With Gas Generation in the Repository

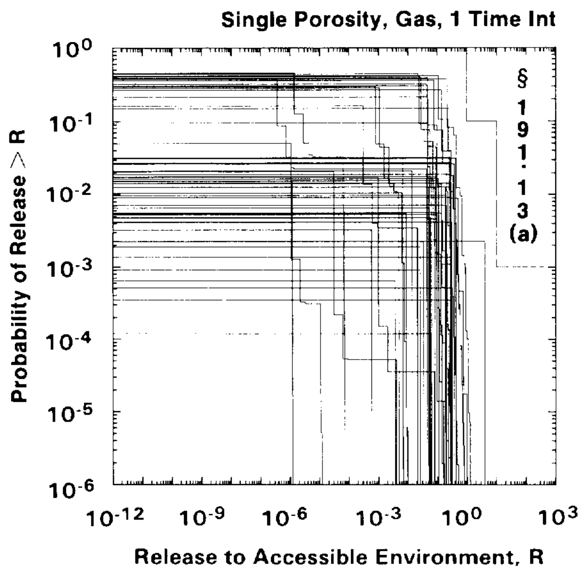

TRI-6342-1577-0

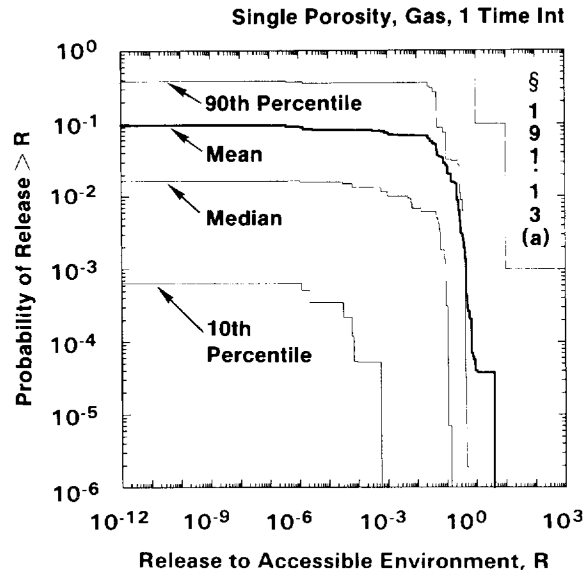

TRI-6342-1579-0

Without Gas Generation in the Repository

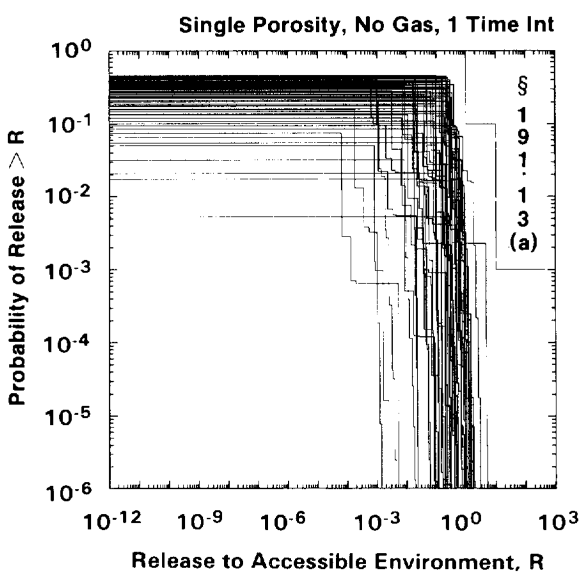

TRI-6342-1617-0

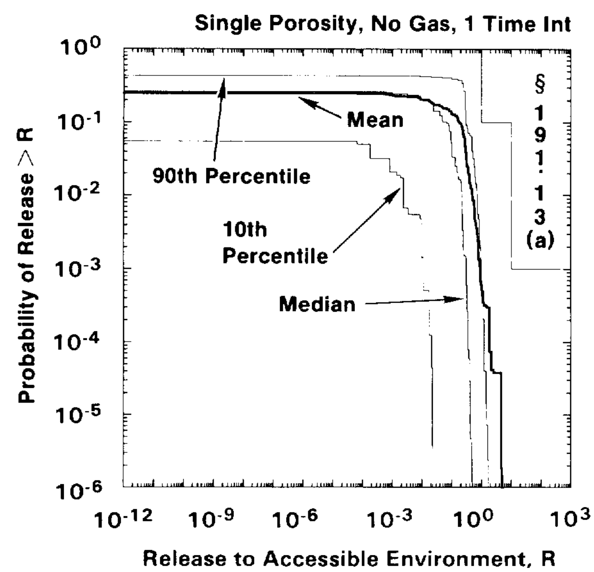

TRI-6342-1618-0

Figure 5.3-3. Comparison of Complementary Cumulative Distribution Functions for Normalized Release to the Accessible Environment with Gas Generation in the Repository (upper two frames) and without Gas Generation in the Repository (lower two frames) for a Single-Porosity Transport Model in the Culebra Dolomite and the Rate Constant λ in the Poisson Model for Drilling Intrusions Equal to Zero After 2000 Yrs.

the assumption of single-porosity transport without gas generation produces CCDFs that are not substantially shifted from those obtained for single-porosity transport with gas generation. Further, all the individual CCDFs fall below the EPA release limits for both cases.

Sensitivity analyses of groundwater transport results for individual isotopes for scenarios $S(1,0,0,0,0)$ and $S^{+-}(2,0,0,0,0)$ with no gas generation in the repository and a single-porosity model in the Culebra are presented in Tables 5.3-1 and 5.3-2. For convenience, these tables also contain the corresponding sensitivity analysis results for release to the Culebra, although these results have appeared previously in Tables 5.1-2 and 5.1-3.

The groundwater transport results in Table 5.3-1 for scenario $S(1,0,0,0,0)$ tend to be dominated by properties of the individual isotopes. In particular, releases at the quarter, half and full distance to the accessible environment tend to increase as the solubilities increase and decrease as the distribution coefficients increase. Increasing SALPERM (Salado permeability) and SALPRES (Salado pressure) also tends to increase the releases for the individual isotopes. This is consistent with the role indicated for these variables in increasing the release of the individual isotopes to the Culebra for scenario $S(1,0,0,0,0)$. Increasing CULFRPOR (Culebra fracture porosity) tends to decrease the release for the individual isotopes by reducing the groundwater flow rate in the Culebra.

The groundwater transport results in Table 5.3-2 for scenario $S^{+-}(2,0,0,0,0)$ are similar to those in Table 5.3-1 for scenario $S(1,0,0,0,0)$. The releases for the individual isotopes tend to be dominated by the appropriate solubilities and distribution coefficients. The variables BPPRES (brine pocket pressure), CULFRPOR (Culebra fracture porosity) and BHPERM (borehole permeability) are often identified in the analyses for the individual isotopes, with the releases increasing as BPPRES and BHPERM increase and decreasing as CULFRPOR increases. The importance indicated for the solubilities BPPRES and BHPERM results from their role in determining release into the Culebra for scenario $S^{+-}(2,0,0,0,0)$.

The sensitivity analysis results obtained for groundwater transport in the Culebra with a single-porosity model in the absence of gas generation are similar to those previously obtained for single-porosity transport with gas generation with the exception that SALPERM (Salado permeability) does not act as a switch for scenario $S(1,0,0,0,0)$. This is not surprising because the absence of gas generation tends to produce larger releases to the Culebra, especially for scenario $S(1,0,0,0,0)$, but the presence or absence of gas generation itself has no effect on the actual transport that takes place in the Culebra. The patterns in the scatterplots for transport in the absence of gas generation for scenarios $S(1,0,0,0,0)$ and $S^{+-}(2,0,0,0,0)$ are similar

TABLE 5.3-1. STEPWISE REGRESSION ANALYSES WITH RANK-TRANSFORMED DATA FOR SCENARIO $S(1,0,0,0,0)$ WITH NO GAS GENERATION IN THE REPOSITORY, A SINGLE-POROSITY TRANSPORT MODEL IN THE CULEBRA DOLOMITE AND INTRUSION OCCURRING 1000 YRS AFTER REPOSITORY CLOSURE

	Release to Culebra*		Quarter Distance		Half Distance		Full Distance	
Step	Variable	R^2	Variable	R^2	Variable	R^2	Variable	R^2
Dependent Variable: Integrated Discharge Am-241								
1	SOLAM	0.81(+)	FKDAM	0.60 (-)	CULFRPOR	0.20 (-)	FKDAM	0.35 (-)
2	SALPERM	0.90(+)	CULFRPOR	0.65 (-)	FKDAM	0.40 (-)	CULFRPOR	0.50 (-)
3	BHPERM	0.92(+)	MBPOR	0.68 (-)	SOLAM	0.52 (+)		
4	SALPRES	0.93(+)			MBPERM	0.57 (+)		
Dependent Variable: Integrated Discharge Np-237								
1	SOLNP	0.77(+)	FKDNP	0.52 (-)	FKDNP	0.47 (-)	FKDNP	0.52 (-)
2	EHPH	0.86(+)	SOLAM	0.60 (+)	SOLAM	0.55 (+)	SOLNP	0.62 (+)
3	SALPERM	0.90(+)	SOLNP	0.65 (+)	SOLNP	0.62 (+)	SOLAM	0.67 (+)
Dependent Variable: Integrated Discharge Pu-239								
1	SOLPU	0.92(+)	FKDPU	0.66 (-)	FKDPU	0.18 (-)	FKDPU	0.40 (-)
2	SALPERM	0.94(+)	CULTRFLD	0.69 (-)				
3	BHPERM	0.95(+)						
Dependent Variable: Integrated Discharge Pu-240								
1	SOLPU	0.91(+)	FKDPU	0.64 (-)	FKDPU	0.20 (-)	FKDPU	0.53 (-)
2	SALPERM	0.94(+)						
3	BHPERM	0.95(+)						
Dependent Variable: Integrated Discharge Th-230								
1	SOLTH	0.94(+)	FKDTH	0.38 (-)	FKDTH	0.42 (-)	FKDTH	0.49 (-)
2	SALPERM	0.96(+)	SOLTH	0.53 (+)	SOLTH	0.54 (+)	SOLTH	0.56 (+)
3	BHPERM	0.97(+)						
4	SALPRES	0.97(+)						
Dependent Variable: Integrated Discharge U-233								
1	SOLU	0.34(+)	SOLU	0.31 (+)	SOLU	0.30 (+)	SOLU	0.25 (+)
2	SALPERM	0.42(+)	FKDU	0.41 (-)	FKDU	0.42 (-)	FKDU	0.40 (-)
3	SALPRES	0.49(+)	SALPERM	0.49 (+)	SALPERM	0.50 (+)	SALPERM	0.49 (+)
4			SALPRES	0.58 (+)	SALPRES	0.58 (+)	SALPRES	0.57 (+)

*Analysis results in this column are the same as those presented in the corresponding column of Table 5.1-2.

TABLE 5.3-1. STEPWISE REGRESSION ANALYSES WITH RANK-TRANSFORMED DATA FOR SCENARIO *S*(1,0,0,0,0) WITH NO GAS GENERATION IN THE REPOSITORY, A SINGLE-POROSITY TRANSPORT MODEL IN THE CULEBRA DOLOMITE AND INTRUSION OCCURRING 1000 YRS AFTER REPOSITORY CLOSURE (concluded)

	Release to Culebra*		Quarter Distance		Half Distance		Full Distance	
Step	Variable	R^2	Variable	R^2	Variable	R^2	Variable	R^2
Dependent Variable: Integrated Discharge U-234								
1	SOLU	0.29(+)	SOLU	0.32 (+)	SOLU	0.31 (+)	SOLU	0.26 (+)
2	SALPERM	0.37(+)	FKDU	0.41 (-)	FKDU	0.42 (-)	FKDU	0.40 (-)
3	SALPRES	0.43(+)	SALPERM	0.49 (+)	SALPERM	0.50 (+)	SALPERM	0.49 (+)
4			SALPRES	0.57 (+)	SALPRES	0.58 (+)	SALPRES	0.57 (+)
5							SOLU	0.62 (-)
Dependent Variable: EPA Sum for Total Integrated Discharge								
1	SOLAM	0.42(+)	SOLU	0.18 (+)	SOLU	0.20 (+)	SOLU	0.21 (+)
2	SALPERM	0.65(+)	FKDU	0.28 (-)	FKDU	0.31 (-)	FKDU	0.32 (-)
3			SALPERM	0.39 (+)	SALPERM	0.40 (+)	SALPERM	0.42 (+)
4			SALPRES	0.48 (+)	SALPRES	0.49 (+)	SALPRES	0.50 (+)
5			CULFRPOR	0.55 (-)	CULFRPOR	0.56 (-)	CULFRPOR	0.56 (-)
6			FKDPU	0.61 (-)	FKDU	0.62 (-)		

*Analysis results in this column are the same as those presented in the corresponding column of Table 5.1-2.

TABLE 5.3-2. STEPWISE REGRESSION ANALYSES WITH RANK-TRANSFORMED DATA FOR SCENARIO S^{+-}(2,0,0,0,0) WITH NO GAS GENERATION IN THE REPOSITORY, A SINGLE-POROSITY TRANSPORT MODEL IN THE CULEBRA DOLOMITE AND INTRUSION OCCURRING 1000 YRS AFTER REPOSITORY CLOSURE

	Release to Culebra*		Quarter Distance		Half Distance		Full Distance	
Step	Variable	R^2	Variable	R^2	Variable	R^2	Variable	R^2
Dependent Variable: Integrated Discharge Am-241								
1	SOLAM	0.84(+)	FKDAM	0.60 (-)	CULFRPOR	0.21 (-)	FKDAM	0.28 (-)
2	BHPERM	0.93(+)	CULFRPOR	0.65 (-)	FKDAM	0.42 (-)	CULFRPOR	0.47 (-)
3	BPPRES	0.94(+)	MBPOR	0.69 (-)	SOLAM	0.51 (+)	SOLAM	0.52 (+)
4					MBPOR	0.55 (-)		
Dependent Variable: Integrated Discharge Np-237								
1	SOLNP	0.77(+)	FKDNP	0.52 (-)	FKDNP	0.48 (-)	FKDNP	0.51 (-)
2	EHPH	0.84(+)	SOLAM	0.62 (+)	SOLNP	0.57 (+)	SOLNP	0.61 (+)
3	BHPERM	0.88(+)	SOLNP	0.68 (+)	SOLAM	0.63 (+)	SOLAM	0.66 (+)
4	BPPRES	0.91(+)	BHPERM	0.71 (+)				
Dependent Variable: Integrated Discharge Pu-239								
1	SOLPU	0.90(+)	FKDPU	0.59 (-)	FKDPU	0.22 (-)	FKDPU	0.37 (-)
2	BHPERM	0.94(+)	CULTRFLD	0.62 (-)				
3	BPPRES	0.95(+)						
4	BHDIAM	0.96(+)						
5	EHPH	0.96(+)						
Dependent Variable: Integrated Discharge Pu-240								
1	SOLPU	0.90(+)	FKDPU	0.63 (-)	FKDPU	0.21 (-)	FKDPU	0.48 (-)
2	BHPERM	0.94(+)						
3	BPPRES	0.95(+)						
4	BHDIAM	0.96(+)						
5	EHPH	0.96(+)						
Dependent Variable: Integrated Discharge Th-230								
1	SOLTH	0.90(+)	FKDTH	0.36 (-)	FKDTH	0.42 (-)	FKDTH	0.51 (-)
2	BHPERM	0.95(+)	SOLTH	0.54 (+)	SOLTH	0.56 (+)	SOLTH	0.58 (+)
3							BPPRES	0.63 (+)

* Analysis results in this column are the same as those presented in the corresponding column of Table 5.1-3.

TABLE 5.3-2. STEPWISE REGRESSION ANALYSES WITH RANK-TRANSFORMED DATA FOR SCENARIO S^{+-}(2,0,0,0,0) WITH NO GAS GENERATION IN THE REPOSITORY, A SINGLE-POROSITY TRANSPORT MODEL IN THE CULEBRA DOLOMITE AND INTRUSION OCCURRING 1000 YRS AFTER REPOSITORY CLOSURE (concluded)

	Release to Culebra*		Quarter Distance		Half Distance		Full Distance	
Step	Variable	R^2	Variable	R^2	Variable	R^2	Variable	R^2
Dependent Variable: Integrated Discharge U-233								
1	SOLU	0.25 (+)	SOLU	0.24 (+)	SOLU	0.22 (+)	SOLU	0.15 (+)
2	BHPERM	0.39 (+)	FKDU	0.40 (-)	FKDU	0.41 (-)	FKDU	0.30 (-)
3	SOLNP	0.50 (-)	BPPRES	0.48 (+)	BHPERM	0.48 (+)	BPPRES	0.40 (+)
4	BPPRES	0.58 (+)	CULFRPOR	0.56 (-)	BPPRES	0.54 (+)	BHPERM	0.46 (+)
5			BHPERM	0.60 (+)	CULFRPOR	0.59 (-)	CULFRPOR	0.52 (-)
6					CULDISP	0.57 (+)		
Dependent Variable: Integrated Discharge U-234								
1	SOLU	0.20 (+)	SOLU	0.22 (+)	FKDU	0.21 (-)	SOLU	0.15 (+)
2	BHPERM	0.36 (+)	FKDU	0.37 (-)	SOLU	0.40 (+)	FKDU	0.28 (-)
3			BPPRES	0.46 (+)	BPPRES	0.47 (+)	BPPRES	0.40 (+)
4			CULFRPOR	0.52 (-)	BHPERM	0.52 (+)	CULFRPOR	0.47 (-)
5			BHPERM	0.57 (+)	CULFRPOR	0.57 (-)	BHPERM	0.53 (+)
6					CULDISP	0.59 (+)		
Dependent Variable: EPA Sum for Total Integrated Discharge								
1	SOLAM	0.62 (+)	BPPRES	0.13 (+)	SOLU	0.16 (+)	SOLU	0.13 (+)
2	BHPERM	0.71 (+)	FKDU	0.24 (-)	FKDU	0.28 (-)	BPPRES	0.25 (+)
3	SOLPU	0.77 (+)	CULFRPOR	0.34 (-)	BPPRES	0.39 (+)	BHPERM	0.33 (+)
4	BPPRES	0.81 (+)	SOLU	0.44 (+)	BHPERM	0.47 (+)	CULFRPOR	0.41 (-)
5			FKDNP	0.50 (-)	CULFRPOR	0.54 (-)	FKDU	0.48 (-)
6			BHPERM	0.55 (+)	FKDNP	0.59 (-)		
7			SOLAM	0.61 (+)				
8			BPSTOR	0.65 (+)				

* Analysis results in this column are the same as those presented in the corresponding column of Table 5.1-3.

to those appearing in Figures 5.2-6 and 5.2-7 for scenario $S^{+-}(2,0,0,0,0)$ in the presence of gas generation.

5.4 Effect of No Chemical Retardation and Dual-Porosity Transport Model in Culebra Dolomite

As shown in the sensitivity analyses presented in preceding sections, retardation resulting from assumed distribution coefficients (i.e., FKDAM, FKDNP, FKDPU, FKDTH, FKDU, MKDAM, MKDNP, MKDPU, MKDTH, MKDU) for the Culebra Dolomite has an important influence on radionuclide releases to the accessible environment due to groundwater transport. At present, no site-specific observations exist for radionuclide sorption in the Culebra Dolomite, and the distributions characterizing the uncertainty in distribution coefficients were developed through an internal review process at Sandia National Laboratories (SNL) (see Section 2.6.10, Vol. 3, of this report). Due to the indicated importance of distribution coefficients and the absence of site-specific data, the best estimate analyses for the 1991 WIPP performance assessment (i.e., gas generation in the repository and a dual-porosity transport model in the Culebra Dolomite) presented in Chapter 4 were repeated with the distribution coefficients set to zero in each sample element. Under agreement with the State of New Mexico (U.S. DOE and State of New Mexico, 1981, as modified), the effect of zero distribution coefficients will be determined in the annual performance assessments conducted for the WIPP until site-specific information becomes available.

As examination of the scatterplots in Figure 5.4-1 shows, releases to the accessible environment are considerably larger when chemical retardation is assumed to be absent. However, although the releases increase in the absence of chemical retardation, the releases themselves are still relatively small. In particular, only a few sample elements result in normalized releases close to one.

As shown in Figure 4.5-4, approximately half the sample elements for scenario $S(1,0,0,0,0)$ result in no release to the Culebra. For these sample elements, the release to the accessible environment will be zero regardless of the assumptions made with respect to sorption. For scenario $S^{+-}(2,0,0,0,0)$, essentially all sample elements result in releases to the Culebra. As indicated by the points appearing above 10^{-8} in the scatterplot for scenario $S^{+-}(2,0,0,0,0)$ in Figure 5.4-1, many sample elements that produce zero releases in the presence of chemical retardation produce nonzero releases in the absence of chemical retardation. A similar effect can also be seen in the scatterplot for scenario $S(1,0,0,0,0)$ in Figure 5.4-1.

The releases of individual isotopes to the accessible environment on which Figure 5.4-1 is based are shown in Figure 5.4-2. The corresponding release

Scenario: $S(1,0,0,0,0)$, Assumed Intrusion Time: 1000 yrs

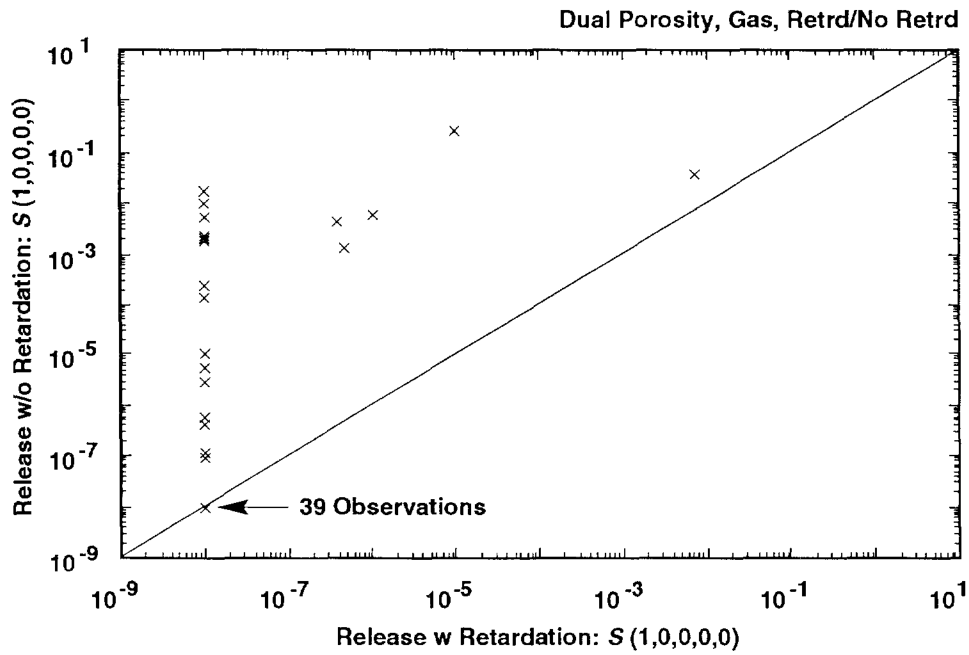

TRI-6342-1642-0

Scenario: $S^{+-}(2,0,0,0,0)$, Assumed Intrusion Time: 1000 yrs

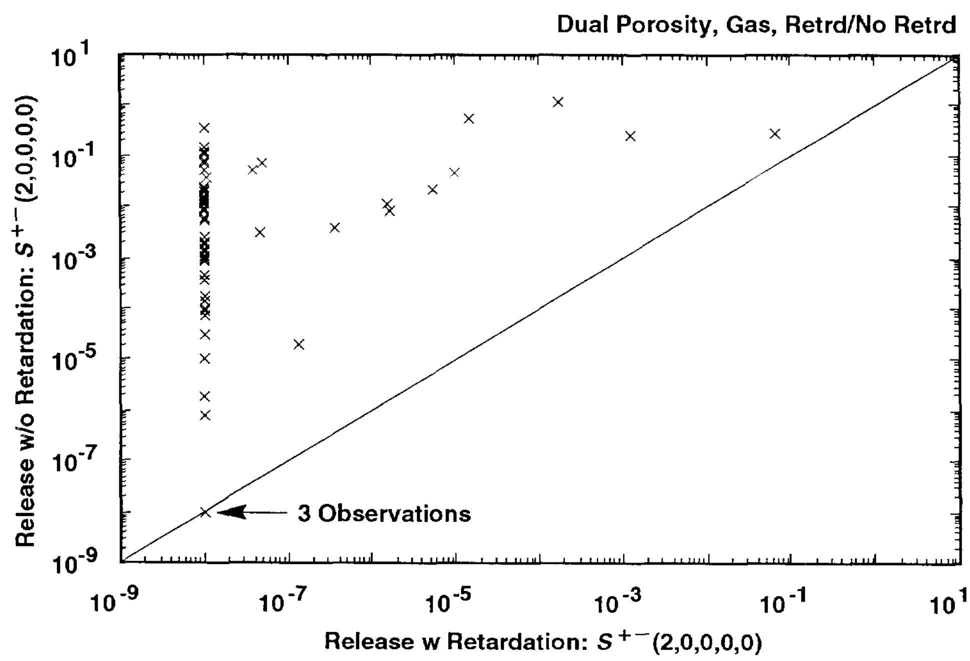

TRI-6342-1643-0

Figure 5.4-1. Scatterplots Comparing Total Normalized Releases to the Accessible Environment Due to Groundwater Transport Calculated by a Dual-Porosity Transport Model with and without Chemical Retardation in the Culebra Dolomite for Gas Generation in the Repository and an Assumed Intrusion Time of 1000 Yrs. For plotting purposes, values less than 10^{-8} are set to 10^{-8}.

Scenario: $S(1,0,0,0,0)$, Assumed Intrusion Time: 1000 yrs

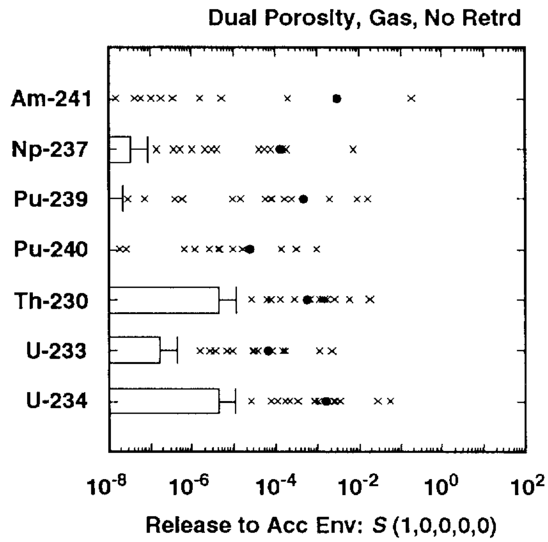

TRI-6342-1556-0

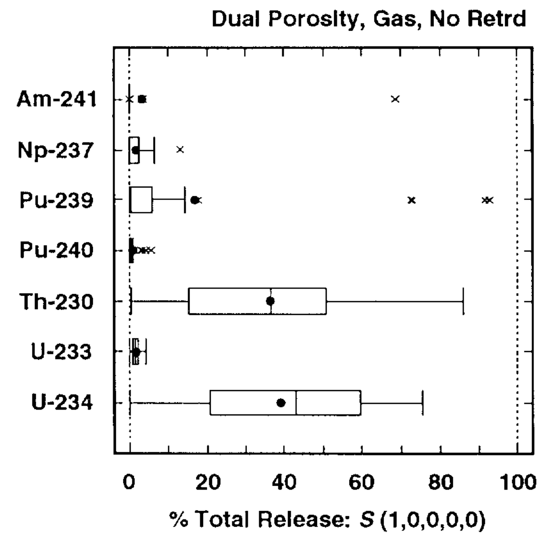

TRI-6342-1557-0

Scenario: $S^{+-}(2,0,0,0,0)$, Assumed Intrusion Time: 1000 yrs

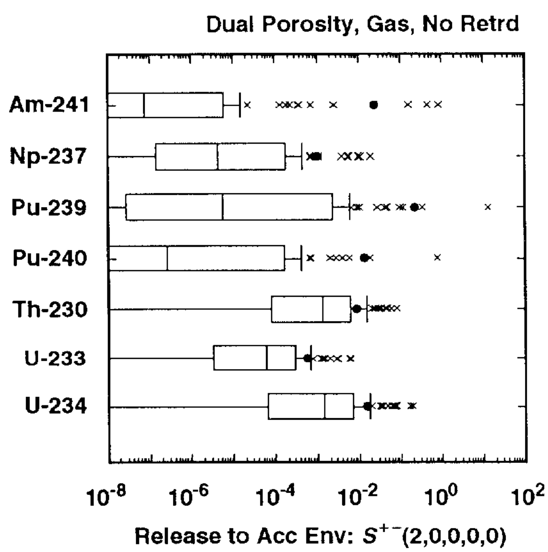

TRI-6342-1558-0

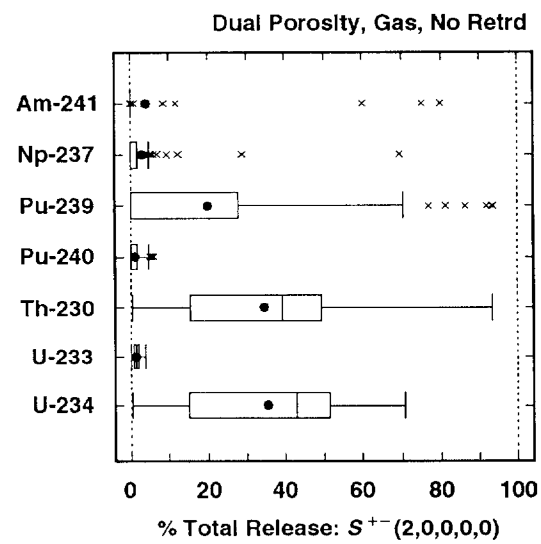

TRI-6342-1559-0

Figure 5.4-2. Normalized Releases for Individual Isotopes to the Accessible Environment Due to Groundwater Transport with Intrusion Occurring at 1000 Yrs, Gas Generation in the Repository and a Dual-Porosity Transport Model without Chemical Retardation in the Culebra Dolomite.

results obtained in the presence of chemical retardation are shown in Figure 4.4-2. As already indicated by the scatterplots appearing in Figure 5.4-1, the releases appearing in Figure 5.4-2 for transport without chemical retardation are considerably larger than those appearing in Figure 4.4-2 for transport with chemical retardation. Further, the major contributors to the total release are also changed. As shown in Figure 4.4-2, U-234 is the major contributor to the total release in the presence of chemical retardation. In contrast, Figure 5.4-2 indicates that Pu-239, Th-230 and U-234 are all important contributors in the absence of chemical retardation; even Am-241 is a dominant contributor for 3 sample elements for scenario $S^{+-}(2,0,0,0,0)$.

As shown in Figure 5.4-1, the assumption of no chemical retardation substantially increases the releases to the accessible environment due to groundwater transport. However, even without chemical retardation, the potential release to the accessible environment over the 10,000-yr period specified in the EPA standard is substantially reduced by groundwater transport in the Culebra. The extent of this reduction is illustrated by the scatterplots appearing in Figure 5.4-3, which show that the releases to the accessible environment due to groundwater transport for many, if not most, sample elements are one or more orders of magnitude less than the original releases to the Culebra.

Transport calculations for no chemical retardation in the Culebra were only performed for intrusions occurring at 1000 yrs (i.e., for scenarios $S(1,0,0,0,0)$ and $S^{+-}(2,0,0,0,0)$). As discussed in conjunction with Figure 5.1-4, these calculations can be used to construct CCDFs for comparison with the EPA release limits under the assumption that the rate constant λ in the Poisson model for drilling intrusions is equal to zero after 2000 yrs. The outcome of this construction is shown in Figure 5.4-4; the corresponding results obtained with retardation in the Culebra appear in the upper two frames of Figure 5.1-4. As comparison of the results in Figures 5.1-4 and 5.4-4 shows, the assumption of no retardation results in CCDFs that are shifted considerably to the right (i.e., closer to the EPA release limits) than the CCDFs obtained with retardation. Even so, only one of the CCDFs obtained without retardation actually crosses the EPA release limits.

Sensitivity analyses of groundwater transport results for individual isotopes for scenarios $S(1,0,0,0,0)$ and $S^{+-}(2,0,0,0,0)$ with gas generation in the repository and a dual-porosity transport model with no chemical retardation in the Culebra are presented in Tables 5.4-1 and 5.4-2. For convenience, these tables also contain the corresponding sensitivity analysis results for release to the Culebra, although these results have appeared previously in Tables 4.5-1 and 4.5-2.

Scenario: $S(1,0,0,0,0)$, Assumed Intrusion Time: 1000 yrs

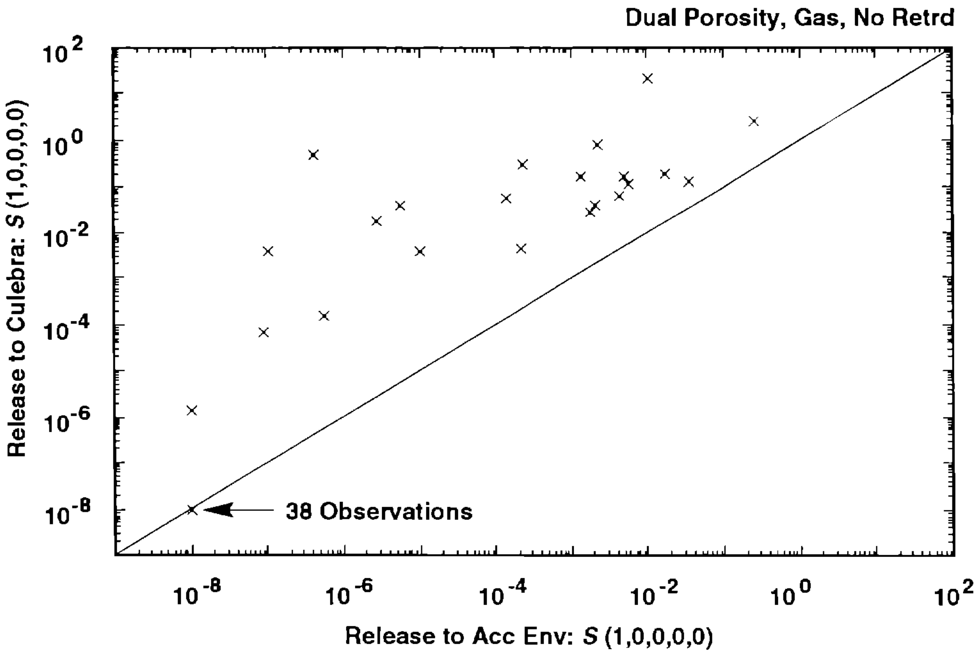

TRI-6342-1644-0

Scenario: $S^{+-}(2,0,0,0,0)$, Assumed Intrusion Time: 1000 yrs

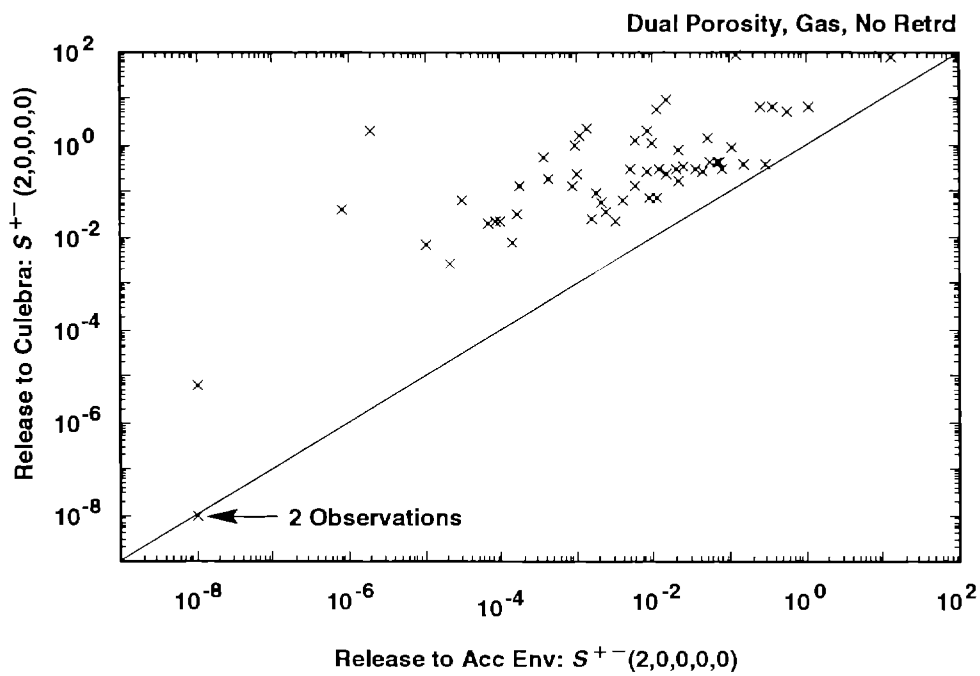

TRI-6342-1645-0

Figure 5.4-3. Scatterplots Comparing Total Normalized Release to the Culebra Dolomite and Total Normalized Release to the Accessible Environment for Scenarios $S(1,0,0,0,0)$ and $S^{+-}(2,0,0,0,0)$ with Gas Generation in the Repository, a Dual-Porosity Transport Model in the Culebra Dolomite, No Chemical Retardation and Intrusion Occurring at 1000 Yrs. For plotting purposes, values less than 10^{-8} are set to 10^{-8}.

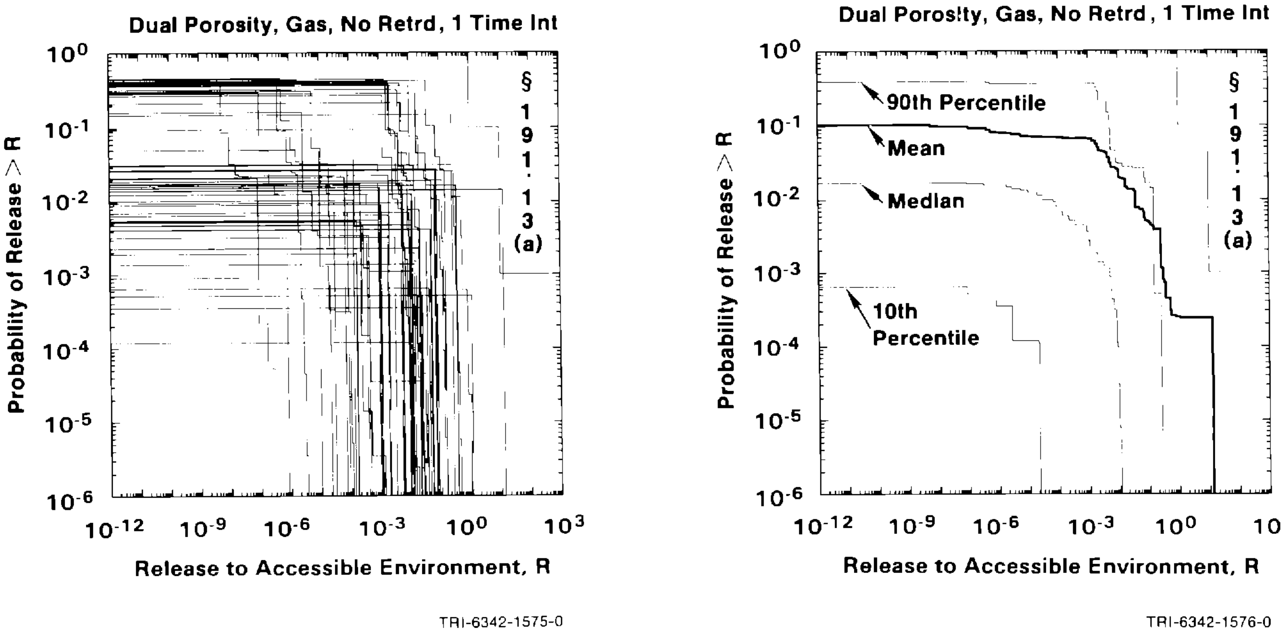

Figure 5.4-4. Complementary Cumulative Distribution Functions for Normalized Release to the Accessible Environment Due to Groundwater Transport for Gas Generation in the Repository, a Dual-Porosity Transport Model in the Culebra Dolomite, No Chemical Retardation and the Rate Constant λ in the Poisson Model for Drilling Intrusions Equal to Zero After 2000 Yrs.

The sensitivity analysis results in Table 5.4-1 for scenario $S(1,0,0,0,0)$ are dominated by SALPERM (Salado permeability). As previously discussed and illustrated by the scatterplots appearing in Figures 4.5-1 and 4.5-4, the importance of SALPERM results from its role as a switch in determining whether or not releases to the Culebra occur. Given that a release to the Culebra occurs, the same factors operate to affect its transport to the accessible environment for scenarios $S(1,0,0,0,0)$ and $S^{+-}(2,0,0,0,0)$. Therefore, as the sensitivity analysis results for scenario $S^{+-}(2,0,0,0,0)$ in Table 5.4-2 are more revealing than those for scenario $S(1,0,0,0,0)$ in Table 5.4-1 due to the absence of SALPERM as a switch, the following discussion will focus on the sensitivity analysis results obtained for $S^{+-}(2,0,0,0,0)$.

The sensitivity analysis results in Table 5.4-2 for scenario $S^{+-}(2,0,0,0,0)$ indicate that the most important variables for integrated transport in the absence of chemical retardation are BHPERM (borehole permeability), BPPRES (brine pocket pressure) and solubilities for the individual elements. These are also the variables that dominate release to the Culebra. However, unlike the analysis results shown in Table 5.4-2 for transport in the Culebra without chemical retardation, the analysis results shown in Table 4.5-2 for transport with chemical retardation are dominated by the distribution

TABLE 5.4-1. STEPWISE REGRESSION ANALYSES WITH RANK-TRANSFORMED DATA FOR SCENARIO *S*(1,0,0,0,0) WITH GAS GENERATION IN THE REPOSITORY AND A DUAL-POROSITY TRANSPORT MODEL WITH NO CHEMICAL RETARDATION IN THE CULEBRA DOLOMITE

	Release to Culebra*		Quarter Distance		Half Distance		Full Distance	
Step	Variable	R^2	Variable	R^2	Variable	R^2	Variable	R^2
Dependent Variable: Integrated Discharge Am-241								
1	SALPERM	0.59(+)	SALPERM	0.58(+)	SALPERM	0.58(+)	SALPERM	0.57(+)
Dependent Variable: Integrated Discharge Np-237								
1	SALPERM	0.53(+)	MBPERM	0.55(+)	SALPERM	0.56(+)	SALPERM	0.56(+)
Dependent Variable: Integrated Discharge Pu-239								
1	SALPERM	0.56(+)	SALPERM	0.56(+)	SALPERM	0.56(+)	SALPERM	0.55(+)
Dependent Variable: Integrated Discharge Pu-240								
1	SALPERM	0.56(+)	SALPERM	0.56(+)	SALPERM	0.56(+)	SALPERM	0.55(+)
Dependent Variable: Integrated Discharge Th-230								
1	SALPERM	0.55(+)	SALPERM	0.58(+)	SALPERM	0.58(+)	SALPERM	0.58(+)
Dependent Variable: Integrated Discharge U-233								
1	SALPERM	0.59(+)	SALPERM	0.59(+)	SALPERM	0.59(+)	SALPERM	0.58(+)
Dependent Variable: Integrated Discharge U-234								
1	SALPERM	0.59(+)	SALPERM	0.58(+)	SALPERM	0.59(+)	SALPERM	0.59(+)
Dependent Variable: EPA Sum for Total Integrated Discharge								
1	SALPERM	0.58(+)	SALPERM	0.57(+)	SALPERM	0.57(+)	SALPERM	0.57(+)

*Analysis results in this column are the same as those presented in the corresponding column of Table 4.5-1.

TABLE 5.4-2. STEPWISE REGRESSION ANALYSES WITH RANK-TRANSFORMED DATA FOR SCENARIO S^{+-}(2,0,0,0,0) WITH GAS GENERATION IN THE REPOSITORY, A DUAL-POROSITY TRANSPORT MODEL WITH NO CHEMICAL RETARDATION IN THE CULEBRA DOLOMITE AND INTRUSION OCCURRING 1000 YRS AFTER REPOSITORY CLOSURE

	Release to Culebra*		Quarter Distance		Half Distance		Full Distance	
Step	Variable	R^2	Variable	R^2	Variable	R^2	Variable	R^2
Dependent Variable: Integrated Discharge Am-241								
1	SOLAM	0.36 (+)	SOLAM	0.22 (-)	CULFRSP	0.23 (+)	CULFRSP	0.33 (+)
2	BHPERM	0.74 (+)	BHPERM	0.47 (+)	BHPERM	0.39 (+)	CULCLIM	0.52 (+)
3	BPPRES	0.78 (+)	CULCLIM	0.61 (+)	SOLAM	0.55 (+)	SOLAM	0.62 (+)
4			CULFRSP	0.71 (+)	CULCLIM	0.72 (+)	BHPERM	0.72 (+)
5			BPPRES	0.75 (+)	BPPRES	0.75 (+)	BPPRES	0.75 (+)
6					CULTRFLD	0.78 (-)	GRCORI	0.77 (-)
7							CULTRFLD	0.80 (-)
Dependent Variable: Integrated Discharge Np-237								
1	SOLNP	0.65 (+)	SOLNP	0.41 (+)	SOLNP	0.37 (+)	SOLNP	0.34 (+)
2	BHPERM	0.78 (+)	BHPERM	0.65 (+)	BHPERM	0.60 (+)	BHPERM	0.53 (+)
3	BPPRES	0.82 (+)	BPPRES	0.71 (+)	BPPRES	0.66 (+)	CULCLIM	0.62 (+)
4	EHPH	0.85 (+)	EHPH	0.75 (+)	EHPH	0.71 (+)	BPPRES	0.68 (+)
5	GRCORI	0.88 (-)	SOLAM	0.79 (+)	SOLAM	0.75 (+)	CULFRSP	0.73 (+)
6			CULCLIM	0.82 (+)	CULCLIM	0.79 (+)	SOLAM	0.76 (+)
7			GRCORI	0.84 (-)	GRCORI	0.82 (-)	EHPH	0.79 (+)
8							GRCORI	0.81 (-)
Dependent Variable: Integrated Discharge Pu-239								
1	SOLPU	0.74 (+)	SOLPU	0.70 (+)	SOLPU	0.68 (+)	SOLPU	0.63 (+)
2	BHPERM	0.85 (+)	BHPERM	0.82 (+)	BHPERM	0.81 (+)	BHPERM	0.75 (+)
3					CULFRSP	0.83 (+)	CULFRSP	0.80 (+)
4							CULCLIM	0.82 (+)
Dependent Variable: Integrated Discharge Pu-240								
1	SOLPU	0.74 (+)	SOLPU	0.69 (+)	SOLPU	0.68 (+)	SOLPU	0.62 (+)
2	BHPERM	0.85 (+)	BHPERM	0.82 (+)	BHPERM	0.80 (+)	BHPERM	0.74 (+)
3					CULFRSP	0.83 (+)	CULFRSP	0.80 (+)
4							CULCLIM	0.83 (+)

*Analysis results in this column are the same as those presented in the corresponding column of Table 4.5-2.

TABLE 5.4-2. STEPWISE REGRESSION ANALYSES WITH RANK-TRANSFORMED DATA FOR SCENARIO S^{+-}(2,0,0,0,0) WITH GAS GENERATION IN THE REPOSITORY, A DUAL-POROSITY TRANSPORT MODEL WITH NO CHEMICAL RETARDATION IN THE CULEBRA DOLOMITE AND INTRUSION OCCURRING 1000 YRS AFTER REPOSITORY CLOSURE (concluded)

	Release to Culebra*		Quarter Distance		Half Distance		Full Distance	
Step	Variable	R^2	Variable	R^2	Variable	R^2	Variable	R^2
Dependent Variable: Integrated Discharge Th-230								
1	SOLTH	0.69 (+)	BHPERM	0.43 (+)	BHPERM	0.44 (+)	BHPERM	0.31 (+)
2	BHPERM	0.82 (+)	BPPRES	0.60 (+)	BPPRES	0.59 (+)	BPPRES	0.44 (+)
3			SOLU	0.65 (+)	SOLU	0.65 (+)	CULCLIM	0.56 (+)
4			SOLTH	0.69 (+)	CULCLIM	0.69 (+)	CULFRSP	0.62 (+)
5					CULPOR	0.73 (-)	CULPOR	0.68 (-+)
6					SOLTH	0.76 (+)	SOLU	0.73 (+)
Dependent Variable: Integrated Discharge U-233								
1	BHPERM	0.43 (+)	BHPERM	0.43 (+)	BHPERM	0.41 (+)	BHPERM	0.28 (+)
2	SOLU	0.58 (+)	BPPRES	0.58 (+)	BPPRES	0.54 (+)	CULCLIM	0.40 (+)
3	BPPRES	0.70 (+)	SOLU	0.68 (+)	SOLU	0.62 (+)	BPPRES	0.52 (+)
4	SOLNP	0.74 (-)	CULCLIM	0.72 (+)	CULCLIM	0.68 (+)	CULFRSP	0.63 (+)
5					CULPOR	0.72 (-)	SOLU	0.68 (+)
6					CULFRSP	0.76 (+)	CULPOR	0.73 (-)
7							SALPRES	0.75 (+)
Dependent Variable: Integrated Discharge U-234								
1	BHPERM	0.47 (+)	BHPERM	0.43 (+)	BHPERM	0.39 (+)	BHPERM	0.27 (+)
2	SOLU	0.60 (+)	BPPRES	0.56 (+)	BPPRES	0.52 (-)	CULCLIM	0.39 (+)
3	BPPRES	0.72 (+)	SOLU	0.68 (+)	SOLU	0.62 (+)	BPPRES	0.51 (+)
4			CULCLIM	0.72 (+)	CULCLIM	0.68 (+)	CULFRSP	0.59 (+)
5			CULPOR	0.75 (-)	CULPOR	0.73 (-)	CULPOR	0.65 (-)
6					SOLU	0.72 (+)		
Dependent Variable: EPa Sum for Total Integrated Discharge								
1	BHPERM	0.46 (+)	BHPERM	0.47 (+)	BHPERM	0.43 (+)	BHPERM	0.31 (+)
2	SOLAM	0.57 (+)	BPPRES	0.61 (+)	BPPRES	0.58 (+)	CULCLIM	0.46 (+)
3	BPPRES	0.66 (+)	CULCLIM	0.68 (+)	CULCLIM	0.67 (+)	BPPRES	0.60 (+)
4	SOLPU	0.69 (+)	BPSTOR	0.71 (+)			CULFRSP	0.69 (+)
5	BPSTOR	0.73 (+)	CULPOR	0.74 (-)			CULPOR	0.72 (-)
6	SOLU	0.76 (+)	BHDIAM	0.77 (+)				

*Analysis results in this column are the same as those presented in the corresponding column of Table 4.5-2.

coefficients for the individual elements. The effects of the distribution coefficients on the transport results analyzed in Table 4.5-2 are so strong that the effects of other variables that have lesser influence on transport are obscured. As shown in Figure 4.5-6 for transport only one-quarter the distance to the accessible environment, transport is essentially shut off over the 10,000-yr period under consideration due to chemical retardation in the matrix. In contrast, the analyses of transport results obtained without chemical retardation presented in Table 5.4-2 are able to identify the effects of some of these other variables. In particular, integrated releases tend to increase as CULCLIM (recharge amplitude factor for Culebra) and CULFRSP (fracture spacing in Culebra) increase and decrease as CULPOR (matrix porosity in Culebra) increases. However, the most important variables overall in the absence of chemical retardation are those that influence release to the Culebra (i.e., BHPERM, BPPRES and elemental solubilities).

As seen previously, the examination of scatterplots often helps provide perspective on regression-based sensitivity analysis and sometimes reveals relationships that are not apparent in the regression models. Other than the previously identified role of SALPERM (Salado permeability) as a switch for scenario $S(1,0,0,0,0)$, examination of scatterplots for the no-retardation calculations did not reveal any unusual patterns. However, it is still useful to examine a few scatterplots to develop a feeling for the relationships indicated in Table 5.4-2.

Scatterplots for normalized release of Am-241 and Pu-239 to the accessible environment for scenario $S^{+-}(2,0,0,0,0)$ are given in Figure 5.4-5. The scatterplot for Am-241 involves CULFRSP (Culebra fracture spacing), which is the first variable selected in the regression model presented in Table 5.4-2 for release to the accessible environment (i.e., for the "Full Distance" results). The rank-regression model presented in Table 5.4-2 indicates that release increases as CULFRSP increases and that this variable can account for approximately 33% of the variability in the release. This result is consistent with the pattern shown in Figure 5.4-5, where the release tends to increase as CULFRSP increases but with considerable variability around this trend.

The scatterplot for Pu-239 in Figure 5.4-5 involves SOLPU (solubility for Pu), which again is the first variable selected in the regression model presented in Table 5.4-2 for release to the accessible environment. In this case, the rank-regression model involving only SOLPU indicates that release increases as SOLPU increases and that SOLPU can account for approximately 63% of the variability in the release. This increasing relationship between release and SOLPU for Pu-239 can be readily seen in the scatterplot in

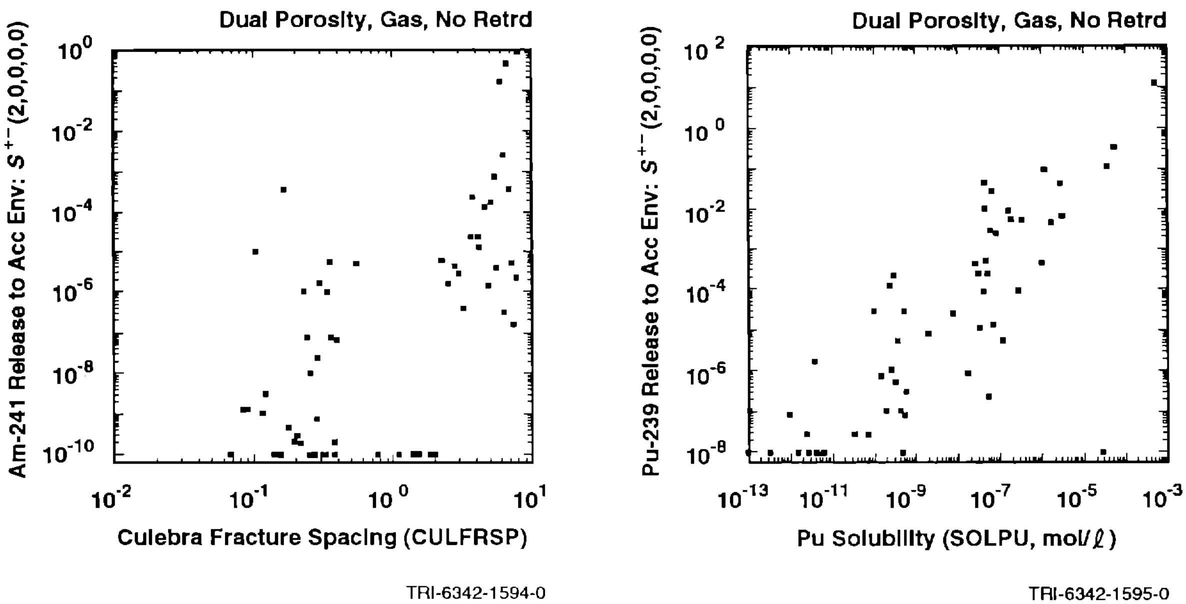

Figure 5.4-5. Scatterplots for Normalized Release of Am-241 and Pu-239 to the Accessible Environment Due to Groundwater Transport for Variables CULFRSP (Culebra fracture spacing) and SOLPU (solubility for Pu) for Scenario S^{+-}(2,0,0,0,0) with Gas Generation in the Repository, a Dual-Porosity Transport Model in the Culebra Dolomite, No Chemical Retardation and Intrusion Occurring at 1000 Yrs.

Figure 5.4-5. Further, as indicated by the R^2 values in the regression models in Table 5.4-2 (i.e., 0.33 for Am-241 and 0.63 for Pu-239), the relationship in the scatterplot for Pu-239 is considerably tighter than the one in the scatterplot for Am-241.

Scatterplots appear in Figure 5.4-6 for the release of U-234 to the accessible environment for scenario S^{+-}(2,0,0,0,0) and the variables BHPERM (borehole permeability), CULCLIM (recharge amplitude factor for Culebra) and SOLU (solubility for U). As shown in Table 5.4-2 for the release of U-234 to the accessible environment, increasing each of these variables tends to increase the release although no single variable dominates. For example, BHPERM is the most influential variable (i.e., is selected first in the stepwise regression analysis with rank-transformed data) but can account for only 27% of the observed variability. This pattern is apparent in the scatterplots in Figure 5.4-6, where release tends to increase with each of BHPERM, CULCLIM and SOLU but with much variability around this increasing trend.

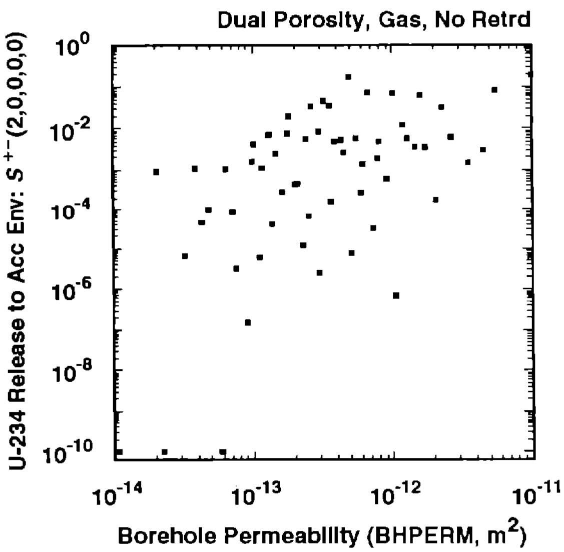

TRI-6342-1596-0

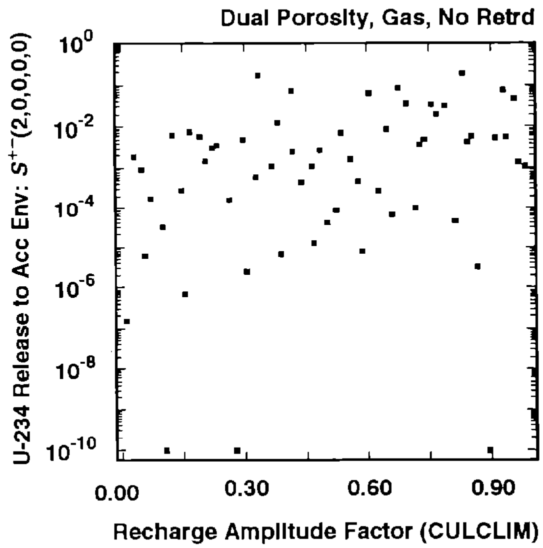

TRI-6342-1598-0

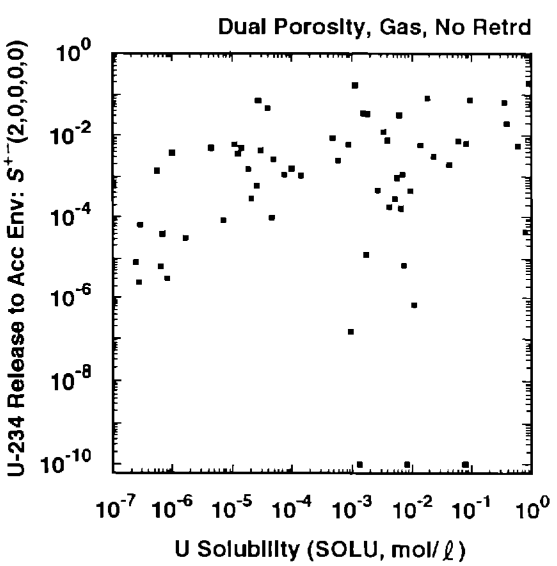

TRI-6342-1597-0

Figure 5.4-6. Scatterplots for Normalized Release of U-234 to the Accessible Environment Due to Groundwater Transport for Variables BHPERM (borehole permeability), CULCLIM (recharge amplitude factor for Culebra) and SOLU (solubility of U) for Scenario S^{+-}(2,0,0,0,0) with Gas Generation in the Repository, A Dual-Porosity Transport Model in the Culebra Dolomite, No Chemical Retardation and Intrusion Occurring at 1000 Yrs.

This is a natural point at which to consider the importance of the variable CULFRPOR (fracture porosity in Culebra). As shown in the scatterplots appearing in Figures 4.5-7 and 5.2-8 for groundwater transport with chemical retardation, increasing CULFRPOR increases groundwater transport when a dual-porosity transport model is used and decreases groundwater transport when a single-porosity transport model is used. Further, CULFRPOR is not identified as being an important variable in the sensitivity analyses presented in Table 5.4-2 for groundwater transport with a dual-porosity transport model and no chemical retardation. The reason for the absence of CULFRPOR from the analyses presented in Table 5.4-2 is easily seen from the scatterplot appearing in Figure 5.4-7, which shows little relationship between CULFRPOR and total release to the accessible environment.

As discussed in Section 5.2, the negative effect of CULFRPOR (fracture porosity in Culebra) on radionuclide release for a single-porosity transport model results from the decrease in groundwater velocity that occurs as CULFRPOR increases. For dual-porosity transport, the presence of a positive effect for CULFRPOR when chemical retardation takes place and the absence of this effect when chemical retardation does not take place suggests that CULFRPOR is involved in the implementation of chemical retardation for the dual-porosity transport model. This is indeed the case, with both CULFRPOR and CULFRSP (Culebra fracture spacing) being involved in the definition of a "skin resistance" that controls radionuclide movement from a fracture to the surrounding matrix for the dual-porosity transport model implemented in STAFF2D (Huyakorn, et al., 1989).

The skin resistance in STAFF2D is defined by

$$\zeta = \left(\frac{b_s}{b_f}\right) \left(\frac{\phi_f \; B}{(1-\phi_f) \; \tau D^{*}}\right) , \qquad (5.4\text{-}1)$$

where

ζ = skin resistance (s/m),

b_s = width of clay lining in fracture (m),

b_f = width of fracture (m),

ϕ_f = fracture porosity (i.e., the sampled variable CULFRPOR in Table 3-1),

B = half the distance between fractures (m) (i.e., one-half the sampled variable CULFRSP in Table 3-1),

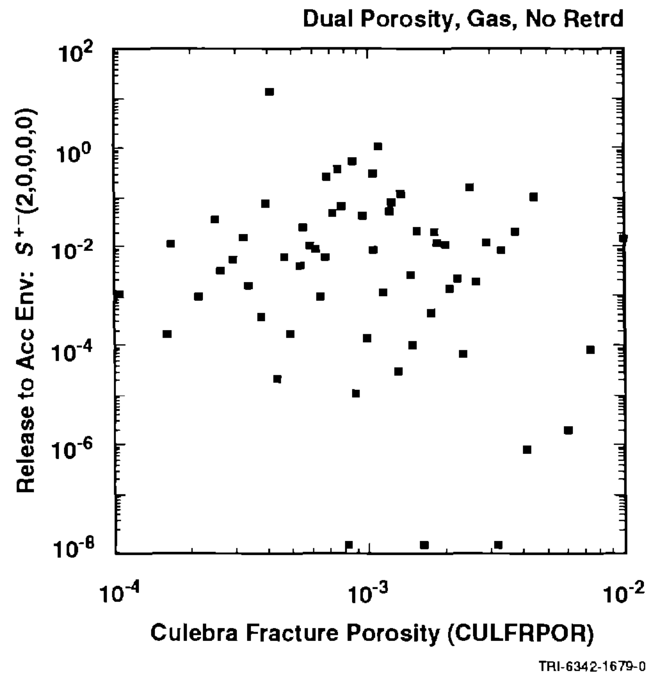

Figure 5.4-7. Scatterplot for Fracture Porosity in Culebra Dolomite (CULFRPOR) versus Total Normalized Release to the Accessible Environment Due to Groundwater Transport for Scenario S^{+-}(2,0,0,0,0) with Gas Generation in the Repository, a Dual-Porosity Transport Model in the Culebra Dolomite, No Chemical Retardation and Intrusion Occurring at 1000 Yrs.

τ = clay tortuosity, which was fixed at 1.2 x 10^{-2} in the 1991 WIPP performance assessment (Vol. 3, Section 2.6.7)

and

D^{α} = molecular diffusion coefficient (m^2/s), which was fixed at the median elemental values shown in Table 3.3-12, Vol. 3, for the 1991 WIPP performance assessment.

As skin resistance increases, the rate of radionuclide movement from a fracture to the surrounding matrix will decrease.

For the 1991 WIPP performance assessment, the ratio b_s/b_f in Eq. 5.4-1 is assumed to equal 0.1. Further, τ is fixed at 1.2 x 10^{-2}; D^{α} is fixed for each element at the median value shown in Table 3.3-12, Vol. 3, and 1-ϕ_f is close to one (i.e., ϕ_f is the sampled variable CULFRPOR shown in Table 3-1, which has a range from 1 x 10^{-4} to 1 x 10^{-2}). As a result, the skin resistance ζ is proportional to the product ϕ_f B, which is the product CULFRPOR*CULFRSP/2 in the notation used in this report. Thus, ζ should increase, with the result that radionuclide transport in the Culebra should also increase, as CULFRPOR and CULFRSP increase, which is exactly the pattern that has been observed (e.g., see the scatterplots for CULFRSP and CULFRPOR in Figure 4.5-7 and the regression analyses in Tables 5.1-2 and 5.1-3). Further, as shown in Figure 5.4-8, a stronger relationship exists between release to the accessible environment and the product CULFRSP*CULFRPOR (i.e., $2\,\phi_f\,B$) than appears in Figure 4.5-7 for either variable by itself.

5.5 Effect of Climate Change

The 1991 WIPP performance assessment used the variable CULCLIM (recharge amplitude factor for Culebra) to study the effects of uncertainty in the future climate in southeastern New Mexico. Specifically, CULCLIM is used in the relationship

$$\frac{h_f(t)}{h_p} = \frac{3A_m + 1}{4} - \frac{A_m - 1}{2}\left(\cos\Theta t + \frac{1}{2}\cos\Phi t - \sin\frac{1}{2}\Phi t\right) \qquad (5.5\text{-}1)$$

to define time-dependent heads in the Culebra, where

$h_f(t)$ = head (m) in Culebra at time t (sec),
h_p = estimate of present-day boundary head in Culebra (e.g., 880 m),
A_m = recharge amplitude factor (dimensionless) for Culebra (i.e., CULCLIM),
Θ = frequency (Hz) for Pleistocene glaciations (i.e., 1.7×10^{-12} Hz),
Φ = frequency (Hz) for second-order climatic fluctuations (i.e., 2×10^{-10} Hz)

and

t = time (sec), with t=0 corresponding to closure of the WIPP.

As discussed in Section 4.4 of Vol. 3, this function is not used to predict future climates, but rather is designed to provide a simple way to examine the influence of possible climatic changes during the next 10,000 yrs. The periodicity of the function is based on approximately 30,000 yrs of paleoclimatic data from southeastern New Mexico and the surrounding region and the global record of Pleistocene glaciations (Swift, in press). The glacial frequency term Θ produces a maximum value of the function $h_f(t)$ at 60,000 yrs, and has little effect during the regulatory period. Most of the introduced variability results from second-order fluctuations controlled by the higher-frequency term Φ. This variability corresponds conceptually to the frequency of nonglacial climatic fluctuations observed in both late Pleistocene and Holocene paleoclimatic data.

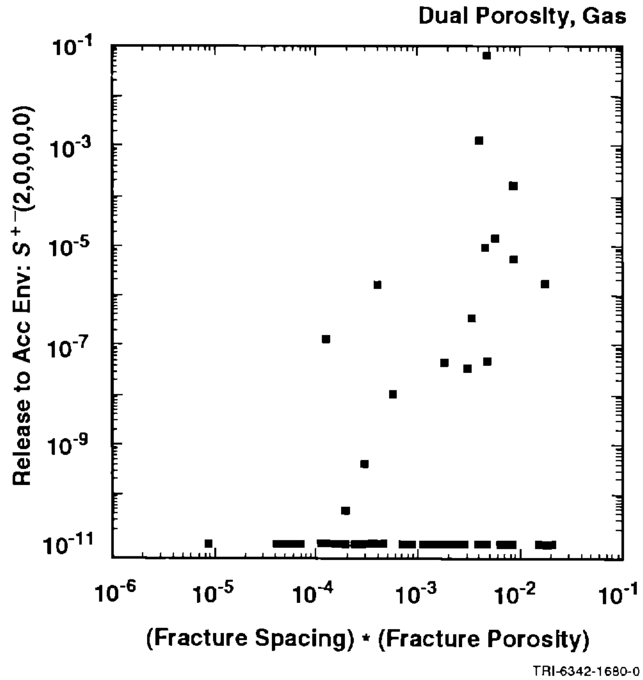

Figure 5.4-8. Scatterplot for Total Normalized Release to the Accessible Environment Due to Groundwater Transport versus the Product of Culebra Fracture Spacing (CULFRSP, m) and Culebra Fracture Porosity (CULFRPOR) (i.e., the product CULFRSP*CULFRPOR) for Scenario $S^{+-}(2,0,0,0,0)$ with Gas Generation in the Repository, a Dual-Porosity Transport Model in the Culebra Dolomite and Intrusion Occurring at 1000 Yrs.

As discussed in Section 6.4.2 of Vol. 2, climatic fluctuations are linked to the groundwater-flow model through the sampled variable CULCLIM (i.e., A_m), which is a scaling factor used to modify hydraulic heads in the Culebra Dolomite along a portion of the northern boundary of the model domain. At its minimum value of 1, CULCLIM results in no change in prescribed boundary heads during the 10,000-yr period. At its maximum value of 1.16, CULCLIM results in boundary heads varying from their estimated present values (e.g., 880 m) to maximum values corresponding to the ground surface (e.g., 1030 m). Intermediate values for CULCLIM result in maximum heads at elevations between their present evaluation and the ground surface.

Considerable interest exists in the effects of climatic variation. Therefore, although the original Latin hypercube sample indicated in Eq. 2.1-5 contained CULCLIM as a variable, analyses for single- and dual-porosity transport in the Culebra with gas generation in the repository and chemical retardation were repeated with CULCLIM set to 1 and to 1.16.

The results of these calculations for total normalized release to the accessible environment are summarized by the scatterplots appearing in Figures 5.5-1 and 5.5-2 for dual- and single-porosity transport, respectively, with the ordinate displaying the results for CULCLIM = 1 and

Scenario: *S*(1,0,0,0,0), Assumed Intrusion Time: 1000 yrs

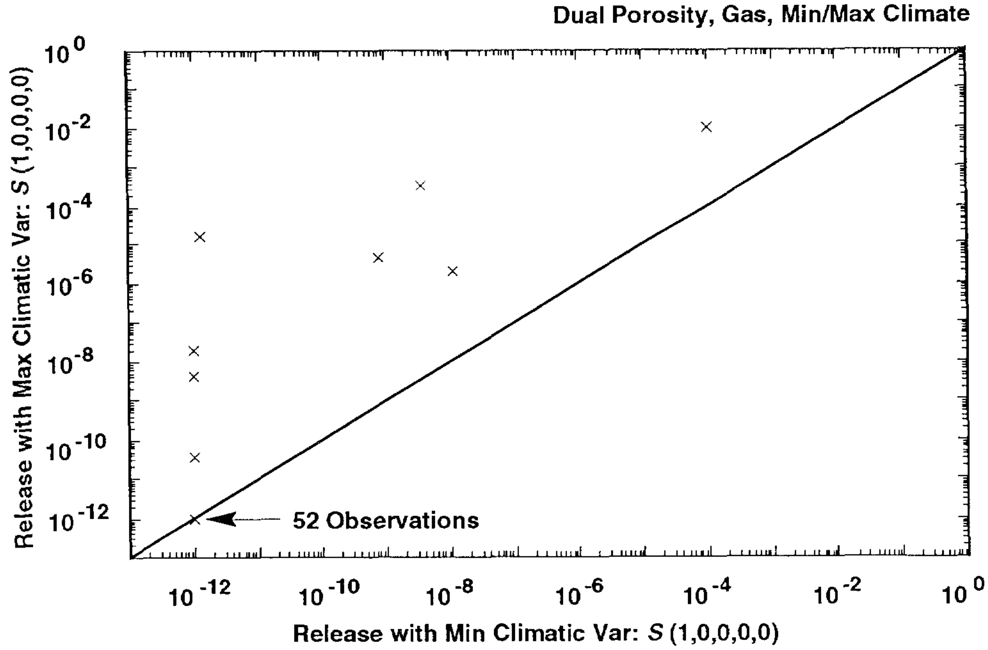

TRI-6342-1646-0

Scenario: S^{+-}(2,0,0,0,0), Assumed Intrusion Time: 1000 yrs

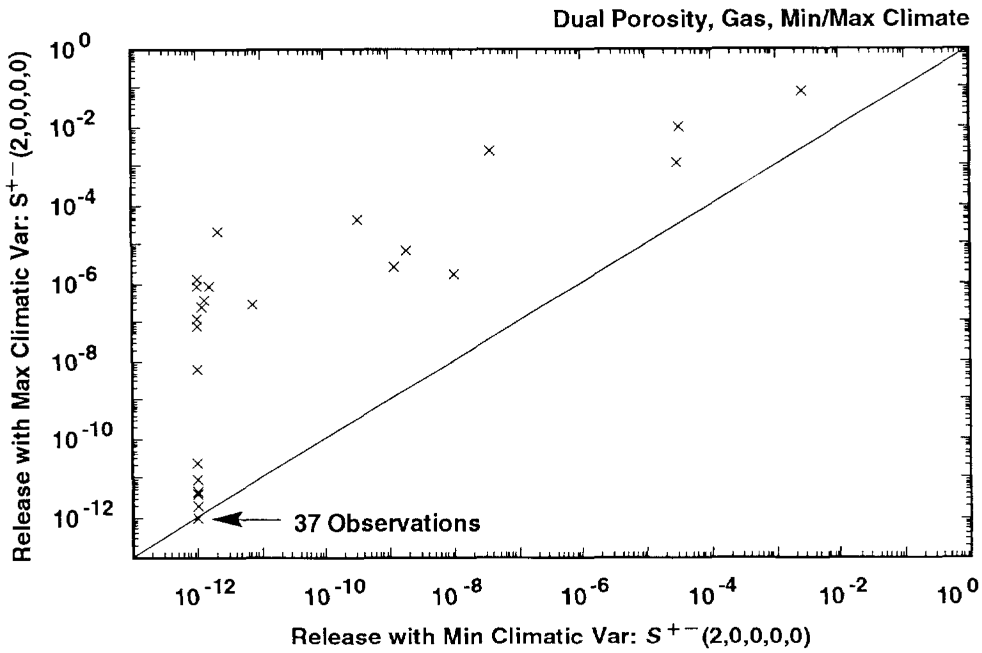

TRI-6342-1647-0

Figure 5.5-1. Scatterplots for Total Normalized Release to the Accessible Environment Due to Groundwater Transport with Minimum (i.e., CULCLIM = 1) and Maximum (i.e., CULCLIM = 1.16) Climatic Variation for Gas Generation in the Repository, a Dual-Porosity Transport Model with Chemical Retardation in the Culebra and Intrusion Occurring at 1000 Yrs. For plotting purposes, values less than 10^{-12} are set to 10^{-12}.

Scenario: S(1,0,0,0,0), Assumed Intrusion Time: 1000 yrs

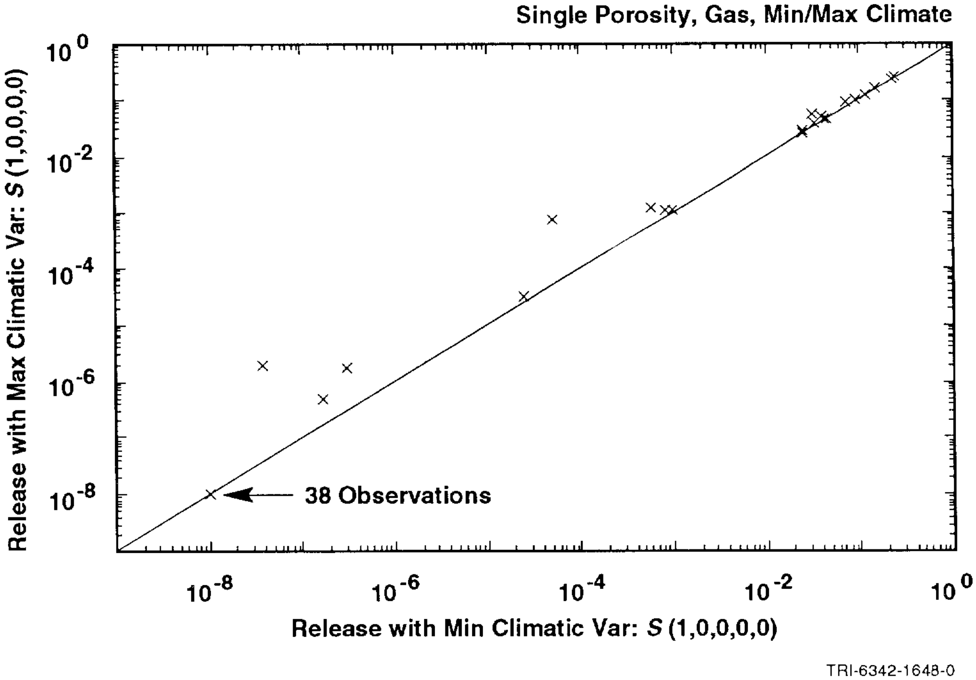

Scenario: S^{+-}(2,0,0,0,0), Assumed Intrusion Time: 1000 yrs

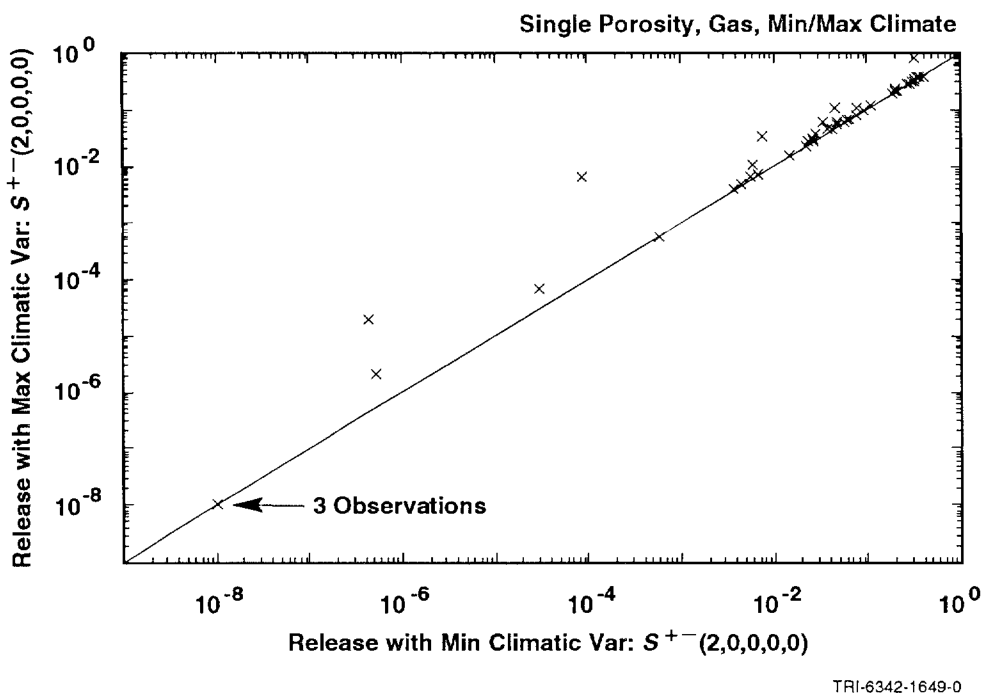

Figure 5.5-2. Scatterplots for Total Normalized Release to the Accessible Environment Due to Groundwater Transport with Minimum (i.e., CULCLIM = 1) and Maximum (i.e., CULCLIM = 1.16) Climatic Variation for Gas Generation in the Repository, a Single-Porosity Transport Model with Chemical Retardation in the Culebra and Intrusion Occurring at 1000 Yrs. For plotting purposes, values less than 10^{-8} are set to 10^{-8}.

the abscissa displaying the results for CULCLIM = 1.16. As shown in Figure 5.5-1, an assumption of increased rainfall, and hence increased head at the northern recharge boundary used for the Culebra, leads to increased releases for the dual-porosity transport model. However, these increased releases are too small to cause a violation of the EPA release limits. In contrast, the results in Figure 5.5-2 show that an assumption of increased rainfall has almost no effect on the releases for the single-porosity transport model.

As shown in Figure 5.5-3, most U-234 releases to the Culebra are transported to the accessible environment within the 10,000-yr time period specified in the EPA standard when a single-porosity transport model is used. The observations shown in Figure 5.5-3 in which this does not occur tend to be those in which uranium has one of its larger distribution coefficient values, in which case the total release is dominated by some other isotope that has a small distribution coefficient value. Thus, the total releases to the accessible environment for single-porosity transport in the Culebra and CULCLIM=1 are dominated by isotopes whose entire release to the Culebra is transported to the accessible environment within the 10,000-yr period in the EPA standard. As a reminder, most releases are dominated by U-234 (see Figure 5.2-5). Thus, although increasing CULCLIM to 1.16 will increase groundwater flow and hence result in earlier releases to the accessible environment, an increased release over 10,000 yrs will not take place. For the dual-porosity transport model, the releases to the accessible environment are substantially less than the releases to the Culebra for all isotopes (e.g., compare the results in Figures 5.1-2 and 5.1-3). In this case, increasing the groundwater flow rate will increase the release to the accessible environment, although the total releases remain small.

Transport calculations for CULCLIM = 1 and CULCLIM = 1.16 were only performed for scenarios $S(1,0,0,0,0)$ and $S^{+-}(2,0,0,0,0)$. As a result, CCDFs for comparison with the EPA release limits using nonzero intrusion probabilities over 10,000 yrs cannot be constructed. However, as already shown in Figures 5.1-4, 5.3-3 and 5.4-3, CCDFs can be constructed for comparison with the EPA release limits under the assumption that the rate constant λ in the Poisson model for drilling intrusions is equal to zero after 2000 yrs. The result of this construction for dual-porosity transport in the Culebra is shown in Figure 5.5-4. As examination of this figure shows, the CCDFs obtained for the maximum recharge case (i.e., CULCLIM = 1.16) are shifted to the right relative to those obtained with present-day recharge (i.e., CULCLIM = 1). However, even for the maximum recharge, the releases due to groundwater transport are substantially smaller than the release due to cuttings removal summarized in the CCDFs shown in Figure 4.1-2. The small effect indicated for CULCLIM in Figure 5.5-4 is consistent with the small effect indicated for

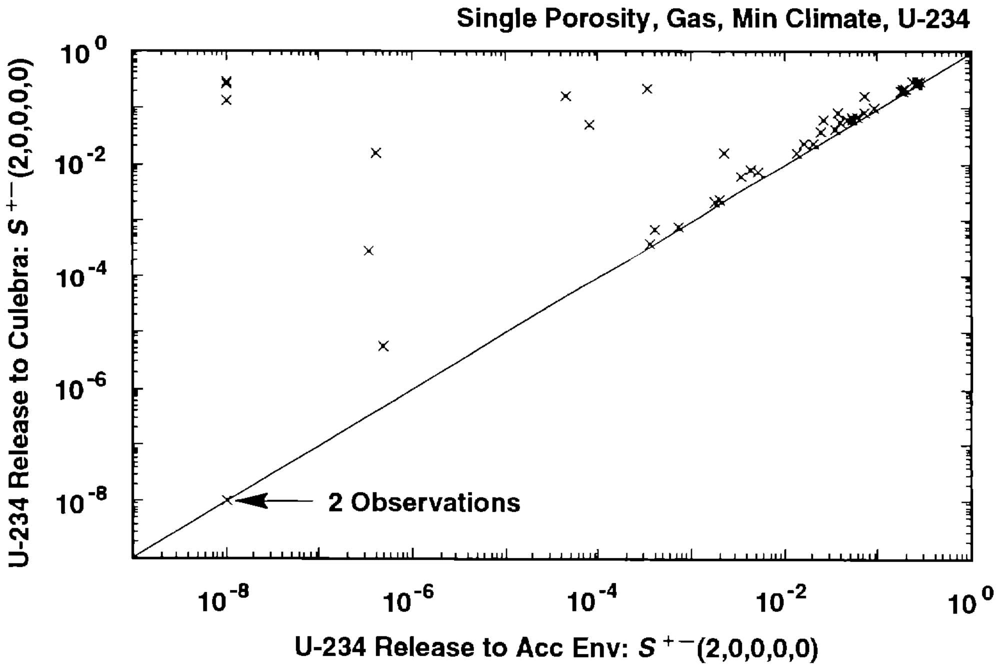

TRI-6342-1692-0

Figure 5.5-3. Scatterplot for Normalized U-234 Release to the Culebra Dolomite versus Normalized U-234 Release to the Accessible Environment Due to Groundwater Transport with Minimum (i.e., CULCLIM = 1) Climatic Variation for Scenario $S^{+-}(2,0,0,0,0)$ with Gas Generation in the Repository, a Single-Porosity Transport Model with Chemical Retardation in the Culebra and Intrusion Occurring at 1000 Yrs. For plotting purposes, values less than 10^{-8} are set to 10^{-8}.

CULCLIM in the scatterplot appearing in Figure 5.4-6 for the release of U-234 to the accessible environment with a dual-porosity transport model and no chemical retardation, where the relative effect of CULCLIM is actually greater than in the analyses presented in this section due to the absence of chemical retardation.

The CCDFs in Figure 5.5-4 are for dual-porosity transport in the Culebra. A similar figure could be generated for single-porosity transport. However, as shown in Figure 5.5-2, the release results for CULCLIM = 1 and CULCLIM = 1.16 are essentially identical when the single-porosity transport model is used, and so the resultant CCDFs would also be the same.

Present-Day Recharge (CULCLIM = 1)

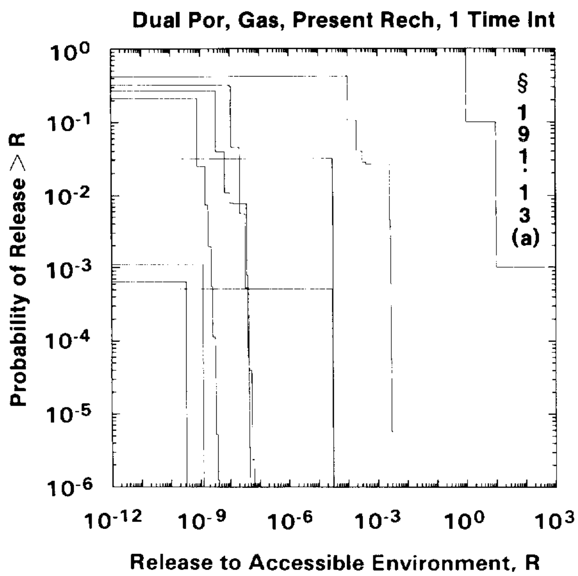

TRI-6342-1571-0

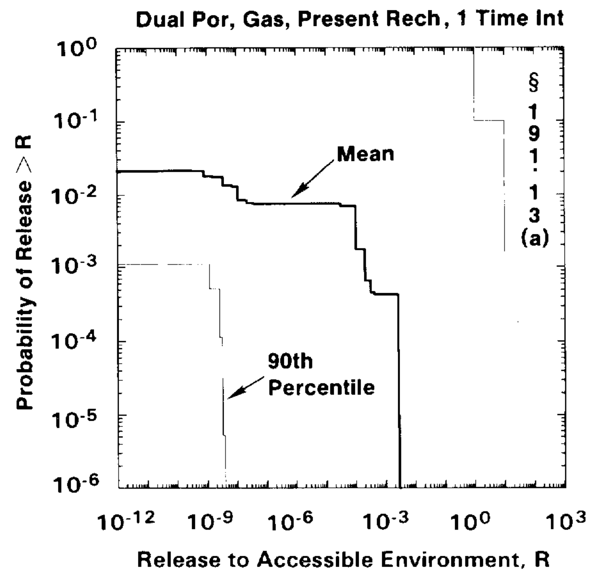

TRI-6342-1572-0

Maximum Recharge (CULCLIM = 1.16)

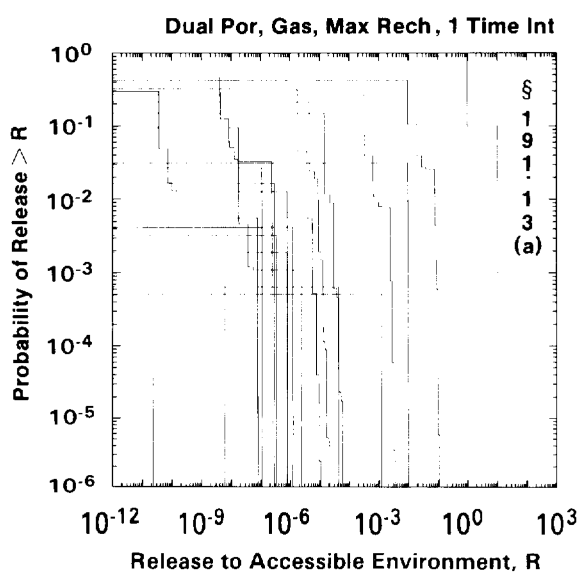

TRI-6342-1573-0

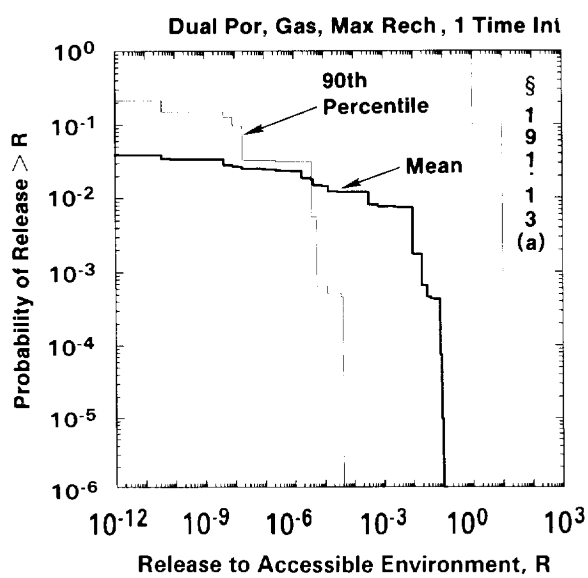

TRI-6342-1574-0

Figure 5.5-4. Comparison of Complementary Cumulative Distribution Functions for Normalized Release to the Accessible Environment with Present-Day Recharge (CULCLIM = 1) and Maximum Recharge (CULCLIM = 1.16) for Gas Generation in the Repository, a Dual-Porosity Transport Model in the Culebra Dolomite and the Rate Constant λ in the Poisson Model for Drilling Intrusions Equal to Zero After 2000 Yrs.

6. DISCUSSION

At present, the most appropriate conceptual model for use in performance assessment at the WIPP is believed to include gas generation due to corrosion and microbial action in the repository and a dual-porosity (matrix and fracture porosity) representation for solute transport in the Culebra Dolomite. Under these assumptions, CCDFs summarizing radionuclide releases to the accessible environment due to both cuttings removal and groundwater transport fall substantially below the release limits promulgated by the EPA. This is the case even when the current estimates of the uncertainty in analysis inputs are incorporated into the performance assessment. Although the results of this analysis offer encouragement with respect to the suitability of the WIPP as a disposal facility for transuranic waste, they should be regarded as preliminary (Table 11-1, Vol. 1).

The best-estimate performance-assessment results indicated in the preceding paragraph are dominated by cuttings removal. The releases to the accessible environment due to groundwater transport make very small contributions to the total release. The variability in the distribution of CCDFs that must be considered in comparisons with the EPA release limits is dominated by the variable LAMBDA (rate constant in Poisson model for drilling intrusions).

The variability in releases to the accessible environment due to individual drilling intrusions was controlled by DBDIAM (drill bit diameter), which was the only imprecisely known variable considered in the model for cuttings removal. If cuttings removal continues to dominate the CCDFs for releases to the accessible environment in future analyses, a more detailed analysis of the variables used in the modeling of cuttings removal should be performed.

Most of the imprecisely known variables considered in the 1991 WIPP performance assessment relate to radionuclide releases to the accessible environment due to groundwater transport. For a single borehole (i.e., an E2-type scenario), whether or not a release from the repository to the Culebra even occurs is controlled by the variable SALPERM (Salado permeability), with no releases for small values (i.e., $< 5 \times 10^{-21}$ m^2) of this variable. When SALPERM is small, the repository never fills with brine and so there is no flow up an intruding borehole that can transport radionuclides to the Culebra. Further, releases that do reach the Culebra for larger values of SALPERM are small and usually do not reach the accessible environment.

A potentially important scenario for the WIPP involves two or more boreholes through the same waste panel, of which at least one penetrates a pressurized brine pocket and at least one does not (i.e., an E1E2-type scenario). For these scenarios, the uncertainty in release to the Culebra is dominated by the variables BHPERM (borehole permeability), BPPRES (brine pocket pressure), and the solubilities for the individual elements in the projected radionuclide inventory for the WIPP (i.e., Am, Np, Pu, Th, U). Once radionuclides are released to the Culebra, the matrix distribution coefficients for the individual elements are important, with releases to the Culebra often failing to reach the accessible environment over the 10,000-yr period specified in the EPA regulations. As an example, Pu-239 dominates the releases to the accessible environment due to cuttings removal, is an important contributor to the total release to the Culebra, and yet is rarely a significant contributor to the total release to the accessible environment due to groundwater transport as a result of the large distribution coefficients associated with plutonium (e.g., median values for fracture and matrix distribution coefficients are 2.02×10^{2} and 2.61×10^{-1} m^3/kg, respectively). In contrast, U-234 has relatively small distribution coefficient values (e.g., median values for fracture and matrix distribution coefficients for uranium are 7.5×10^{-3} and 2.58×10^{-2} m^3/kg, respectively) and usually dominates the releases to the accessible environment due to groundwater transport.

As indicated by the preceding discussion, a small subset of the 45 variables presented in Table 3-1 dominates the best-estimate results obtained in the 1991 WIPP performance assessment. The most important variable overall is LAMBDA (rate constant in Poisson model for drilling intrusions). As shown in Figure 4.6-1, LAMBDA completely dominates the uncertainty in the CCDFs that must be compared against the EPA release limits. The releases to the accessible environment due to groundwater transport are very small in the best-estimate analyses (i.e., gas generation in the repository and a dual-porosity transport model in the Culebra), with the result that the releases to the accessible environment are dominated by cuttings removal. Although the uncertainty in cuttings removal for individual boreholes is determined by DBDIAM (drill bit diameter) in the 1991 WIPP performance assessment, the variables that determine, or prevent, releases to the accessible environment due to groundwater transport are more important due to the larger quantities of radionuclides that have the potential to be released.

The following variables are important in determining radionuclide releases to the accessible environment due to groundwater transport: solubilities for the individual elements (i.e., SOLAM, SOLNP4, SOLNP5, SOLPU4, SOLPU5, SOLTH, SOLU4, SOLU6), borehole permeability (BHPERM), Salado permeability (SALPERM), and matrix distribution coefficients (i.e., MKDAM, MKDNP, MKDPU, MKDTH, MKDU). It is difficult to put an absolute ranking on the importance of these variables. For example, any one of the following three conditions is sufficient to effectively prevent radionuclide releases to the accessible environment due to groundwater transport: (1) low solubilities, (2) low borehole permeability, and (3) high matrix distribution coefficients. Further, for intrusions involving a single borehole, low values for Salado permeability prevent releases to the Culebra and hence to the accessible environment. The uncertainty in the WIPP performance assessment results for groundwater transport to the accessible environment would be reduced by better characterizations of the possible values for these variables.

The solubilities and distribution coefficients for the individual elements are not equally important. Due to the large inventory and long half-life of Pu-239 (see Figure 2.4-2), the solubility and distribution coefficient for plutonium are important variables. A similar, but slightly less strong statement, can be made for americium because of the presence of Am-241 in the WIPP inventory. However, the properties of americium are less important than those of plutonium due to the relatively short half-life of Am-241 (i.e., 432 yrs) relative to the 10,000-yr period that must be considered in comparison with EPA release limits. The solubilities and distribution coefficients for neptunium and thorium are relatively unimportant due to the small amounts of Np-237 and Th-230 in the WIPP inventory (see Figure 2.4-2). Uranium presents an intermediate situation. The estimated inventory of U-234 in one waste panel is approximately 0.3 EPA units or, equivalently, 3 EPA units in the entire repository (see Figure 2.4-2). Relatively high solubilities and low distribution coefficients result in U-234 tending to dominate the releases to the accessible environment even though the inventory of Pu-239 in a single waste panel is much higher (i.e., approximately 70 EPA units). Due to large contributions of U-234 to the total normalized release to the accessible environment due to groundwater transport, improvements in the estimates for the solubility and distribution coefficient for uranium could reduce the uncertainty in the total releases due to groundwater transport. In summary and conditional on current estimates of the waste to be disposed of at the WIPP, the most important elements for the characterization of solubilities and distribution coefficients for comparisons with the EPA release limits are plutonium, uranium and americium.

After the preceding variables, the sensitivity analyses for groundwater transport with gas generation in the repository and a dual-porosity transport model in the Culebra identified several other variables that had lesser effects, including CULFRPOR (Culebra fracture porosity), CULFRSP (Culebra fracture spacing), CULCLIM (recharge amplitude factor for Culebra) and several variables related to gas generation. The variable BPPRES (brine pocket pressure) was also selected in analyses for E1E2-type scenarios. Increasing each of CULFRPOR, CULFRSP, CULCLIM and BPPRES tends to increase releases. Increasing gas generation tended to decrease releases, although none of the individual variables related to gas generation appeared to have a large effect. However, SALPERM (Salado permeability) acted as a switch for releases into the Culebra for a single borehole only in the presence of gas generation. Increasing fracture distribution coefficients (i.e., FKDAM, FKDNP, FKDPU, FKDTH, FKDU) tended to decrease releases due to groundwater transport, although the effects of these distribution coefficients were generally smaller than the effects of the corresponding matrix distribution coefficients. Although solubilities were important, the use of solubilities defined on the basis of oxidation states for neptunium (i.e., SOLNP4 and SOLNP5), plutonium (i.e., SOLPU4 and SOLPU5) and uranium (i.e., SOLU4 and SOLU6) had little effect on the releases from the repository to the Culebra, with both oxidation states for each element producing overlapping releases.

Sensitivity analysis results depend on both the ranges assigned to variables and the impact that incremental changes in these variables have on the predicted variable of interest. As a result, variables with large ranges and/or large incremental effects can obscure the effects of other variables. In analyses such as those presented in this report, sensitivity analysis results are conditional on the characterizations of subjective uncertainty assigned to the input variables selected for consideration. In particular, as the knowledge base for individual variables is improved (i.e., as subjective uncertainty is reduced), these variables may cease to be important contributors to uncertainty in the outcome of a performance assessment and thus be superseded in importance by other previously less important variables. However, with the assumption that new sources of uncertainty are not identified, the overall uncertainty in the results of the analysis should decrease as the uncertainty in important variables is reduced.

Sensitivity analysis results only measure the effects of the sampled variables and thus are conditional on the conceptual models analyzed and on the numerical representations employed for these conceptual models. Therefore, the following variants of the 1991 WIPP performance assessment have also been considered to provide additional perspective on the impact of subjective uncertainty: (1) no gas generation in the repository and a dual-porosity transport model in the Culebra, (2) gas generation in the repository and a single-porosity (fracture porosity) transport model in the Culebra, (3) no gas generation in the repository and a single-porosity transport model in the Culebra, (4) gas generation in the repository and a dual-porosity transport model in the Culebra without chemical retardation, and (5) gas generation in the repository, a dual-porosity transport model in the Culebra, and extremes of climatic variation. All of these variations relate to groundwater transport and thus do not affect releases due to cuttings removal, which were found to dominate the results of the 1991 WIPP performance assessment. However, these variations do have the potential to increase the importance of releases due to groundwater transport relative to releases due to cuttings removal. Further, these variations remove the effects of some of the dominant variables identified in the sensitivity analyses for gas generation in the repository and a dual-porosity transport model in the Culebra, and thus provide an opportunity to observe the impact of additional variables listed in Table 3-1.

The presence of gas generation was found to reduce releases to the Culebra for an E2-type scenario. When gas generation is present, the variable SALPERM (Salado permeability) acts as a switch that determines whether or not a release to the Culebra will occur. The role of SALPERM as a switch goes away when gas generation is not considered. In this case, the repository is generally brine saturated by the time the first drilling intrusion occurs (i.e., at 1000 yrs in the 1991 WIPP performance assessment) and release to the Culebra is dominated by the solubilities for the individual elements (i.e., Am, Np, Pu, Th, U), with a lesser effect due to SALPERM as a result of its influence on the amount of fluid flowing up the borehole. Sample elements that result in zero releases to the Culebra with gas generation in the repository result in nonzero releases without gas generation. Further, nonzero releases in the presence of gas generation in the repository tend to be larger in the absence of gas generation. The absence of gas generation also results in larger releases to the Culebra for E1E2-type scenarios. Since the absence of gas generation can result in larger releases to the Culebra, it can also lead to larger releases to the accessible environment due to groundwater transport. However, when the dual-porosity transport model is used, many releases to the accessible environment are zero and even the nonzero releases tend to be small (usually substantially less than 0.1). As a result, total releases to the accessible environment due to cuttings removal and groundwater transport are also dominated by cuttings removal when no gas generation in the repository and a dual-porosity transport model in the Culebra are assumed.

The use of a single-porosity rather than a dual-porosity transport model in the Culebra was found to result in substantially larger releases to the accessible environment due to groundwater transport. Specifically, normalized releases are often several orders of magnitude higher when a single-porosity transport model is used, and many zero releases with the dual-porosity transport model are nonzero with the single-porosity transport model. However, despite these increases in groundwater releases, the CCDFs for total releases to the accessible environment constructed with results obtained for gas generation in the repository and a single-porosity transport model in the Culebra are below the EPA release limits, although they are considerably above the corresponding CCDFs constructed with dual-porosity results. Unlike results obtained with the dual-porosity transport model, many of the groundwater releases to the accessible environment obtained with the single-porosity transport model are larger than the corresponding cuttings releases. For comparison, the mean CCDFs for cuttings removal, groundwater transport with a dual-porosity transport model, and groundwater transport with a single-porosity transport model are shown in Figure 6-1.

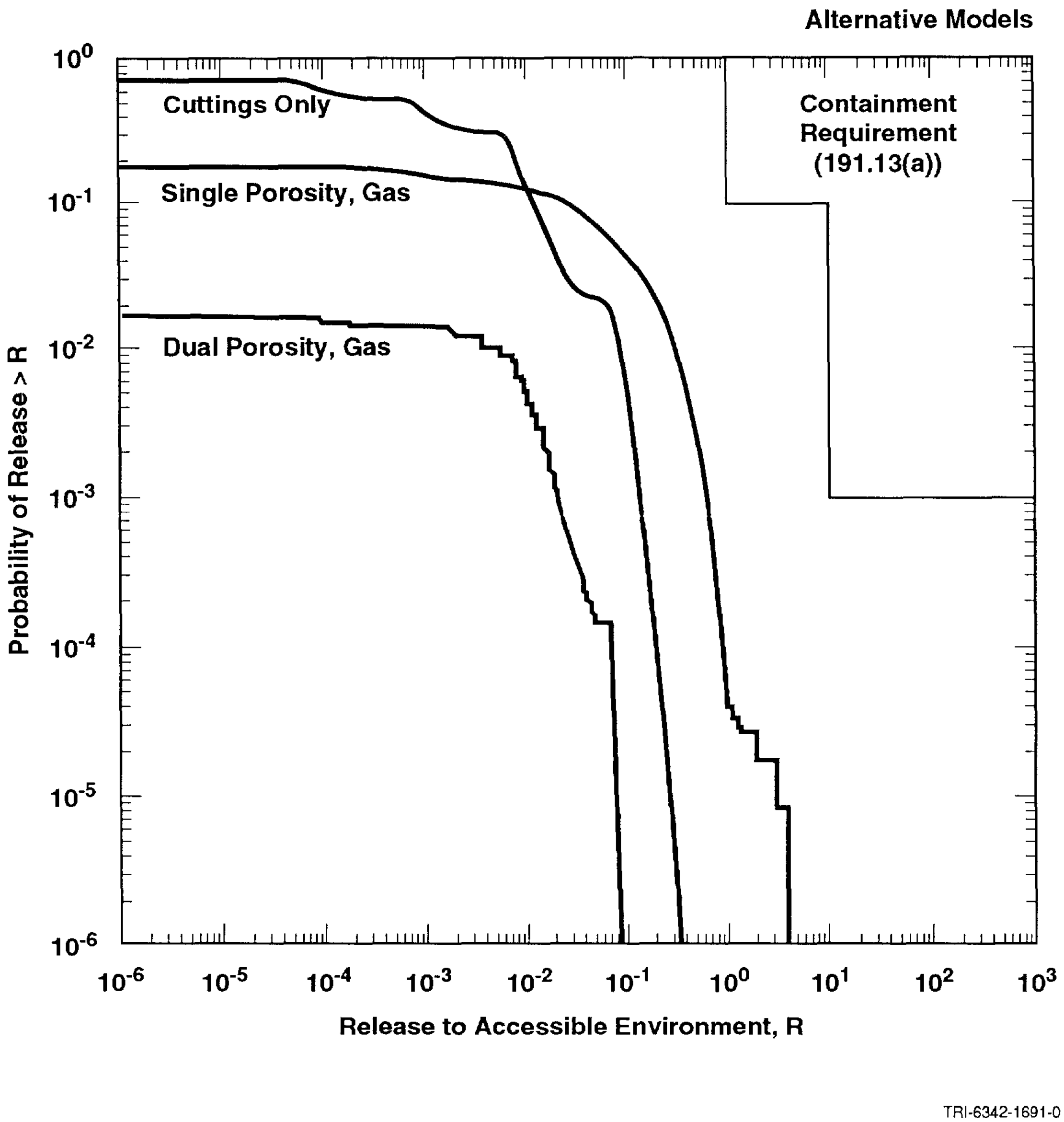

Figure 6-1. Mean Complementary Cumulative Distribution Functions for Normalized Releases to the Accessible Environment for Cuttings Removal, Groundwater Transport with Gas Generation in the Repository and a Dual-Porosity Transport Model in the Culebra Dolomite, and Groundwater Transport with Gas Generation in the Repository and a Single-Porosity Transport Model in the Culebra Dolomite. The distributions of CCDFs on which the mean CCDFs in this figure are based appear in Figures 4.1-2 and 5.2-1.

As already discussed, the absence of gas generation in the repository results in larger releases to the Culebra than the presence of gas generation, and the use of a single-porosity transport model in the Culebra results in larger releases to the accessible environment than the use of a dual-porosity model. Thus, rather unsurprisingly, even larger groundwater-transport releases result for no gas generation in the repository and a single-porosity transport model in the Culebra. The analyses for no gas generation in the repository and a single-porosity transport model in the Culebra were performed for intrusions occurring only at 1000 yrs. Thus, it is not possible to construct the CCDFs used for comparison with the EPA release limits that include intrusions occurring after 1000 yrs. However, given the releases observed for intrusions at 1000 yrs, some of the resultant CCDFs would probably intersect the EPA release limits, although the bulk of the CCDF distribution would be below these limits.

At present, no experimental data are available for the Culebra Dolomite that can be used to estimate radionuclide retardation during transport by flowing groundwater. As a result, there is significant uncertainty in what the appropriate values should be for these quantities. The 1991 WIPP performance assessment considered a range of elemental distribution coefficients developed through an internal review process at SNL (Section 2.3.4, Vol. 3), which in turn lead to retardations for use within the transport calculations. To help provide perspective on the importance of chemical retardation, dual-porosity transport calculations without chemical retardation were performed for the Culebra for intrusions occurring at 1000 yrs and releases into the Culebra predicted with gas generation in the repository. As should be the case, these calculationd lead to larger releases to the accessible environment than were obtained with chemical retardation. However, these releases are still small, with few releases exceeding 0.1 EPA release units and most releases much smaller. The releases predicted for no gas generation in the repository and a single-porosity transport model with chemical retardation in the Culebra are generally larger than the releases predicted for gas generation in the repository and a dual-porosity transport model without chemical retardation in the Culebra. The analyses for gas generation in the repository and a dual-porosity transport model without chemical retardation in the Culebra were performed only for intrusions occurring at 1000 yrs. Thus, with the available results, it is not possible to construct CCDFs for comparison with the EPA release limits that include intrusions occurring after 1000 yrs. However, given the releases observed for intrusions at 1000 yrs, few if any of these CCDFs would intersect the EPA release limits and most of the CCDFs would be considerably below the EPA limits.

Summaries of the releases to the accessible environment obtained under different modeling assumptions are provided in Figures 6-2 and 6-3 for

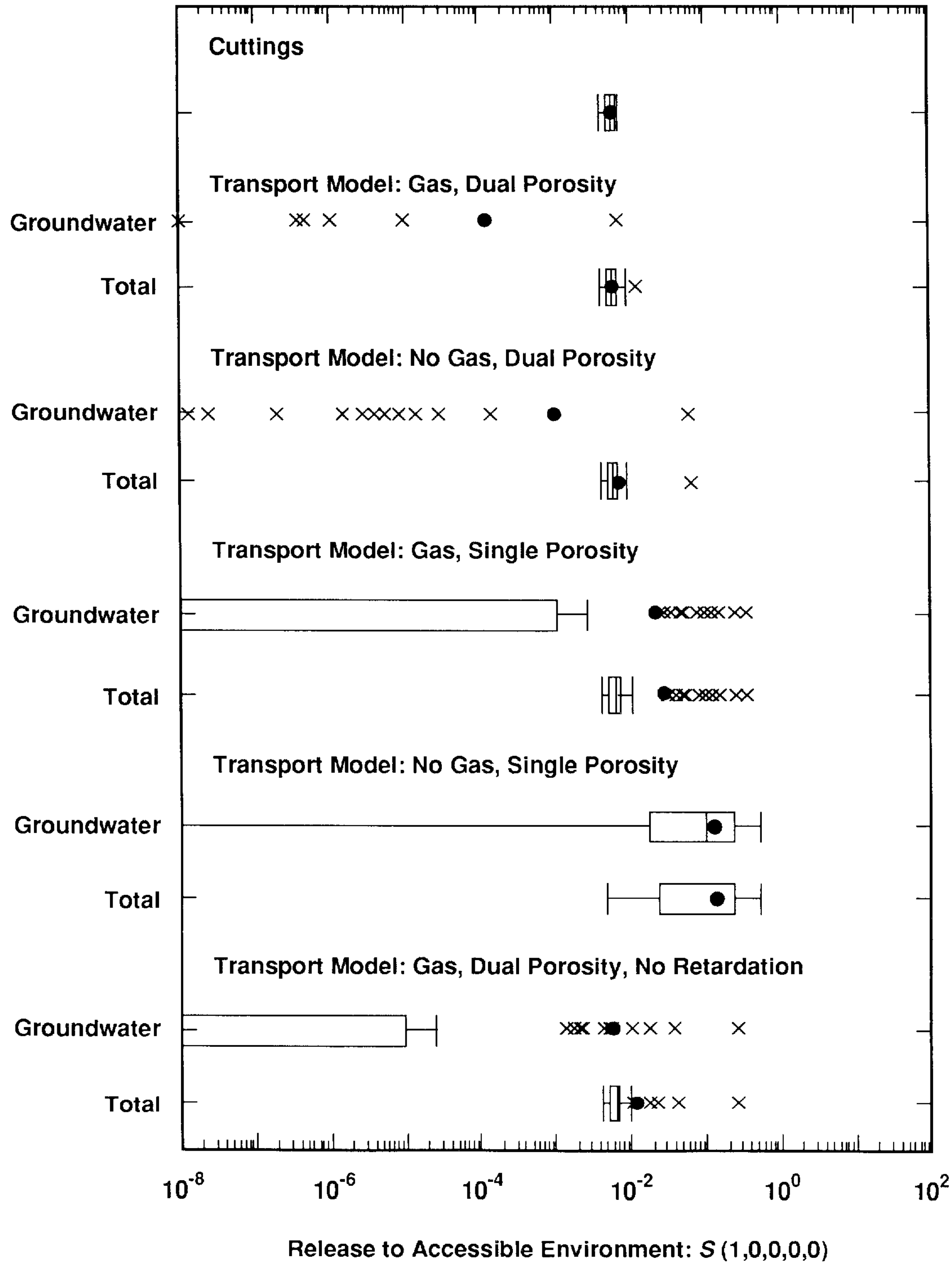

3 Figure 6-2. Summary of Normalized Releases to the Accessible Environment for E2-type Scenarios with
4 Intrusion Occurring at 1000 Yrs (i.e., for scenario *S*(1,0,0,0,0)).

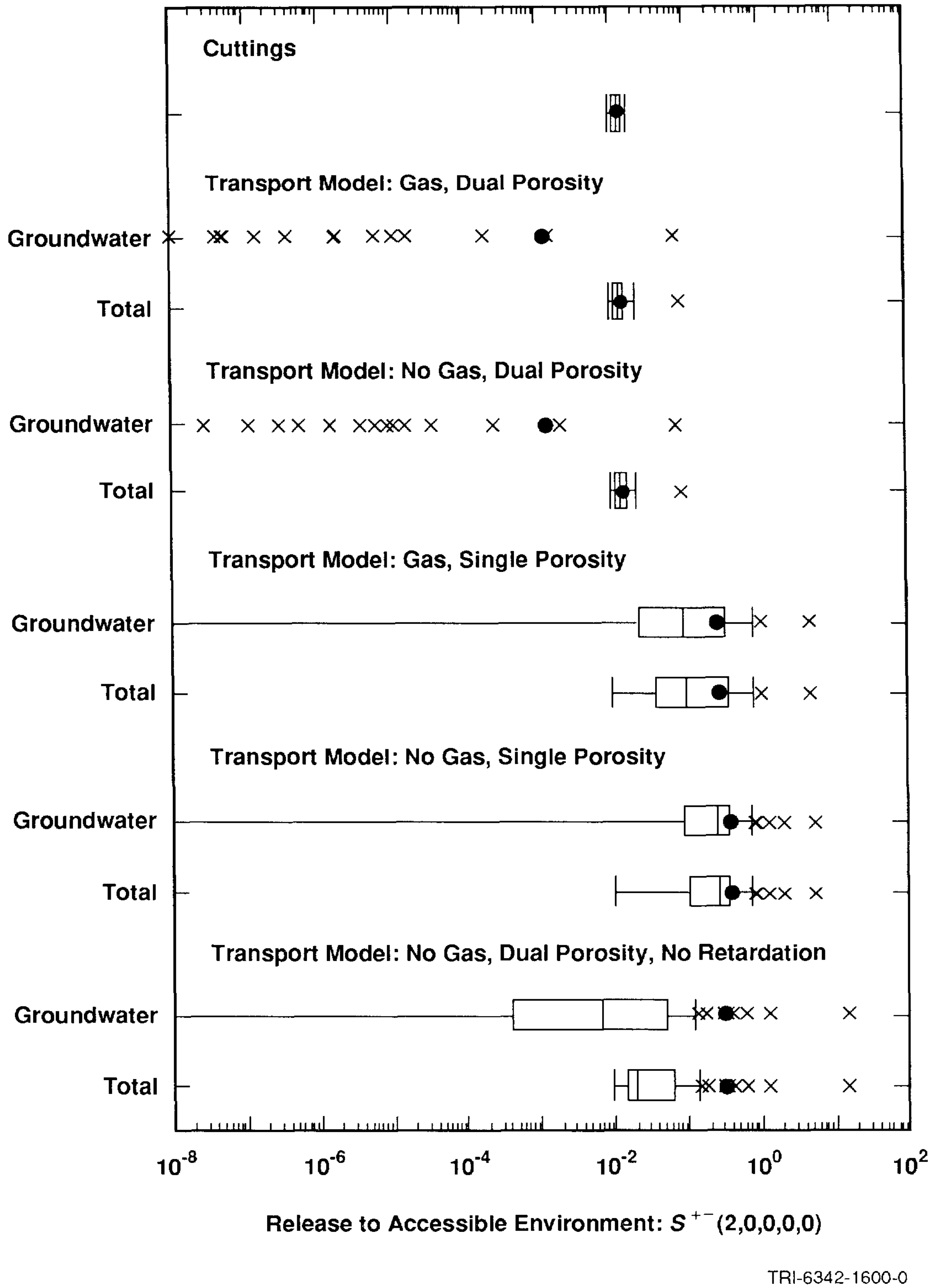

3 Figure 6-3. Summary of Normalized Releases to the Accessible Environment for E1E2-type Scenarios
4 with Intrusion Occurring at 1000 Yrs (i.e., for scenario $S^{+-}(2,0,0,0,0)$).

E2- and E1E2-type scenarios, respectively, for intrusions occurring at 1000 yrs (i.e., for scenarios $S(1,0,0,0,0)$ and $S^{+-}(2,0,0,0,0)$ in the more explicit notation used in the body of the report). As examination of these figures shows, dual-porosity transport in conjunction with chemical retardation results in releases to the accessible environment that are completely dominated by cuttings removal. Even when dual-porosity transport in conjunction with no chemical retardation is assumed, the median release due to cuttings removal is larger than the median release due to groundwater transport. In contrast, the releases to the accessible environment for single-porosity transport are often larger than the corresponding releases due to cuttings removal.

Mean CCDFs for releases to the accessible environment due to groundwater transport are shown in Figure 6-4 for the various alternative conceptual models considered in the 1991 WIPP performance assessment. For several of the alternative conceptual models, calculations were performed only for intrusions occurring at 1000 yrs. As a result, the CCDFs in Figure 6-4 were constructed with the assumption that the rate constant in the Poisson model for drilling intrusions (i.e., LAMBDA) is equal to zero after 2000 yrs. This assumption is consistent with recommendations made in an expert review of future human intrusions at the WIPP (Hora et al., 1991). As examination of Figure 6-4 shows, all of the alternative conceptual models result in mean CCDFs for release to the accessible environment that are below the EPA release limits, although there is considerable variation in the location of the individual CCDFs.

The final variant on the best-estimate analysis for the 1991 WIPP performance assessment was the consideration of two extremes of climatic variation, with one extreme resulting in boundary heads in the Culebra remaining constant at present-day values (e.g., 880 m) and the other extreme resulting in time-dependent fluctuations in heads along a recharge strip at the northern boundary of the model domain that ranged from present-day values to a maximum value corresponding to the surrounding land surface (e.g., 1030 m). As shown in Figures 6-5 and 6-6, these variations were found to have limited effect on the releases to the accessible environment due to groundwater transport with either a dual-porosity or a single-porosity transport model in the Culebra. However, additional investigations of the effects of uncertainty and variability in future climatic conditions will be performed as alternative conceptual models for regional groundwater recharge and flow are examined (e.g., Beauheim and Holt, 1990). Although climatic fluctuations have little impact on releases calculated using the current conceptual model for recharge, results presented in this report should not be extrapolated to other models for the location and amount of recharge to the Culebra.

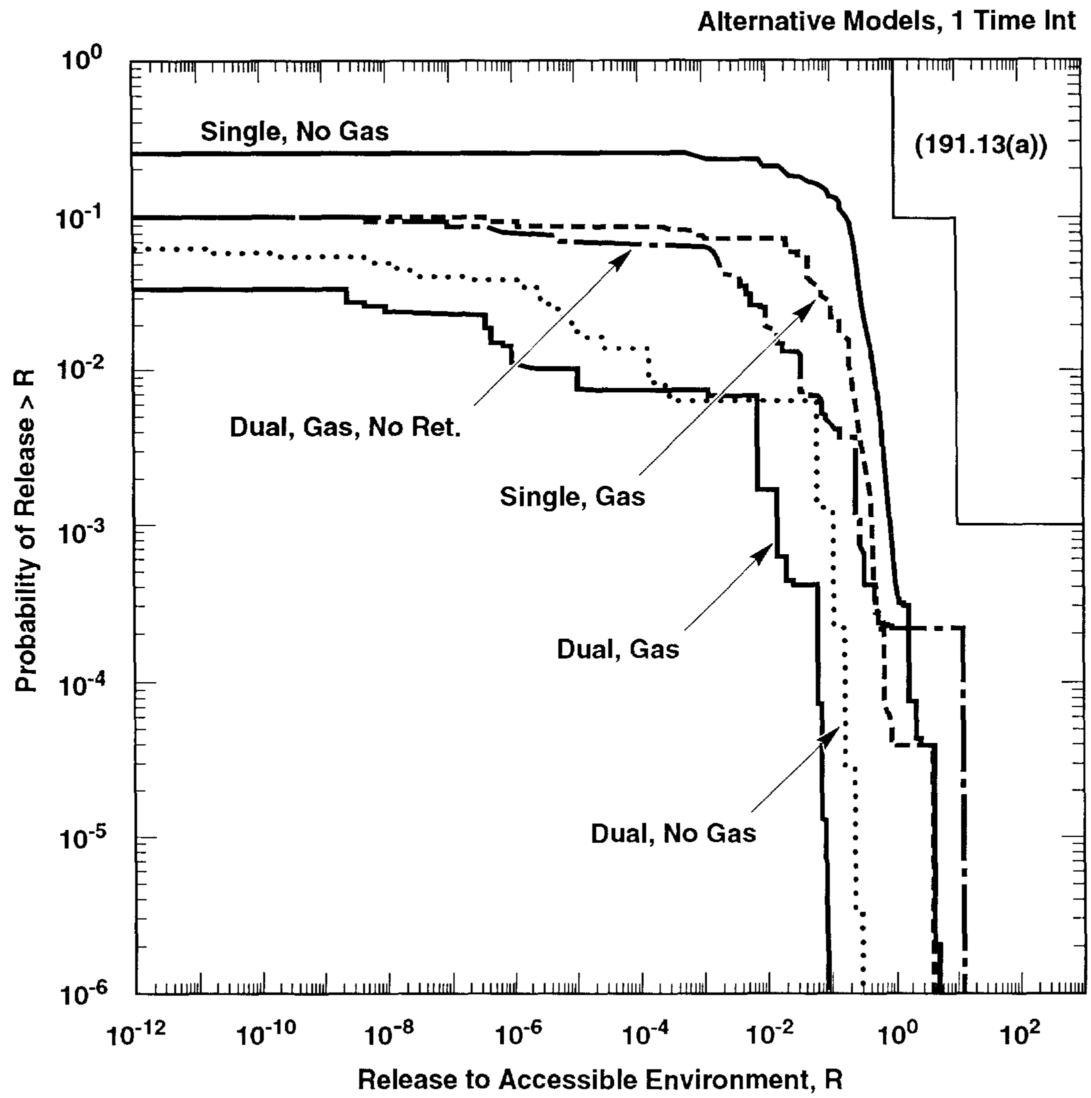

TRI-6342-1690-0

Figure 6-4. Mean Complementary Cumulative Distribution Functions for Normalized Releases to the Accessible Environment Due to Groundwater Transport Obtained with Alternative Conceptual Models and the Rate Constant λ in the Poisson Model for Drilling Intrusions Set to Zero After 2000 Yrs. The distributions of CCDFs on which the mean CCDFs in this figure are based appear in Figures 5.1-4, 5.3-3 and 5.4-4.

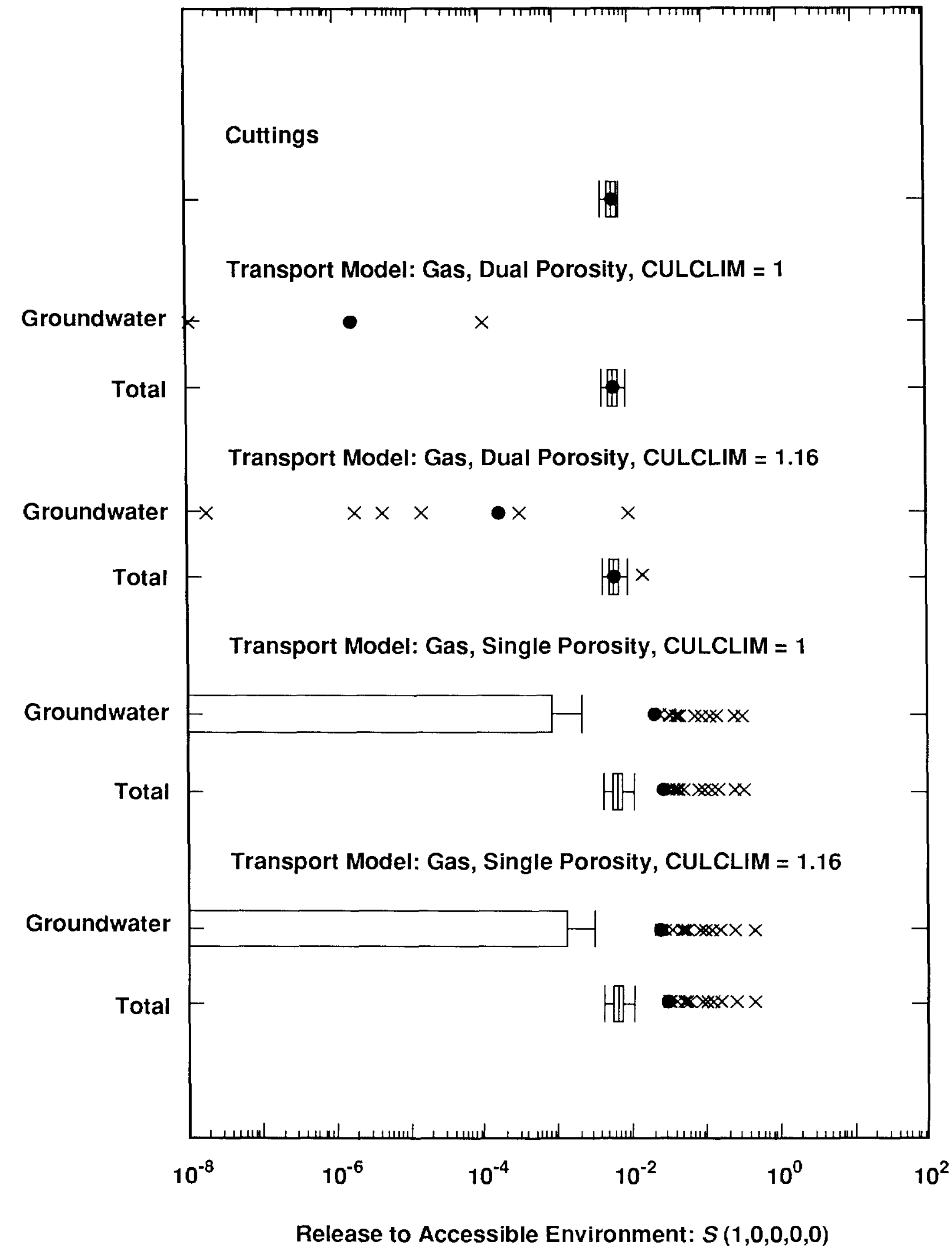

Figure 6-5. Summary of Normalized Releases to the Accessible Environment for Present-Day Recharge (CULCLIM = 1) and Maximum Recharge (CULCLIM = 1.16) of the Culebra Dolomite for E2-type Scenarios with Intrusion Occurring at 1000 Yrs (i.e., for scenario *S*(1,0,0,0,0)).

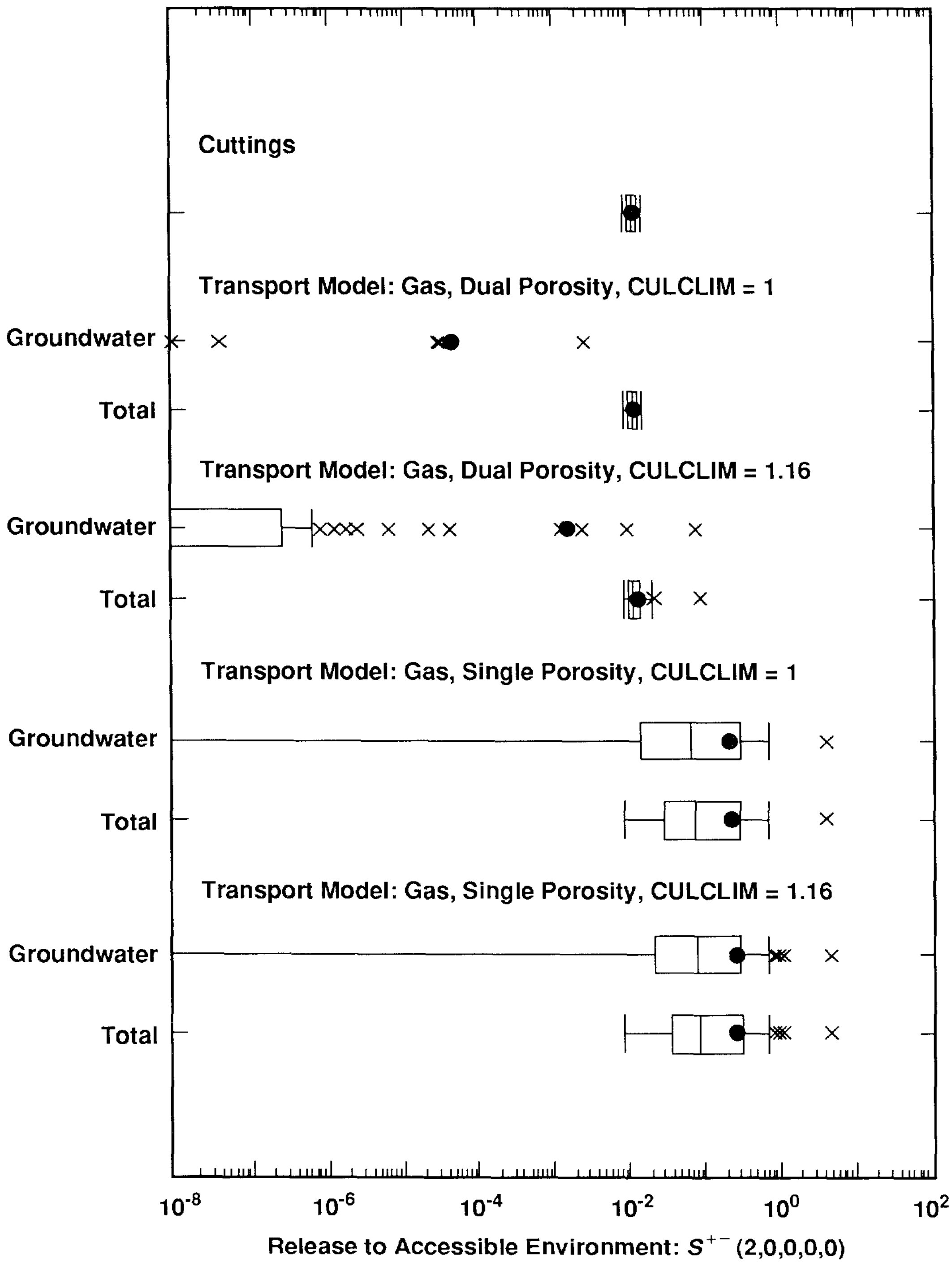

Figure 6-6. Summary of Normalized Releases to the Accessible Environment for Present-Day Recharge (CULCLIM = 1) and Maximum Recharge (CULCLIM = 1.16) of the Culebra Dolomite for E1E2-type Scenarios with Intrusion Occurring at 1000 Yrs (i.e., for scenario S^{+-}(2,0,0,0,0)).

A summary of the relative importance of the 45 imprecisely known variables considered in the 1991 WIPP performance assessment (i.e., the variables listed in Table 3-1) is presented in Table 6-1. As previously discussed, the importance of individual variables is conditional on both the conceptual model in use and the assessed uncertainty in the other variables under consideration. The summary in Table 6-1 is based on results obtained in the analyses for the alternative conceptual models, with special emphasis being placed on the results obtained in the best-estimate analysis (i.e., gas generation in the repository and a dual-porosity transport model in the Culebra). Although this report contains many formal sensitivity analyses, the summary results presented in Table 6-1 are not taken directly from specific analyses but rather are based on an overall impression of the results obtained in many individual sensitivity analyses. Alterations in the ordering of variable importance given in Table 6-1 are possible as variables are added or deleted from consideration, the assessed uncertainty in individual variables is changed, and the conceptual model in use is refined. Further, the selection of a specific conceptual model and its associated numerical implementation for use in the WIPP performance assessment could alter the relative importance of individual variables indicated in Table 6-1. To date the uncertainty associated with plausible alternative conceptual models has not been incorporated into a representation for the overall uncertainty in WIPP performance-assessment results.

Annual performance assessments, including uncertainty and sensitivity analysis, are performed for the WIPP to provide perspective on compliance with the EPA regulations and guidance for additional research to support a final decision on the acceptability or unacceptability of the WIPP as a disposal facility for transuranic waste. The following insights have emerged from these analyses and are providing guidance to current research efforts:

(1) The rate constant in the Poisson model for drilling intrusions (LAMBDA) is a, if not the, dominant determinant of the CCDFs used for comparison with the EPA release limits. An expert review process is being used to develop a better understanding of this important parameter (Hora et al., 1991; Vol. 1, Section 4.3).

(2) Given that a drilling intrusion has occurred, the interplay between Salado permeability and gas generation is an important determinant of both whether or not a release to the Culebra occurs and the size of such a release should it occur. Research programs are underway to study both Salado permeability (Saulnier, 1988 and 1991; Wawersik and Beauheim, 1991) and gas generation in the repository (Brush, 1990).

TABLE 6-1. SUMMARY OF VARIABLE IMPORTANCE IN THE 1991 WIPP PERFORMANCE ASSESSMENT. The summary presented in this table is based on results obtained in the sensitivity analyses associated with the alternative conceptual models, with special emphasis being placed on results obtained in the best-estimate analysis (i.e., gas generation in the repository and a dual-porosity transport model in the Culebra Dolomite), and is conditional on these conceptual models, the numerical implementation of these conceptual models in the WIPP performance assessment, the assessed subjective uncertainty in the 45 variables listed in Table 3-1 and the fixed values used for other variables required in the performance assessment.

IMPORTANT
Borehole permeability (BHPERM)
Culebra fracture porosity (CULFRPOR)
Culebra fracture spacing (CULFRSP)
Drill bit diameter (DBDIAM)
Fracture distribution coefficients (FKDAM, FKDNP, FDKPU, FDKTH, FKDU, with plutonium, americium and uranium being the most important elements)
Matrix distribution coefficients for individual elements (MKDAM, MKDNP, MKDPU, MKDTH, MKDU)
Rate constant in Poisson model for drilling intrusions (LAMBDA)
Salado permeability (SALPERM)
Solubilities for individual elements (SOLAM, SOLNP4, SOLNP5, SOLPU4, SOLPU5, SOLTH, SOLU4, SOLU6)
SMALL EFFECTS OBSERVED
Brine pocket pressure (BPPRES)
Brine pocket storativity (BPSTOR)
Culebra dispersivity (CULDISP)
Culebra porosity (CULPOR)
Culebra transmissivity field (CULTRFLD)
Gas Generation rate for corrosion of steel under inundated conditions (GRCORI). The individual variables related to gas generation (GRCORH, GRCORI, GRMICH, GRMICI, STOICCOR, STOICMIC, VMETAL, VWOOD) had limited identifiable impacts on analysis results. However, the presence or absence of gas generation had an important effect on radionuclide release to the Culebra and on the effect that Salado permeability has on this release.

TABLE 6-1. SUMMARY OF VARIABLE IMPORTANCE IN THE 1991 WIPP PERFORMANCE ASSESSMENT. The summary presented in this table is based on results obtained in the sensitivity analyses associated with the alternative conceptual models, with special emphasis being placed on results obtained in the best-estimate analysis (i.e., gas generation in the repository and a dual-porosity transport model in the Culebra Dolomite), and is conditional on these conceptual models, the numerical implementation of these conceptual models in the WIPP performance assessment, the assessed subjective uncertainty in the 45 variables listed in Table 3-1 and the fixed values used for other variables required in the performance assessment. (concluded)

SMALL EFFECTS OBSERVED (continued)
Index variable used to select relative areas of the stability regimes for different oxidation states of neptunium, plutonium and uranium (EHPH)
Marker Bed 139 permeability (MBPERM, 0.8 rank correlation with Salado permeability)
Recharge amplitude factor for Culebra (CULCLIM)
Salado pressure (SALPRES)
LIMITED OR NO EFFECTS OBSERVED
Fraction of total waste volume that is occupied by IDB (Integrated Data Base) metals and glass waste category (VMETAL)
Fraction of total waste volume that is occupied by IDB combustible waste category (VWOOD)
Fraction of waste panel area underlain by a pressurized brine pocket (BPAREAFR, effect overwhelmed by uncertainty in rate constant in Poisson model for drilling intrusions)
Gas generation rate due to microbial degradation of cellulosics under humid conditions (GRMICH)
Gas generation rate due to microbial degradation of cellulosics under inundated conditions (GRMICI)
Gas generation rate for corrosion of steel under humid conditions (GRCORH)
Initial fluid (brine) saturation of waste (BRSAT)
Marker Bed 139 porosity (MBPOR)
Stoichiometric coefficient for corrosion of steel (STOICCOR)
Stoichiometric coefficient for microbial degradation of cellulosics (STOICMIC)
Threshold displacement pressure in Marker Bed 139 (MBTHPRES)

(3) Elemental solubilities are important determinants of the amounts of radionuclides that can be transported from the repository to the Culebra by brine flowing up an intruding borehole. An experimental program is underway to determine the chemical conditions that could exist in the repository (Brush, 1990) and the solubilities that would exist under such conditions (Brush, 1990; Phillips and Molecke, in review).

(4) Distribution coefficients are important determinants of radionuclide transport in the Culebra. Laboratory experiments with cores removed from the Culebra Dolomite are currently underway to provide estimates of both physical and chemical retardation (Gelbard and Novak, 1992).

(5) The use of a single- or dual-porosity transport model has significant impact on predicted radionuclide transport in the Culebra. Existing information, INTRAVAL evaluations and additional experiments are being utilized to assess the appropriateness of these two models.

(6) In the absence of chemical retardation, the flow patterns in the Culebra can have a significant impact on radionuclide transport to the accessible environment. An extensive effort is underway to estimate the range of transmissivity fields for the Culebra that is consistent with available field data (Vol. 2, Section 6.2).

The following possibilities for additional investigation also arise from the uncertainty and sensitivity analyses performed in support of the 1991 WIPP performance assessment, although they are not being pursued at present:

(1) Cuttings removal is important in the 1991 WIPP performance assessment. The releases associated with drilling intrusions may be increased by processes involving spalling into the borehole. Due to the indicated importance of cuttings removal, processes that could affect these releases need to be considered.

(2) The variable BHPERM (borehole permeability) has a significant impact on the amount of brine that can flow up an intruding borehole and hence on resultant radionuclide releases to the Culebra. Additional investigation of this variable may be appropriate, although difficult due to the dependence of BHPERM on future drilling practices.

(3) The possible existence of pressurized brine pockets in the Castile Formation below the WIPP leads to the scenarios in the current

WIPP performance assessment with the largest releases to the accessible environment. Realistic representation of the extent to which such pockets exist beneath the repository would improve WIPP performance-assessment results.

Now that the 1991 WIPP performance assessment, together with associated uncertainty and sensitivity analyses, has been completed, the following possible improvements to the 1992 performance assessment can be identified:

(1) Use of more resolution in the time at which drilling intrusions occur; in particular, consideration of drilling intrusions at times earlier than 1000 yrs to better incorporate the effects of radioactive decay.

(2) Use of more activity levels in the waste for cuttings removal, possibly in conjunction with a refined activity distribution that takes into account random mixing of waste in the loading of the repository.

(3) Use of separate calculations to determine releases into the Culebra for single boreholes that penetrate pressurized brine pockets (i.e., E1-type scenarios) and single boreholes that do not penetrate pressurized brine pockets (i.e., E2-type scenarios). In the 1991 WIPP performance assessment, these releases were assumed to be the same but this may not be the case in the presence of gas generation in the repository.

(4) Evaluation of direct releases to the surface environment due to brine flow for scenarios that involve penetration of a pressurized brine pocket.

(5) Improved estimation of probabilities for E1E2-type scenarios. At present, these scenarios involve a very specific combination of plug failures in boreholes that is not taken into account in the calculation of their probabilities.

REFERENCES

Beauheim, R. L., and R. M. Holt, 1990. "Hydrogeology of the WIPP Site," in *Geological and Hydrological Studies of Evaporites in the Northern Delaware Basin for the Waste Isolation Pilot Plant (WIPP), New Mexico. Geological Society of America 1990 Annual Meeting Field Trip #14 Guidebook.* Dallas, TX: The Dallas Geological Society. 131-180.

Bertram-Howery, S. G., M. G. Marietta, R. P. Rechard, P. N. Swift, D. R. Anderson, B. L. Baker, J. E. Bean, Jr., W. Beyeler, K. F. Brinster, R. V. Guzowski, J. C. Helton, R. D. McCurley, D. K. Rudeen, J. D. Schreiber, and P. Vaughn. 1990. *Preliminary Comparison with 40 CFR Part 191, Subpart B for the Waste Isolation Pilot Plant, December 1990.* SAND90-2347. Albuquerque, NM: Sandia National Laboratories.

Brush, L. H., 1990. *Test Plan for Laboratory and Modeling Studies of Repository and Radionuclide Chemistry for the Waste Isolation Pilot Plant.* SAND90-0266. Albuquerque, NM: Sandia National Laboratories.

Cranwell, R. M., R. V. Guzowski, J. E. Campbell, and N. R. Ortiz. 1990. *Risk Methodology for Geologic Disposal of Radioactive Waste: Scenario Selection Procedure.* NUREG/CR-1667, SAND80-1429. Albuquerque, NM: Sandia National Laboratories.

Freeze, R. A., and J. A. Cherry. 1979. *Groundwater.* New Jersey: Prentice-Hall, Inc.

Gelbard, F., and C. F. Novak. 1992. "Program Plan to Determine Radionuclide Retardation for the WIPP Site." Copy on file at Waste Management Transportation Library. Albuquerque, NM: Sandia National Laboratories.

Helton, J. C., J. W. Garner, R. D. McCurley, and D. K. Rudeen. 1991. *Sensitivity Analysis Techniques and Results for Performance Assessment at the Waste Isolation Pilot Plant.* SAND90-7103. Albuquerque, NM: Sandia National Laboratories.

Hora, S. C., D. von Winterfeldt, and K. M. Trauth. 1991. *Expert Judgement on Inadvertent Human Intrusion into the Waste Isolation Pilot Plant.* SAND90-3063. Albuquerque, NM: Sandia National Laboratories.

Huyakorn, P. S., H. O. White, Jr., and S. Panday. 1989. *STAFF2D Solute Transport and Fracture Flow in Two Dimensions.* Herndon, VA: Hydrogeologic, Inc.

IAEA (International Atomic Energy Agency). 1989. *Evaluating the Reliability of Predictions Made Using Environmental Transfer Models.* Safety Series Report No. 100. Vienna: International Atomic Energy Agency.

Iman, R. L., and W. J. Conover. 1979. "The Use of the Rank Transform in Regression." *Technometrics* 21: 499-509.

Iman, R. L., and W. J. Conover. 1982. "A Distribution-Free Approach to Inducing Rank Correlation Among Input Variables." *Communications in Statistics,* vol. B11, no. 3: 311-334.

Iman, R. L., and M. J. Shortencarier. 1984. *A FORTRAN 77 Program and User's Guide for the Generation of Latin Hypercube and Random Samples for Use with Computer Models.* NUREG/CR-3624, SAND83-2365. Albuquerque, NM: Sandia National Laboratories.

Iman, R. L., J. M. Davenport, E. L. Frost, and M. J. Shortencarier. 1980. *Stepwise Regression with PRESS and Rank Regression (Program User's Guide).* SAND79-1472. Albuquerque, NM: Sandia National Laboratories.

Iman, R. L., M. J. Shortencarier, and J. D. Johnson. 1985. *A FORTRAN 77 Program and User's Guide for the Calculation of Partial Correlation and Standardized Regression Coefficients.* NUREG/CR-4122, SAND85-0044. Albuquerque, NM: Sandia National Laboratories.

Kaplan, S., and B. J. Garrick. 1981. "On the Quantitative Definition of Risk." *Risk Analysis* 1: 11-27.

Kelly, V. A., and G. J. Saulnier, Jr. 1990. *Core Analysis From the Culebra Dolomite at the Waste Isolation Pilot Plant.* SAND90-7011. Albuquerque, NM: Sandia National Laboratories.

Lappin, A. R., R. L. Hunter, D. P. Garber, P. B. Davies, R. L. Beauheim, D. J. Borns, L. H. Brush, B. M. Butcher, T. Cauffman, M. S. Y. Chu, L. S. Gomez, R. V. Guzowski, H. J. Iuzzolino, V. Kelley, S. J. Lambert, M. G. Marietta, J. W. Mercer, E. J. Nowak, J. Pickens, R. P. Rechard, M. Reeves, K. L. Robinson, and M. D. Siegel. 1989. *Systems Analysis, Long-Term Radionuclide Transport, and Dose Assessments, Waste Isolation Pilot Plant (WIPP), Southeastern New Mexico; March 1989.* SAND89-0462. Albuquerque, NM: Sandia National Laboratories.

McKay, M. D., W. J. Conover, and R. J. Beckman. 1979. "A Comparison of Three Methods for Selecting Values of Input Variables in the Analysis of Output From a Computer Code." *Technometrics* vol. 21, no. 2: 239-245.

Parry, G. W. 1988. "On the Meaning of Probability in Probabilistic Safety Assessment." *Reliability Engineering and System Safety* 23: 309-314.

Paté-Cornell, M. E. 1986. "Probability and Uncertainty in Nuclear Safety Decisions." *Nuclear Engineering and Design* 93: 319-327.

Phillips, M. L. F., and M. A. Molecke. In review. *Technical Requirements for the CH-TRU Waste Source Term Program.* SAND91-2111. Albuquerque, NM: Sandia National Laboratories.

Popielak, R. S., R. L. Beauheim, S. R. Black, W. E. Coons, C. T. Ellingson, and R. L. Olson. 1983. *Brine Reservoirs in the Castile Fm., Waste Isolation Pilot Plant (WIPP) Project, Southeastern New Mexico.* TME-3153. Carlsbad, NM: U.S. Department of Energy.

Reeves, M., V. A. Kelley, and J. S. Pickens. 1987. *Regional Double-Porosity Solute Transport in the Culebra Dolomite: An Analysis of Parameter Sensitivity and Importance at the Waste Isolation Pilot Plant (WIPP) Site.* SAND87-7105. Albuquerque, NM: Sandia National Laboratories.

Saulnier, G. J., Jr. 1988. *Field Operations Plan for Permeability Testing in the WIPP Underground Facility*. Albuquerque, NM: Sandia National Laboratories.

Saulnier, G. J., Jr. 1991. *Field Operations Plan for Permeability Testing in the WIPP Underground Facility, Addendum I*. Albuquerque, NM: Sandia National Laboratories.

Swift, P. N. In press. "Long-Term Climate Variability at the Waste Isolation Pilot Plant, Southeastern New Mexico," to appear in *Environmental Management.*

Trauth, K. M., R. P. Rechard, and S. C. Hora. 1991. "Expert Judgment as Input to Waste Isolation Pilot Plant Performance Assessment Calculations: Probability Distributions of Significant System Parameters" in *Mixed Waste: Proceedings of the First International Symposium, August 26-29, Baltimore, Maryland*. Eds. A. A. Moghissi and G. A. Benda. American Society of Mechanical Engineers, U.S. Department of Energy, U.S. Environmental Protection Agency, and the University of Maryland

U.S. DOE (Department of Energy) and State of New Mexico. 1981, as modified. "Agreement for Consultation and Cooperation" on WIPP by the State of New Mexico and U.S. Department of Energy, modified 11/30/84 and 8/4/87.

U.S. EPA (Environmental Protection Agency). 1985. *Environmental Standards for the Management and Disposal of Spent Nuclear Fuel, High-Level and Transuranic Radioactive Waste; Final Rule,* 40 CFR Part 191, *Federal Register* **50**: 38066-38089.

Vesely, W. E. and D. M. Rasmusen. 1984. "Uncertainties in Nuclear Probabilistic Risk Analyses." *Risk Analysis* 4: 313-322.

Wawersik, W. R., and R. L. Beauheim. 1991. *Test Plan--Hydraulic Fracturing and Hydrologic Tests in Marker Beds 139 and 140*. Albuquerque, NM: Sandia National Laboratories.

Distribution

FEDERAL AGENCIES

U. S. Department of Energy (2)
Office of Environmental Restoration
and Waste Management
Attn: L. P. Duffy, EM-1
C. Frank, EM-50
Washington, DC 20585

U.S. Department of Energy (3)
Office of Environmental Restoration
and Waste Management
Attn: M. Frei, EM-34 (Trevion II)
Washington, DC 20585-0002

U.S. Department of Energy
Office of Environmental Restoration
and Waste Management
Attn: J. Lytle, EM-30 (Trevion II)
Washington, DC 20585-0002

U.S. Department of Energy
Office of Environmental Restoration
and Waste Management
Attn: S. Schneider, EM-342
(Trevion II)
Washington, DC 20585-0002

U.S. Department of Energy (3)
WIPP Task Force
Attn: G. H. Daly
S. Fucigna
J. Rhoderick
12800 Middlebrook Rd.
Suite 400
Germantown, MD 20874

U.S. Department of Energy (4)
Office of Environment, Safety and
Health
Attn: R. P. Berube, EH-20
C. Borgstrum, EH-25
R. Pelletier, EH-231
K. Taimi, EH-232
Washington, DC 20585

U. S. Department of Energy (4)
WIPP Project Integration Office
Attn: W. J. Arthur III
L. W. Gage
P. J. Higgins
D. A. Olona
P.O. Box 5400
Albuquerque, NM 87115-5400

U. S. Department of Energy (11)
WIPP Project Site Office (Carlsbad)
Attn: A. Hunt (4)
V. Daub (4)
J. Lippis
K. Hunter
R. Becker
P.O. Box 3090
Carlsbad, NM 88221-3090

U. S. Department of Energy, (5)
Office of Civilian Radioactive Waste
Management
Attn: Deputy Director, RW-2
Associate Director, RW-10
Office of Program
Administration and
Resources Management
Associate Director, RW-20
Office of Facilities
Siting and
Development
Associate Director, RW-30
Office of Systems
Integration and
Regulations
Associate Director, RW-40
Office of External
Relations and Policy
Office of Geologic Repositories
Forrestal Building
Washington, DC 20585

U. S. Department of Energy
Attn: National Atomic Museum Library
Albuquerque Operations Office
P.O. Box 5400
Albuquerque, NM 87185

U. S. Department of Energy
Research & Waste Management Division
Attn: Director
P.O. Box E
Oak Ridge, TN 37831

U. S. Department of Energy (2)
Idaho Operations Office
Fuel Processing and Waste
Management Division
785 DOE Place
Idaho Falls, ID 83402

U.S. Department of Energy
Savannah River Operations Office
Defense Waste Processing
Facility Project Office
Attn: W. D. Pearson
P.O. Box A
Aiken, SC 29802

U.S. Department of Energy (2)
Richland Operations Office
Nuclear Fuel Cycle & Production
Division
Attn: R. E. Gerton
825 Jadwin Ave.
P.O. Box 500
Richland, WA 99352

U.S. Department of Energy (3)
Nevada Operations Office
Attn: J. R. Boland
D. Livingston
P. K. Fitzsimmons
2753 S. Highland Drive
Las Vegas, NV 87183-8518

U.S. Department of Energy (2)
Technical Information Center
P.O. Box 62
Oak Ridge, TN 37831

U.S. Department of Energy (2)
Chicago Operations Office
Attn: J. C. Haugen
9800 South Cass Avenue
Argonne, IL 60439

U.S. Department of Energy
Los Alamos Area Office
528 35th Street
Los Alamos, NM 87544

U.S. Department of Energy (3)
Rocky Flats Area Office
Attn: W. C. Rask
G. Huffman
T. Lukow
P.O. Box 928
Golden, CO 80402-0928

U.S. Department of Energy
Dayton Area Office
Attn: R. Grandfield
P.O. Box 66
Miamisburg, OH 45343-0066

U.S. Department of Energy
Attn: E. Young
Room E-178
GAO/RCED/GTN
Washington, DC 20545

U.S. Bureau of Land Management
101 E. Mermod
Carlsbad, NM 88220

U.S. Bureau of Land Management
New Mexico State Office
P.O. Box 1449
Santa Fe, NM 87507

U.S. Environmental Protection
Agency (2)
Office of Radiation Protection
Programs (ANR-460)
Attn: Richard Guimond (2)
Washington, D.C. 20460

U.S. Nuclear Regulatory Commission
Division of Waste Management
Attn: H. Marson
Mail Stop 4-H-3
Washington, DC 20555

U.S. Nuclear Regulatory Commission
(4)
Advisory Committee on Nuclear Waste
Attn: Dade Moeller
Martin J. Steindler
Paul W. Pomeroy
William J. Hinze
7920 Norfolk Avenue
Bethesda, MD 20814

U.S. Nuclear Regulatory Commission (2)
Attn: C. Lui
J. Glynn
Mail Stop NLS-372
Washington, DC 20555

U.S. Nuclear Regulatory Commission
Attn: A. Buslik
Mail Stop NLS-377
Washington, DC 20555

Defense Nuclear Facilities Safety Board
Attn: Dermot Winters
625 Indiana Avenue NW
Suite 700
Washington, DC 20004

Nuclear Waste Technical Review Board (2)
Attn: Dr. Don A. Deere
Dr. Sidney J. S. Parry
Suite 910
1100 Wilson Blvd.
Arlington, VA 22209-2297

Katherine Yuracko
Energy and Science Division
Office of Management and Budget
725 17th Street NW
Washington, DC 20503

U.S. Geological Survey (2)
Water Resources Division
Attn: Cathy Peters
Suite 200
4501 Indian School, NE
Albuquerque, NM 87110

STATE AGENCIES

Environmental Evaluation Group (5)
Attn: Robert Neill
Suite F-2
7007 Wyoming Blvd., N.E.
Albuquerque, NM 87109

New Mexico Bureau of Mines and Mineral Resources
Socorro, NM 87801

New Mexico Energy, Minerals and Natural Resources Department
Attn: Librarian
2040 South Pacheco
Santa Fe, NM 87505

New Mexico Energy, Minerals and Natural Resources Department
New Mexico Radioactive Task Force (2)
(Governor's WIPP Task Force)
Attn: Anita Lockwood, Chairman
Chris Wentz, Coordinator/Policy Analyst
2040 South Pacheco
Santa Fe, NM 87505

Bob Forrest
Mayor, City of Carlsbad
P.O. Box 1569
Carlsbad, NM 88221

Chuck Bernard
Executive Director
Carlsbad Department of Development
P.O. Box 1090
Carlsbad, NM 88221

New Mexico Environment Department
Secretary of the Environment
Attn: J. Espinosa (3)
P.O. Box 968
1190 St. Francis Drive
Santa Fe, NM 87503-0968

New Mexico Environment Department
Attn: Pat McCausland
WIPP Project Site Office
P.O. Box 3090
Carlsbad, NM 88221-3090

New Mexico State Engineer's Office
Attn: Dr. Mustafa Chudnoff
P.O. Box 25102
Santa Fe, NM 87504-5102

ADVISORY COMMITTEE ON NUCLEAR FACILITY SAFETY

John F. Ahearne
Executive Director, Sigma Xi
99 Alexander Drive
Research Triangle Park, NC 27709

James E. Martin
109 Observatory Road
Ann Arbor, MI 48109

Dr. Gerald Tape
Assoc. Universities
1717 Massachusetts Ave. NW
Suite 603
Washington, DC 20036

WIPP PANEL OF NATIONAL RESEARCH COUNCIL'S BOARD ON RADIOACTIVE WASTE MANAGEMENT

Charles Fairhurst, Chairman
Department of Civil and
Mineral Engineering
University of Minnesota
500 Pillsbury Dr. SE
Minneapolis, MN 55455-0220

John O. Blomeke
3833 Sandy Shore Drive
Lenoir City, TN 37771-9803

John D. Bredehoeft
Western Region Hydrologist
Water Resources Division
U.S. Geological Survey (M/S 439)
345 Middlefield Road
Menlo Park, CA 94025

Fred M. Ernsberger
1325 NW 10th Avenue
Gainsville, FL 32601

Rodney C. Ewing
Department of Geology
University of New Mexico
200 Yale, NE
Albuquerque, NM 87131

B. John Garrick
4590 MacArthur Blvd., #400
Newport Beach, CA 92660-2027

Leonard F. Konikow
U.S. Geological Survey
431 National Center
Reston, VA 22092

Jeremiah O'Driscoll
505 Valley Hill Drive
Atlanta, GA 30350

Christopher Whipple
Clement International Corp.
160 Spear St.
Suite 1380
San Francisco, CA 94105-1535

National Research Council (3)
Board on Radioactive
Waste Management
RM HA456
Attn: Peter B. Myers, Staff
Director (2)
Dr. Geraldine J. Grube
2101 Constitution Avenue
Washington, DC 20418

PERFORMANCE ASSESSMENT PEER REVIEW PANEL

G. Ross Heath
College of Ocean and
Fishery Sciences HN-15
583 Henderson Hall
University of Washington
Seattle, WA 98195

Thomas H. Pigford
Department of Nuclear Engineering
4159 Etcheverry Hall
University of California
Berkeley, CA 94720

Thomas A. Cotton
JK Research Associates, Inc.
4429 Butterworth Place, NW
Washington, DC 20016

Robert J. Budnitz
President, Future Resources
Associates, Inc.
2000 Center Street
Suite 418
Berkeley, CA 94704

C. John Mann
Department of Geology
245 Natural History Bldg.
1301 West Green Street
University of Illinois
Urbana, IL 61801

Frank W. Schwartz
Department of Geology and Mineralogy
The Ohio State University
Scott Hall
1090 Carmack Rd.
Columbus, OH 43210

NATIONAL LABORATORIES

Argonne National Labs (2)
Attn: A. Smith
D. Tomasko
9700 South Cass, Bldg. 201
Argonne, IL 60439

Battelle Columbus Laboratories (3)
Attn: Paul Baybutt
R. S. Denning
Steve Unwin
505 King Avenue
Columbus, OH 43201

Battelle Northwest
Attn: Pamela Doctor
P.O. Box 999
Richland, WA 99352

Battelle Pacific Northwest Laboratories (3)
Attn: R. E. Westerman
S. Bates
H. C. Burkholder
Battelle Boulevard
Richland, WA 99352

Los Alamos National Laboratory
Attn: B. Erdal, CNC-11
P.O. Box 1663
Los Alamos, NM 87544

Los Alamos National Laboratory
Attn: A. Meijer
Mail Stop J514
Los Alamos, NM 87545

Los Alamos National Laboratory (3)
HSE-8
Attn: M. Enoris
L. Soholt
J. Wenzel
P.O. Box 1663
Los Alamos, NM 87544

Los Alamos National Laboratory (2)
HSE-7
Attn: A. Drypolcher
S. Kosciewiscz
P.O. Box 1663
Los Alamos, NM 87544

Los Alamos National Laboratory (2)
Analysis and Assessment Division, A-1, MS F600
Attn: M. D. McKay
M. A. Meyer
P.O. Box 1663
Los Alamos, NM 87544

Oak Ridge National Laboratory
Computer Sciences
Attn: Darryl Downing
Building 2029, P.O. Box X
Oak Ridge, TN 37830

Oak Ridge National Laboratory (3)
Engineering Physics and Mathematics Division
Attn: E. M. Oblow
Francois G. Pin
Brian A. Worley
P.O. Box X
Oak Ridge, TN 37830

Oak Ridge National Laboratory (2)
Environmental Sciences Division
Attn: Steve Bartell
R. H. Gardner
P.O. Box X
Oak Ridge, TN 37830

Oak Ridge National Laboratory (2)
Health and Safety Research Division
Attn: David G. Kocher
F. O. Hoffman
P.O. Box X
Oak Ridge, TN 37830

Oak Ridge National Laboratory
Martin Marietta Systems, Inc.
Attn: J. Setaro
P.O. Box 2008, Bldg. 3047
Oak Ridge, TN 37831-6019

Savannah River Laboratory (3)
Attn: N. Bibler
M. J. Plodinec
G. G. Wicks
Aiken, SC 29801

Savannah River Plant (2)
Attn: Richard G. Baxter
Building 704-S
K. W. Wierzbicki
Building 703-H
Aiken, SC 29808-0001

CORPORATIONS/MEMBERS OF THE PUBLIC

Benchmark Environmental Corp. (3)
Attn: John Hart
C. Frederickson
K. Lickliter
4501 Indian School Rd., NE
Suite 105
Albuquerque, NM 87110

Deuel and Associates, Inc.
Attn: R. W. Prindle
7208 Jefferson, NE
Albuquerque, NM 87109

Disposal Safety, Inc.
Attn: Benjamin Ross
Suite 314
1660 L Street NW
Washington, DC 20006

Ecodynamics Research Associates (2)
Attn: Pat Roache
Rebecca Blaine
P.O. Box 8172
Albuquerque, NM 87198

E G & G Idaho (3)
1955 Fremont Street
Attn: C. Atwood
C. Hertzler
T. I. Clements
Idaho Falls, ID 83415

Geomatrix
Attn: Kevin Coppersmith
100 Pine Street #1000
San Francisco, CA 94111

Golden Associates, Inc. (3)
Attn: Mark Cunnane
Richard Kossik
Ian Miller
4104 148th Avenue NE
Redmond, WA 98052

In-Situ, Inc. (2)
Attn: S. C. Way
C. McKee
209 Grand Avenue
Laramie, WY 82070

INTERA, Inc.
Attn: A. M. LaVenue
8100 Mountain Road NE
Suite 213
Albuquerque, NM 87110

INTERA, Inc.
Attn: J. F. Pickens
Suite #300
6850 Austin Center Blvd.
Austin, TX 78731

INTERA, Inc.
Attn: Wayne Stensrud
P.O. Box 2123
Carlsbad, NM 88221

INTERA, Inc.
Attn: William Nelson
101 Convention Center Drive
Suite 540
Las Vegas, NV 89109

IT Corporation (2)
Attn: P. Drez
J. Myers
Regional Office - Suite 700
5301 Central Avenue, NE
Albuquerque, NM 87108

MACTEC (2)
Attn: J. A. Thies
D. K. Duncan
8418 Zuni Road SE
Suite 200
Albuquerque, NM 87108

Pacific Northwest Laboratory
Attn: Bill Kennedy
Battelle Blvd.
P.O. Box 999
Richland, WA 99352

RE/SPEC, Inc. (2)
Attn: W. Coons
Suite 300
4775 Indian School NE
Albuquerque, NM 87110

RE/SPEC, Inc.
Attn: J. L. Ratigan
P.O. Box 725
Rapid City, SD 57709

Reynolds Elect/Engr. Co., Inc.
Building 790, Warehouse Row
Attn: E. W. Kendall
P.O. Box 98521
Las Vegas, NV 89193-8521

Roy F. Weston, Inc.
CRWM Tech. Supp. Team
Attn: Clifford J. Noronha
955 L'Enfant Plaza, S.W.
North Building, Eighth Floor
Washington, DC 20024

Science Applications International Corporation
Attn: Howard R. Pratt, Senior Vice President
10260 Campus Point Drive
San Diego, CA 92121

Science Applications International Corporation (2)
Attn: George Dymmel
Chris G. Pflum
101 Convention Center Dr.
Las Vegas, NV 89109

Science Applications International Corporation (2)
Attn: John Young
Dave Lester
18706 North Creek Parkway
Suite 110
Bothell, WA 98011

Science Applications International Corporation
Attn: David C. Aldrich
1710 Goodridge Drive
P.O. Box 1303
McLean, VA 22102

Science Applications International Corporation
Attn: Mark D. Otis
P.O. Box 50697
101 S. Park Ave.
Idaho Falls, ID 83405

Southwest Research Institute
Center for Nuclear Waste Regulatory Analysis (2)
Attn: P. K. Nair
6220 Culebra Road
San Antonio, Texas 78228-0510

W. K. Summers
The City of Albuquerque
Public Works Department
Utility Planning Division
P.O. Box 1293
Albuquerque, NM 87103

Systems, Science, and Software (2)
Attn: E. Peterson
P. Lagus
Box 1620
La Jolla, CA 92038

TASC
Attn: Steven G. Oston
55 Walkers Brook Drive
Reading, MA 01867

Tech. Reps., Inc. (6)
Attn: Janet Chapman
Debbie Marchand
John Stikar
Denise Bissell
Dan Scott
5000 Marble NE
Suite 222
Albuquerque, NM 87110

Tolan, Beeson, & Associates
Attn: Terry L. Tolan
2320 W. 15th Avenue
Kennewick, WA 99337

TRW Environmental Safety Systems (TESS)
Attn: Ivan Saks
10306 Eaton Place
Suite 300
Fairfax, VA 22030

Westinghouse Electric Corporation (4)
Attn: Library
L. Trego
C. Cox
L. Fitch
R. F. Kehrman
P.O. Box 2078
Carlsbad, NM 88221

Westinghouse Hanford Company
Attn: Don Wood
P.O. Box 1970
Richland, WA 99352

Western Water Consultants
Attn: D. Fritz
1949 Sugarland Drive #134
Sheridan, WY 82801-5720

Western Water Consultants
Attn: P. A. Rechard
P.O. Box 4128
Laramie, WY 82071

D. G. Cacuci
Dept. of Nuclear Engineering
University of Illinois
103 South Goodwin Avenue
Urbana, IL 61801-2984

W. J. Conover
College of Business Administration
Texas Tech University
Lubbock, TX 79409

Neville Cook
Rock Mechanics Engineering
Mine Engineering Dept.
University of California
Berkeley, CA 94720

John Evans
Harvard School of Public Health
665 Huntington Avenue
Boston, MA 02115

F. E. Haskin
Dept. of Chemical & Nuclear Engr.
University of New Mexico
Albuquerque, NM 87131

Max Henrion
Dept. of Engineering and Public Policy
Carnegie-Mellon University
Pittsburgh, PA 15213

Carl Irwin
Department of Mathematics
West Virginia University
Morgantown, WV 26505

Stan Kaplan
Pickard, Lowe and Garrick, Inc.
2260 University Drive
Newport Beach, CA 92660

Thomas B. Kirchner
Natural Resource Ecology Lab
Colorado State University
Fort Collins, CO 85023

Greg McRae
Dept. of Chemical Engineering
Carnegie-Mellon University
Pittsburgh, PA 15213

M. Granger Morgan
Dept. of Engineering and Public Policy
Carnegie-Mellon University
Pittsburgh, PA 15213

Dennis W. Powers
Star Route Box 87
Anthony, TX 79821

H. Rabitz
Department of Chemistry
Princeton University
Princeton, NJ 08544

K. H. Reckhow
School of Forestry and Environmental Studies
Duke University
Durham, NC 27706

S. K. Seaholm
University of Minnesota
Div. of Health Computer Science
Box 511 UMHC
420 Delaware St., SE
Minneapolis, MN 55455

Shirley Thieda
P.O. Box 2109, RR1
Bernalillo, NM 87004

Jack Urich
c/o CARD
144 Harvard SE
Albuquerque, NM 87106

F. Ward Whicker
Dept. of Radiology and Radiation Biology
Colorado State University
Fort Collins, CO 80523

UNIVERSITIES

University of California
Mechanical, Aerospace, and Nuclear Engineering Department (3)
Attn: W. Kastenberg
D. Browne
G. Apostolakis
5532 Boelter Hall
Los Angeles, CA 90024

University of Hawaii at Hilo
Attn: S. Hora
Business Administration
Hilo, HI 96720-4091

University of New Mexico
Geology Department
Attn: Library
Albuquerque, NM 87131

University of New Mexico
Research Administration
Attn: H. Schreyer
102 Scholes Hall
Albuquerque, NM 87131

University of Wyoming
Department of Civil Engineering
Attn: V. R. Hasfurther
Laramie, WY 82071

University of Wyoming
Department of Geology
Attn: J. I. Drever
Laramie, WY 82071

University of Wyoming
Department of Mathematics
Attn: R. E. Ewing
Laramie, WY 82071

LIBRARIES

Thomas Brannigan Library
Attn: Don Dresp, Head Librarian
106 W. Hadley St.
Las Cruces, NM 88001

Hobbs Public Library
Attn: Marcia Lewis, Librarian
509 N. Ship Street
Hobbs, NM 88248
New Mexico State Library
Attn: Norma McCallan
325 Don Gaspar
Santa Fe, NM 87503

New Mexico Tech
Martin Speere Memorial Library
Campus Street
Socorro, NM 87810

New Mexico Junior College
Pannell Library
Attn: Ruth Hill
Lovington Highway
Hobbs, NM 88240

Carlsbad Municipal Library
WIPP Public Reading Room
Attn: Lee Hubbard, Head Librarian
101 S. Halagueno St.
Carlsbad, NM 88220

University of New Mexico
General Library
Government Publications Department
Albuquerque, NM 87131

NEA/PERFORMANCE ASSESSMENT ADVISORY GROUP (PAAC)

P. Duerden
ANSTO
Lucas Heights Research Laboratories
Private Mail Bag No. 1
Menai, NSW 2234
AUSTRAILIA

Gordon S. Linsley
Division of Nuclear Fuel Cycle and Waste Management
International Atomic Energy Agency
P.O. Box 100
A-1400 Vienna
AUSTRIA

Nicolo Cadelli
Commission of the European Communities
200, Rue de la Loi
B-1049 Brussels
BELGIUM

R. Heremans
Organisme National des Déchets Radioactifs et des Matiéres Fissiles
ONDRAF
Place Madou 1, Boitec 24/25
B-1030 Brussels
BELGIUM

J. Marivoet
Centre d'Etudes de l'Energie Nucléaire
CEN/SCK
Boeretang 200
B-2400 Mol
BELGIUM

P. Conlon
Waste Management Division
Atomic Energy Control Board (AECB)
P.O. Box 1046
Ottawa, Canada KIP 559
CANADA

A. G. Wikjord
Manager, Environmental and Safety Assessment Branch
Atomic Energy of Canada Limited (AECL)
Whiteshell Nuclear Research Establishment
Pinawa, Manitoba ROE 1LO
CANADA

Jukka-Pekka Salo
Teollisuuden Voima Oy (TVO)
Fredrikinkatu 51-53 B
SF-00100 Helsinki
FINLAND

Timo Vieno
Technical Research Centre of Finland (VTT)
Nuclear Energy Laboratory
P.O. Box 208
SF-02151 Espoo
FINLAND

Timo Äikäs
Teollisuuden Voima Oy (TVO)
Fredrikinkatu 51-53 B
SF-00100 Helsinki
FINLAND

M. Claude Ringeard
Division de la Sécurité et de la
Protection de l'Environment (DSPE)
Commissariat á l'Energie Atomique
Agence Nationale pour la Gestion des
Déchets Radioactifs (ANDRA)
Route du Panorama Robert Schuman
B. P. No. 38
F-92266 Fontenay-aux-Roses Cedex
FRANCE

Gérald Ouzounian
Agence Nationale pour la Gestion des
Déchets Radioactifs (ANDRA)
Route du Panorama Robert Schuman
B. P. No. 38
F-92266 Fontenay-aux-Roses Cedex
FRANCE

Claudio Pescatore
Division of Radiation Protection and
Waste Management
OECD Nuclear Energy Agency
38, Boulevard Suchet
F-75016 Paris
FRANCE

M. Dominique Greneche
Commissariat á l'Energie Atomique
IPSN/DAS/SASICC/SAED
B. P. No. 6
F-92265 Fontenay-aux-Roses Cedex
FRANCE

Robert Fabriol
Bureau de Recherches géologiques et
miniéres (BRGM)
B. P. 6009
45060 Orléans Cedex 2
FRANCE

P. Bogorinski
Gesellschaft für Reaktorsicherheit
(GRS) mbH
Schwertnergasse 1
D-5000 Köln 1
GERMANY

R. Storck
GSF - Institut für Tieflagerung
Theodor-Heuss-Strabe 4
D-3300 Braunschweig
GERMANY

Ferrucio Gera
ISMES S.p.A
Via del Crociferi 44
I-00187 Roma
ITALY

Hideo Matsuzuru
Head, Environmental Assessment
Laboratory
Dept. of Environmental Safety
Research
Nuclear Safety Research Center
Tokai Research Establishment, JAERI
Tokai-mura, Naka-gun
Ibaraki-ken
JAPAN

Hiroyuki Umeki
Isolation System Research Program
Radioactive Waste Management Project
Power Reactor and Nuclear Fuel
Development Corporation (PNC)
1-9-13, Akasaka
Minato-ku
Tokyo 107
JAPAN

P. Carboneras Martinez
ENRESA
Calle Emilio Vargas 7
R-28043 Madrid
SPAIN

Tönis Papp
Swedish Nuclear Fuel and Waste
Management Co.
Box 5864
S 102 48 Stockholm
SWEDEN

Conny Hägg
Swedish Radiation Protection
Institute (SSI)
Box 60204
S-104 01 Stockholm
SWEDEN

J. Hadermann
Paul Scherrer Institute
Waste Management Programme
CH-5232 Villigen PSI
SWITZERLAND

J. Vigfusson
USK- Swiss Nuclear Safety
Inspectorate
Federal Office of Energy
CH-5303 Würenlingen
SWITZERLAND

D. E. Billington
Departmental Manager - Assessment
Studies
Radwaste Disposal R&D Division
AEA Decommissioning & Radwaste
Harwell Laboratory, B60
Didcot Oxfordshire OX11 ORA
UNITED KINGDOM

P. Grimwood
Waste Management Unit
BNFL
Sellafield
Seascale, Cumbria CA20 1PG
UNITED KINGDOM

Alan J. Hooper
UK Nirex Ltd
Curie Avenue
Harwell, Didcot
Oxfordshire, OX11 ORH
UNITED KINGDOM

Jerry M. Boak
Yucca Mountain Project Office
U.S. Department of Energy
P.O. Box 98608
Las Vegas, NV 89193
UNITED STATES

Seth M. Coplan (Chairman)
U.S. Nuclear Regulatory Commission
Division of High-Level Waste
Management
Mail Stop 4-H-3
Washington, DC 20555
UNITED STATES

A. E. Van Luik
Intera/M&O
The Valley Bank Center
101 Convention Center Dr.
Las Vegas, NV 89109
UNITED STATES

NEA/PSAG USER'S GROUP

Alexander Nies (PSAC Chairman)
Gesellschaft für Strahlen- und
Institut für Tieflagerung
Abteilung für Endlagersicherheit
Theodor-Heuss-Strasse 4
D-3300 Braunscheweig
GERMANY

Eduard Hofer
Gesellschaft für Reaktorsicherheit
(GRS) MBH
Forschungsgelände
D-8046 Garching
GERMANY

Takashi Sasahara
Environmental Assessment Laboratory
Department of Environmental Safety
Research
Nuclear Safety Research Center,
Tokai Research Establishment, JAERI
Tokai-mura, Naka-gun
Ibaraki-ken
JAPAN

Alejandro Alonso
Cátedra de Tecnología Nuclear
E.T.S. de Ingenieros Industriales
José Gutiérrez Abascal, 2
E-28006 Madrid
SPAIN

Pedro Prado
CIEMAT
Instituto de Tecnología Nuclear
Avenida Complutense, 22
E-28040 Madrid
SPAIN

Miguel Angel Cuñado
ENRESA
Emilio Vargas, 7
E-28043 Madrid
SPAIN

Francisco Javier Elorza
ENRESA
Emilio Vargas, 7
E-28043 Madrid
SPAIN

Nils A. Kjellbert
Swedish Nuclear Fuel and Waste
Management Company (SKB)
Box 5864
S-102 48 Stockholm
SWEDEN

Björn Cronhjort
Swedish National Board for Spent
Nuclear Fuel (SKN)
Sehlsedtsgatan 9
S-115 28 Stockholm
SWEDEN

Richard A. Klos
Paul-Scherrer Institute (PSI)
CH-5232 Villingen PSI
SWITZERLAND

NAGRA (2)
Attn: Charles McCombie
Fritz Van Dorp
Parkstrasse 23
CH-5401 Baden
SWITZERLAND

Daniel A. Galson
Intera Information Technologies
Park View House, 14B Burton Street
Melton Mowbray
Leicestershire, LEI3, 1AE
UNITED KINGDOM

Brian G. J. Thompson
Department of the Environment
Her Majesty's Inspectorate of
Pollution
Room A5.33, Romney House
43 Marsham Street
London SW1P 2PY
UNITED KINGDOM

INTERA/ECL
Attn: Trevor J. Sumerling
Chiltern House
45 Station Road
Henley-on-Thames
Oxfordshire RG9 1AT
UNITED KINGDOM

U.S. Nuclear Regulatory Commission
(2)
Attn: Richard Codell
Norm Eisenberg
Mail Stop 4-H-3
Washington, D.C. 20555

Paul W. Eslinger
Battelle Pacific Northwest
Laboratories (PNL)
P.O. Box 999, MS K2-32
Richland, WA 99352

Andrea Saltelli
Commission of the European
Communities
Joint Research Centre od Ispra
I-21020 Ispra (Varese)
ITALY

Budhi Sagar
Center for Nuclear Waste Regulatory
Analysis (CNWRA)
Southwest Research Institute
P.O. Drawer 28510
6220 Culebra Road
San Antonio, TX 78284

Shaheed Hossain
Division of Nuclear Fuel Cycle and
Waste Management
International Atomic Energy Agency
Wagramerstrasse 5
P.O. Box 100
A-1400 Vienna
AUSTRIA

Claudio Pescatore
Division of Radiation Protection and
Waste Management
38, Boulevard Suchet
F-75016 Paris
FRANCE

GEOSTATISTICS EXPERT WORKING GROUP (GXG)

Rafael L. Bras
R.L. Bras Consulting Engineers
44 Percy Road
Lexington, MA 02173

Jesus Carrera
Universidad Politecnica de Cataluña
E.T.S.I. Caminos
Jordi, Girona 31
E-08034 Barcelona
SPAIN

Gedeon Dagan
Department of Fluid Mechanics and
Heat Transfer
Tel Aviv University
P.O. Box 39040
Ramat Aviv, Tel Aviv 69978
ISRAEL

Ghislain de Marsily (GXG Chairman)
University Pierre et Marie Curie
Laboratorie de Geologie Applique
4, Place Jussieu - T.26 - 5^{e} etage
75252 Paris Cedex 05
FRANCE

Alain Galli
Centre de Geostatistique
Ecole des Mines de Paris
35 rue St. Honore
77035 Fontainebleau
FRANCE

Steve Gorelick
Department of Applied Earth Sciences
Stanford University
Stanford, CA 94305-2225

Peter Grindrod
Intera Information Technologies Ltd.
Chiltern House, 45 Station Road
Henley-on-Thames
Oxfordshire, RG9 1AT
UNITED KINGDOM

Alan Gutjahr
Department of Mathematics
New Mexico Institute of Mining and
Technology
Socorro, NM 87801

C. Peter Jackson
Harwell Laboratory
Theoretical Studies Department
Radwaste Disposal Division
Bldg. 424.4
Oxfordshire Didcot Oxon OX11 ORA
UNITED KINDGOM

Peter Kitanidis
60 Peter Coutts Circle
Stanford, CA 94305

Ray Mackay
Department of Civil Engineering
University of Newcastle Upon Tyne
Newcastle Upon Tyne NE1 7RU
UNITED KINGDOM

Dennis McLaughlin
Parsons Laboratory
Room 48-209
Department of Civil Engineering
Massachusetts Institute of Technology
Cambridge, MA 02139

Shlomo P. Neuman
College of Engineering and Mines
Department of Hydrology and Water
Resources
University of Arizona
Tucson, AZ 85721

Christian Ravenne
Geology and Geochemistry Division
Institut Francais du Pétrole
1 & 4, av. de Bois-Préau BP311
92506 Rueil Malmaison Cedex
FRANCE

Yorim Rubin
Department of Civil Engineering
University of California, Berkeley
Berkeley, CA 94720

FOREIGN ADDRESSES

Radiation Protection Program CEC
Attn: G. Neale Kelly
Rue de la Loi, 200
B-1049 Bruxelles
BELGIUM

Radiation Protection Program CEC
Attn: Jaak Sinnaeve
Rue de la Loi, 200
B-1049 Bruxelles
BELGIUM

Studiecentrum Voor Kernenergie
Centre D'Energie Nucleaire
Attn: A. Bonne
SCK/CEN
Boeretang 200
B-2400 Mol
BELGIUM

Atomic Energy of Canada, Ltd. (3)
Whiteshell Research Estab.
Attn: Michael E. Stevens
Bruce W. Goodwin
Donna Wushke
Pinewa, Manitoba
ROE 1LO
CANADA

National Water Research Institute
Attn: E. Halfon
Canada Centre for Inland Waters
Burlington, Ontario
CANADA

Esko Peltonen
Industrial Power Company Ltd.
TVO
Fredrikinkatu 51-53
SF-00100 Helsinki 10
FINLAND

Jean-Pierre Olivier
OECD Nuclear Energy Agency (2)
38, Boulevard Suchet
F-75016 Paris
FRANCE

D. Alexandre, Deputy Director
ANDRA
31 Rue de la Federation
75015 Paris
FRANCE

Claude Sombret
Centre D'Etudes Nucleaires
De La Vallee Rhone
CEN/VALRHO
S.D.H.A. BP 171
30205 Bagnols-Sur-Ceze
FRANCE

BGA/ISH/ZBD
Attn: Anton Bayer
P.O. Box 1108
D-8042 Neuherberg
GERMANY

Bundesministerium fur Forschung und Technologie
Postfach 200 706
5300 Bonn 2
GERMANY

Bundesanstalt fur Geowissenschaften und Rohstoffe
Attn: Michael Langer
Postfach 510 153
3000 Hannover 51
GERMANY

Gesellschaft fur Reaktorsicherheit
Attn: Bernard Krzykacz
D-8046 Garching
GERMANY

Gesellschaft fur Reaktorsicherheit (GRS) mb (2)
Attn: Bruno Baltes
Wolfgang Muller
Schwertnergasse 1
D-5000 Cologne
GERMANY

Hahn-Mietner-Institut fur Kernforschung
Attn: Werner Lutze
Glienicker Strasse 100
100 Berlin 39
GERMANY

Institut fur Tieflagerung (2)
Attn: K. Kuhn
Theodor-Heuss-Strasse 4
D-3300 Braunschweig
GERMANY

Kernforschungszentrum Karlsruhe/INR
Attn: Joachim Ehrhardt
Postfach 3640
D-7500 Karlsruhe 1
GERMANY

Kernforschungszentrum Karlsruhe/INR
Attn: Friedmar Fischer
Postfach 3640
D-7500 Karlsruhe 1
GERMANY

Physikalisch-Technische Bundesanstalt
Attn: Peter Brenneke
Postfach 33 45
D-3300 Braunschweig
GERMANY

Japan Atomic Energy Research Institute
Department of Reactor Safety Research
Attn: T. Ishigami
Tokai-mura, Naka-gun, Ibaraki-ken
319-11
JAPAN

Shingo Tashiro
Japan Atomic Energy Research Institute
Tokai-Mura, Ibaraki-Ken
319-11
JAPAN

Catholic University Brabant
Attn: J. P. C. Kleijnen
Tilburg
THE NETHERLANDS

Delft University of Technology
Dept. of Mathematics
Attn: Roger Cooke
Julianalaan 132
Delft
THE NETHERLANDS

Netherlands Energy Research Foundation
ECN
Attn: L. H. Vons
3 Westerduinweg
P.O. Box 1
1755 ZG Petten
THE NETHERLANDS

Johan Andersson
Swedish Nuclear Power Inspectorate
Statens Kärnkraftinspektion (SKI)
Box 27106
S-102 52 Stockholm
SWEDEN

Fred Karlsson
Svensk Karnbransleforsorjning AB
SKB
Box 5864
S-102 48 Stockholm
SWEDEN

Abtielung fur die Sicherheit der Kernanlagen
Attn: S. Chakraborty
Eidgenossisches Amt fur Energiewirtschaft
CH-5303
Wurenlingen
SWITZERLAND

Nationale Genossenschaft fur die Lagerung Radioaktiver Abfalle (NAGRA) (2)
Attn: Stratis Vomvoris
Piet Zuidema
Hardstrasse 73
CH-5430 Wettingen
SWITZERLAND

D. R. Knowles
British Nuclear Fuels, plc
Risley, Warrington, Cheshire WA3 6AS
1002607 UNITED KINGDOM

AEA Technology
Attn: J.H. Rees
D5W/29 Culham Laboratory
Abington
Oxfordshire OX14 3DB
UNITED KINGDOM

AEA Technology
Attn: W. R. Rodwell
044/A31 Winfrith Technical Centre
Dorchester
Dorset DT2 8DH
UNITED KINGDOM

AEA Technology
Attn: J. E. Tinson
B4244 Harwell Laboratory
Didcot
Oxfordshire OX11 ORA
UNITED KINGDOM

The University of Reading
Department of Statistics
Attn: Derek J. Pike
Whiteknights
Reading RG6 2AN
UNITED KINGDOM

National Radiological Protection
Board
Attn: M. Crick
Chilton, Didcot
Oxon OX11 ORQ
UNITED KINGDOM

National Radiological Protection
Board
Attn: Marion Hill
Chilton, Didcot
Oxon OX11 ORQ
UNITED KINGDOM

National Radiological Protection
Board
Attn: J. A. Jones
Chilton, Didcot
Oxon OX11 ORQ
UNITED KINGDOM

United Kingdom Atomic Energy
Authority
Attn: William Nixon
Safety & Reliability Directorate
Wigshaw Lane
Culcheth
Warrington WA3 4NE
UNITED KINGDOM

INTERNAL

1 A. Narath
20 O. E. Jones
1502 J. C. Cummings
1511 D. K. Gartling
3151 S. M. Wayland
6000 D. L. Hartley
6119 R. L. Beauheim
6119 P. B. Davies
6119 E. D. Gorham
6119 C. F. Novak
6119 S. W. Webb
6121 D. E. Munson
6121 E. J. Nowak
6121 J. R. Tillerson
6233 J. C. Eichelberger
6300 D. E. Miller
6301 E. J. Bonano
6302 T. E. Blejwas, Acting
6303 S. Y. Pickering
6303 W. D. Weart
6312 F. W. Bingham
6313 Supervisor
6313 L. S. Costin
6315 Supervisor
6316 R. P. Sandoval
6320 R. E. Luna, Acting
6341 J. M. Covan
6341 D. P. Garber
6341 A. L. Stevens
6341 J. Orona*
6341 Sandia WIPP Central Files (250)
6342 D. R. Anderson
6342 S. Bertram-Howery
6342 B. M. Butcher
6342 D. P. Gallegos
6342 L. S. Gomez
6342 M. Gruebel
6342 R. Guzowski
6342 R. D. Klett
6342 M. G. Marietta
6342 A. C. Peterson
6342 R. P. Rechard
6342 P. Swift
6342 M. Tierney
6342 K. M. Trauth
6342 B. L. Baker*
6342 J. Bean*
6342 J. Berglund*
6342 W. Beyeler*
6342 T. Blaine*
6342 K. Brinster*
6342 K. Byle*
6342 L. Clements*
6342 J. Garner*
6342 A. Gilkey*
6342 H. Iuzzolino*
6342 J. Logothetis*
6342 R. McCurley*
6342 J. Rath*
6342 D. Rudeen*
6342 J. Sandha*
6342 J. Schreiber*
6342 P. Vaughn*
6343 T. M. Schultheis
6345 R. Beraun
6345 L. Brush
6345 R. C. Lincoln
6345 F. T. Mendenhall
6345 M. A. Molecke
6347 Supervisor
6347 D. R. Schafer
6400 D. J. McCloskey
6400 N. R. Ortiz
6411 R. J. Breeding
6412 A. L. Camp
6412 S. E. Dingman
6412 A. C. Payne
6413 F. T. Harper
6413 J. C. Helton (20)
6413 J. L. Sprung
6416 D. A. Zimmerman
6419 M. P. Bohn
6453 L. F. Restrepo
6613 J. E. Campbell
6613 R. M. Cranwell
6613 R. L. Iman
6613 C. Leigh
6622 M.S.Y. Chu
9300 J. E. Powell
9330 J. D. Kennedy
8523-2 Central Technical Files
3141 S. A. Landenberger (5)
3145 Document Processing (8) for DOE/OSTI
3151 G. C. Claycomb (3)

*6342/Geo-Centers

☆ U.S. GOVERNMENT PRINTING OFFICE: 1992—673-122/60127